DISCLAIMER

This report was prepared as an account of work sponsored by an agency of the United States Government. Neither the United States Government nor any agency thereof, nor any of their employees, makes any warranty, express or implied, or assumes any legal liability or responsibility for the accuracy, completeness, or usefulness of any information, apparatus, product, or process disclosed, or represents that its use would not infringe privately owned rights. Reference herein to any specific commercial product, process, or service by trade name, trademark, manufacturer, or otherwise does not necessarily constitute or imply its endorsement, recommendation, or favoring by the United States Government or any agency thereof. The views and opinions of authors expressed herein do not necessarily state or reflect those of the United States Government or any agency thereof. Reference herein to any social initiative (including but not limited to Diversity, Equity, and Inclusion (DEI); Community Benefits Plans (CBP); Justice 40; etc.) is made by the Author independent of any current requirement by the United States Government and does not constitute or imply endorsement, recommendation, or support by the United States Government or any agency thereof.

Lawrence Livermore National Laboratory

TEX-Chlorine: Highly Enriched Uranium with Chloride Absorbers to Provide Validation Benchmarks for Y-12 Electrorefining Facility

IER-499 CED-4b Report

Eric Aboud, Jesse Norris, Paul Maggi, and Konner Casanova

External (Unlimited)

September 8, 2025

LLNL-TR-2002677

Disclaimer

Lawrence Livermore National Laboratory is operated by Lawrence Livermore National Security, LLC, for the U.S. Department of Energy, National Nuclear Security Administration under Contract DE-AC52-07NA27344.

Acknowledgements

This work was supported by the United States Department of Energy (DOE) Nuclear Criticality Safety Program (NCSP), funded and managed by the National Nuclear Security Administration for the DOE. These experiments were executed at the National Criticality Experiments Research Center (NCERC) under the operations of the Los Alamos National Laboratory's Advanced Nuclear Technology Group (NEN-2). The experiments were executed by the following experimenters: Theresa Cutler, Peter Brain, Travis Grove, Rene Sanchez, Alex McSpaden, Kristin Stolte, Zach Lemke, Kenny Valdez, and Charlie Kiehne. The experiments were conducted with facility support by NCERC-FO and Mission Support and Test Services (MSTS).

Internal review was performed by Paul Maggi (LLNL) and external review was performed by Konner Casanova (INL). This benchmark was submitted as HEU-MET-THERM-038 to the ICSBEP Technical Review Group (TRG) in April 2025. The subgroup associated with this benchmark consisted of: Kristin Stolte (LANL), Joetta Goda (LANL), John Bess (JFoster & Associates), Zachariah Lemkre (LANL), Alexander McSpaden (LANL), and Mariya Brovchenko (ASNR).

Table of Contents

Executive Summary

This report documents the final benchmark of the TEX-Chlorine (IER-499) Thermal Epithermal eXperiments (TEX) with highly enriched uranium with chlorine absorbers and high-density polyethylene reflectors and moderators. TEX-Chlorine is a variation of the TEX-HEU baseline assembly with the addition of sodium chloride absorber plates. This evaluation contains three experimental configurations that were performed on Comet at NCERC between July and August 2024. The three configurations, which were acceptable as benchmark cases, spanned from thermal (first two configurations) to fast (third configuration). All three cases were reviewed and accepted by the ICSBEP TRG in April 2025 and was submitted to the ICSBEP in August 2025 after receiving subgroup approval.

Table 1 reports the benchmark k_{eff} values derived experimentally and the resulting benchmark k_{eff} values. The experimentally derived results are calculated via the reactor period, and the uncertainty is based on a rigorous analysis of 33 uncertainty components. The biases represent model simplifications which were taken to simplify the model for the ease of use of the benchmark by a user. The primary sources of uncertainty are from the stack height measurements and the hydrogen thermal scattering law for the thermal configurations.

Table 1: Summary of the experimental and benchmark k_{eff} value for each case.

Case	Moderator Thickness (in)	Neutron Spectrum	Experimental k_{eff}	Bias in k_{eff}	Benchmark k_{eff}
1	0.750	Thermal	1.00041(78)	-0.00024(19)	1.00017(80)
2	1.750	Thermal	1.00065(117)	0.00150(18)	1.00214(119)
3	0.125	Intermediate/Fast	1.00134(70)	-0.00290(20)	0.99845(73)

Table 2 reports the sample calculations results using MCNP6.3 with ENDF/B-VIII.0. A detailed comparison between MCNP6.3, COG11.3, and MONK11A using the nuclear data libraries ENDF/B-VII.1, ENDF/B-VIII.0, and JEFF3.3 was performed in this evaluation. Notably good agreement was found between ENDF/B-VIII.0 and the experimental results for the two thermal configurations. A significant bias was observed between all of the codes and nuclear data libraries and the experimental result for the fast configuration. A C/E plot for all of the assessed codes and nuclear data libraries including comparisons to previous benchmarks and the TEX-HEU baseline configurations is shown in Figure 1.

Table 2: Summary of the Computational/Experimental (C/E) values for each case using MCNP6.3 and ENDF/B-VIII.0.

Case	Calculated k_{eff}	C/E
1	0.99670(4)	0.99653(78)
2	1.00036(4)	0.99822(117)
3	0.98900(4)	0.99054(69)

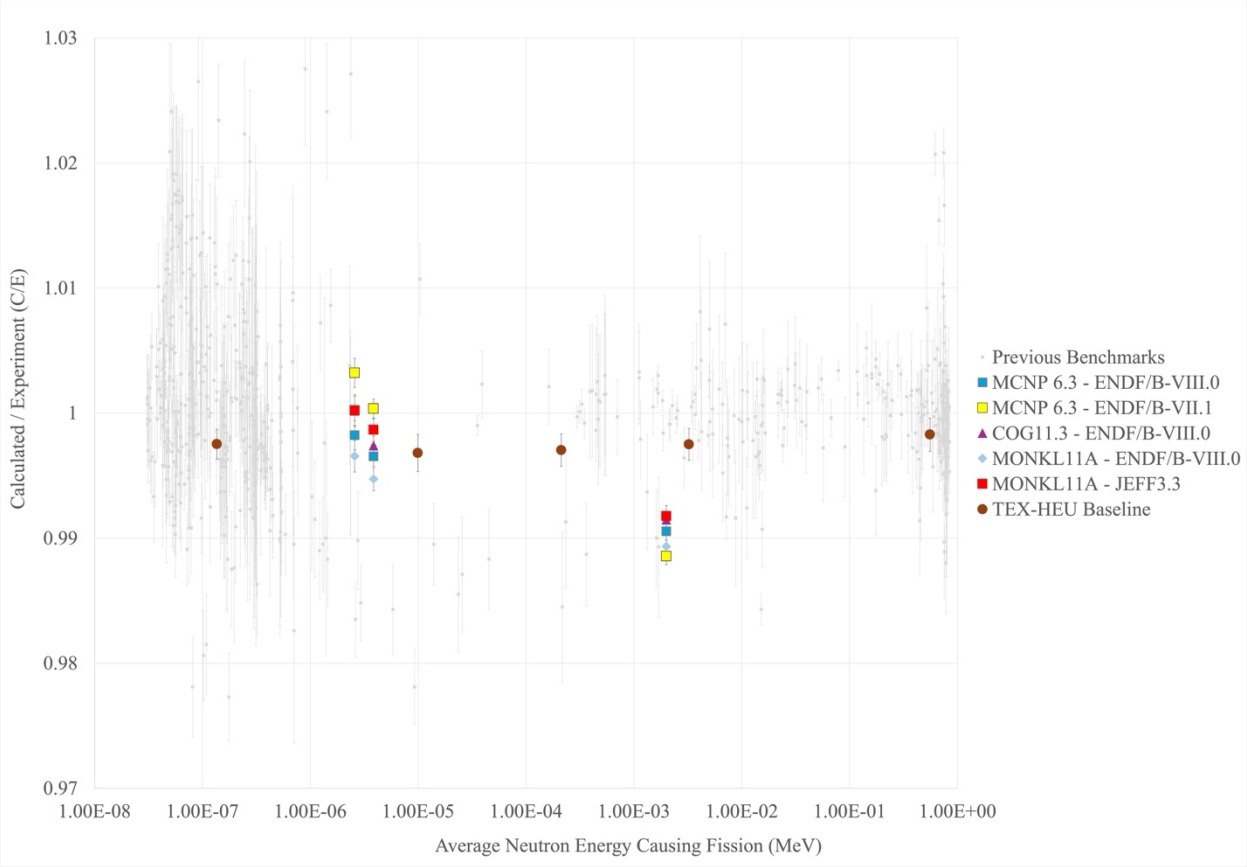

Figure 1: C/E results for the three cases comparing various codes and nuclear data libraries. This also compares to the TEX-HEU baseline configurations.

NEA/NSC/DOC(95)03/II
Volume II

HEU-MET-THERM-038

TEX-CHLORINE ASSEMBLIES: HIGHLY ENRICHED URANIUM PLATES WITH SODIUM CHLORIDE ABSORBERS USING POLYETHYLENE MODERATOR AND POLYETHYLENE REFLECTOR

Evaluator

Eric Aboud
Jesse Norris
Lawrence Livermore National Laboratory

Internal Reviewer

Paul Maggi
Lawrence Livermore National Laboratory

Independent Reviewer

Konner Casanova
Idaho National Laboratory

LLNL-TR-2002677
Lawrence Livermore National Laboratory
7000 East Avenue, P.O. Box 808, L-198, Livermore, California, USA, 94551

DISCLAIMER

ACKNOWLEDGEMENTS

This work was supported by the Nuclear Criticality Safety Program, funded and managed by the National Nuclear Security Administration for the Department of Energy.

HEU-MET-THERM-038

TEX-CHLORINE ASSEMBLIES: HIGHLY ENRICHED URANIUM PLATES WITH SODIUM CHLORIDE ABSORBERS USING POLYETHYLENE MODERATOR AND POLYETHYLENE REFLECTOR

IDENTIFICATION NUMBER: HEU-MET-THERM-038

KEY WORDS: critical experiment, highly enriched uranium, metal, chlorine, high-density polyethylene, polyethylene-moderated, polyethylene-reflected, Comet, Jemima, acceptable

1.0 DETAILED DESCRIPTION

1.1 Overview of the Experiment

This evaluation documents highly enriched uranium (HEU) experimental critical configurations with polyethylene moderators and sodium chloride absorbers conducted as part of the United States Nuclear Criticality Safety Program's Thermal/Epithermal eXperiments (TEX) program. HEU-MET-MIXED-021 provides the benchmark evaluation of five TEX experiments designed to establish baseline configurations with HEU Jemima plates moderated by high density polyethylene (HDPE). The TEX-HEU experiments were designed to cover five different fission energy regimes by varying the thickness of the interstitial HDPE moderator, with varying fractions of thermal, intermediate, and fast fissions, and to be easily modified to accommodate test materials of interest. HEU-MET-INTER-013 documents the first TEX-HEU variation, incorporating hafnium in seven different experimental configurations. This evaluation covers an additional variant that incorporates absorber plates of compacted high-purity sodium chloride salt. These experiments were motivated by a criticality safety need for validation data for uranium purification by means of electrorefining with chloride salts, especially thermal and intermediate energy configurations resulting from moderator upset conditions, and their design was optimized by matching sensitivity profiles from application cases. All three experimental configurations are judged to be acceptable as benchmark cases.

The main parameter varied between the configurations is the thickness of the polyethylene moderators and the sodium chloride absorbers between the HEU plates. Varying the thickness of the polyethylene tunes the neutron energy spectrum between majority thermal (Case 1 and 2) and intermediate (Case 3). The fission fractions, presented in Table 1, are determined calculationally. Case 3 is cross listed as HEU-MET-INTER-014.

Table 1: Comparison of the polyethylene plate thicknesses and resulting fission fractions grouped by neutron energy regime (based on calculations using MCNP® 6.3 with ENDF/B-VIII.0).

Configuration	Nominal Moderator Thickness, in. (cm)	Calculated Fission Fractions		
		Thermal (<0.625 eV)	Intermediate (0.625 eV - 100 keV)	Fast (>100 keV)
1[(a)]	0.750 (1.905)	58.07%	30.15%	11.78%
2	1.750 (4.445)	62.99%	25.51%	11.50%
3	0.125 (0.3175)	13.64%	51.10%	35.26%

[(a)] Sandwich configuration, detailed in Section 1.2.1.

The HEU plates, with enrichment U(93.4 wt-%), an outer diameter of 15 in. (38.1 cm), and a thickness of

0.118 in. (0.29972 cm) (IEU-MET-FAST-002), have a long history of being used in critical experiments, dating back to 1956[1]. The HEU plates have been used in the Big Ten experiments of the 1970s (IEU-MET-FAST-007), the first three Zeus experiments in 1999-2002 (HEU-MET-INTER-006, HEU-MET-FAST-072, and HEU-MET-FAST-073), and the Nb-1Zr experiment in 2004 (HEU-MET-FAST-047). Recently, the HEU plates have been used in the Curie (HEU-MET-INTER-011), TEX-HEU (HEU-MET-MIXED-021), the Zeus with lead (IEU-MET-FAST-025, HEU-MET-FAST-102), and the TEX-Hf (HEU-MET-INTER-013) experiments.

The TEX-Cl experiments were conducted over approximately three weeks in July and August of 2024 at the National Criticality Experiments Research Center (NCERC), located inside the Device Assembly Facility (DAF) at the Nevada National Security Site (NNSS) in the United States of America. The design and execution of the experiments were a collaboration between Lawrence Livermore National Laboratory's (LLNL) Nuclear Criticality Safety Division (NCSD) and Los Alamos National Laboratory's (LANL) Advanced Nuclear Technologies Group (NEN-2), funded by the U.S. Department of Energy's Nuclear Criticality Safety Program. The experiments were designed by Eric Aboud and Ruby Araj of LLNL's NCSD. The experiments were observed and documented by Eric Aboud, Jesse Norris, and Ruby Araj of LLNL's NCSD. The experiments were performed by Theresa Cutler, Peter Brain, Travis Grove, Rene Sanchez, Alex McSpaden, Kristin Stotle, Zach Lemke, Kenny Valdez, and Charlie Kiehne of LANL. The experiments were conducted with facility support by NCERC-FO (Facility Operations) and Mission Support and Test Services (MSTS) personnel.

1.2 Description of Experimental Configuration

1.2.1 Design of the Critical Assembly

The design of the assembly was based on the TEX-HEU template, shown in Figure 1, with layers of HEU, high-density polyethylene (HDPE), and absorber material. The fission neutron energy spectra were tuned by adjusting the interstitial polyethylene moderator thicknesses. When conducting the experiment, the reactivity was coarsely controlled by varing the number of fuel layers and the HEU fuel mass, either by swapping the fuel plate with similar fuel plates or plates with different inner annuli. The reactivity was finely controlled by adjusting the upper reflector thickness, which could be adjusted in 0.03125 in. (0.079375 cm) increments. The annular side and bottomr reflectors are 1 in. thick, which are not varied to tune reactivity. The HDPE ring reflector height was adjusted to match the HEU and HDPE stack to the nearest 0.03125 in. (0.079375 cm). Similar to the TEX-Hf, the absorber material of interest, in this case the sodium chloride absorbers, was placed in each layer with the moderator and fuel plates.

[1] The "early Jemima experiments" in 1952-1954 used HEU plates having a diameter of 10.50 in. and thickness of 0.800 cm (IEU-MET-FAST-001).

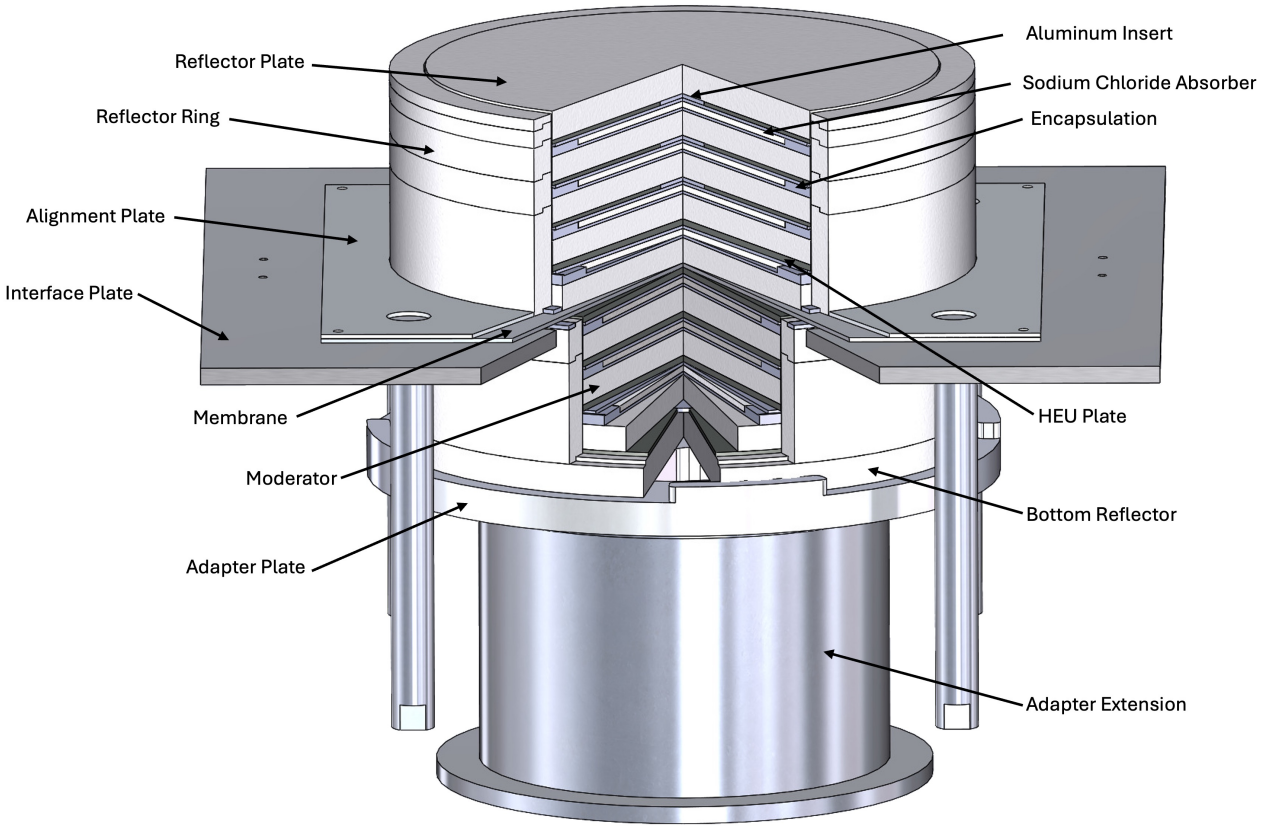

Figure 1: Cut away view of the TEX-Cl configuration.

Two different moderator configurations were used: a standard and a sandwich configuration. Examples of the two configuration types are shown in Figure 2 and Figure 3. The standard stacking method is made up of a repeating pattern of one HEU plate, one HDPE moderator plate, and one absorber plate. The sandwich stacking method has two layers of HDPE sandwiching a sodium chloride asborber between the HEU plates. In the figures the dark gray plates are the HEU plates, the light gray plates are the sodium chloride absorbers, which are enclosed in aluminum, and the white plates are the HDPE moderators or reflectors. Figure 3 shows the top half of the 8-layer sandwich stack on Comet prior to the installation of the HDPE ring reflectors and while the two halves of the assembly are fully separated. Figure 2 shows the top half of the 8-layer standard stack on the granite table used for the coordinate measuring machine (CMM) measurements and also does not show the ring reflectors installed.

Figure 2: TEX-Cl standard stacking method, showing the top stack of the Case 2.

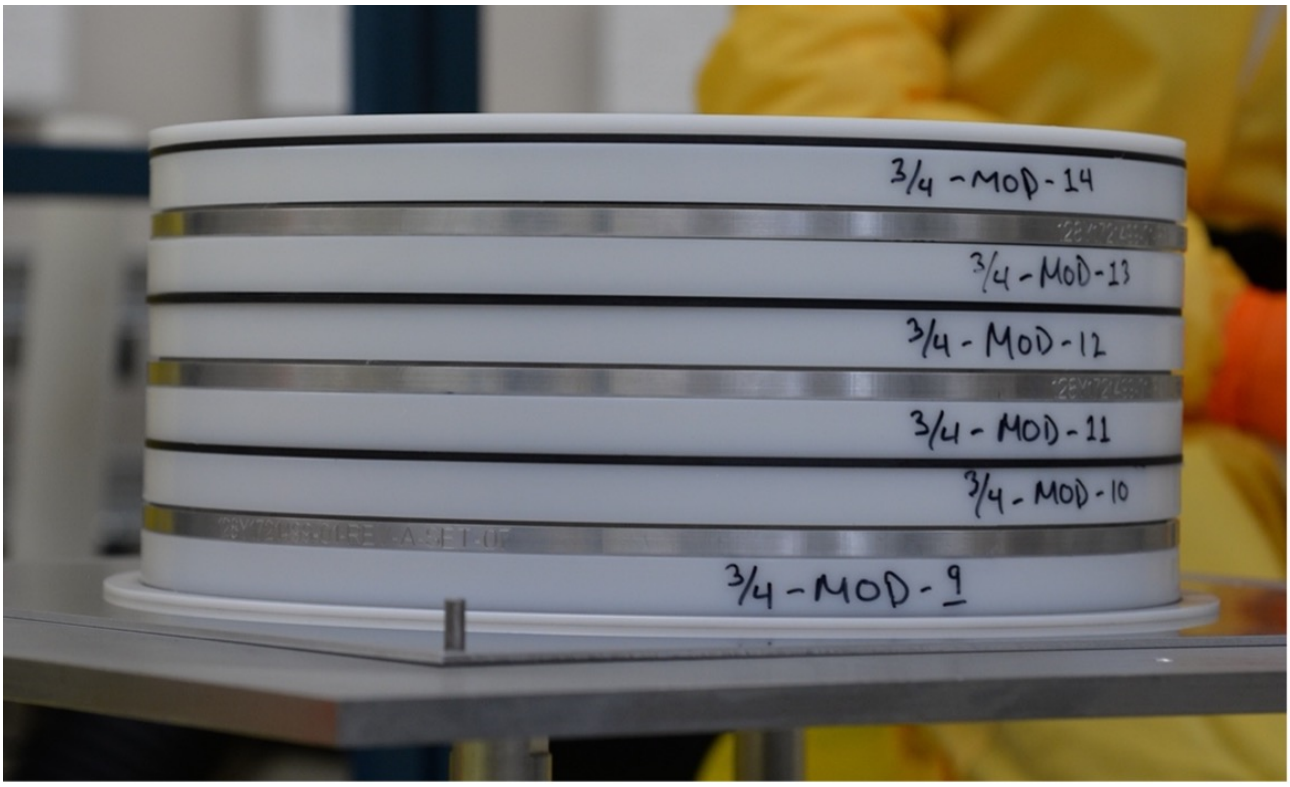

Figure 3: TEX-Cl sandwich stacking method, showing the top stack of the Case 1.

1.2.2 Comet General Purpose Critical Assembly Machine

The Comet General Purpose Critical Assembly Machine is a vertical lift machine used to remotely assemble a critical assembly. Comet, shown in Figure 4, consists of the surrounding structure, stationary platform, and moveable platen. For the TEX-HEU, TEX-Hf, and TEX-Cl campaigns, additional parts were affixed to Comet, including: an experiment platform, which was afixed to the stationary platform, and a lower adapter, which extends the movable platen.

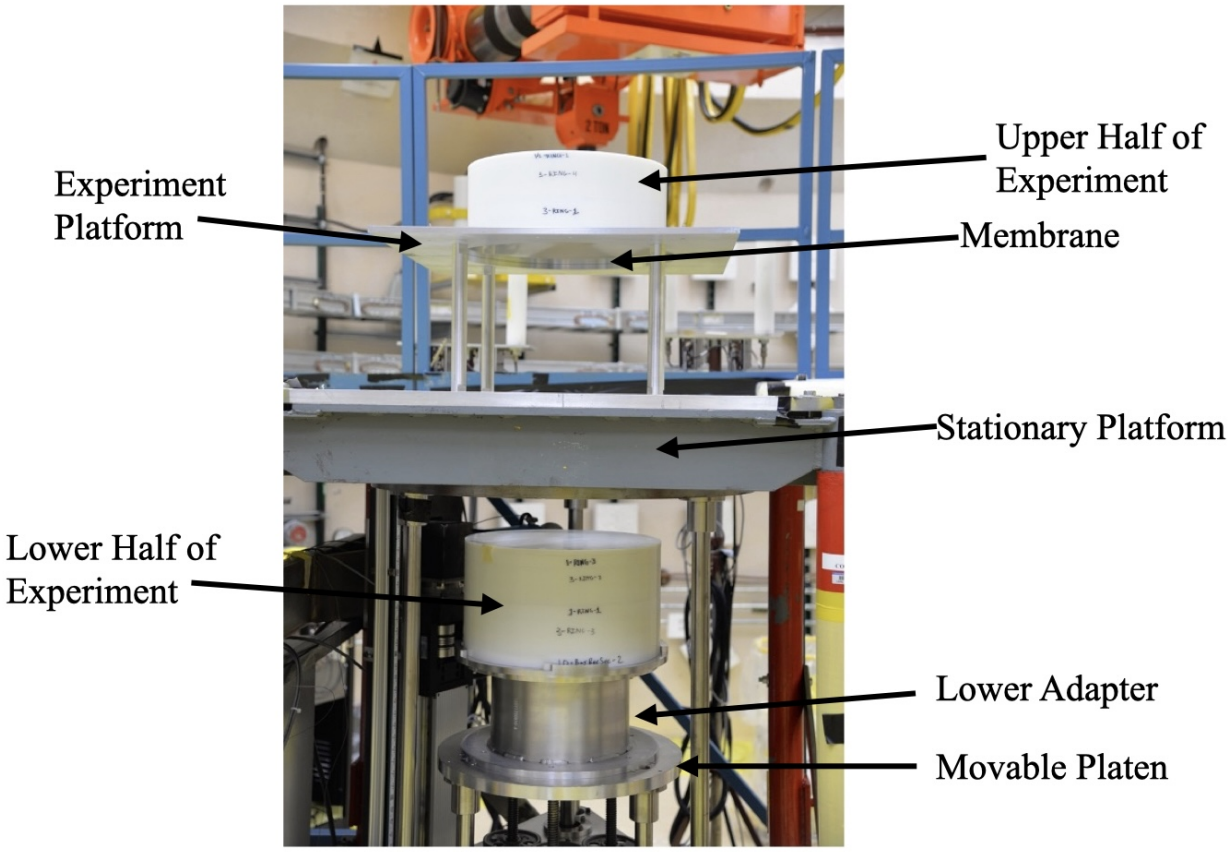

Figure 4: The Comet general purpose critical assembly machine. The Godiva IV fast burst reactor is located to the right of this photo (out of frame).

Roughly half of the experiment is built on the upper experiment platform, referred to as the upper stack, and the other half on the lower adapter, referred to as the lower stack. During operation, the moveable platen is extended vertically to bring the two halves of the assembly together until the upper and lower stacks are in contact. After initial contact the platen is driven in to fully lift the upper stack, ensuring no gaps between the two halves. Once fully assembled, the two halves are separated by a thin aluminum membrane, which holds the upper stack on the experimental platform.

The Godiva IV fast burst reactor is located in the same room as Comet, but is located at greater than 10 ft (3 m) away.

The following sections describe these additional parts on Comet. The design drawings for the components

listed in this section were not able to be attached to this report due to new policies. Instead, they are available as an appendix in HEU-MET-INTER-013.

1.2.2.1 Stationary Platform

The experiment platform holds the upper stack, shown in Figure 5. The platform consists of the interface plate and four standoffs, which connect the interface plate to the stationary platform. The membrane is placed on top of the interface plate, allowing the movable platen to lift the lower half of the experiment as it meets the upper half of the experiment through the membrane, and uses four pegs to hold the membrane and alignment plate in place while allowing vertical movement. The original drawings of the stationary platform, interface plate, standoffs, and membrane, with dimensions and tolerances, can be found in HEU-MET-INTER-013.

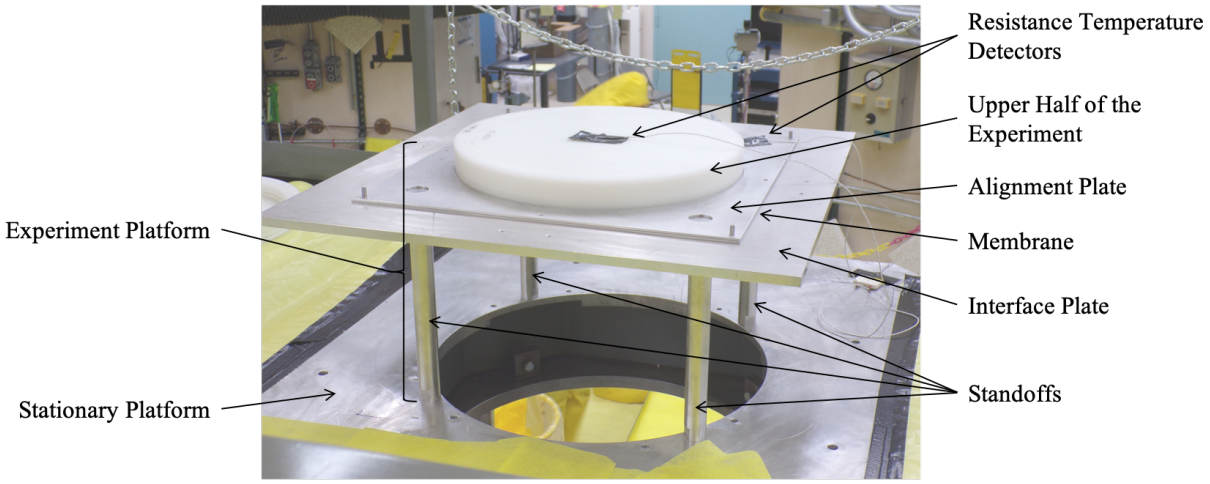

Figure 5: Upper stationary platform of the Comet, with the experiment platform. During the benchmark measurements, the resistance temperature detectors and alignment plate were removed.

The interface plate is a 28 in. × 28 in. × 0.5 in. (71.12 cm × 71.12 cm × 1.27 cm) Al-6061 plate with a 19 in. (48.26 cm) diameter hole through its center. The standoffs are 12 in. (30.48 cm) long Al-6061 cylinders with a 1.25 in. (3.175 cm) diameter. The membrane is a 21 in. × 21 in. (53.34 cm × 53.34 cm) Al-6061 plate with a thickness of 0.125 in. (0.3175 cm), report in Table 2. The membrane includes four small holes, one in each corner, which match the four pegs in the interface plate, ensuring consistent alignment during placement. This design allows the membrane to be lifted up to 0.75 in. (1.905 cm) from the top surface of the interface plate.

Table 2: Membrane nominal dimensions and tolerances.

Part Type	Thickness [in. (cm)]	Side Length [in. (cm)]
Membrane	0.125 ± 0.010 (0.3175 ± 0.0254)	21.000 ± 0.030 (53.3400 ± 0.0762)

1.2.2.2 Lower Adapter

The adapter plate, shown in Figure 6, holds the lower stack and has been updated since the TEX-HEU and TEX-Hf experiments. Namely, the redesign incorporates a new lip design which allows access to the source holder in the bottom reflector, which has also been redesigned and is described in Section 1.2.5. The lip, which originally was a single height around the entire circumference, is now limited to four sections where the gaps between the sections allow full access to the bottom reflector. The adapter plate has an outer diameter of 18.5 in. (46.99 cm) and a thickness of 0.53 in. (1.3462 cm). The plate features an inner diameter of 17.150 in. (43.561 cm) with a cross spoke design in the center, shown in Figure 7. The adapter plate has a lip height of 0.47 in. (1.1938 cm), giving it a total height of 1 in. (2.54 cm) where there are lips.

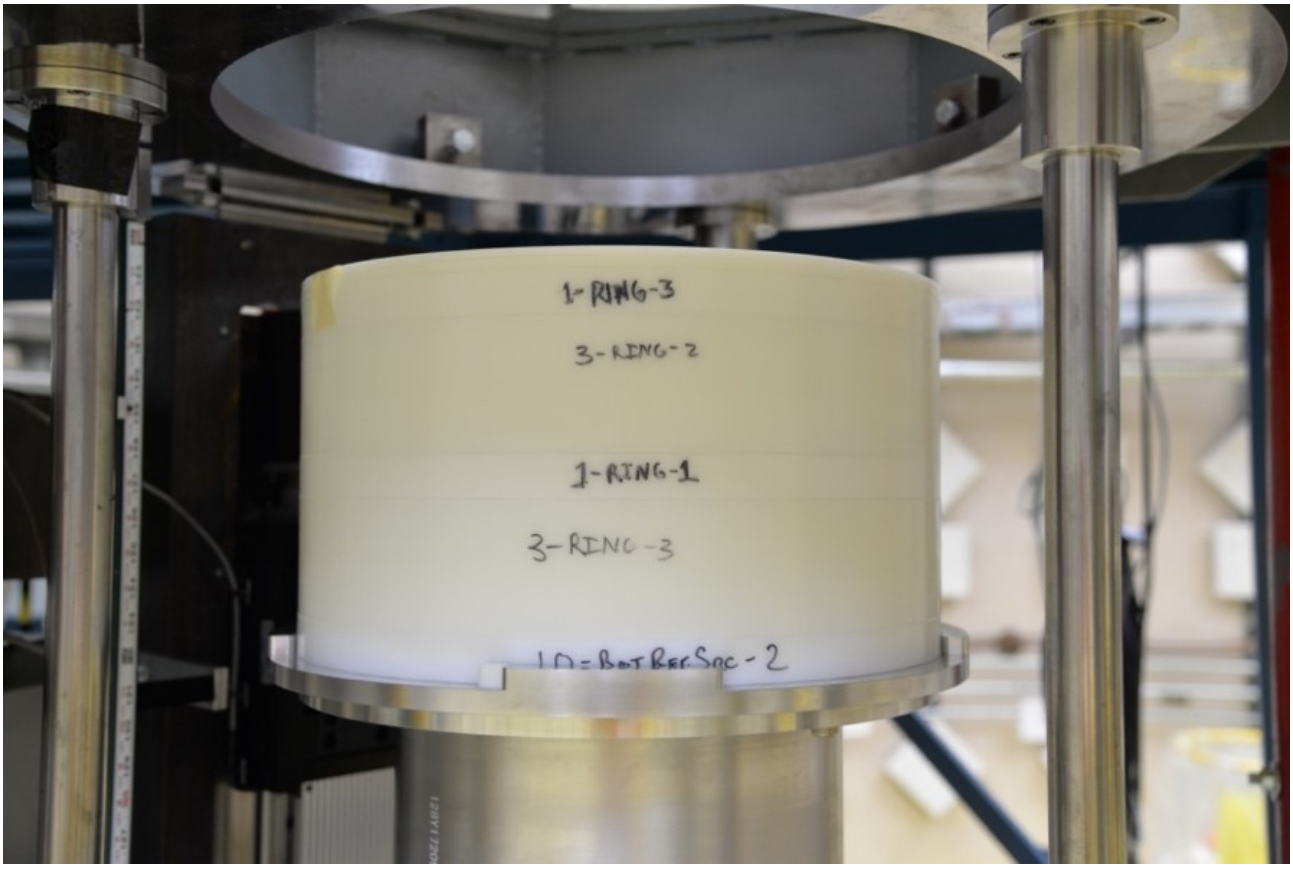

Figure 6: Lower movable platen of Comet from TEX-HEU, with the lower adapter. A similar photograph was not taken with the new adapter plate.

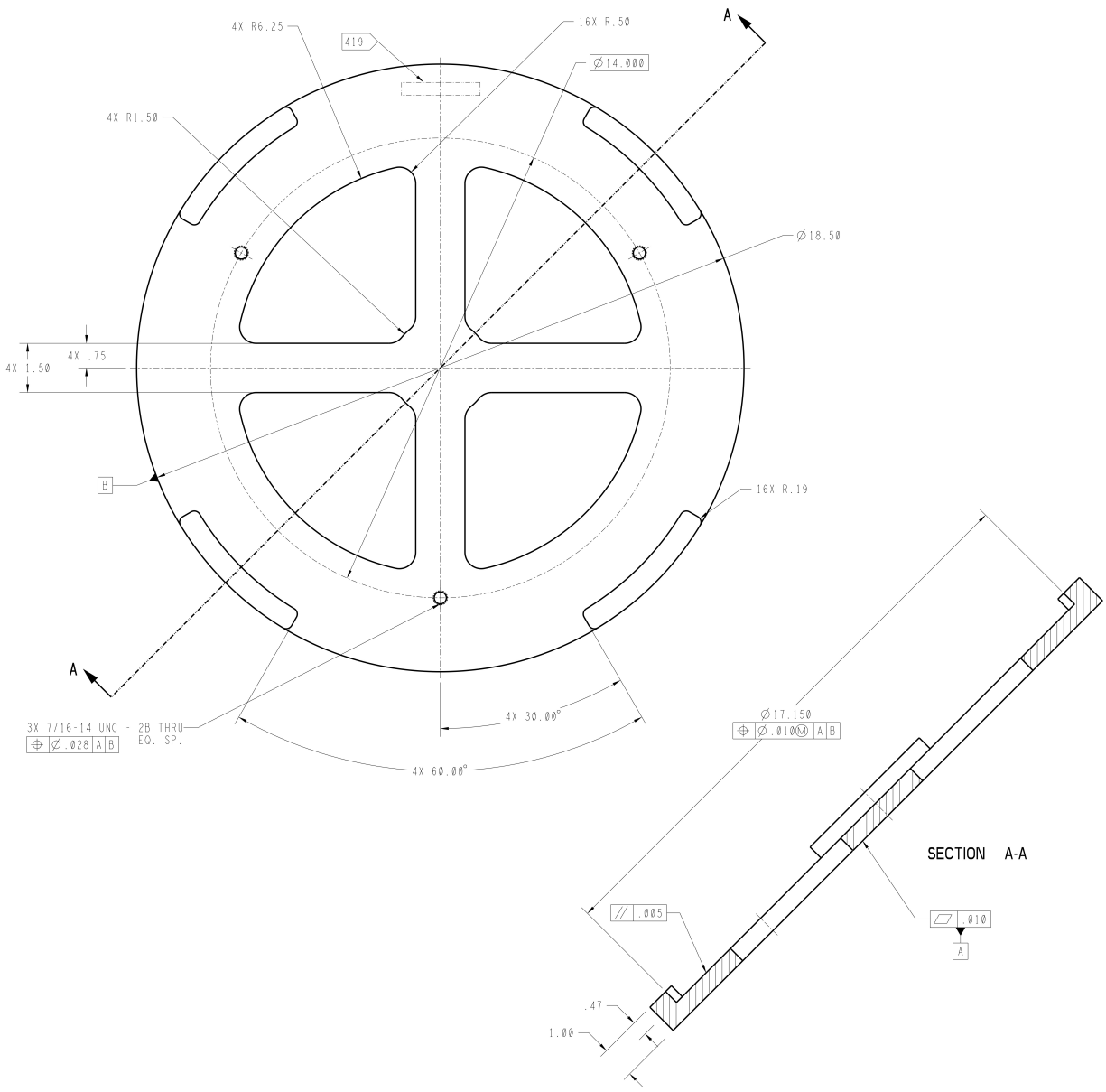

Figure 7: A drawing of the adapter plate given rough dimensions. This figure highlights the lip features of the new design.

The adapter plate sits on the adapter extension and when combine the two components make up the lower adapter. The adapter extension is an 8 in. (20.32 cm) tall annular cylinder with a wall thickness of 0.25 in. (0.635 cm) and a 12 in. (30.48 cm) outer diameter. The adapter extension also includes a 2.5 in. (6.35 cm) wide and 0.5 in. (1.27 cm) thick top and bottom flange to affix it to the adapter plate and the movable platen. The lower adapter sits on the movable platen, shown in Figure 8.

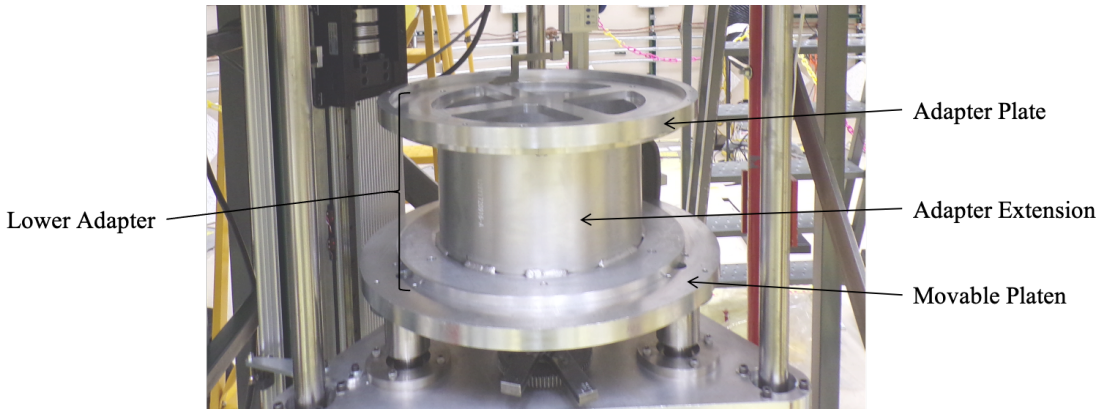

Figure 8: Lower adapter which shows the individual components: adapter plate, adapter extension, and moveable platen.

Both components of the lower adapter are made from Al-6061.

The new adapter plate was measured by Los Alamos National Laboratory upon acceptance with an Ohaus EX35001 Balance (Serial Number: C032910287; Calibration Number: 348452), a 0-6 inch Digital Caliper (Serial Number: A23151184; Calibration Number: KBF08P39L), and a 0-24 inch Digital Caliper (Serial Number: 74337; Calibration Number: 10044797). The measurements also utilized a 0-1" micrometer (Serial Number: 9298165; Calibration Number:377132-466024). The micrometer has a measurement precision of 0.00002 inches. The balance reported to the nearest tenth of a gram with a total measurement uncertainty of 0.3 grams, including linearity, corner loading, and repeatability. The two digital calipers reported to nearest 0.0001 in. (0.000254 cm) with a total measurement uncertainty of 0.0010 in. (0.00254 cm) up to 8 inches, or the entire range of the 0-6" Digital Caliper, a total uncertainty of 0.0015 in. (0.00381 cm) between 8 inches and 12 inches, and a total uncertainty of 0.0020 in. (0.00508 cm) above 12 inches The measurements of the adapter plate are given in Table 3. The mass of the adapter plate was measured to be 4509.1 ± 0.3 g.

Table 3: Adapter plate dimensional measurements.

Parameter	**Nominal [in. (cm)]**	**Measurement [in. (cm)]**
Outer Diameter	18.50 ± 0.01 (46.9900 ± 0.0254)	18.4975 ± 0.0020 (46.98365 ± 0.00508)
Total Height with Lip	1.00 ± 0.01 (2.5400 ± 0.0254)	0.9995 ± 0.0010 (2.53873 ± 0.00254)
	1.00 ± 0.01 (2.5400 ± 0.0254)	0.9950 ± 0.0010 (2.52730 ± 0.00254)
	1.00 ± 0.01 (2.5400 ± 0.0254)	1.0000 ± 0.0010 (2.54000 ± 0.00254)
	1.00 ± 0.01 (2.5400 ± 0.0254)	0.9965 ± 0.0010 (2.53111 ± 0.00254)
Average Total Height with Lip		0.9978 ± 0.0010 (2.53441 ± 0.00254)

1.2.3 Highly Enriched Uranium Plates

The HEU plates are nominally 0.118 in. (0.29972 cm) thick, 15 in. (38.1 cm) outer diameter U(93+) plates, commonly referred to as the "Jemima" plates. These plates are either full or annular cylinders with inner annuli of 2.5 in. (6.35 cm), 6 in. (15.24 cm), or 10 in. (25.4 cm). The annulus removes some of the HEU mass which results in lower or higher mass plate variants, which may be exploited for reactivity control. The plates are identified based on their outer radius and their inner (annular) radius: 15/0-HEU (Full, HEU1), 15/2.5-HEU (2.5", HEU2, Id. No. 403), 15/6-HEU (6", HEU4, "Six Inch", Id. No. 401), and 15/10-HEU (10", "Ten Inch", Id. No. 402). An overview of the variants are shown in Figure 9. The nominal plate dimensions and tolerances are tabulated in Table 4.

Table 4: HEU plate nominal dimensions and tolerances (see Fig. 9 for dimensions)[2].

Part Type	Inner Diameter, *b* [in. (cm)]	Outer Diameter, *a* [in. (cm)][(a)]	Thickness, *c* [in. (cm)]
15/0-HEU	-	15 +0.000/-0.005 (38.1 +0.0000/-0.0127)	0.118 (0.29972)
15/2.5-HEU	2.510 +0.005/-0.000 (6.3754 +0.0127/-0.0000)		
15/6-HEU	6.005 +0.005/-0.000 (15.2527 +0.0127/-0.0000)		
15/10-HEU	10.005 +0.005/-0.000 (25.4127 +0.0127/-0.0000)		
6/0-HEU	-	6 +0.000/-0.005 (15.24 +0.0000/-0.0127)	

[(a)] A recent report characterizing the HEU plate dimensions using a coordinate measuring machine included original drawings of the 15/2.5-HEU, 15/6-HEU, and 15/10-HEU plates[3]. These drawings indicate a symmetric tolerance on the outer diameter of ±0.005 in.; which is in disagreement with the asymmetric tolerenace reported in HEU-MET-INTER-006, HEU-MET-FAST-072, and HEU-MET-FAST-073. However, the measurements of the outer diameters in that report indiciate an average outer diameter of 14.996 in. with a range of 14.993 in. to 15.000 in.; which is in agreement with the asymmetric tolerance. Therefore, the reported asymmetric tolerance from HEU-MET-INTER-006, HEU-MET-FAST-072, and HEU-MET-FAST-073 is presented.

The measured thicknesses of the HEU plates and the mass measurement performed in the past two decades, including those performed during the TEX-Hf epxerimental campaign, are shown in Table 5. The mass measurements in 2022, during the TEX-Hf campaign, were performed with a Mettler Toledo Electronic Scale with a maximum capacity of 16,200 grams, precision of 0.1 grams, and linearity of 0.2 grams. The measurement procedure is described in detail in HEU-MET-INTER-013. The reported thickness measurements were taken from those described in [1] performed during MIX-MET-FAST-016 in 2019. The measurements were performed using an IP67 Mitutoyo caliper (CD-24"C) with a resolution of ±0.02 in. (±0.0508 cm).

[1]The HEU notation (HEU1, HEU2, and HEU4) is used in the Zeus benchmarks HEU-MET-INTER-006, HEU-MET-FAST-072, and HEU-MET-FAST-073 and the Id. No. notation in used in the Big Ten benchmark IEU-MET-FAST-007.

[2]The inner and outer diameter dimensions and tolerances are based on descriptions of the 15/0-HEU and 15/2.5-HEU plates in HEU-MET-INTER-006 and HEU-MET-FAST-072 and the 15/6-HEU plates in HEU-MET-FAST-073.

[3]K. Amundson et al. *HEU Pancake (Jemima) Plate Preliminary Characterization Report*. LA-UR-24-20414. Los Alamos National Laboratory, 2024. DOI: 10.2172/2282508.

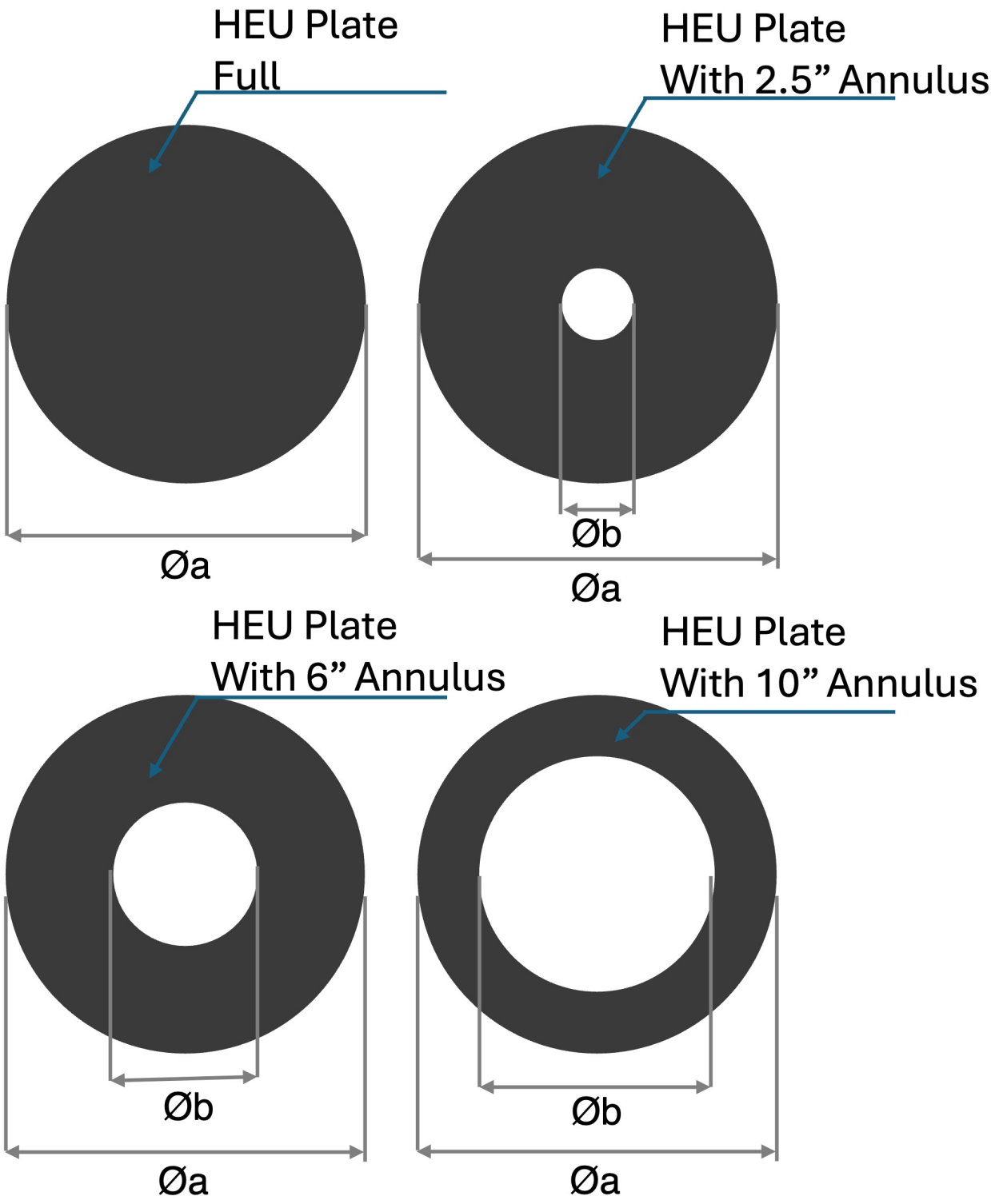

Figure 9: Diagram of the HEU plates, showing four part types.

Table 5: HEU plate mass and dimension measurements (see Fig. 9 for dimensions).

Part Type	Part ID	Mass (g)				Thickness, *c* [in. (cm)][(c)]
		2023[(a)]	2022[(b)]	2020[(c)]	2005[(d)]	
15/0-HEU	11150	6404.4	6404.7	6410.3	6415.4	0.1218 (0.30937)
	11149	6382.4	6382.2	6383.6	6409.2	0.1222 (0.31039)
	11147	6511.9	6512.4	6517.3	6526.2	0.1195 (0.30353)
	11019	6468.6	6469.2	6470.0	6476.9	0.1190 (0.30226)
	11017	6497.8	6497.8	6501.6	6518.6	0.1208 (0.30683)
15/2.5-HEU	10491	6391.6	6391.6	6392.4	6393.8	0.1238 (0.31445)
	10489	6343.5	6343.7	6343.8	6345.0	0.1232 (0.31293)
	10487	6274.8	6275.4	6274.9	6276.4	0.1203 (0.30556)
	10475	6228.0	6228.5	6230.0	6236.2	0.1285 (0.32639)
	10470	6278.3	6278.6	6279.0	6261.0	0.1227 (0.31166)
	10467	6335.6	6335.6	6335.8	6336.6	0.1245 (0.31623)
	10464	6258.3	6258.4	6258.5	6259.3	0.1195 (0.30353)
15/6-HEU	11018	5369.0	5369.6	5369.9	5375.4	0.1192 (0.30277)
	10935	-	5434.9	-	5435.9	-
	10933	-	5437.4	-	5439.9	-
	10932	-	5432.9	-	5436.5	0.1250 (0.31750)
	10477	5498.5	5498.9	5499.2	5498.6	0.1235 (0.31369)
	10457	5574.1	5573.9	5574.1	5574.0	0.1255 (0.31877)
15/10-HEU	10485	-	3604.3	-	3605.5	-
	10481	-	3594.3	-	3593.6	0.1205 (0.30607)
	10479	3564.3	3564.6	3564.7	3565.4	0.1198 (0.30429)
	10473	-	3606.9	-	3607.3	-
	10472	3586.1	3586.4	3585.7	3587.2	0.1220 (0.30988)
	10463	3632.4	3631.7	3631.7	3627.0	0.1233 (0.31318)
	10458	-	3617.9	-	3618.3	-
6/0-HEU	Q2-16	1074.9	1075.6	-	1077.8	0.1252 (0.31801)

[(a)] Reproduced from HEU-MET-FAST-106.
[(b)] Reproduced from HEU-MET-INTER-013.
[(c)] Reproduced from HEU-MET-MIXED-021.
[(d)] Reproduced from [1].

The derived volumes and densities using the data presented in Table 4 and Table 5 are shown below in Table 6

Table 6: Derived HEU plate volumes and densities.

Part Type	Part ID	Volume (cm^3)	Density (g/cm^3)
15/0-HEU	**11150**	**352.7125**	**18.1584**
	11149	353.8708	18.0354
	11147	346.0521	18.8191
	11019	344.6042	18.7728
	11017	349.8167	18.5749
15/2.5-HEU	10491	348.4659	18.3421
	10489	346.7770	18.2933
	10487	338.6143	18.5326
	10475	361.6952	17.2203
	10470	345.3697	18.1794
	10467	350.4362	18.0792
	10464	336.3625	18.6061
15/6-HEU	11018	289.8619	18.5247
	10935	286.9438	18.9406
	10933	286.9438	18.9494
	10932	303.9659	17.8734
	10477	300.3183	18.3102
	10457	305.1818	18.2642
15/10-HEU	10485	189.6860	19.0014
	10481	193.7048	18.5556
	10479	192.5796	18.5098
	10473	189.6860	19.0151
	10472	196.1161	18.2871
	10463	198.2058	18.3229
	10458	189.6860	19.0731
6/0-HEU	Q2-16	58.0093	18.5418

1.2.4 Sodium Chloride Absorbers

The sodium chloride absorbers are composed of granular sodium chloride (NaCl) salt encapsulated by an aluminum alloy 6061 (Al-6061) container. The sodium chloride salt, marketed as BioXtra (Catalogue Number: S7653), was procured through Millipore Sigma with a purity of $\geq$ 99.5%. The sodium chloride salt was procured from a single batch in April 2024. Two types of sodium chloride absorbers were designed for these experiments: a set of 0.250 in-thick (0.635 cm) and a set of 0.1875 in-thick (0.47625 cm) active absorber region plates. The diameter of the salt containing cavity for both variations is 12 in. (30.48 cm). The base of the vessel, shown in Figure 10, includes the salt cavity, an interface surface for the lid, and a retaining lip for the lid. The lip has a nominal thickness of 0.23 in. (0.5842 cm) and height of 0.03 in. (0.0762 cm) with a nominal inner diameter of 14.77 in. (37.5158 cm). The base has a nominal outer diameter of 15 in. (38.1 cm). The lid, shown in Figure 11, has a nominal outer diameter of 14.625 in. (37.1475 cm) and a thickness of 0.100 in. (0.254 cm). The lid and base are held together with aluminum alloy 2024 (Al-2024) screws of specific dimensions present in Figure 12. The screw holes were match drilled for each of the sodium chloride absorbers, therefore the holes are not shown in following figures. Each of the sodium chloride absorbers has 16 screw holes located at a

diameter of 12.750 inches with equal spacing of 22.50 degrees.

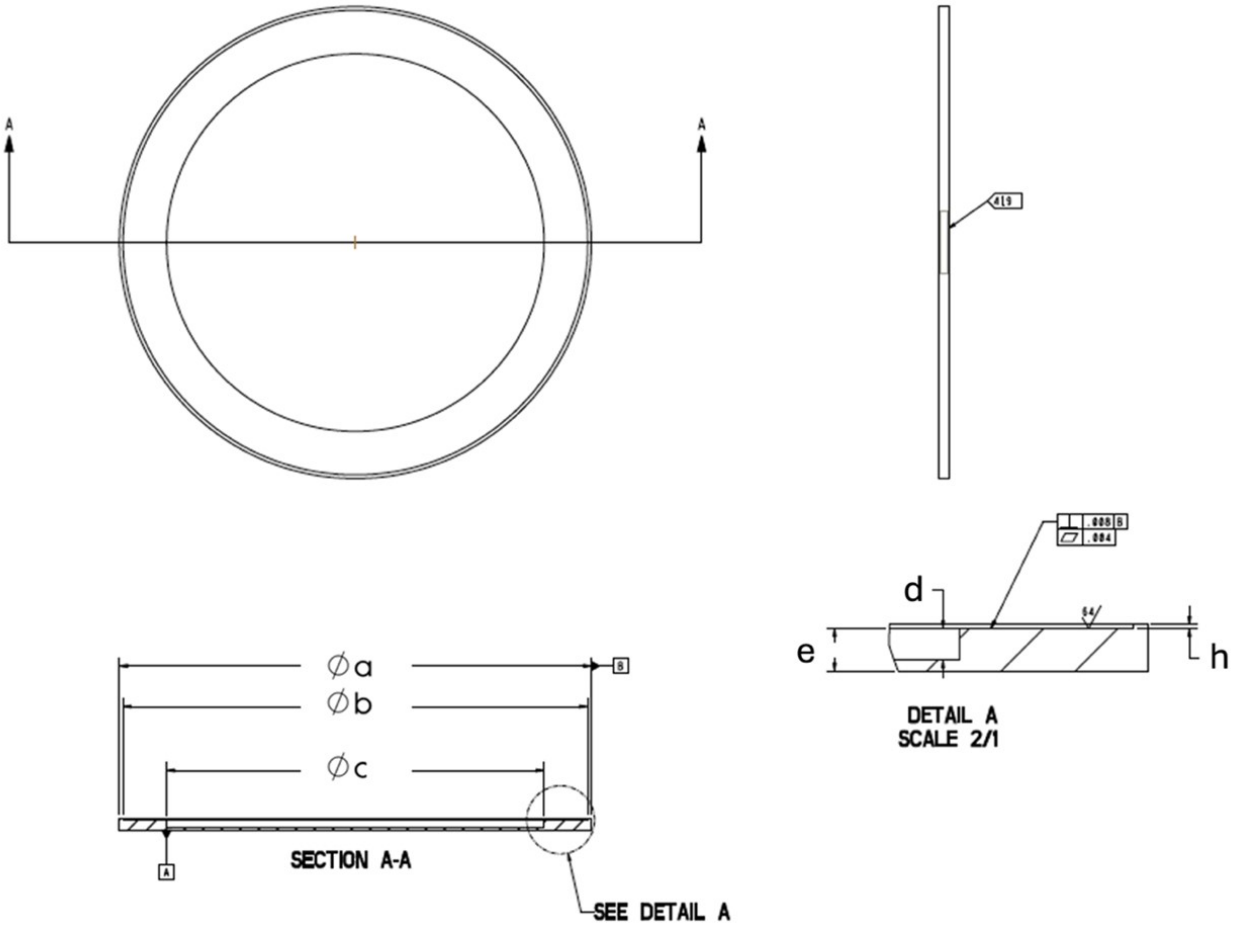

Figure 10: Drawing of the base of the sodium chloride absorber encapsulation. The labels for the dimensions correspond to the measurements reported in the tables in Sections 1.2.4.3 and 1.2.4.4.

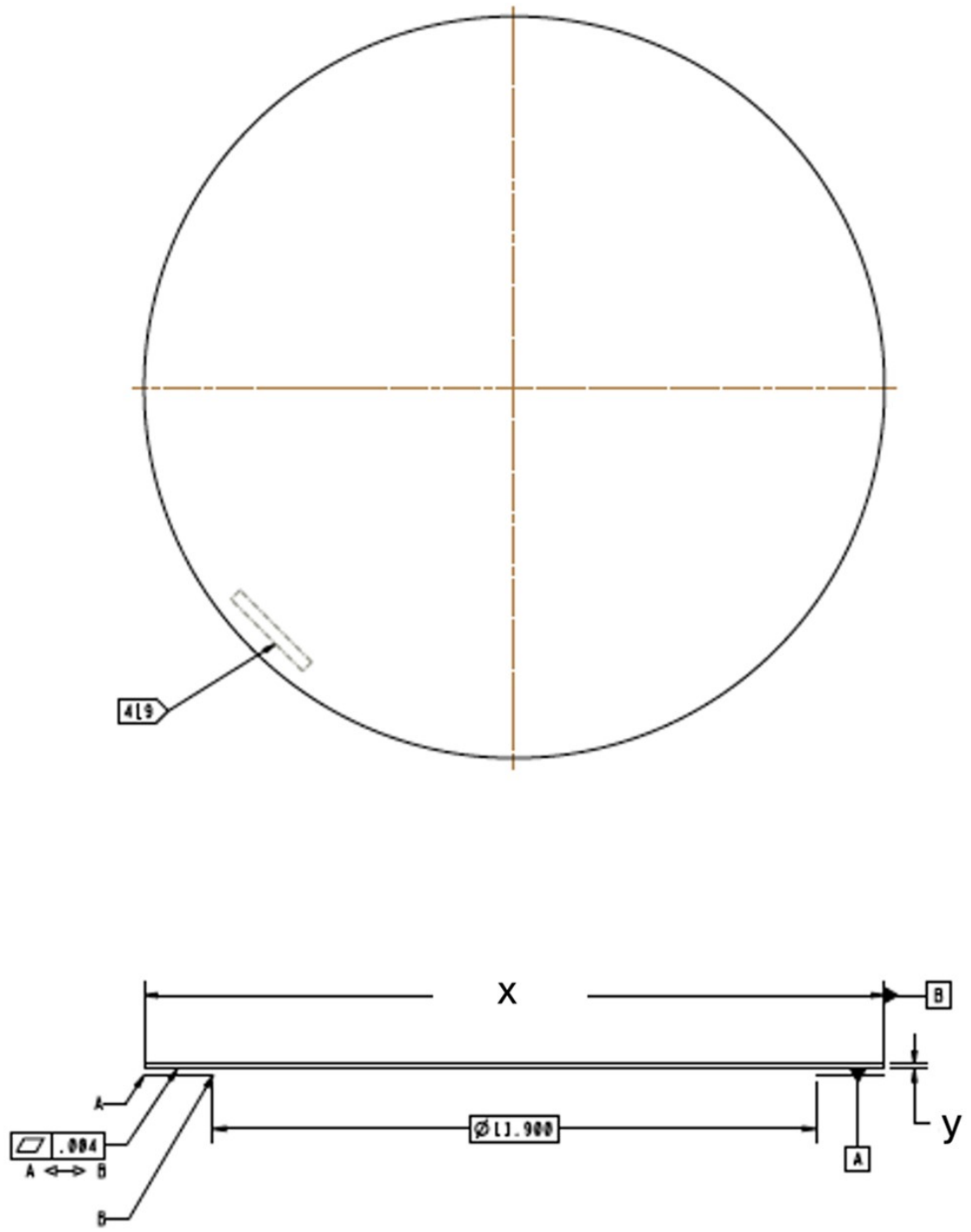

Figure 11: Drawing of the lid of the sodium chloride absorber encapsulation. The labels for the dimensions correspond to the measurements reported in the tables in Sections 1.2.4.3 and 1.2.4.4.

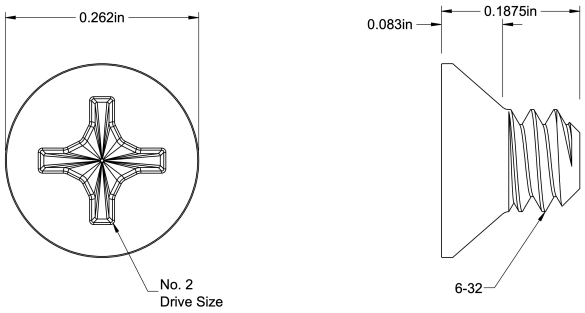

Figure 12: Drawing of the screws used for the sodium chloride absorber encapsulation.

The encapsulations were procured by LANL and shipped to LLNL for filling. The filling procedure is described in detail in Section 1.2.4.1. After filling the plates, they were shipped to the NNSS to prepare for experimental execution.

Acceptance measurements of the encapsulation plates were performed by LANL after receiving them from the manufacturer and before they were shipped to LLNL. Acceptance measurements were performed twice, once with a coordinate measuring machine (CMM) and once with traditional measurement techniques. The CMM has a measurement precision of 0.00635 cm. The traditional measurement techniques include the 0-6" digital caliper, 0-24" digital caliper, and 0-1" micrometer specified in Section 1.2.2.2.

Initial mass measurements of the encapsulation plate components, and assembled encapsulation plates, were also performed by LANL during acceptance. Acceptance mass measurements were performed with an Ohaus EX35001 Balance (Calibration Number: 348452) which has a total measurement uncertainty of 0.3 grams, including linearity, corner loading, and repeatability. Mass measurements were performed by LLNL immediately after filling was complete and before shipment to NNSS. The mass measurements at LLNL were performed with an Ohaus PX4202/E balance (Calibration Number: 19-E8S6X-20-1) which has a total measurement uncertainty of 0.1 grams, including linearity and sensitivity. Final mass measurements were performed by LANL immediately following the experimental execution at NCERC. The final measurements, which were taken at NCERC, were performed with a Mettler Toledo MS16001L balance (Calibration Number: 2024001052) which has a total measurement uncertainty of 0.3 grams, including linearity, shift, and repeatability.

1.2.4.1 Sodium Chloride Absorber Filling Procedure

The sodium chloride salt was procured in one order, from a single batch, in four separate containers. The procedure started by baking the sodium chloride salt in an oven overnight prior to filling ($>100^{\circ}$C), shown in Figure 13. This was done to drive off any accumulated moisture. While the salt is lowly hygroscopic, it is assumed that over a long period of time the salt would accumulate a measurable amount of moisture. A test subject (small vial), using the same salt, was filled well before the bulk of the plates were filled. This test subject was an experiment to test the water accumulation over time. The subject was weight at initial fill and periodically over the next six months using a scale with a precision of 0.1 grams. No increase of mass was measured over the period of the test.

Figure 13: A picture of the oven process to back the salt before filling.

As provided in 1.2.4.3 and 1.2.4.4, mass measurements were performed on the plates at initial fill, prior to shipment to the NNSS, and directly after the experiment. This was done to ensure that the method of baking the salt and the seal of the containers was sufficient to prevent the accumulation of moisture. There was no accumulation of moisture that was observed.

After the baking process, at the time of filling, a sample of the salt being filled into each of the plates was taken and sealed into a glass vial. These glass vials, described in more detail in Section 1.3.2, were samples to be sent off to a laboratory for impurity and moisture content testing. The details of the tests are also described in Section 1.3.2.

The sodium chloride absorbers were filled through a process of vibrational packing. A pneumatic vibration tool (serial number and type unknown) was used to pack the salt, shown in Figure 14. To ensure even packing of the plate, the sodium chloride absorbers were packed with the plate resting on the thin edge. A thick cover plate with a funnel at one edge (the top when standing on the thin edge of the plate) was added to the procedure after the first few fills to optimize the process. The packing was performed with the lid secured.

Figure 14: A picture of the vibrational packing. Note that this does not include the thick cover plate as described in the text.

The progress of filling was monitored by removing the lid and checking the amount of void, as shown in Figure 15. Salt was continually added until that void disappeared. The void would shrink to a point where it could no longer be filled via bulk additions or funnel, see Figure 16, and minor salt additions would be added until no void would appear when packing. During each fill step the mass of the entire plate assembly (to include the salt and the encapsulations) were measured with the balance described in Section 1.2.4 to accurately monitor the total amount of salt added to the plates. Eventually, no additional salt could be added as no void would appear when using the vibrational packer, this is shown in Figure 17.

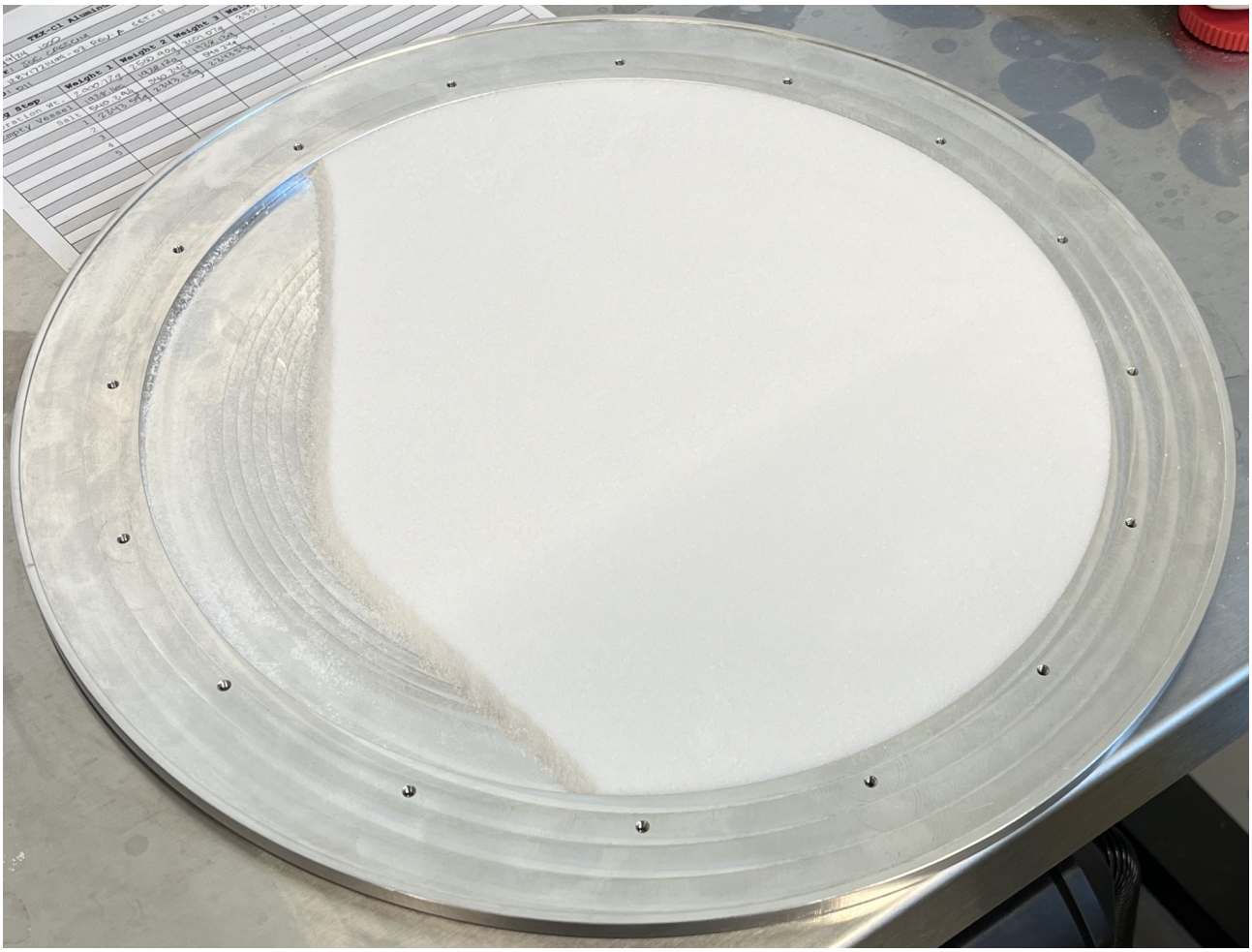

Figure 15: A picture showing an example of what a void looks like as to monitor the progress of filling.

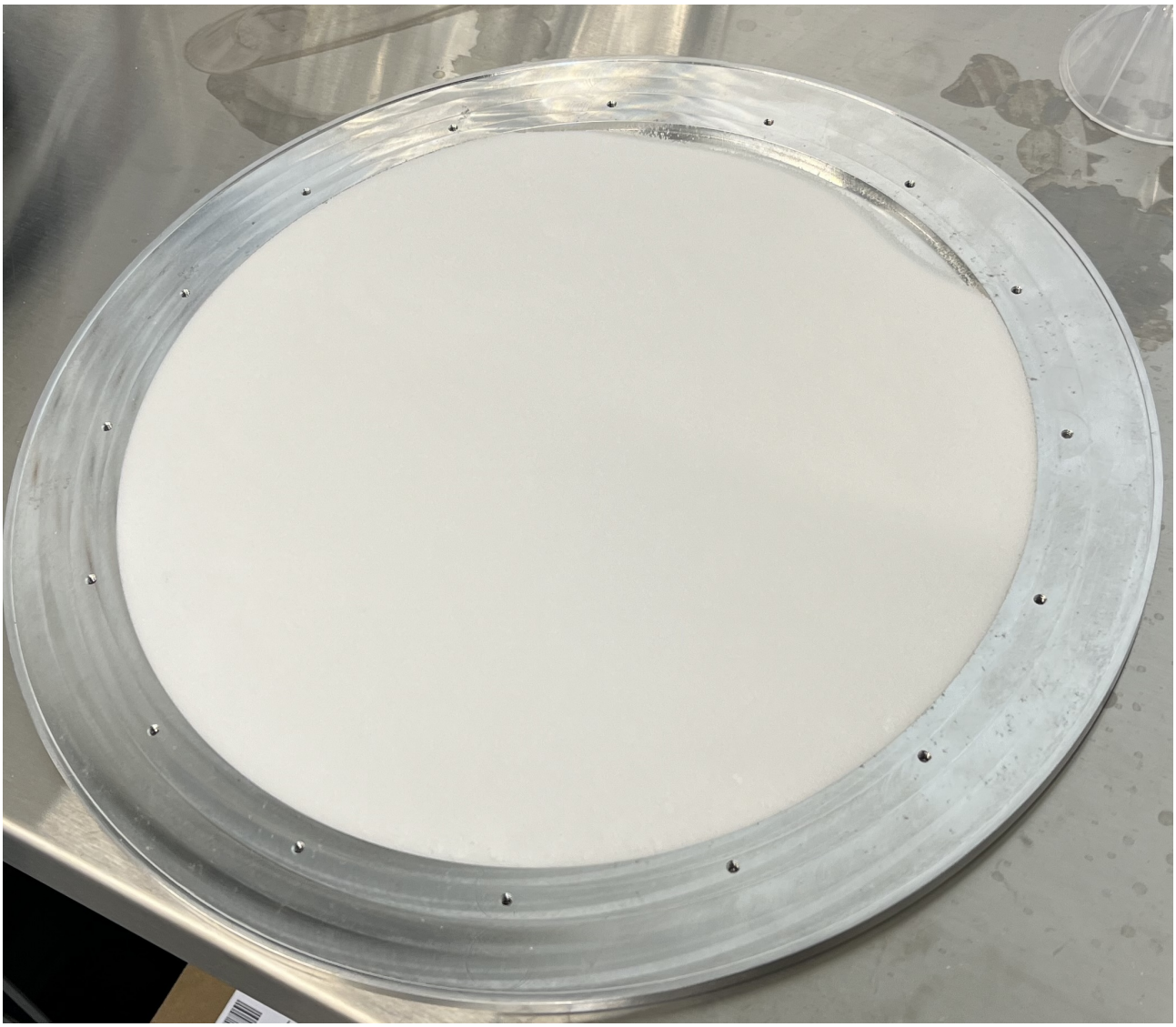

Figure 16: A picture showing an example of what a void looks like just before the final filling steps.

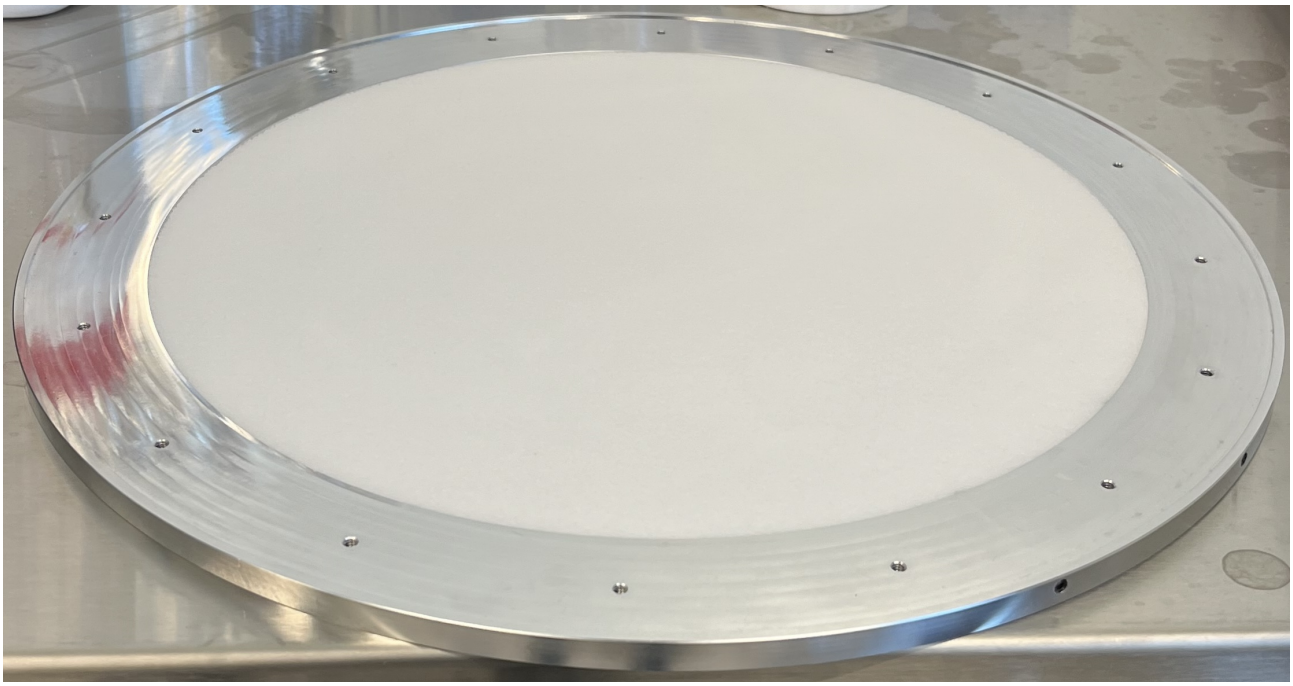

Figure 17: A picture showing an example of what the sodium chloride absorbers look like once fully filled.

1.2.4.2 Sodium Chloride Absorber Packing Fraction

The particle size of the salt was nonhomogeneous, meaning that the particle size was variable and had no known uniformity. As such, the maximum expected packing fraction for a random distribution of particle sizes is 70% [2]. The achieved packing fraction for all sodium chloride absorbers was between 65% and 70%, depending on the plate thickness. More information about the densities can be found in Section 1.3.2.

1.2.4.3 3/16" Sodium Chloride Absorbers

Twenty-three 0.1875-inch (0.47625 cm; labeled 3/16") sodium chloride absorbers were procured for this experiment. Upon receipt from the manufacturer, LANL performed acceptance mass measurements, which are reported in the following tables: Table 7 and Table 8, CMM dimensional measurements, Tables 9, 10, 11, 12, and traditional dimensional measurements, Tables 13, 14, and 15. Mass measurements were performed during the plate filling process, which are reported in the following tables: Table 16, prior to shipment from LLNL to NCERC, Table 17, and after experimental execution, Table 18. The derived volumes and densities are presented in Table 19, Table 20, and Table 21.

Table 7: Sodium chloride absorber component weights via acceptance measurements performed by LANL.

Part ID	Mass (g)			
	Base	Lid	Assembled (No Salt)	Screws (Difference)
SaltPlate3/16-1	1197.9	721.4	1920.9	1.60
SaltPlate3/16-2	1209.0	721.3	1932.3	2.00
SaltPlate3/16-3	1218.1	720.0	1940.5	2.40
SaltPlate3/16-4	1207.8	721.6	1931.7	2.30
SaltPlate3/16-5	1205.5	721.0	1928.8	2.30
SaltPlate3/16-6	1210.5	720.2	1932.3	1.60
SaltPlate3/16-7	1213.0	719.8	1935.1	2.30
SaltPlate3/16-8	1209.5	722.5	1934.2	2.20
SaltPlate3/16-9	1201.6	720.7	1924.4	2.10
SaltPlate3/16-10	1204.0	720.9	1926.8	1.90
SaltPlate3/16-11	1215.0	720.3	1937.5	2.20
SaltPlate3/16-12	1218.0	720.9	1941.1	2.20
SaltPlate3/16-13	1211.8	721.5	1935.5	2.20
SaltPlate3/16-14	1204.3	720.1	1926.7	2.30
SaltPlate3/16-15	1211.6	718.3	1932.1	2.20
SaltPlate3/16-16	1210.9	719.9	1932.9	2.10
SaltPlate3/16-17	1197.2	719.3	1918.7	2.20
SaltPlate3/16-18	1214.6	722.6	1939.6	2.40
SaltPlate3/16-19	1203.5	718.9	1924.6	2.20
SaltPlate3/16-20	1207.1	718.9	1928.2	2.20
SaltPlate3/16-21	1209.6	719.5	1931.3	2.20
SaltPlate3/16-22	1206.3	720.8	1929.3	2.20
SaltPlate3/16-23	1211.9	720.7	1934.6	2.00

Table 8: Sodium chloride absorber assembled unfilled weights via acceptance measurements performed by LANL.

Part ID	Mass of Empty Vessel (g)			
	Measurement 1	Measurement 2	Measurement 3	Average$\pm 1\sigma$[(a)]
SaltPlate3/16-1	1922.1	1922.1	1922.1	1922.1 ± 0.0
SaltPlate3/16-2	1933.1	1933.1	1933.1	1933.1 ± 0.0
SaltPlate3/16-3	1941.2	1941.2	1941.1	1941.1 ± 0.0
SaltPlate3/16-4	1932.1	1932.1	1932.1	1932.1 ± 0.0
SaltPlate3/16-5	1929.3	1929.3	1929.3	1929.3 ± 0.0
SaltPlate3/16-6	1933.6	1933.6	1933.6	1933.6 ± 0.0
SaltPlate3/16-7	1935.6	1935.6	1935.6	1935.6 ± 0.0
SaltPlate3/16-8	1934.8	1934.8	1934.8	1934.8 ± 0.0
SaltPlate3/16-9	1924.9	1924.9	1924.9	1924.9 ± 0.0
SaltPlate3/16-10	1927.3	1927.3	1927.3	1927.3 ± 0.0
SaltPlate3/16-11	1938.2	1938.1	1938.1	1938.1 ± 0.0
SaltPlate3/16-12	1941.6	1941.6	1941.6	1941.6 ± 0.0
SaltPlate3/16-13	1935.9	1936.0	1935.9	1935.9 ± 0.0
SaltPlate3/16-14	1927.2	1927.2	1927.2	1927.2 ± 0.0
SaltPlate3/16-15	1932.6	1932.6	1932.7	1932.6 ± 0.0
SaltPlate3/16-16	1933.5	1933.5	1933.5	1933.5 ± 0.0
SaltPlate3/16-17	1919.3	1919.2	1919.3	1919.3 ± 0.0
SaltPlate3/16-18	1940.1	1940.1	1940.1	1940.1 ± 0.0
SaltPlate3/16-19	1925.1	1925.1	1925.1	1925.1 ± 0.0
SaltPlate3/16-20	1928.1	1928.1	1928.1	1928.1 ± 0.0
SaltPlate3/16-21	1931.9	1931.9	1931.9	1931.9 ± 0.0
SaltPlate3/16-22	1929.9	1929.9	1929.9	1929.9 ± 0.0
SaltPlate3/16-23	1935.1	1935.1	1935.1	1935.1 ± 0.0

[(a)] The standard deviation of the measurements are zero, but still shown for completeness.

Table 9: Sodium chloride absorber encapsulation base acceptance measurements via CMM measurements performed by LANL (see Figure 10).

Part ID	Inner Diameter, c [in (cm)]	Outer Diameter, a [in (cm)]	Bottom Thickness, e-d [in (cm)]
SaltPlate3/16-1	12.001 (30.4825)	14.999 (38.0975)	0.096 (0.2438)
SaltPlate3/16-2	12.000 (30.4800)	14.996 (38.0898)	0.095 (0.2413)
SaltPlate3/16-3	11.999 (30.4775)	14.996 (38.0898)	0.100 (0.2540)
SaltPlate3/16-4	11.998 (30.4749)	14.996 (38.0898)	0.101 (0.2565)
SaltPlate3/16-5	11.999 (30.4775)	14.996 (38.0898)	0.094 (0.2388)
SaltPlate3/16-6	11.999 (30.4775)	14.997 (38.0924)	0.100 (0.2540)
SaltPlate3/16-7	12.000 (30.4800)	14.997 (38.0924)	0.092 (0.2337)
SaltPlate3/16-8	12.000 (30.4800)	14.997 (38.0924)	0.098 (0.2489)
SaltPlate3/16-9	12.000 (30.4800)	14.997 (38.0924)	0.094 (0.2388)
SaltPlate3/16-10	12.000 (30.4800)	14.996 (38.0898)	0.097 (0.2464)
SaltPlate3/16-11	11.999 (30.4775)	14.996 (38.0898)	0.094 (0.2388)
SaltPlate3/16-12	11.998 (30.4749)	14.999 (38.0975)	0.099 (0.2515)
SaltPlate3/16-13	12.000 (30.4800)	14.997 (38.0924)	0.098 (0.2489)
SaltPlate3/16-14	12.002 (30.4851)	14.997 (38.0924)	0.091 (0.2311)
SaltPlate3/16-15	12.000 (30.4800)	14.996 (38.0898)	0.098 (0.2489)
SaltPlate3/16-16	12.000 (30.4800)	14.997 (38.0924)	0.093 (0.2362)
SaltPlate3/16-17	11.999 (30.4775)	14.996 (38.0898)	0.095 (0.2413)
SaltPlate3/16-18	12.000 (30.4800)	14.995 (38.0873)	0.097 (0.2464)
SaltPlate3/16-19	11.999 (30.4775)	14.996 (38.0898)	0.093 (0.2362)
SaltPlate3/16-20	11.999 (30.4775)	14.995 (38.0873)	0.093 (0.2362)
SaltPlate3/16-21	11.999 (30.4775)	14.996 (38.0898)	0.095 (0.2413)
SaltPlate3/16-22	12.000 (30.4800)	14.996 (38.0898)	0.096 (0.2438)
SaltPlate3/16-23	12.000 (30.4800)	14.996 (38.0898)	0.097 (0.2464)

Table 10: Sodium chloride absorber encapsulation base acceptance measurements via CMM measurements performed by LANL (see Figure 10).

Part ID	**Pocket Depth, d [in (cm)]**			
	Measurement 1	**Measurement 2**	**Measurement 3**	**Average$\pm 1\sigma$**
SaltPlate3/16-1	0.187 (0.4750)	0.185 (0.4699)	0.183 (0.4648)	0.185±0.002 (0.4699±0.0051)
SaltPlate3/16-2	0.187 (0.4750)	0.188 (0.4775)	0.184 (0.4674)	0.186±0.002 (0.4733±0.0053)
SaltPlate3/16-3	0.186 (0.4724)	0.185 (0.4699)	0.186 (0.4724)	0.186±0.001 (0.4716±0.0015)
SaltPlate3/16-4	0.187 (0.4750)	0.187 (0.4750)	0.184 (0.4674)	0.186±0.002 (0.4724±0.0044)
SaltPlate3/16-5	0.185 (0.4699)	0.185 (0.4699)	0.187 (0.4750)	0.186±0.001 (0.4716±0.0029)
SaltPlate3/16-6	0.186 (0.4724)	0.185 (0.4699)	0.185 (0.4699)	0.185±0.001 (0.4707±0.0015)
SaltPlate3/16-7	0.186 (0.4724)	0.187 (0.4750)	0.186 (0.4724)	0.186±0.001 (0.4733±0.0015)
SaltPlate3/16-8	0.187 (0.4750)	0.187 (0.4750)	0.187 (0.4750)	0.187±0.000 (0.4750±0.0000)
SaltPlate3/16-9	0.187 (0.4750)	0.185 (0.4699)	0.187 (0.4750)	0.186±0.001 (0.4733±0.0029)
SaltPlate3/16-10	0.187 (0.4750)	0.188 (0.4775)	0.186 (0.4724)	0.187±0.001 (0.4750±0.0025)
SaltPlate3/16-11	0.185 (0.4699)	0.185 (0.4699)	0.189 (0.4801)	0.186±0.002 (0.4733±0.0059)
SaltPlate3/16-12	0.186 (0.4724)	0.185 (0.4699)	0.187 (0.4750)	0.186±0.001 (0.4724±0.0025)
SaltPlate3/16-13	0.187 (0.4750)	0.187 (0.4750)	0.189 (0.4801)	0.188±0.001 (0.4767±0.0029)
SaltPlate3/16-14	0.187 (0.4750)	0.187 (0.4750)	0.186 (0.4724)	0.187±0.001 (0.4741±0.0015)
SaltPlate3/16-15	0.187 (0.4750)	0.186 (0.4724)	0.186 (0.4724)	0.186±0.001 (0.4733±0.0015)
SaltPlate3/16-16	0.188 (0.4775)	0.185 (0.4699)	0.187 (0.4750)	0.187±0.002 (0.4741±0.0039)
SaltPlate3/16-17	0.185 (0.4699)	0.188 (0.4775)	0.187 (0.4750)	0.187±0.002 (0.4741±0.0039)
SaltPlate3/16-18	0.187 (0.4750)	0.185 (0.4699)	0.185 (0.4699)	0.186±0.001 (0.4716±0.0029)
SaltPlate3/16-19	0.184 (0.4674)	0.185 (0.4699)	0.181 (0.4597)	0.183±0.002 (0.4657±0.0053)

Table 10 Continued.

Part ID	Pocket Depth, d [in (cm)]			
	Measurement 1	**Measurement 2**	**Measurement 3**	**Average$\pm 1\sigma$**
SaltPlate3/16-20	0.186 (0.4724)	0.187 (0.4750)	0.186 (0.4724)	0.186$\pm$0.001 (0.4733$\pm$0.0015)
SaltPlate3/16-21	0.186 (0.4724)	0.187 (0.4750)	0.186 (0.4724)	0.186$\pm$0.001 (0.4733$\pm$0.0015)
SaltPlate3/16-22	0.187 (0.4750)	0.190 (0.4826)	0.186 (0.4724)	0.188$\pm$0.002 (0.4767$\pm$0.0053)
SaltPlate3/16-23	0.188 (0.4775)	0.187 (0.4750)	0.185 (0.4699)	0.187$\pm$0.002 (0.4741$\pm$0.0039)

Table 11: Sodium chloride absorber encapsulation lid acceptance measurements via CMM measurements performed by LANL (see Figure 11).

Part ID	**Diameter, x [in (cm)]**	**Thickness, y [in (cm)]**			
		Measurement 1	**Measurement 2**	**Measurement 3**	**Average**$\pm 1\sigma$
SaltPlate3/16-1	14.649 (37.2085)	0.099 (0.2515)	0.099 (0.2515)	0.098 (0.2489)	0.099±0.001 (0.2506±0.0015)
SaltPlate3/16-2	14.647 (37.2034)	0.098 (0.2489)	0.101 (0.2565)	0.098 (0.2489)	0.099±0.002 (0.2515±0.0044)
SaltPlate3/16-3	14.650 (37.2110)	0.099 (0.2515)	0.099 (0.2515)	0.098 (0.2489)	0.099±0.001 (0.2506±0.0015)
SaltPlate3/16-4	14.649 (37.2085)	0.098 (0.2489)	0.098 (0.2489)	0.098 (0.2489)	0.098±0.000 (0.2489±0.0000)
SaltPlate3/16-5	14.650 (37.2110)	0.098 (0.2489)	0.098 (0.2489)	0.099 (0.2515)	0.098±0.001 (0.2498±0.0015)
SaltPlate3/16-6	14.648 (37.2059)	0.099 (0.2515)	0.098 (0.2489)	0.098 (0.2489)	0.098±0.001 (0.2498±0.0015)
SaltPlate3/16-7	14.650 (37.2110)	0.098 (0.2489)	0.098 (0.2489)	0.099 (0.2515)	0.098±0.001 (0.2498±0.0015)
SaltPlate3/16-8	14.649 (37.2085)	0.098 (0.2489)	0.099 (0.2515)	0.098 (0.2489)	0.098±0.001 (0.2498±0.0015)
SaltPlate3/16-9	14.644 (37.1958)	0.098 (0.2489)	0.098 (0.2489)	0.098 (0.2489)	0.098±0.000 (0.2489±0.0000)
SaltPlate3/16-10	14.646 (37.2008)	0.098 (0.2489)	0.098 (0.2489)	0.098 (0.2489)	0.098±0.000 (0.2489±0.0000)
SaltPlate3/16-11	14.643 (37.1932)	0.098 (0.2489)	0.098 (0.2489)	0.098 (0.2489)	0.098±0.000 (0.2489±0.0000)
SaltPlate3/16-12	14.643 (37.1932)	0.098 (0.2489)	0.099 (0.2515)	0.098 (0.2489)	0.098±0.001 (0.2498±0.0015)
SaltPlate3/16-13	14.646 (37.2008)	0.099 (0.2515)	0.098 (0.2489)	0.098 (0.2489)	0.098±0.001 (0.2498±0.0015)
SaltPlate3/16-14	14.647 (37.2034)	0.098 (0.2489)	0.098 (0.2489)	0.098 (0.2489)	0.098±0.000 (0.2489±0.0000)
SaltPlate3/16-15	14.650 (37.2110)	0.099 (0.2515)	0.098 (0.2489)	0.098 (0.2489)	0.098±0.001 (0.2498±0.0015)
SaltPlate3/16-16	14.650 (37.2110)	0.098 (0.2489)	0.098 (0.2489)	0.097 (0.2464)	0.098±0.001 (0.2481±0.0015)
SaltPlate3/16-17	14.648 (37.2059)	0.099 (0.2515)	0.098 (0.2489)	0.098 (0.2489)	0.098±0.001 (0.2498±0.0015)
SaltPlate3/16-18	14.646 (37.2008)	0.099 (0.2515)	0.101 (0.2565)	0.098 (0.2489)	0.099±0.002 (0.2523±0.0039)
SaltPlate3/16-19	14.648 (37.2059)	0.098 (0.2489)	0.097 (0.2464)	0.098 (0.2489)	0.098±0.001 (0.2481±0.0015)

Table 11 Continued.

Part ID	Diameter, x [in (cm)]	Thickness, y [in (cm)]			
		Measurement 1	Measurement 2	Measurement 3	Average$\pm 1\sigma$
SaltPlate3/16-20	14.650 (37.2110)	0.098 (0.2489)	0.097 (0.2464)	0.098 (0.2489)	0.098$\pm$0.001 (0.2481$\pm$0.0015)
SaltPlate3/16-21	14.649 (37.2085)	0.098 (0.2489)	0.098 (0.2489)	0.098 (0.2489)	0.098$\pm$0.000 (0.2489$\pm$0.0000)
SaltPlate3/16-22	14.645 (37.1983)	0.098 (0.2489)	0.098 (0.2489)	0.098 (0.2489)	0.098$\pm$0.000 (0.2489$\pm$0.0000)
SaltPlate3/16-23	14.645 (37.1983)	0.098 (0.2489)	0.097 (0.2464)	0.098 (0.2489)	0.098$\pm$0.001 (0.2481$\pm$0.0015)

Table 12: Sodium chloride absorber encapsulation assembled thickness via CMM measurements performed by LANL.

Part ID	Assembled Thickness [in (cm)]			
	Measurement 1	Measurement 2	Measurement 3	Average$\pm 1\sigma$
SaltPlate3/16-1	0.386 (0.980)	0.372 (0.9449)	0.380 (0.9652)	0.379±0.007 (0.9635±0.0178)
SaltPlate3/16-2	0.384 (0.975)	0.375 (0.9525)	0.380 (0.9652)	0.380±0.005 (0.9644±0.0115)
SaltPlate3/16-3	0.374 (0.950)	0.390 (0.9906)	0.384 (0.9754)	0.383±0.008 (0.9720±0.0205)
SaltPlate3/16-4	0.374 (0.950)	0.380 (0.9652)	0.382 (0.9703)	0.379±0.004 (0.9618±0.0106)
SaltPlate3/16-5	0.384 (0.975)	0.373 (0.9474)	0.380 (0.9652)	0.379±0.006 (0.9627±0.0141)
SaltPlate3/16-6	0.375 (0.953)	0.387 (0.9830)	0.382 (0.9703)	0.381±0.006 (0.9686±0.0153)
SaltPlate3/16-7	0.387 (0.983)	0.375 (0.9525)	0.377 (0.9576)	0.380±0.006 (0.9644±0.0163)
SaltPlate3/16-8	0.379 (0.963)	0.399 (1.0135)	0.382 (0.9703)	0.387±0.011 (0.9821±0.0274)
SaltPlate3/16-9	0.389 (0.988)	0.373 (0.9474)	0.385 (0.9779)	0.382±0.008 (0.9711±0.0211)
SaltPlate3/16-10	0.373 (0.947)	0.389 (0.9881)	0.379 (0.9627)	0.380±0.008 (0.9660±0.0205)
SaltPlate3/16-11	0.389 (0.988)	0.373 (0.9474)	0.382 (0.9703)	0.381±0.008 (0.9686±0.0204)
SaltPlate3/16-12	0.374 (0.950)	0.382 (0.9703)	0.384 (0.9754)	0.380±0.005 (0.9652±0.0134)
SaltPlate3/16-13	0.400 (1.016)	0.377 (0.9576)	0.393 (0.9982)	0.390±0.012 (0.9906±0.0299)
SaltPlate3/16-14	0.371 (0.942)	0.385 (0.9779)	0.374 (0.9500)	0.377±0.007 (0.9567±0.0187)
SaltPlate3/16-15	0.388 (0.986)	0.377 (0.9576)	0.396 (1.0058)	0.387±0.010 (0.9830±0.0242)
SaltPlate3/16-16	0.390 (0.991)	0.374 (0.9500)	0.382 (0.9703)	0.382±0.008 (0.9703±0.0203)
SaltPlate3/16-17	0.382 (0.970)	0.391 (0.9931)	0.372 (0.9449)	0.382±0.010 (0.9694±0.0241)
SaltPlate3/16-18	0.395 (1.003)	0.377 (0.9576)	0.376 (0.9550)	0.383±0.011 (0.9720±0.0272)
SaltPlate3/16-19	0.378 (0.960)	0.372 (0.9449)	0.397 (1.0084)	0.382±0.013 (0.9711±0.0332)

Table 12 Continued.

Part ID	Assembled Thickness [in (cm)]			
	Measurement 1	**Measurement 2**	**Measurement 3**	**Average**$\pm 1\sigma$
SaltPlate3/16-20	0.389 (0.988)	0.386 (0.9804)	0.372 (0.9449)	0.382$\pm$0.009 (0.9711$\pm$0.0230)
SaltPlate3/16-21	0.380 (0.965)	0.379 (0.9627)	0.384 (0.9754)	0.381$\pm$0.003 (0.9677$\pm$0.0067)
SaltPlate3/16-22	0.381 (0.968)	0.397 (1.0084)	0.373 (0.9474)	0.384$\pm$0.012 (0.9745$\pm$0.0310)
SaltPlate3/16-23	0.384 (0.975)	0.382 (0.9703)	0.392 (0.9957)	0.386$\pm$0.005 (0.9804$\pm$0.0134)

Table 13: Sodium chloride absorber encapsulation base lip inner diameter acceptance measurements via hand tool measurements performed by LANL (see Figure 10).

Part ID	**Lip Inner Diameter, b [in (cm)]**			
	Measurement 1	**Measurement 2**	**Measurement 3**	**Average**$\pm 1\sigma$
SaltPlate3/16-1	14.768 (37.511)	14.766 (37.504)	14.768 (37.511)	14.767±0.001 (37.5086±0.0037)
SaltPlate3/16-2	14.765 (37.502)	14.765 (37.502)	14.767 (37.507)	14.765±0.001 (37.5035±0.0029)
SaltPlate3/16-3	14.768 (37.509)	14.768 (37.509)	14.769 (37.513)	14.768±0.001 (37.5107±0.0022)
SaltPlate3/16-4	14.765 (37.503)	14.771 (37.517)	14.768 (37.511)	14.768±0.003 (37.5103±0.0070)
SaltPlate3/16-5	14.765 (37.503)	14.767 (37.507)	14.765 (37.503)	14.766±0.001 (37.5044±0.0022)
SaltPlate3/16-6	14.766 (37.504)	14.772 (37.521)	14.766 (37.504)	14.768±0.004 (37.5099±0.0095)
SaltPlate3/16-7	14.766 (37.504)	14.766 (37.506)	14.769 (37.512)	14.767±0.002 (37.5073±0.0041)
SaltPlate3/16-8	14.763 (37.497)	14.771 (37.517)	14.764 (37.499)	14.766±0.004 (37.5044±0.0111)
SaltPlate3/16-9	14.766 (37.506)	14.771 (37.517)	14.770 (37.515)	14.769±0.002 (37.5124±0.0060)
SaltPlate3/16-10	14.767 (37.508)	14.768 (37.511)	14.766 (37.506)	14.767±0.001 (37.5082±0.0025)
SaltPlate3/16-11	14.767 (37.508)	14.765 (37.503)	14.770 (37.515)	14.767±0.002 (37.5086±0.0057)
SaltPlate3/16-12	14.770 (37.515)	14.766 (37.504)	14.772 (37.520)	14.769±0.003 (37.5128±0.0078)
SaltPlate3/16-13	14.769 (37.512)	14.772 (37.520)	14.753 (37.473)	14.764±0.010 (37.5014±0.0252)
SaltPlate3/16-14	14.719 (37.385)	14.744 (37.448)	14.755 (37.476)	14.739±0.018 (37.4366±0.0469)
SaltPlate3/16-15	14.771 (37.517)	14.769 (37.512)	14.771 (37.518)	14.770±0.001 (37.5158±0.0034)
SaltPlate3/16-16	14.769 (37.513)	14.769 (37.513)	14.768 (37.509)	14.769±0.001 (37.5120±0.0022)
SaltPlate3/16-17	14.771 (37.517)	14.767 (37.507)	14.769 (37.513)	14.769±0.002 (37.5124±0.0051)
SaltPlate3/16-18	14.774 (37.525)	14.766 (37.506)	14.771 (37.517)	14.770±0.004 (37.5158±0.0096)
SaltPlate3/16-19	14.770 (37.515)	14.767 (37.508)	14.768 (37.511)	14.768±0.001 (37.5111±0.0032)

Table 13 Continued.

Part ID	Lip Inner Diameter, b [in (cm)]			
	Measurement 1	**Measurement 2**	**Measurement 3**	**Average$\pm 1\sigma$**
SaltPlate3/16-20	14.763 (37.498)	14.766 (37.506)	14.770 (37.516)	14.766$\pm$0.004 (37.5065$\pm$0.0089)
SaltPlate3/16-21	14.766 (37.504)	14.771 (37.517)	14.769 (37.512)	14.768$\pm$0.003 (37.5111$\pm$0.0064)
SaltPlate3/16-22	14.770 (37.516)	14.766 (37.504)	14.770 (37.516)	14.769$\pm$0.003 (37.5120$\pm$0.0066)
SaltPlate3/16-23	14.764 (37.499)	14.770 (37.515)	14.763 (37.498)	14.765$\pm$0.004 (37.5039$\pm$0.0092)

Table 14: Sodium chloride absorber encapsulation lid acceptance measurements via hand tool measurements performed by LANL (see Figure 11).

Part ID	**Diameter, x [in (cm)]**			
	Measurement 1	**Measurement 2**	**Measurement 3**	**Average$\pm 1\sigma$**
SaltPlate3/16-1	14.647 (37.2021)	14.651 (37.2123)	14.641 (37.1876)	14.646±0.005 (37.2007±0.0124)
SaltPlate3/16-2	14.645 (37.1970)	14.648 (37.2047)	14.647 (37.2034)	14.646±0.002 (37.2017±0.0041)
SaltPlate3/16-3	14.654 (37.2212)	14.649 (37.2072)	14.654 (37.2212)	14.652±0.003 (37.2165±0.0081)
SaltPlate3/16-4	14.650 (37.2110)	14.654 (37.2199)	14.647 (37.2021)	14.650±0.003 (37.2110±0.0089)
SaltPlate3/16-5	14.650 (37.2110)	14.655 (37.2237)	14.648 (37.2059)	14.651±0.004 (37.2135±0.0092)
SaltPlate3/16-6	14.647 (37.2034)	14.654 (37.2212)	14.651 (37.2123)	14.651±0.003 (37.2123±0.0089)
SaltPlate3/16-7	14.648 (37.2059)	14.649 (37.2085)	14.651 (37.2123)	14.649±0.001 (37.2089±0.0032)
SaltPlate3/16-8	14.648 (37.2059)	14.650 (37.2110)	14.648 (37.2059)	14.649±0.001 (37.2076±0.0029)
SaltPlate3/16-9	14.646 (37.1996)	14.641 (37.1881)	14.644 (37.1958)	14.644±0.002 (37.1945±0.0058)
SaltPlate3/16-10	14.650 (37.2097)	14.645 (37.1983)	14.649 (37.2085)	14.648±0.002 (37.2055±0.0063)
SaltPlate3/16-11	14.767 (37.5069)	14.644 (37.1958)	14.648 (37.2047)	14.686±0.070 (37.3024±0.1771)
SaltPlate3/16-12	14.640 (37.1843)	14.648 (37.2059)	14.640 (37.1856)	14.643±0.005 (37.1920±0.0121)
SaltPlate3/16-13	14.646 (37.1996)	14.653 (37.2174)	14.645 (37.1983)	14.648±0.004 (37.2051±0.0107)
SaltPlate3/16-14	14.650 (37.2097)	14.648 (37.2059)	14.646 (37.1996)	14.648±0.002 (37.2051±0.0051)
SaltPlate3/16-15	14.651 (37.2135)	14.651 (37.2135)	14.649 (37.2085)	14.650±0.001 (37.2118±0.0029)
SaltPlate3/16-16	14.652 (37.2148)	14.650 (37.2097)	14.651 (37.2123)	14.651±0.001 (37.2123±0.0025)
SaltPlate3/16-17	14.653 (37.2174)	14.649 (37.2085)	14.649 (37.2072)	14.650±0.002 (37.2110±0.0055)
SaltPlate3/16-18	14.649 (37.2072)	14.645 (37.1983)	14.646 (37.1996)	14.646±0.002 (37.2017±0.0048)
SaltPlate3/16-19	14.653 (37.2186)	14.648 (37.2059)	14.652 (37.2161)	14.651±0.003 (37.2135±0.0067)

Table 14 Continued.

Part ID	Diameter, x [in (cm)]			
	Measurement 1	**Measurement 2**	**Measurement 3**	**Average$\pm 1\sigma$**
SaltPlate3/16-20	14.645 (37.1983)	14.650 (37.2097)	14.653 (37.2186)	14.649$\pm$0.004 (37.2089$\pm$0.0102)
SaltPlate3/16-21	14.654 (37.2212)	14.648 (37.2059)	14.654 (37.2199)	14.652$\pm$0.003 (37.2157$\pm$0.0085)
SaltPlate3/16-22	14.648 (37.2059)	14.643 (37.1920)	14.647 (37.2021)	14.646$\pm$0.003 (37.2000$\pm$0.0072)
SaltPlate3/16-23	14.646 (37.2008)	14.647 (37.2021)	14.650 (37.2110)	14.648$\pm$0.002 (37.2047$\pm$0.0055)

Table 15: Sodium chloride absorber encapsulation assembled thickness via hand tool measurements performed by LANL.

Part ID	Assembled Thickness [in (cm)]			
	Measurement 1	Measurement 2	Measurement 3	Average$\pm 1\sigma$
SaltPlate3/16-1	0.369 (0.9373)	0.372 (0.9449)	0.371 (0.9423)	0.371±0.002 (0.9415±0.0039)
SaltPlate3/16-2	0.371 (0.9423)	0.371 (0.9423)	0.373 (0.9474)	0.372±0.001 (0.9440±0.0029)
SaltPlate3/16-3	0.372 (0.9449)	0.370 (0.9398)	0.374 (0.9500)	0.372±0.002 (0.9449±0.0051)
SaltPlate3/16-4	0.371 (0.9423)	0.371 (0.9423)	0.371 (0.9423)	0.371±0.000 (0.9423±0.0000)
SaltPlate3/16-5	0.370 (0.9398)	0.370 (0.9398)	0.374 (0.9500)	0.371±0.002 (0.9432±0.0059)
SaltPlate3/16-6	0.372 (0.9449)	0.372 (0.9449)	0.373 (0.9474)	0.372±0.001 (0.9457±0.0015)
SaltPlate3/16-7	0.371 (0.9423)	0.373 (0.9474)	0.369 (0.9373)	0.371±0.002 (0.9423±0.0051)
SaltPlate3/16-8	0.373 (0.9474)	0.371 (0.9423)	0.372 (0.9449)	0.372±0.001 (0.9449±0.0025)
SaltPlate3/16-9	0.373 (0.9474)	0.370 (0.9398)	0.372 (0.9449)	0.372±0.002 (0.9440±0.0039)
SaltPlate3/16-10	0.373 (0.9474)	0.369 (0.9373)	0.373 (0.9474)	0.372±0.002 (0.9440±0.0059)
SaltPlate3/16-11	0.375 (0.9525)	0.371 (0.9423)	0.373 (0.9474)	0.373±0.002 (0.9474±0.0051)
SaltPlate3/16-12	0.373 (0.9474)	0.371 (0.9423)	0.374 (0.9500)	0.373±0.002 (0.9466±0.0039)
SaltPlate3/16-13	0.373 (0.9474)	0.371 (0.9423)	0.372 (0.9449)	0.372±0.001 (0.9449±0.0025)
SaltPlate3/16-14	0.370 (0.9398)	0.371 (0.9423)	0.370 (0.9398)	0.370±0.001 (0.9406±0.0015)
SaltPlate3/16-15	0.373 (0.9474)	0.370 (0.9398)	0.371 (0.9423)	0.371±0.002 (0.9432±0.0039)
SaltPlate3/16-16	0.373 (0.9474)	0.372 (0.9449)	0.371 (0.9423)	0.372±0.001 (0.9449±0.0025)
SaltPlate3/16-17	0.371 (0.9423)	0.371 (0.9423)	0.371 (0.9423)	0.371±0.000 (0.9423±0.0000)
SaltPlate3/16-18	0.374 (0.9500)	0.371 (0.9423)	0.372 (0.9449)	0.372±0.002 (0.9457±0.0039)
SaltPlate3/16-19	0.373 (0.9474)	0.371 (0.9423)	0.372 (0.9449)	0.372±0.001 (0.9449±0.0025)

Table 12 Continued.

Part ID	Assembled Thickness [in (cm)]			
	Measurement 1	Measurement 2	Measurement 3	Average$\pm1\sigma$
SaltPlate3/16-20	0.373 (0.9474)	0.371 (0.9423)	0.372 (0.9449)	0.372$\pm$0.001 (0.9449$\pm$0.0025)
SaltPlate3/16-21	0.373 (0.9474)	0.372 (0.9449)	0.371 (0.9423)	0.372$\pm$0.001 (0.9449$\pm$0.0025)
SaltPlate3/16-22	0.372 (0.9449)	0.369 (0.9373)	0.373 (0.9474)	0.371$\pm$0.002 (0.9432$\pm$0.0053)
SaltPlate3/16-23	0.373 (0.9474)	0.370 (0.9398)	0.373 (0.9474)	0.372$\pm$0.002 (0.9449$\pm$0.0044)

Table 16: Sodium chloride absorber mass measurements immediately after being filled with the NaCl salt. For formatting, the column "Part ID" is the number following the nomenclature "SaltPlate3/16".

Part ID	Date	Mass of Filled Vessel (g)			
		Measurement 1	Measurement 2	Measurement 3	Average$\pm1\sigma$[(a)]
-1	May 01, 2024	2464.6	2464.6	2464.6	2464.6$\pm$0.0
-2	May 02, 2024	2454.2	2454.2	2454.2	2454.2$\pm$0.0
-3	May 02, 2024	2456.0	2456.0	2456.0	2456.0$\pm$0.0
-4	May 07, 2024	2447.8	2447.8	2447.8	2447.8$\pm$0.0
-5	May 07, 2024	2446.1	2446.1	2446.1	2446.1$\pm$0.0
-6	May 07, 2024	2456.5	2456.5	2456.5	2456.5$\pm$0.0
-7	May 08, 2024	2445.6	2445.6	2445.6	2445.6$\pm$0.0
-8	May 08, 2024	2449.8	2449.8	2449.8	2449.8$\pm$0.0
-9	May 08, 2024	2433.3	2433.3	2433.3	2433.3$\pm$0.0
-10	May 09, 2024	2425.4	2425.4	2425.4	2425.4$\pm$0.0
-11	May 09, 2024	2449.6	2449.6	2449.6	2449.6$\pm$0.0
-12	May 09, 2024	2457.6	2457.6	2457.6	2457.6$\pm$0.0
-13	May 10, 2024	2446.6	2446.6	2446.6	2446.6$\pm$0.0
-14	May 10, 2024	2437.8	2437.8	2437.8	2437.8$\pm$0.0
-15	May 13, 2024	2445.6	2445.6	2445.6	2445.6$\pm$0.0
-16	May 13, 2024	2448.5	2448.4	2448.5	2448.4$\pm$0.0
-17	May 13, 2024	2425.1	2425.1	2425.1	2425.1$\pm$0.0
-18	May 14, 2024	2442.0	2442.0	2442.0	2442.0$\pm$0.0
-19	May 14, 2024	2430.9	2430.9	2430.9	2430.9$\pm$0.0
-20	May 15, 2024	2424.4	2424.4	2424.4	2424.4$\pm$0.0
-21	May 15, 2024	2432.3	2432.3	2432.3	2432.3$\pm$0.0
-22	May 20, 2024	2425.4	2425.4	2425.4	2425.4$\pm$0.0
-23	May 21, 2024	2451.1	2451.1	2451.1	2451.1$\pm$0.0

[(a)] The standard deviation of the measurements are zero, but still shown for completeness.

Table 17: Sodium chloride absorber mass measurements prior to shipment from LLNL to NCERC. For formatting, the column "Part ID" is the number following the nomenclature "SaltPlate3/16".

Part ID	**Date**	**Mass of Filled Vessel (g)**			
		Measurement 1	**Measurement 2**	**Measurement 3**	**Average**$\pm 1\sigma$
-1	May 31, 2024	2464.7	2464.7	2464.7	2464.7±0.0
-2	May 31, 2024	2454.2	2454.2	2454.2	2454.2±0.0
-3	May 31, 2024	2456.0	2456.0	2456.0	2456.0±0.0
-4	May 31, 2024	2447.8	2447.8	2447.7	2447.8±0.0
-5	May 31, 2024	2446.2	2446.2	2446.2	2446.2±0.0
-6	May 31, 2024	2456.0	2455.7	2455.8	2455.9±0.1
-7	May 31, 2024	2455.6	2455.6	2455.6	2455.6±0.0
-8	May 31, 2024	2449.8	2449.9	2449.9	2449.8±0.0
-9	May 31, 2024	2433.3	2433.3	2433.3	2433.3±0.0
-10	May 31, 2024	2425.5	2425.4	2425.4	2425.4±0.1
-11	May 31, 2024	2449.6	2449.6	2449.7	2449.6±0.0
-12	May 31, 2024	2457.5	2457.5	2457.6	2457.5±0.0
-13	May 31, 2024	2446.6	2446.5	2446.6	2446.6±0.1
-14	May 31, 2024	2437.7	2437.7	2437.7	2437.7±0.0
-15	May 31, 2024	2445.6	2445.6	2445.5	2445.6±0.0
-16	May 31, 2024	2448.3	2448.4	2448.4	2448.4±0.1
-17	May 31, 2024	2425.3	2425.3	2425.3	2425.3±0.0
-18	May 31, 2024	2442.1	2442.2	2442.1	2442.1±0.1
-19	May 31, 2024	2431.0	2430.9	2431.0	2431.0±0.0
-20	May 31, 2024	2424.5	2424.6	2424.6	2424.5±0.0
-21	May 31, 2024	2432.5	2432.5	2432.4	2432.4±0.1
-22	May 31, 2024	2425.7	2425.5	2425.5	2425.6±0.1
-23	May 31, 2024	2451.1	2451.1	2451.1	2451.1±0.0

Table 18: Sodium chloride absorber mass measured at NCERC directly after the experiments. Only the plates used in the experiments were measured.

Part ID	Date	Measurement (g)
SaltPlate3/16-1	Aug 05, 2024	-
SaltPlate3/16-2	Aug 05, 2024	2453.5
SaltPlate3/16-3	Aug 05, 2024	2455.1
SaltPlate3/16-4	Aug 05, 2024	2446.9
SaltPlate3/16-5	Aug 05, 2024	2445.3
SaltPlate3/16-6	Aug 05, 2024	2454.9
SaltPlate3/16-7	Aug 05, 2024	-
SaltPlate3/16-8	Aug 05, 2024	2448.9
SaltPlate3/16-9	Aug 05, 2024	2432.5
SaltPlate3/16-10	Aug 05, 2024	2424.5
SaltPlate3/16-11	Aug 05, 2024	2448.8
SaltPlate3/16-12	Aug 05, 2024	2456.7
SaltPlate3/16-13	Aug 05, 2024	2445.8
SaltPlate3/16-14	Aug 05, 2024	2436.7
SaltPlate3/16-15	Aug 05, 2024	2444.4
SaltPlate3/16-16	Aug 05, 2024	2447.1
SaltPlate3/16-17	Aug 05, 2024	2423.9
SaltPlate3/16-18	Aug 05, 2024	2440.8
SaltPlate3/16-19	Aug 05, 2024	2429.6
SaltPlate3/16-20	Aug 05, 2024	-
SaltPlate3/16-21	Aug 05, 2024	-
SaltPlate3/16-22	Aug 05, 2024	-
SaltPlate3/16-23	Aug 05, 2024	-

Table 19: Derived volumes and densities for the sodium chloride absorber salt.

Part ID Salt Plate 1/4 -	Mass (g)	Volume (cm^3)	Density (g/cm^3)
03	514.0	344.0449	1.4939
04	514.8	344.6051	1.4939
05	516.0	344.0449	1.4998
06	521.3	343.4272	1.5180
08	514.1	346.5733	1.4834
09	507.6	345.3378	1.4698
10	497.2	346.5733	1.4345
11	510.7	345.2802	1.4790
12	515.1	344.6051	1.4946
13	509.9	347.8089	1.4659
14	509.5	346.0709	1.4722
15	511.8	345.3378	1.4820
16	513.6	345.9555	1.4847
17	504.7	345.8979	1.4590
18	500.7	344.1022	1.4552
19	504.5	339.7211	1.4850

Table 20: Derived volumes and densities for the sodium chloride absorber encapsulation base.

Part ID Salt Plate 1/4 -	Mass (g)	Volume (cm^3)	Density (g/cm^3)
03	1218.1	487.1241	2.5006
04	1207.8	490.4261	2.4628
05	1205.5	469.8058	2.5660
06	1210.5	486.9128	2.4861
08	1209.5	482.8429	2.5050
09	1201.6	470.5098	2.5538
10	1204.0	479.7908	2.5094
11	1215.0	470.4683	2.5825
12	1218.0	485.0065	2.5113
13	1211.8	483.5593	2.5060
14	1204.3	462.6241	2.6032
15	1211.6	481.9341	2.5140
16	1210.9	467.9654	2.5876
17	1197.2	473.6812	2.5274
18	1214.6	478.2174	2.5398
19	1203.5	464.4313	2.5913

Table 21: Derived volumes and densities for the sodium chloride absorber encapsulation lid.

Part ID Salt Plate 1/4 -	Mass (g)	Volume (cm^3)	Density (g/cm^3)
03	720.0	272.5441	2.6418
04	721.6	270.6656	2.6660
05	721.0	271.6233	2.6544
06	720.2	271.5492	2.6522
08	722.5	271.5862	2.6603
09	720.7	270.4809	2.6645
10	720.9	270.5548	2.6645
11	720.3	270.4439	2.6634
12	720.9	271.3638	2.6566
13	721.5	271.4750	2.6577
14	720.1	270.5917	2.6612
15	718.3	271.6233	2.6445
16	719.9	269.7818	2.6685
17	719.3	271.5492	2.6489
18	722.6	274.2358	2.6350
19	718.9	269.7081	2.6655

1.2.4.4 1/4" Sodium Chloride Absorbers

Thirteen 0.25-inch (0.635 cm; labeled 1/4") sodium chloride absorbers were procured for this experiment. Upon receipt from the manufacturer, LANL performed acceptance mass measurements, which are reported in the following tables: Table 22 and Table 23, CMM dimensional measurements, Tables 24, 25, 26, and 27, and traditional dimensional measurements, Tables 28, 29, and 30. Mass measurements were performed during the plate filling process, which are reported in the following tables: Table 16, prior to shipment from LLNL to NCERC, Table 32, and after experimental execution, Table 18. The derived volumes and densities are presented in Table 34.

Table 22: Sodium chloride absorber component weights via acceptance measurements performed by LANL.

Part ID	Mass (g)			
	Base	Lid	Assembled (No Salt)	Screws (Difference)
Salt Plate 1/4-01	1373.0	719.0	2094.3	2.30
Salt Plate 1/4-02	1374.4	721.5	2098.4	2.50
Salt Plate 1/4-03	1388.3	722.0	2112.5	2.20
Salt Plate 1/4-04	1383.9	722.1	2107.9	1.90
Salt Plate 1/4-05	1390.1	722.0	2114.4	2.30
Salt Plate 1/4-06	1384.6	721.7	2108.5	2.20
Salt Plate 1/4-07	1402.0	722.7	2126.8	2.10
Salt Plate 1/4-08	1385.6	721.0	2108.8	2.20
Salt Plate 1/4-09	1392.9	722.7	2118.0	2.40
Salt Plate 1/4-10	1390.9	722.6	2115.9	2.40
Salt Plate 1/4-11	1383.1	722.0	2107.3	2.20
Salt Plate 1/4-12	1386.7	720.9	2109.7	2.10
Salt Plate 1/4-13	1385.1	721.4	2108.9	2.40

Table 23: Sodium chloride absorber assembled unfilled weights via acceptance measurements performed by LANL.

Part ID	Mass of Empty Vessel (g)			
	Measurement 1	Measurement 2	Measurement 3	Average$\pm 1\sigma$
Salt Plate 1/4-01	2094.8	2094.8	2094.8	2094.8 ± 0.0
Salt Plate 1/4-02	2098.9	2098.9	2098.9	2098.9 ± 0.0
Salt Plate 1/4-03	2113.1	2113.1	2113.1	2113.1 ± 0.0
Salt Plate 1/4-04	2108.8	2108.8	2108.8	2108.8 ± 0.0
Salt Plate 1/4-05	2115.1	2115.1	2115.1	2115.1 ± 0.0
Salt Plate 1/4-06	2109.1	2109.1	2109.1	2109.1 ± 0.0
Salt Plate 1/4-07	2127.4	2127.4	2127.4	2127.4 ± 0.0
Salt Plate 1/4-08	2109.3	2109.3	2109.3	2109.3 ± 0.0
Salt Plate 1/4-09	2118.5	2118.5	2118.5	2118.5 ± 0.0
Salt Plate 1/4-10	2116.3	2116.3	2116.3	2116.3 ± 0.0
Salt Plate 1/4-11	2107.8	2107.8	2107.8	2107.8 ± 0.0
Salt Plate 1/4-12	2110.3	2110.2	2110.3	2110.3 ± 0.0
Salt Plate 1/4-13	2109.4	2109.4	2109.4	2109.4 ± 0.0

Table 24: Sodium chloride absorber encapsulation base acceptance measurements via CMM measurements performed by LANL (see Figure 10).

Part ID	**Inner Diameter, c [in (cm)]**	**Outer Diameter, a [in (cm)]**	**Bottom Thickness, e-d [in (cm)]**
Salt Plate 1/4-01	11.997 (30.4724)	15.004 (38.1102)	0.100 (0.254)
Salt Plate 1/4-02	11.996 (30.4698)	15.000 (38.1000)	0.091 (0.2311)
Salt Plate 1/4-03	12.000 (30.4800)	14.997 (38.0924)	0.092 (0.2337)
Salt Plate 1/4-04	12.000 (30.4800)	14.998 (38.0949)	0.093 (0.2362)
Salt Plate 1/4-05	12.000 (30.4800)	14.996 (38.0898)	0.091 (0.2311)
Salt Plate 1/4-06	12.000 (30.4800)	14.996 (38.0898)	0.093 (0.2362)
Salt Plate 1/4-07	12.000 (30.4800)	14.997 (38.0924)	0.091 (0.2311)
Salt Plate 1/4-08	12.000 (30.4800)	14.997 (38.0924)	0.092 (0.2337)
Salt Plate 1/4-09	12.000 (30.4800)	14.997 (38.0924)	0.093 (0.2362)
Salt Plate 1/4-10	12.000 (30.4800)	14.998 (38.0949)	0.093 (0.2362)
Salt Plate 1/4-11	12.000 (30.4800)	14.998 (38.0949)	0.091 (0.2311)
Salt Plate 1/4-12	12.000 (30.4800)	14.998 (38.0949)	0.094 (0.2388)
Salt Plate 1/4-13	11.999 (30.4775)	14.999 (38.0975)	0.095 (0.2413)

Table 25: Sodium chloride absorber encapsulation base acceptance measurements via CMM measurements performed by LANL (see Figure 10).

Part ID	**Pocket Depth, d [in (cm)]**			
	Measurement 1	**Measurement 2**	**Measurement 3**	**Average**$\pm 1\sigma$
Salt Plate 1/4-01	0.248 (0.6299)	0.246 (0.6248)	0.246 (0.6248)	0.247±0.001 (0.6265±0.0029)
Salt Plate 1/4-02	0.247 (0.6274)	0.246 (0.6248)	0.246 (0.6248)	0.246±0.001 (0.6257±0.0015)
Salt Plate 1/4-03	0.248 (0.6299)	0.248 (0.6299)	0.248 (0.6299)	0.248±0.000 (0.6299±0.0000)
Salt Plate 1/4-04	0.248 (0.6299)	0.247 (0.6274)	0.246 (0.6248)	0.247±0.001 (0.6274±0.0025)
Salt Plate 1/4-05	0.248 (0.6299)	0.248 (0.6299)	0.246 (0.6248)	0.247±0.001 (0.6282±0.0029)
Salt Plate 1/4-06	0.247 (0.6274)	0.247 (0.6274)	0.247 (0.6274)	0.247±0.000 (0.6274±0.0000)
Salt Plate 1/4-07	0.248 (0.6299)	0.246 (0.6248)	0.247 (0.6274)	0.247±0.001 (0.6274±0.0025)
Salt Plate 1/4-08	0.248 (0.6299)	0.247 (0.6274)	0.248 (0.6299)	0.248±0.001 (0.6291±0.0015)
Salt Plate 1/4-09	0.248 (0.6299)	0.249 (0.6325)	0.248 (0.6299)	0.248±0.001 (0.6308±0.0015)
Salt Plate 1/4-10	0.249 (0.6325)	0.248 (0.6299)	0.248 (0.6299)	0.248±0.001 (0.6308±0.0015)
Salt Plate 1/4-11	0.248 (0.6299)	0.248 (0.6299)	0.248 (0.6299)	0.248±0.000 (0.6299±0.0000)
Salt Plate 1/4-12	0.248 (0.6299)	0.248 (0.6299)	0.249 (0.6325)	0.248±0.001 (0.6308±0.0015)
Salt Plate 1/4-13	0.249 (0.6325)	0.249 (0.6325)	0.248 (0.6299)	0.249±0.001 (0.6316±0.0015)

Table 26: Sodium chloride absorber encapsulation lid acceptance measurements via CMM measurements performed by LANL (see Figure 11).

Part ID	**Diameter, x [in (cm)]**	**Thickness, y [in (cm)]**
Salt Plate 1/4-01	14.651 (37.2135)	0.098 (0.2489)
Salt Plate 1/4-02	14.647 (37.2034)	0.098 (0.2489)
Salt Plate 1/4-03	14.648 (37.2059)	0.098 (0.2489)
Salt Plate 1/4-04	14.648 (37.2059)	0.098 (0.2489)
Salt Plate 1/4-05	14.647 (37.2034)	0.099 (0.2515)
Salt Plate 1/4-06	14.643 (37.1932)	0.099 (0.2515)
Salt Plate 1/4-07	14.646 (37.2008)	0.100 (0.2540)
Salt Plate 1/4-08	14.641 (37.1881)	0.100 (0.2540)
Salt Plate 1/4-09	14.647 (37.2034)	0.099 (0.2515)
Salt Plate 1/4-10	14.648 (37.2059)	0.099 (0.2515)
Salt Plate 1/4-11	14.647 (37.2034)	0.099 (0.2515)
Salt Plate 1/4-12	14.642 (37.1907)	0.099 (0.2515)
Salt Plate 1/4-13	14.647 (37.2034)	0.099 (0.2515)

Table 27: Sodium chloride absorber encapsulation assembled thickness via CMM measurements performed by LANL.

Part ID	**Assembled Thickness [in (cm)]**			
	Measurement 1	**Measurement 2**	**Measurement 3**	**Average**$\pm 1\sigma$
Salt Plate 1/4-01	0.432 (1.0973)	0.454 (1.1532)	0.442 (1.1227)	0.443$\pm$0.011 (1.1244$\pm$0.0280)
Salt Plate 1/4-02	0.432 (1.0973)	0.451 (1.1455)	0.446 (1.1328)	0.443$\pm$0.010 (1.1252$\pm$0.0250)
Salt Plate 1/4-03	0.434 (1.1024)	0.451 (1.1455)	0.448 (1.1379)	0.444$\pm$0.009 (1.1286$\pm$0.0230)
Salt Plate 1/4-04	0.433 (1.0998)	0.451 (1.1455)	0.452 (1.1481)	0.445$\pm$0.011 (1.1311$\pm$0.0272)
Salt Plate 1/4-05	0.434 (1.1024)	0.443 (1.1252)	0.445 (1.1303)	0.441$\pm$0.006 (1.1193$\pm$0.0149)
Salt Plate 1/4-06	0.440 (1.1176)	0.447 (1.1354)	0.450 (1.1430)	0.446$\pm$0.005 (1.1320$\pm$0.0130)
Salt Plate 1/4-07	0.439 (1.1151)	0.436 (1.1074)	0.440 (1.1176)	0.438$\pm$0.002 (1.1134$\pm$0.0053)
Salt Plate 1/4-08	0.448 (1.1379)	0.436 (1.1074)	0.446 (1.1328)	0.443$\pm$0.006 (1.1261$\pm$0.0163)
Salt Plate 1/4-09	0.451 (1.1455)	0.436 (1.1074)	0.443 (1.1252)	0.443$\pm$0.008 (1.1261$\pm$0.0191)
Salt Plate 1/4-10	0.447 (1.1354)	0.441 (1.1201)	0.453 (1.1506)	0.447$\pm$0.006 (1.1354$\pm$0.0152)
Salt Plate 1/4-11	0.446 (1.1328)	0.434 (1.1024)	0.439 (1.1151)	0.440$\pm$0.006 (1.1168$\pm$0.0153)
Salt Plate 1/4-12	0.452 (1.1481)	0.435 (1.1049)	0.444 (1.1278)	0.444$\pm$0.009 (1.1269$\pm$0.0216)
Salt Plate 1/4-13	0.434 (1.1024)	0.456 (1.1582)	0.450 (1.1430)	0.447$\pm$0.011 (1.1345$\pm$0.0289)

Table 28: Sodium chloride absorber encapsulation base lip inner diameter acceptance measurements via hand tool measurements performed by LANL (see Figure 10).

Part ID	**Lip Inner Diameter, b [in (cm)]**			
	Measurement 1	**Measurement 2**	**Measurement 3**	**Average**$\pm 1\sigma$
Salt Plate 1/4-01	14.766 (37.504)	14.765 (37.503)	14.767 (37.508)	14.766$\pm$0.001 (37.5052$\pm$0.0026)
Salt Plate 1/4-02	14.767 (37.507)	14.767 (37.507)	14.767 (37.507)	14.767$\pm$0.000 (37.5069$\pm$0.0000)
Salt Plate 1/4-03	14.769 (37.513)	14.772 (37.521)	14.767 (37.508)	14.769$\pm$0.003 (37.5141$\pm$0.0064)
Salt Plate 1/4-04	14.768 (37.509)	14.767 (37.507)	14.772 (37.521)	14.769$\pm$0.003 (37.5124$\pm$0.0074)
Salt Plate 1/4-05	14.763 (37.498)	14.747 (37.457)	14.771 (37.517)	14.760$\pm$0.012 (37.4908$\pm$0.0305)
Salt Plate 1/4-06	14.767 (37.508)	14.770 (37.516)	14.768 (37.509)	14.768$\pm$0.002 (37.5111$\pm$0.0041)
Salt Plate 1/4-07	14.766 (37.504)	14.769 (37.512)	14.766 (37.504)	14.767$\pm$0.002 (37.5069$\pm$0.0044)
Salt Plate 1/4-08	14.763 (37.498)	14.769 (37.512)	14.767 (37.507)	14.766$\pm$0.003 (37.5056$\pm$0.0071)
Salt Plate 1/4-09	14.765 (37.503)	14.765 (37.502)	14.766 (37.506)	14.765$\pm$0.001 (37.5035$\pm$0.0019)
Salt Plate 1/4-10	14.761 (37.492)	14.771 (37.517)	14.769 (37.513)	14.767$\pm$0.005 (37.5073$\pm$0.0137)
Salt Plate 1/4-11	14.770 (37.515)	14.769 (37.512)	14.763 (37.498)	14.767$\pm$0.004 (37.5082$\pm$0.0089)
Salt Plate 1/4-12	14.767 (37.507)	14.762 (37.495)	14.759 (37.487)	14.762$\pm$0.004 (37.4963$\pm$0.0102)
Salt Plate 1/4-13	14.762 (37.495)	14.761 (37.492)	14.765 (37.502)	14.762$\pm$0.002 (37.4966$\pm$0.0048)

Table 29: Sodium chloride absorber encapsulation lid acceptance measurements via hand tool measurements performed by LANL (see Figure 11).

Part ID	**Diameter, x [in (cm)]**			
	Measurement 1	**Measurement 2**	**Measurement 3**	**Average**$\pm 1\sigma$
Salt Plate 1/4-01	14.642 (37.1894)	14.654 (37.2199)	14.648 (37.2059)	14.648±0.006 (37.2051±0.0153)
Salt Plate 1/4-02	14.650 (37.2110)	14.644 (37.1945)	14.649 (37.2072)	14.647±0.003 (37.2042±0.0086)
Salt Plate 1/4-03	14.650 (37.2110)	14.650 (37.2097)	14.648 (37.2059)	14.649±0.001 (37.2089±0.0026)
Salt Plate 1/4-04	14.649 (37.2085)	14.650 (37.2097)	14.645 (37.1970)	14.648±0.003 (37.2051±0.0070)
Salt Plate 1/4-05	14.643 (37.1920)	14.647 (37.2021)	14.650 (37.2110)	14.646±0.004 (37.2017±0.0095)
Salt Plate 1/4-06	14.648 (37.2059)	14.643 (37.1932)	14.647 (37.2034)	14.646±0.003 (37.2008±0.0067)
Salt Plate 1/4-07	14.647 (37.2034)	14.649 (37.2072)	14.645 (37.1970)	14.647±0.002 (37.2025±0.0051)
Salt Plate 1/4-08	14.643 (37.1920)	14.641 (37.1869)	14.639 (37.1831)	14.641±0.002 (37.1873±0.0045)
Salt Plate 1/4-09	14.644 (37.1958)	14.653 (37.2186)	14.645 (37.1983)	14.647±0.005 (37.2042±0.0125)
Salt Plate 1/4-10	14.640 (37.1856)	14.644 (37.1958)	14.644 (37.1945)	14.643±0.002 (37.1920±0.0055)
Salt Plate 1/4-11	14.678 (37.2821)	14.645 (37.1970)	14.648 (37.2047)	14.657±0.019 (37.2279±0.0471)
Salt Plate 1/4-12	14.635 (37.1729)	14.639 (37.1818)	14.646 (37.2008)	14.640±0.006 (37.1852±0.0143)
Salt Plate 1/4-13	14.645 (37.1983)	14.644 (37.1945)	14.650 (37.2110)	14.646±0.003 (37.2013±0.0086)

Table 30: Sodium chloride absorber encapsulation assembled thickness via hand tool measurements performed by LANL.

Part ID	**Assembled Thickness [in (cm)]**			
	Measurement 1	**Measurement 2**	**Measurement 3**	**Average**$\pm 1\sigma$
Salt Plate 1/4-01	0.432 (1.0973)	0.429 (1.0897)	0.432 (1.0973)	0.431$\pm$0.002 (1.0947$\pm$0.0044)
Salt Plate 1/4-02	0.433 (1.0998)	0.429 (1.0897)	0.435 (1.1049)	0.432$\pm$0.003 (1.0981$\pm$0.0078)
Salt Plate 1/4-03	0.435 (1.1049)	0.433 (1.0998)	0.433 (1.0998)	0.434$\pm$0.001 (1.1015$\pm$0.0029)
Salt Plate 1/4-04	0.434 (1.1024)	0.430 (1.0922)	0.433 (1.0998)	0.432$\pm$0.002 (1.0981$\pm$0.0053)
Salt Plate 1/4-05	0.435 (1.1049)	0.432 (1.0973)	0.434 (1.1024)	0.434$\pm$0.002 (1.1015$\pm$0.0039)
Salt Plate 1/4-06	0.435 (1.1049)	0.433 (1.0998)	0.433 (1.0998)	0.434$\pm$0.001 (1.1015$\pm$0.0029)
Salt Plate 1/4-07	0.435 (1.1049)	0.436 (1.1074)	0.433 (1.0998)	0.435$\pm$0.002 (1.1041$\pm$0.0039)
Salt Plate 1/4-08	0.436 (1.1074)	0.434 (1.1024)	0.430 (1.0922)	0.433$\pm$0.003 (1.1007$\pm$0.0078)
Salt Plate 1/4-09	0.436 (1.1074)	0.434 (1.1024)	0.433 (1.0998)	0.434$\pm$0.002 (1.1032$\pm$0.0039)
Salt Plate 1/4-10	0.436 (1.1074)	0.435 (1.1049)	0.433 (1.0998)	0.435$\pm$0.002 (1.1041$\pm$0.0039)
Salt Plate 1/4-11	0.433 (1.0998)	0.435 (1.1049)	0.435 (1.1049)	0.434$\pm$0.001 (1.1032$\pm$0.0029)
Salt Plate 1/4-12	0.436 (1.1074)	0.432 (1.0973)	0.433 (1.0998)	0.434$\pm$0.002 (1.1015$\pm$0.0053)
Salt Plate 1/4-13	0.436 (1.1074)	0.434 (1.1024)	0.433 (1.0998)	0.434$\pm$0.002 (1.1032$\pm$0.0039)

Table 31: Sodium chloride absorber mass measurements immediately after being filled with the NaCl salt. For formatting, the column "Part ID" is the number following the nomenclature "Salt Plate 1/4".

Part ID	Date	Mass of Filled Vessel (g)			
		Measurement 1	Measurement 2	Measurement 3	Average$\pm 1\sigma$[(a)]
-01	May 21, 2024	2751.3	2751.3	2751.3	2751.3±0.0
-02	May 21, 2024	2761.0	2760.9	2760.9	2760.9±0.0
-03	May 21, 2024	2773.5	2773.5	2773.4	2773.5±0.0
-04	May 21, 2024	2764.8	2764.8	2764.8	2764.8±0.0
-05	May 21, 2024	2761.7	2761.7	2761.7	2761.7±0.0
-06	May 22, 2024	2764.8	2764.8	2764.8	2764.8±0.0
-07	May 22, 2024	2781.2	2781.2	2781.2	2781.2±0.0
-08	May 23, 2024	2762.1	2762.1	2762.1	2762.1±0.0
-09	May 23, 2024	2777.9	2777.9	2777.9	2777.9±0.0
-10	May 23, 2024	2793.2	2793.2	2793.2	2793.2±0.0
-11	May 23, 2024	2774.5	2774.5	2774.5	2774.5±0.0
-12	May 23, 2024	2790.1	2790.1	2790.1	2790.1±0.0
-13	May 24, 2024	2783.2	2783.2	2783.2	2783.2±0.0

[(a)] The standard deviation of the measurements are zero, but still shown for completeness.

Table 32: Sodium chloride absorber mass measurements prior to shipment from LLNL to NCERC. For formatting, the column "Part ID" is the number following the nomenclature "Salt Plate 1/4".

Part ID	Date	Mass of Filled Vessel (g)			
		Measurement 1	Measurement 2	Measurement 3	Average$\pm 1\sigma$
-01	May 31, 2024	2751.3	2751.2	2751.3	2751.3±0.1
-02	May 31, 2024	2760.9	2761.0	2761.0	2760.9±0.1
-03	May 31, 2024	2773.4	2773.3	2773.4	2773.4±0.1
-04	May 31, 2024	2764.9	2764.9	2764.8	2764.8±0.1
-05	May 31, 2024	2761.5	2761.6	2761.8	2761.6±0.2
-06	May 31, 2024	2763.9	2763.9	2763.8	2763.8±0.1
-07	May 31, 2024	2781.3	2781.3	2781.3	2781.3±0.0
-08	May 31, 2024	2762.2	2762.2	2762.2	2762.2±0.0
-09	May 31, 2024	2778.0	2778.0	2777.9	2778.0±0.1
-10	May 31, 2024	2793.2	2793.2	2793.1	2793.2±0.0
-11	May 31, 2024	2774.6	2774.6	2774.7	2774.6±0.0
-12	May 31, 2024	2790.2	2790.2	2790.2	2790.2±0.0
-13	May 31, 2024	2783.5	2783.4	2783.3	2783.4±0.1

Table 33: Sodium chloride absorber mass measured at NCERC directly after the experiments. Only the plates used in the experiments were measured.

Part ID	Date	Measurement (g)
Salt Plate 1/4-01	Aug 05, 2024	-
Salt Plate 1/4-02	Aug 05, 2024	2760.1
Salt Plate 1/4-03	Aug 05, 2024	2772.6
Salt Plate 1/4-04	Aug 05, 2024	2764.0
Salt Plate 1/4-05	Aug 05, 2024	2760.8
Salt Plate 1/4-06	Aug 05, 2024	-
Salt Plate 1/4-07	Aug 05, 2024	2780.3
Salt Plate 1/4-08	Aug 05, 2024	2761.3
Salt Plate 1/4-09	Aug 05, 2024	2777.0
Salt Plate 1/4-10	Aug 05, 2024	-
Salt Plate 1/4-11	Aug 05, 2024	-
Salt Plate 1/4-12	Aug 05, 2024	-
Salt Plate 1/4-13	Aug 05, 2024	-

Table 34: Derived volumes and densities for the sodium chloride absorbers.

Part ID Salt Plate 1/4 -	**Mass (g)**	**Volume (cm^3)**	**Density (g/cm^3)**
Salt			
02	661.2	456.2335	1.4492
03	659.5	459.6267	1.4348
04	655.2	457.7733	1.4314
05	645.7	458.3911	1.4086
07	652.9	457.7733	1.4262
08	652.0	459.0089	1.4205
09	658.5	460.2444	1.4307
Encapsulation Base			
02	1374.4	525.1004	2.6174
03	1388.3	528.9239	2.6248
04	1383.9	530.9404	2.6065
05	1390.1	525.3592	2.6460
07	1402.0	525.0417	2.6703
08	1385.6	528.6401	2.6211
09	1392.9	532.2448	2.6170
Encapsulation Lid			
02	721.5	270.5917	2.6664
03	722.0	270.6286	2.6679
04	722.1	270.6286	2.6682
05	722.0	273.3528	2.6413
07	722.7	276.0763	2.6178
08	721.0	275.8878	2.6134
09	722.7	273.3528	2.6438

1.2.5 Polyethylene Parts

The HDPE parts include moderator (MOD) plates, reflector (REF) plates, a bottom reflector (BOTREFSRC), reflector rings (RING), and caps (CAP,BOTCAP). Figure 18 shows a diagram of how these parts fit together. The moderator plates sit inside of the stack while the rest of the HDPE parts serve externally as reflector components. The reflector ring parts create a nominal 1 in. (2.54 cm) reflector surrounding the core stack. The bottom reflector, reflector rings, and reflector caps include step joints which allow the parts to mate together and limit neutron streaming paths. The caps are used to fill the open step joints to complete the reflectors.

All parts from the TEX-Hf campaign were weighed and measured, using a coordinate measuring machine (CMM) with a precision of 0.00635 cm, by LLNL's Dimensional Inspection Laboratory prior to the experiment. All new parts procured for this experimental campaign were weighed and measured, using a coordinate measuring machine (CMM), by Los Alamos National Laboratory prior to the experiment. The dimensional measurements performed by the CMM report minimum, maximum, and average values for the diameters and a single value for the thicknesses. The diameter measurements result from measuring many cord lengths of the diameter. The thickness measurements result from creating a best-fit plane of the top surface using many points measured at that surface. The thickness represents the distance between the base and this plane. The following sections report the mass and dimensional measurements for the polyethylene parts.

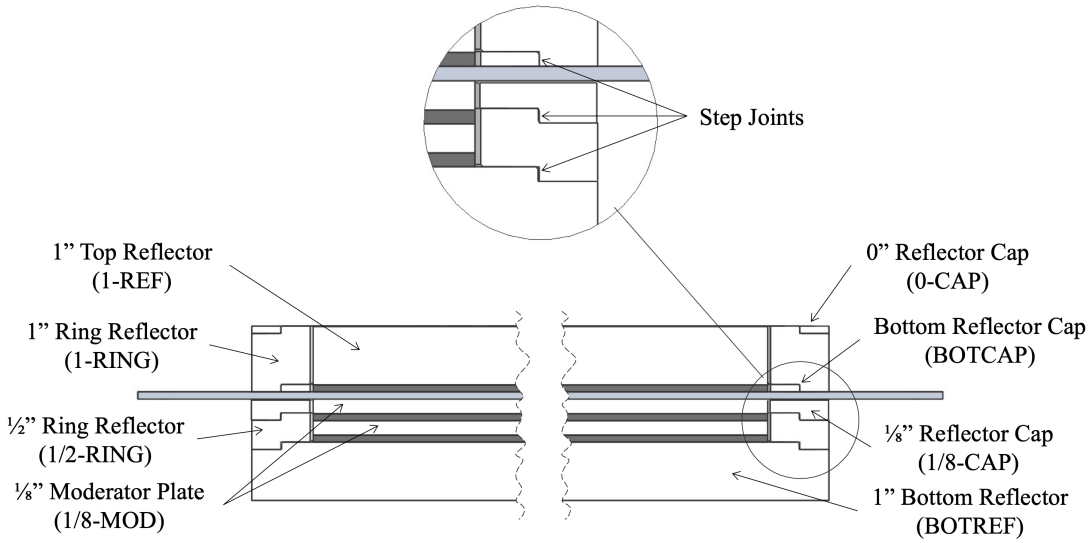

Figure 18: Diagram of the polyethylene parts.

1.2.5.1 Moderator and Reflector Plates

The polyethylene moderator and reflector plates are cylindrical with a nominal diameter of 15 in. (38.1 cm) and varying thicknesses, reported in Table 35. Figure 19 shows a schematic of the moderator and reflector plate part. The moderator plates are placed between the HEU plates with five nominal thicknesses: 0.125 in. (0.3175 cm), 0.25 in. (0.635 cm), 0.5 in. (1.27 cm), 0.75 in. (1.905 cm), and 1.5 in. (3.81 cm). The reflector plates are used as the top reflector and provide fine reactivity control with three nominal thicknesses: 0.03125 in. (0.079375 cm), 0.0625 in. (0.15875 cm), and 1 in. (2.54 cm). The moderator plates were also used in the top reflector. The original drawings of the moderator plates, with dimensions and tolerances, are included in Appendix **??**, except the 3/4-MOD plates which are not included.

Tables 36, 38, 40, 42, 44, and 46 report the mass and dimensional measurements of the polyethylene moderator and reflector plates. Tables 37, 39, 41, 43, and 45 report the derived volumes and densities of the moderator plates. A description of these measurements is included in Section 1.2.5.

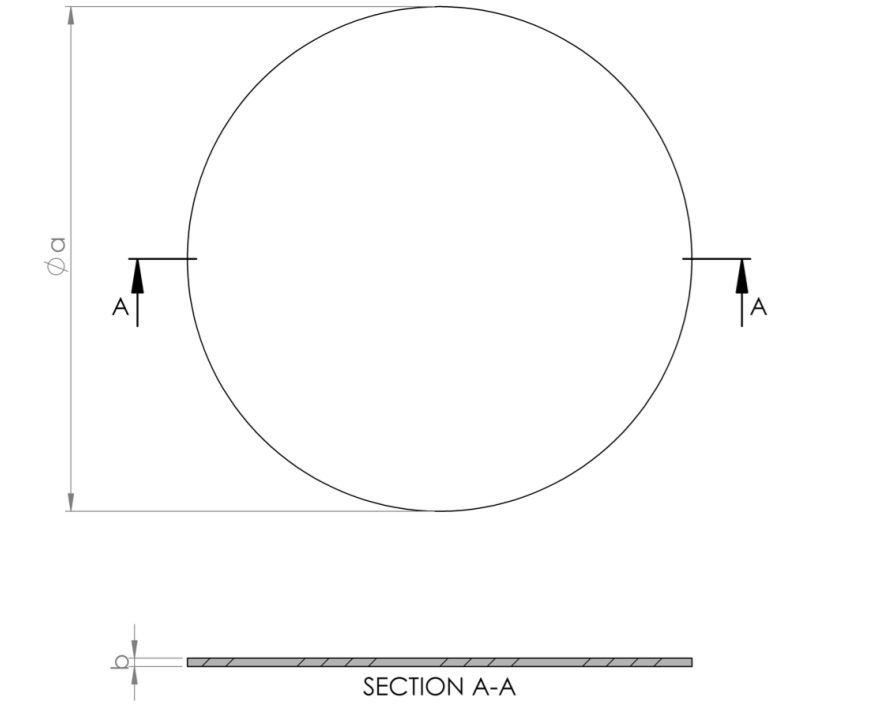

Figure 19: Schematic of the polyethylene moderator and reflector plate.

Table 35: Polyethylene moderator and reflector plate nominal dimensions (see Figure 19).

Part Type	**Thickness, *b* [in. (cm)]**	**Diameter, *a* [in. (cm)]**
1/8-MOD	0.125 ± 0.005 (0.3175 ± 0.0127)	15.000 ± 0.010 (38.1000 ± 0.0254)
1/4-MOD	0.250 ± 0.005 (0.6350 ± 0.0127)	
1/2-MOD	0.500 ± 0.005 (1.2700 ± 0.0127)	
3/4-MOD	0.750 ± 0.005 (1.9050 ± 0.0127)	
1.5-MOD	1.500 ± 0.005 (3.8100 ± 0.0127)	
1/16-REF	0.0625 ± 0.0005 (0.15875 ± 0.00127)	
1-REF	1.000 ± 0.005 (2.5400 ± 0.0127)	

Table 36: Mass and dimension measurements of the 1/8-MOD parts (see Figure 19).

Part ID	Mass (g)	Thickness, *b* [in. (cm)]	Diameter, *a* [in. (cm)]		
			Min	Max	Average
1/8-MOD-1	343.0	0.1249 (0.3172)	14.9894	14.9979	14.9948 (38.0868)
1/8-MOD-2	342.1	0.1259 (0.3198)	14.9895	14.9991	14.9947 (38.0865)
1/8-MOD-3	344.0	0.1253 (0.3183)	14.9894	14.9993	14.9950 (38.0873)
1/8-MOD-4	344.3	0.1251 (0.3178)	14.9878	14.9999	14.9944 (38.0858)
1/8-MOD-5	343.0	0.1246 (0.3165)	14.9913	14.9995	14.9955 (38.0886)
1/8-MOD-6	344.7	0.1255 (0.3188)	14.9934	15.0018	14.9965 (38.0911)
1/8-MOD-7	345.0	0.1248 (0.3170)	14.9908	15.0017	14.9959 (38.0896)
1/8-MOD-8	345.2	0.1251 (0.3178)	14.9901	15.0003	14.9956 (38.0888)
1/8-MOD-9	343.4	0.1248 (0.3170)	14.9885	14.9969	14.9940 (38.0848)
1/8-MOD-10	343.5	0.1266 (0.3216)	14.9904	15.0004	14.9962 (38.0903)
1/8-MOD-11	343.2	0.1249 (0.3172)	14.9901	14.9998	14.9954 (38.0883)
1/8-MOD-12	344.6	0.1264 (0.3211)	14.9876	15.0001	14.9951 (38.0876)
1/8-MOD-13	343.9	0.1250 (0.3175)	14.9895	15.0002	14.9945 (38.0860)
1/8-MOD-14	345.4	0.1259 (0.3198)	14.9908	15.0006	14.9964 (38.0909)
1/8-MOD-15	345.3	0.1256 (0.3190)	14.9927	14.9986	14.9961 (38.0901)
1/8-MOD-16	343.8	0.1247 (0.3167)	14.9931	15.0005	14.9972 (38.0929)
1/8-MOD-17	344.0	0.1253 (0.3183)	14.9921	14.9991	14.9957 (38.0891)
1/8-MOD-18	344.7	0.1255 (0.3188)	14.9917	15.0000	14.9964 (38.0909)
1/8-MOD-19	350.8	0.1275 (0.3239)	14.9917	15.0013	14.9967 (38.0916)
1/8-MOD-20	350.2	0.1280 (0.3251)	14.9888	14.9980	14.9943 (38.0855)
1/8-MOD-21	350.6	0.1285 (0.3264)	14.9893	14.9995	14.9953 (38.0881)
1/8-MOD-22	351.0	0.1274 (0.3236)	14.9905	15.0001	14.9961 (38.0901)
1/8-MOD-23	351.4	0.1274 (0.3236)	14.9899	14.9998	14.9955 (38.0886)
1/8-MOD-24	351.4	0.1271 (0.3228)	14.9916	14.9987	14.9958 (38.0893)
1/8-MOD-25	349.4	0.1268 (0.3221)	14.9903	14.9995	14.9951 (38.0876)
1/8-MOD-26	351.9	0.1269 (0.3223)	14.9919	15.0000	14.9957 (38.0891)
1/8-MOD-27	349.3	0.1263 (0.3208)	14.9937	15.0004	14.9965 (38.0911)
1/8-MOD-28	349.3	0.1272 (0.3231)	14.9922	15.0015	14.9974 (38.0934)
1/8-MOD-29	347.9	0.1314 (0.3338)	14.9894	14.9999	14.9957 (38.0891)
1/8-MOD-30	348.3	0.1283 (0.3259)	14.9908	15.0003	14.9950 (38.0873)
1/8-MOD-31	351.1	0.1268 (0.3221)	14.9886	14.9990	14.9953 (38.0881)
1/8-MOD-32	348.8	0.1270 (0.3226)	14.9890	14.9992	14.9952 (38.0878)
1/8-MOD-33	350.0	0.1271 (0.3228)	14.9892	14.9990	14.9948 (38.0868)
1/8-MOD-34	351.3	0.1277 (0.3244)	14.9880	14.9979	14.9942 (38.0853)
1/8-MOD-35	351.2	0.1288 (0.3272)	14.9909	14.9984	14.9957 (38.0891)
1/8-MOD-36	348.3	0.1306 (0.3317)	14.9908	15.0015	14.9965 (38.0911)
1/8-MOD-37	347.3	0.1293 (0.3284)	14.9922	15.0009	14.9963 (38.0906)
1/8-MOD-38	351.1	0.1321 (0.3355)	14.9923	15.0008	14.9973 (38.0931)
1/8-MOD-39	350.5	0.1276 (0.3241)	14.9864	15.0007	14.9946 (38.0863)

Table 37: Derived volumes and densities of the 1/8-MOD parts.

Part ID	Mass (g)	Volume (cm^3)	Density (g/cm^3)
1/8-MOD-1	**343.0**	**361.4388**	**0.9490**
1/8-MOD-2	342.1	364.3278	0.9390
1/8-MOD-3	344.0	362.6060	0.9487
1/8-MOD-4	344.3	361.9983	0.9511
1/8-MOD-5	343.0	360.6044	0.9512
1/8-MOD-6	344.7	363.2575	0.9489
1/8-MOD-7	345.0	361.2025	0.9551
1/8-MOD-8	345.2	362.0562	0.9534
1/8-MOD-9	343.4	361.1109	0.9510
1/8-MOD-10	343.5	366.4268	0.9374
1/8-MOD-11	343.2	361.4678	0.9495
1/8-MOD-12	344.6	365.7942	0.9421
1/8-MOD-13	343.9	361.7138	0.9508
1/8-MOD-14	345.4	364.4104	0.9478
1/8-MOD-15	345.3	363.5275	0.9499
1/8-MOD-16	343.8	360.9756	0.9524
1/8-MOD-17	344.0	362.6399	0.9486
1/8-MOD-18	344.7	363.2526	0.9489
1/8-MOD-19	350.8	369.0563	0.9505
1/8-MOD-20	350.2	370.3850	0.9455
1/8-MOD-21	350.6	371.8814	0.9428
1/8-MOD-22	351.0	368.7373	0.9519
1/8-MOD-23	351.4	368.7078	0.9531
1/8-MOD-24	351.4	367.8543	0.9553
1/8-MOD-25	349.4	366.9518	0.9522
1/8-MOD-26	351.9	367.2706	0.9581
1/8-MOD-27	349.3	365.5731	0.9555
1/8-MOD-28	349.3	368.2223	0.9486
1/8-MOD-29	347.9	380.2944	0.9148
1/8-MOD-30	348.3	371.2878	0.9381
1/8-MOD-31	351.1	366.9616	0.9568
1/8-MOD-32	348.8	367.5355	0.9490
1/8-MOD-33	350.0	367.8053	0.9516
1/8-MOD-34	351.3	369.5120	0.9507
1/8-MOD-35	351.2	372.7695	0.9421
1/8-MOD-36	348.3	378.0194	0.9214
1/8-MOD-37	347.3	374.2465	0.9280
1/8-MOD-38	351.1	382.4019	0.9181
1/8-MOD-39	350.5	369.2423	0.9492

Table 38: Mass and dimension measurements of the 1/4-MOD parts (see Figure 19).

Part ID	Mass (g)	Thickness, *b* [in. (cm)]	Diameter, *a* [in. (cm)]		
			Min	Max	Average
1/4-MOD-1	690.2	0.2512 (0.6380)	14.9835	14.9910	14.9879 (38.0693)
1/4-MOD-2	689.1	0.2532 (0.6431)	14.9821	14.9912	14.9866 (38.0660)
1/4-MOD-3	688.0	0.2497 (0.6342)	14.9804	14.9915	14.9853 (38.0627)
1/4-MOD-4	689.7	0.2558 (0.6497)	14.9824	14.9903	14.9868 (38.0665)
1/4-MOD-5	689.2	0.2555 (0.6490)	14.9822	14.9923	14.9869 (38.0667)
1/4-MOD-6	687.5	0.2539 (0.6449)	14.9806	14.9909	14.9862 (38.0649)
1/4-MOD-7	688.4	0.2531 (0.6429)	14.9792	14.9872	14.9843 (38.0601)
1/4-MOD-8	689.2	0.2524 (0.6411)	14.9786	14.9903	14.9855 (38.0632)
1/4-MOD-9	688.8	0.2540 (0.6452)	14.9850	14.9913	14.9883 (38.0703)
1/4-MOD-10	689.5	0.2514 (0.6386)	14.9792	14.9887	14.9844 (38.0604)
1/4-MOD-11	688.1	0.2499 (0.6347)	14.9790	14.9885	14.9849 (38.0616)
1/4-MOD-12	688.5	0.2516 (0.6391)	14.9842	14.9909	14.9872 (38.0675)
1/4-MOD-13	689.4	0.2511 (0.6378)	14.9806	14.9899	14.9864 (38.0655)
1/4-MOD-14	689.5	0.2507 (0.6368)	14.9803	14.9897	14.9858 (38.0639)
1/4-MOD-15	689.1	0.2515 (0.6388)	14.9806	14.9893	14.9858 (38.0639)
1/4-MOD-16	688.2	0.2532 (0.6431)	14.9815	14.9924	14.9872 (38.0675)
1/4-MOD-17	687.6	0.2605 (0.6617)	14.9796	14.9899	14.9851 (38.0622)
1/4-MOD-18	688.9	0.2530 (0.6426)	14.9812	14.9898	14.9859 (38.0642)
1/4-MOD-19	688.2	0.2547 (0.6469)	14.9769	14.9887	14.9838 (38.0589)
1/4-MOD-20	688.7	0.2599 (0.6601)	14.9814	14.9890	14.9860 (38.0644)
1/4-MOD-21	686.9	0.2600 (0.6604)	14.9804	14.9877	14.9840 (38.0594)
1/4-MOD-22	688.2	0.2605 (0.6617)	14.9817	14.9889	14.9851 (38.0622)
1/4-MOD-23	688.0	0.2499 (0.6347)	14.9775	14.9879	14.9841 (38.0596)
1/4-MOD-24	688.3	0.2528 (0.6421)	14.9810	14.9878	14.9854 (38.0629)
1/4-MOD-25	687.6	0.2525 (0.6414)	14.9800	14.9903	14.9849 (38.0616)
1/4-MOD-26	688.4	0.2542 (0.6457)	14.9812	14.9907	14.9860 (38.0644)
1/4-MOD-27	687.9	0.2574 (0.6538)	14.9803	14.9881	14.9849 (38.0616)
1/4-MOD-28	687.9	0.2595 (0.6591)	14.9820	14.9887	14.9857 (38.0637)
1/4-MOD-29	688.0	0.2621 (0.6657)	14.9830	14.9924	14.9864 (38.0655)
1/4-MOD-30	688.3	0.2594 (0.6589)	14.9837	14.9914	14.9870 (38.0670)
1/4-MOD-31	688.2	0.2515 (0.6388)	14.9821	14.9892	14.9861 (38.0647)
1/4-MOD-32	688.2	0.2509 (0.6373)	14.9807	14.9910	14.9859 (38.0642)
1/4-MOD-33	688.3	0.2511 (0.6378)	14.9815	14.9922	14.9871 (38.0672)
1/4-MOD-34	687.7	0.2581 (0.6556)	14.9810	14.9887	14.9849 (38.0616)
1/4-MOD-35	688.2	0.2583 (0.6561)	14.9830	14.9918	14.9879 (38.0693)
1/4-MOD-36	688.1	0.2576 (0.6543)	14.9833	14.9900	14.9875 (38.0683)

Table 39: Derived volumes and densities of the 1/4-MOD parts.

Part ID	Mass (g)	Volume (cm^3)	Density (g/cm^3)
1/4-MOD-1	**690.2**	**726.2602**	**0.9503**
1/4-MOD-2	689.1	731.9155	0.9415
1/4-MOD-3	688.0	721.6730	0.9533
1/4-MOD-4	689.7	739.4510	0.9327
1/4-MOD-5	689.2	738.5936	0.9331
1/4-MOD-6	687.5	733.8998	0.9368
1/4-MOD-7	688.4	731.4019	0.9412
1/4-MOD-8	689.2	729.4959	0.9448
1/4-MOD-9	688.8	734.3946	0.9379
1/4-MOD-10	689.5	726.4990	0.9491
1/4-MOD-11	688.1	722.2125	0.9528
1/4-MOD-12	688.5	727.3487	0.9466
1/4-MOD-13	689.4	725.8258	0.9498
1/4-MOD-14	689.5	724.6115	0.9515
1/4-MOD-15	689.1	726.9238	0.9480
1/4-MOD-16	688.2	731.9741	0.9402
1/4-MOD-17	687.6	752.8666	0.9133
1/4-MOD-18	688.9	731.2691	0.9421
1/4-MOD-19	688.2	735.9764	0.9351
1/4-MOD-20	688.7	751.2228	0.9168
1/4-MOD-21	686.9	751.3113	0.9143
1/4-MOD-22	688.2	752.8666	0.9141
1/4-MOD-23	688.0	722.1354	0.9527
1/4-MOD-24	688.3	730.6422	0.9420
1/4-MOD-25	687.6	729.7265	0.9423
1/4-MOD-26	688.4	734.7474	0.9369
1/4-MOD-27	687.9	743.8875	0.9247
1/4-MOD-28	687.9	750.0366	0.9172
1/4-MOD-29	688.0	757.6222	0.9081
1/4-MOD-30	688.3	749.8777	0.9179
1/4-MOD-31	688.2	726.9529	0.9467
1/4-MOD-32	688.2	725.1993	0.9490
1/4-MOD-33	688.3	725.8936	0.9482
1/4-MOD-34	687.7	745.9105	0.9220
1/4-MOD-35	688.2	746.7875	0.9215
1/4-MOD-36	688.1	744.7239	0.9240

Table 40: Mass and dimension measurements of the 1/2-MOD parts (see Figure 19).

Part ID	Mass (g)	Thickness, *b* [in. (cm)]	Diameter, *a* [in. (cm)]		
			Min	Max	Average
1/2-MOD-1	1377.9	0.5079 (1.2901)	14.9884	14.9953	14.9925 (38.0810)
1/2-MOD-2	1377.8	0.5047 (1.2819)	14.9866	14.9957	14.9909 (38.0769)
1/2-MOD-3	1385.0	0.5095 (1.2941)	14.9880	14.9951	14.9914 (38.0782)
1/2-MOD-4	1378.1	0.5044 (1.2812)	14.9877	14.9974	14.9926 (38.0812)
1/2-MOD-5	1380.2	0.5033 (1.2784)	14.9882	14.9950	14.9913 (38.0779)
1/2-MOD-6	1378.2	0.5003 (1.2708)	14.9870	14.9955	14.9910 (38.0771)
1/2-MOD-7	1383.7	0.5068 (1.2873)	14.9882	14.9963	14.9917 (38.0789)
1/2-MOD-8	1386.3	0.5047 (1.2819)	14.9854	14.9925	14.9888 (38.0716)
1/2-MOD-9	1385.4	0.5035 (1.2789)	14.9867	14.9912	14.9888 (38.0716)
1/2-MOD-10	1379.6	0.5045 (1.2814)	14.9861	14.9939	14.9890 (38.0721)
1/2-MOD-11	1384.5	0.5068 (1.2873)	14.9849	14.9937	14.9889 (38.0718)
1/2-MOD-12	1376.8	0.5005 (1.2713)	14.9867	14.9937	14.9901 (38.0749)
1/2-MOD-13	1385.5	0.5061 (1.2855)	14.9900	14.9961	14.9923 (38.0804)
1/2-MOD-14	1378.1	0.5079 (1.2901)	14.9841	14.9947	14.9884 (38.0705)
1/2-MOD-15	1381.5	0.5060 (1.2852)	14.9839	14.9936	14.9896 (38.0736)
1/2-MOD-16	1378.8	0.5063 (1.2860)	14.9848	14.9943	14.9891 (38.0723)
1/2-MOD-17	1378.8	0.5075 (1.2891)	14.9856	14.9942	14.9886 (38.0710)
1/2-MOD-18	1384.9	0.5127 (1.3023)	14.9840	14.9949	14.9892 (38.0726)
1/2-MOD-19	1380.5	0.5105 (1.2967)	14.9825	14.9922	14.9871 (38.0672)
1/2-MOD-20	1378.2	0.5016 (1.2741)	14.9862	14.9924	14.9893 (38.0728)
1/2-MOD-21	1379.3	0.5005 (1.2713)	14.9867	14.9921	14.9896 (38.0736)
1/2-MOD-22	1377.0	0.5030 (1.2776)	14.9858	14.9925	14.9888 (38.0716)
1/2-MOD-23	1385.3	0.5104 (1.2964)	14.9858	14.9934	14.9896 (38.0736)
1/2-MOD-24	1378.2	0.5092 (1.2934)	14.9854	14.9937	14.9887 (38.0713)
1/2-MOD-25	1385.6	0.5109 (1.2977)	14.9842	14.9920	14.9890 (38.0721)
1/2-MOD-26	1377.8	0.5066 (1.2868)	14.9837	14.9928	14.9870 (38.0670)
1/2-MOD-27	1385.1	0.5082 (1.2908)	14.9833	14.9934	14.9886 (38.0710)
1/2-MOD-28	1377.3	0.4996 (1.2690)	14.9855	14.9931	14.9889 (38.0718)
1/2-MOD-29	1376.3	0.5041 (1.2804)	14.9874	14.9942	14.9901 (38.0749)
1/2-MOD-30	1377.5	0.5084 (1.2913)	14.9857	14.9935	14.9900 (38.0746)
1/2-MOD-31	1377.8	0.5051 (1.2830)	14.9878	14.9952	14.9915 (38.0784)
1/2-MOD-32	1381.2	0.5073 (1.2885)	14.9862	14.9937	14.9889 (38.0718)

Table 41: Derived volumes and densities of the 1/2-MOD parts.

Part ID	Mass (g)	Volume (cm^3)	Density (g/cm^3)
1/2-MOD-1	**1377.9**	**1469.3233**	**0.9378**
1/2-MOD-2	1377.8	1459.7543	0.9439
1/2-MOD-3	1385.0	1473.7357	0.9398
1/2-MOD-4	1378.1	1459.2175	0.9444
1/2-MOD-5	1380.2	1455.7827	0.9481
1/2-MOD-6	1378.2	1447.0474	0.9524
1/2-MOD-7	1383.7	1465.9846	0.9439
1/2-MOD-8	1386.3	1459.3453	0.9499
1/2-MOD-9	1385.4	1455.8755	0.9516
1/2-MOD-10	1379.6	1458.8059	0.9457
1/2-MOD-11	1384.5	1465.4370	0.9448
1/2-MOD-12	1376.8	1447.4520	0.9512
1/2-MOD-13	1385.5	1464.0769	0.9463
1/2-MOD-14	1378.1	1468.5198	0.9384
1/2-MOD-15	1381.5	1463.2605	0.9441
1/2-MOD-16	1378.8	1464.0303	0.9418
1/2-MOD-17	1378.8	1467.4024	0.9396
1/2-MOD-18	1384.9	1482.5565	0.9341
1/2-MOD-19	1380.5	1475.7812	0.9354
1/2-MOD-20	1378.2	1450.4784	0.9502
1/2-MOD-21	1379.3	1447.3554	0.9530
1/2-MOD-22	1377.0	1454.4297	0.9468
1/2-MOD-23	1385.3	1475.9845	0.9386
1/2-MOD-24	1378.2	1472.3375	0.9361
1/2-MOD-25	1385.6	1477.3121	0.9379
1/2-MOD-26	1377.8	1464.4874	0.9408
1/2-MOD-27	1385.1	1469.4264	0.9426
1/2-MOD-28	1377.3	1444.6179	0.9534
1/2-MOD-29	1376.3	1457.8633	0.9441
1/2-MOD-30	1377.5	1470.2793	0.9369
1/2-MOD-31	1377.8	1461.0281	0.9430
1/2-MOD-32	1381.2	1466.8828	0.9416

Table 42: Mass and dimension measurements of the 3/4-MOD parts (see Figure 19).

Part ID	Mass (g)	Thickness, *b* [in. (cm)]	Diameter, *a* [in. (cm)]
3/4-MOD-1	2117.4	0.7700 (1.95580)	14.9900 (38.07460)
3/4-MOD-2	2117.2	0.7638 (1.93993)	14.9970 (38.09238)
3/4-MOD-3	2116.9	0.7758 (1.97041)	14.9920 (38.07968)
3/4-MOD-4	2116.6	0.7643 (1.94120)	14.9960 (38.08984)
3/4-MOD-5	2107.7	0.7683 (1.95136)	14.9960 (38.08984)
3/4-MOD-6	2115.7	0.7658 (1.94501)	14.9940 (38.08476)
3/4-MOD-7	2116.7	0.7608 (1.93231)	14.9940 (38.08476)
3/4-MOD-8	2116.2	0.7570 (1.92278)	14.9970 (38.09238)
3/4-MOD-9	2116.9	0.7573 (1.92342)	14.9960 (38.08984)
3/4-MOD-10	2112.5	0.7598 (1.92977)	14.9970 (38.09238)
3/4-MOD-11	2111.8	0.7548 (1.91707)	14.9960 (38.08984)
3/4-MOD-12	2112.3	0.7555 (1.91897)	14.9970 (38.09238)
3/4-MOD-13	2116.3	0.7588 (1.92723)	14.9920 (38.07968)
3/4-MOD-14	2118.1	0.7630 (1.93802)	14.9940 (38.08476)
3/4-MOD-15	2117.0	0.7630 (1.93802)	14.9980 (38.09492)
3/4-MOD-16	2109.6	0.7545 (1.91643)	14.9950 (38.08730)
3/4-MOD-17	2112.5	0.7558 (1.91961)	14.9980 (38.09492)
3/4-MOD-18	2117.1	0.7648 (1.94247)	14.9960 (38.08984)
3/4-MOD-19	2117.1	0.7643 (1.94120)	14.9960 (38.08984)
3/4-MOD-20	2119.2	0.7650 (1.94310)	14.9980 (38.09492)
3/4-MOD-21	2117.7	0.7693 (1.95390)	14.9980 (38.09492)
3/4-MOD-22	2118.0	0.7653 (1.94374)	14.9970 (38.09238)

Table 43: Derived volumes and densities of the 3/4-MOD parts.

Part ID	Mass (g)	Volume (cm^3)	Density (g/cm^3)
3/4-MOD-1	**2117.4**	**2226.8195**	**0.9509**
3/4-MOD-2	2117.2	2210.8081	0.9577
3/4-MOD-3	2116.9	2244.0471	0.9433
3/4-MOD-4	2116.6	2211.9604	0.9569
3/4-MOD-5	2107.7	2223.5375	0.9479
3/4-MOD-6	2115.7	2215.7107	0.9549
3/4-MOD-7	2116.7	2201.2431	0.9616
3/4-MOD-8	2116.2	2191.2690	0.9657
3/4-MOD-9	2116.9	2191.7003	0.9659
3/4-MOD-10	2112.5	2199.2294	0.9606
3/4-MOD-11	2111.8	2184.4646	0.9667
3/4-MOD-12	2112.3	2186.9270	0.9659
3/4-MOD-13	2116.3	2194.8704	0.9642
3/4-MOD-14	2118.1	2207.7535	0.9594
3/4-MOD-15	2117.0	2208.9316	0.9584
3/4-MOD-16	2109.6	2183.4498	0.9662
3/4-MOD-17	2112.5	2187.9424	0.9655
3/4-MOD-18	2117.1	2213.4075	0.9565
3/4-MOD-19	2117.1	2211.9604	0.9571
3/4-MOD-20	2119.2	2214.7217	0.9569
3/4-MOD-21	2117.7	2227.0257	0.9509
3/4-MOD-22	2118.0	2215.1501	0.9561

Table 44: Mass and dimension measurements of the 1.5-MOD parts (see Figure 19).

Part ID	Mass (g)	Thickness, *b* [in. (cm)]	Diameter, *a* [in. (cm)]		
			Min	Max	Average
1.5-MOD-1	4150.8	1.4998 (3.8095)	14.9962	15.0107	15.0035 (38.1089)
1.5-MOD-2	4132.6	1.5100 (3.8354)	14.9968	14.9977	14.9933 (38.0830)
1.5-MOD-3	4125.6	1.5087 (3.8321)	14.9846	14.9962	14.9988 (38.0970)
1.5-MOD-4	4136.2	1.5146 (3.8471)	14.9879	15.0005	14.9946 (38.0863)
1.5-MOD-5	4147.2	1.4945 (3.7960)	14.9967	15.0075	15.0038 (38.1097)
1.5-MOD-6	4173.6	1.5086 (3.8318)	14.9811	14.9896	14.9859 (38.0642)
1.5-MOD-7	4167.4	1.5241 (3.8712)	14.9851	14.9984	14.9913 (38.0779)
1.5-MOD-8	4175.3	1.5105 (3.8367)	14.9803	14.9896	14.9856 (38.0634)
1.5-MOD-9	4135.6	1.5027 (3.8169)	14.9879	14.9949	14.9917 (38.0789)
1.5-MOD-10	4168.4	1.5103 (3.8362)	14.9784	14.9898	14.9841 (38.0596)
1.5-MOD-11	4171.2	1.5263 (3.8768)	14.9827	14.9948	14.9887 (38.0713)
1.5-MOD-12	4146.4	1.5188 (3.8578)	14.9915	15.0022	14.9965 (38.0911)

Table 45: Derived volumes and densities of the 1.5-MOD parts.

Part ID	Mass (g)	Volume (cm^3)	Density (g/cm^3)
1.5-MOD-1	**4150.8**	**4345.1977**	**0.9553**
1.5-MOD-2	4132.6	4368.8028	0.9459
1.5-MOD-3	4125.6	4368.2446	0.9445
1.5-MOD-4	4136.2	4382.8717	0.9437
1.5-MOD-5	4147.2	4330.0158	0.9578
1.5-MOD-6	4173.6	4360.4448	0.9572
1.5-MOD-7	4167.4	4408.4212	0.9453
1.5-MOD-8	4175.3	4365.7618	0.9564
1.5-MOD-9	4135.6	4346.7542	0.9514
1.5-MOD-10	4168.4	4364.3099	0.9551
1.5-MOD-11	4171.2	4413.2535	0.9452
1.5-MOD-12	4146.4	4396.1393	0.9432

Table 46: Mass and dimension measurements of the reflector plate parts (see Figure 19).

Part ID	Mass (g)	Thickness, *b* [in. (cm)]	Diameter, *a* [in. (cm)]		
			Min	Max	Average
1/32-REF-1	85.0	0.0334 (0.0848)	14.9832	14.9996	14.9908 (38.0766)
1/32-REF-2	85.9	0.0325 (0.0826)	14.9833	14.9983	14.9905 (38.0759)
1/16-REF-1	182.4	0.0728 (0.1849)	14.9831	14.9890	14.9858 (38.0639)
1/16-REF-2	182.9	0.0671 (0.1704)	14.9829	14.9884	14.9856 (38.0634)
1-REF-1	2766.9	0.9995 (2.5387)	14.9860	14.9934	14.9902 (38.0751)
1-REF-2	2767.2	1.0015 (2.5438)	14.9844	14.9922	14.9883 (38.0703)

1.2.5.2 Reflector Rings

The polyethylene reflector rings are annular cylinders with varying thicknesses and a nominal inner and outer diameter of 15.1 in. (38.354 cm) and 17.1 in. (43.434 cm), respectively. Figure 20 shows a schematic of the reflector ring part. The reflector rings have four nominal thicknesses: 0.25 in. (0.635 cm), 0.5 in. (1.27 cm), 1 in. (2.54 cm), and 3 in. (7.62 cm). The reflector rings stack around the core stack to provide a nominal 1 in. (2.54 cm) reflector. They are designed to interlock, using step joints, which keep the rings in alignment as they are stacked and reduce neutron streaming paths, shown in Figure 18. The step joints have a nominal height of 0.125 in. (0.3175 cm), identified as label *g* in Figure 20. On the lower half of the experiment, the reflector rings interlock with the bottom reflector (BOTREF). On the upper half of the experiment, the reflector rings sit on the bottom reflector cap (BOTCAP).

Table 47 reports the mass and dimensional measurements of the polyethylene reflector rings. A description of these measurements is included in Section 1.2.5.

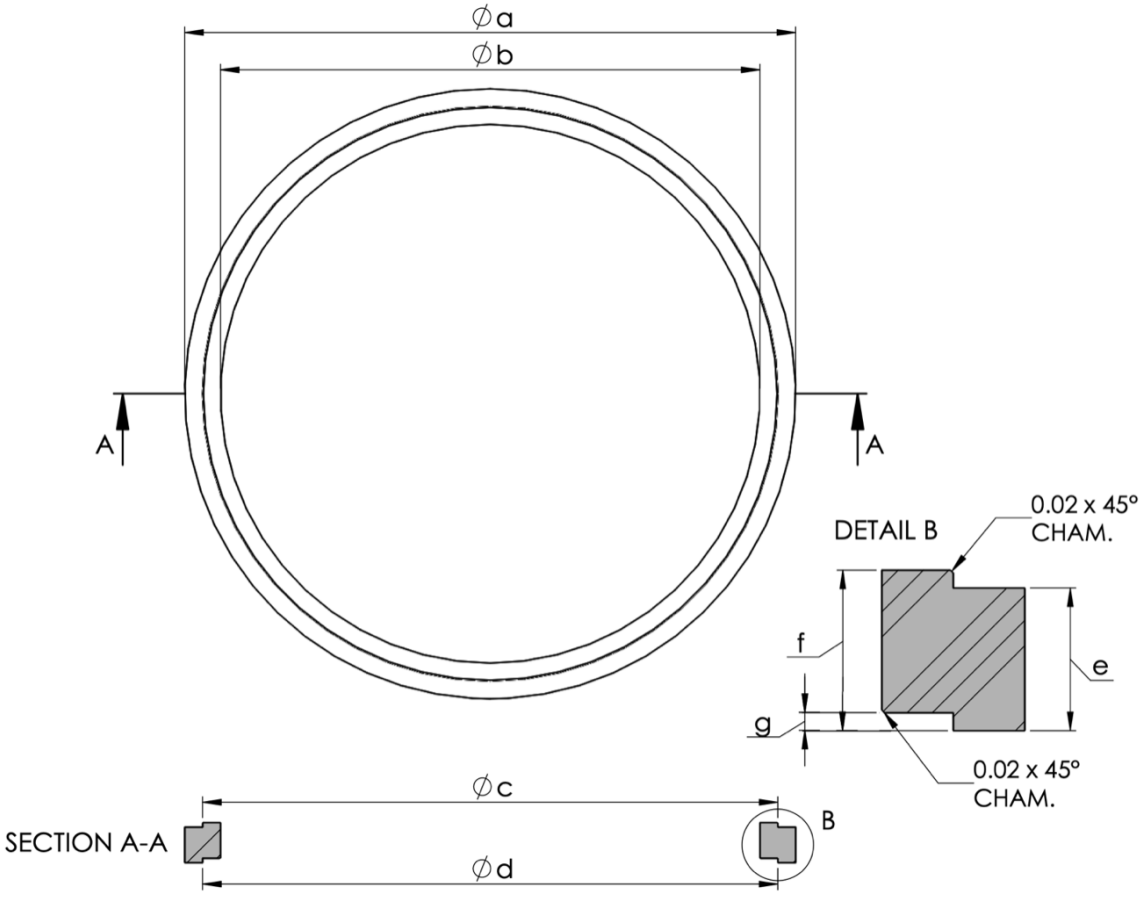

Figure 20: Schematic of the polyethylene reflector ring (dimensions in inches).

Table 47: Mass and dimensions of the reflector ring parts (see Figure 20).

Part ID	Mass (g)	Outer Diameter, *a* [in. (cm)]			Inner Diameter, *b* [in. (cm)]		
		Min	Max	Average	Min	Max	Average
1/4-RING-1	199.1	17.0822	17.1050	17.0933 (43.4170)	15.0657	15.0912	15.0789 (38.3004)
1/4-RING-2	198.9	17.0821	17.1019	17.0927 (43.4155)	15.0690	15.0925	15.0813 (38.3065)
1/4-RING-3	198.7	17.0816	17.1060	17.0939 (43.4185)	15.0699	15.0912	15.0811 (38.3060)
1/4-RING-4	199.4	17.0838	17.1047	17.0937 (43.4180)	15.0681	15.0897	15.0792 (38.3012)
1/2-RING-1	394.1	17.0770	17.0870	17.0818 (43.3878)	15.0620	15.0728	15.0670 (38.2702)
1/2-RING-2	394.4	17.0802	17.0854	17.0830 (43.3908)	15.0660	15.0729	15.0682 (38.2732)
1/2-RING-3	392.9	17.0806	17.0855	17.0828 (43.3903)	15.0652	15.0721	15.0680 (38.2727)
1/2-RING-4	393.3	17.0793	17.0865	17.0822 (43.3888)	15.0650	15.0703	15.0676 (38.2717)
1-RING-1	805.8	17.0787	17.0852	17.0824 (43.3893)	15.0605	15.0691	15.0660 (38.2676)
1-RING-2	805.8	17.0745	17.0781	17.0767 (43.3748)	15.0572	15.0629	15.0609 (38.2547)
1-RING-3	805.8	17.0808	17.0888	17.0837 (43.3926)	15.0622	15.0700	15.0666 (38.2692)
1-RING-4	804.9	17.0696	17.0766	17.0729 (43.3652)	15.0509	15.0606	15.0560 (38.2422)
1-RING-5	804.8	17.0812	17.0868	17.0839 (43.3931)	15.0671	15.0714	15.0691 (38.2755)
1-RING-6	805.8	17.0775	17.0810	17.0788 (43.3802)	15.0595	15.0647	15.0624 (38.2585)
3-RING-1	2384.7	17.0879	17.0916	17.0898 (43.4081)	15.0875	15.0912	15.0896 (38.3276)
3-RING-2	2387.0	17.0877	17.0923	17.0896 (43.4076)	15.0891	15.0932	15.0910 (38.3311)
3-RING-3	2388.8	17.0872	17.0938	17.0915 (43.4124)	15.0880	15.0913	15.0898 (38.3281)
3-RING-4	2388.1	17.0887	17.0928	17.0912 (43.4116)	15.0873	15.0922	15.0905 (38.3299)
3-RING-5	2384.2	17.0855	17.0915	17.0888 (43.4056)	15.0894	15.0928	15.0913 (38.3319)
3-RING-6	2384.7	17.0861	17.0933	17.0892 (43.4066)	15.0877	15.0933	15.0909 (38.3309)

Table 47 (continued): Mass and dimensions of the reflector ring parts (see Figure 20).

Part ID	Top Step Diameter, *c* [in. (cm)]			Bottom Step Diameter, *d* [in. (cm)]		
	Min	**Max**	**Average**	**Min**	**Max**	**Average**
1/4-RING-1	16.0527	16.0778	16.0654 (40.8061)	16.0876	16.1120	16.0990 (40.8915)
1/4-RING-2	16.0532	16.0787	16.0654 (40.8061)	16.0906	16.1096	16.1003 (40.8948)
1/4-RING-3	16.0491	16.0743	16.0630 (40.8000)	16.0896	16.1120	16.1010 (40.8965)
1/4-RING-4	16.0509	16.0746	16.0634 (40.8010)	16.0895	16.1082	16.0993 (40.8922)
1/2-RING-1	16.0480	16.0596	16.0537 (40.7764)	16.0836	16.0956	16.0895 (40.8673)
1/2-RING-2	16.0507	16.0575	16.0533 (40.7754)	16.0871	16.0919	16.0894 (40.8671)
1/2-RING-3	16.0471	16.0528	16.0496 (40.7660)	16.0894	16.0965	16.0922 (40.8742)
1/2-RING-4	16.0495	16.0543	16.0515 (40.7708)	16.0880	16.0938	16.0904 (40.8696)
1-RING-1	16.0564	16.0653	16.0615 (40.7962)	16.0800	16.0845	16.0824 (40.8493)
1-RING-2	16.0517	16.0575	16.0550 (40.7797)	16.0897	16.0939	16.0923 (40.8744)
1-RING-3	16.0590	16.0661	16.0628 (40.7995)	16.0799	16.0862	16.0823 (40.8490)
1-RING-4	16.0420	16.0531	16.0485 (40.7632)	16.0989	16.1075	16.1037 (40.9034)
1-RING-5	16.0624	16.0693	16.0653 (40.8059)	16.0850	16.0906	16.0880 (40.8635)
1-RING-6	16.0554	16.0604	16.0581 (40.7876)	16.0915	16.0967	16.0934 (40.8772)
3-RING-1	16.0726	16.0780	16.0742 (40.8285)	16.0975	16.1006	16.0993 (40.8922)
3-RING-2	16.0713	16.0748	16.0729 (40.8252)	16.0982	16.1025	16.1000 (40.8940)
3-RING-3	16.0685	16.0751	16.0713 (40.8211)	16.0970	16.1014	16.0994 (40.8925)
3-RING-4	16.0714	16.0751	16.0738 (40.8275)	16.0981	16.1035	16.1007 (40.8958)
3-RING-5	16.0710	16.0733	16.0720 (40.8229)	16.0994	16.1029	16.1014 (40.8976)
3-RING-6	16.0710	16.0736	16.0722 (40.8234)	16.1022	16.1048	16.1033 (40.9024)

Table 47 (continued): Mass and dimensions of the reflector ring parts (see Figure 20).

Part ID	**Outer Edge Height, *e* [in. (cm)]**	**Inner Edge Height, *f* [in. (cm)]**	**Bottom Step Height, *g* [in. (cm)]**
1/4-RING-1	0.2568 (0.6523)	0.3727 (0.9467)	0.1205 (0.3061)
1/4-RING-2	0.2585 (0.6566)	0.3748 (0.9520)	0.1209 (0.3071)
1/4-RING-3	0.2575 (0.6541)	0.3721 (0.9451)	0.1205 (0.3061)
1/4-RING-4	0.2566 (0.6518)	0.3711 (0.9426)	0.1199 (0.3045)
1/2-RING-1	0.5027 (1.2769)	0.6140 (1.5596)	0.1198 (0.3043)
1/2-RING-2	0.5042 (1.2807)	0.6156 (1.5636)	0.1205 (0.3061)
1/2-RING-3	0.5053 (1.2835)	0.6166 (1.5662)	0.1179 (0.2995)
1/2-RING-4	0.5050 (1.2827)	0.6156 (1.5636)	0.1184 (0.3007)
1-RING-1	1.0016 (2.5441)	1.1275 (2.8639)	0.1219 (0.3096)
1-RING-2	1.0036 (2.5491)	1.1256 (2.8590)	0.1196 (0.3038)
1-RING-3	1.0014 (2.5436)	1.1268 (2.8621)	0.1219 (0.3096)
1-RING-4	1.0052 (2.5532)	1.1232 (2.8529)	0.1161 (0.2949)
1-RING-5	0.9991 (2.5377)	1.1252 (2.8580)	0.1205 (0.3061)
1-RING-6	1.0036 (2.5491)	1.1255 (2.8588)	0.1190 (0.3023)
3-RING-1	2.9952 (7.6078)	3.1229 (7.9322)	0.1231 (0.3127)
3-RING-2	2.9957 (7.6091)	3.1223 (7.9306)	0.1230 (0.3124)
3-RING-3	2.9974 (7.6134)	3.1235 (7.9337)	0.1232 (0.3129)
3-RING-4	2.9953 (7.6081)	3.1223 (7.9306)	0.1225 (0.3112)
3-RING-5	2.9961 (7.6101)	3.1243 (7.9357)	0.1231 (0.3127)
3-RING-6	2.9951 (7.6076)	3.1226 (7.9314)	0.1224 (0.3109)

1.2.5.3 Reflector Caps

The polyethylene reflector caps are rings with varying thicknesses. They may have step joints to mate with the annular reflectors to cap the top or bottom of the annular reflector. The purpose of the caps is to end the annular reflector, otherwise there would be an open step joint left the the top of each half stack. They have a nominal inner and outer diameter of 15.1 in. (38.354 cm) and 17.1 in. (43.434 cm), respectively. The polyethylene bottom reflector caps (BOTCAP) are rings with a nominal thickness of 0.125 in. (0.3175 cm) and inner and outer diameter of 15.1 in. (38.354 cm) and 16.05 in. (40.767 cm), respectively. Figures 21 and 22 show a schematic of the reflector cap part types. The reflector caps provide fine height adjustment on the top of the reflector rings while the bottom reflector caps serve as the base for the first reflector ring in upper half of the experiment on the membrane. The reflector caps allow the ring reflector to be brought to within 0.03125 in. (0.079375 cm) of the top reflector height. Like the polyethylene reflector rings, the step joints have a nominal height of 0.125 in. (0.3175 cm). There is also a zero-height reflector cap (0-CAP) with a nominal thickness of 0.125 in. (0.3175 cm) and inner and outer diameter of 16.08 in. (40.8432 cm) and 17.1 in. (43.434 cm), respectively. The zero-height reflector cap finishes the top of the reflector rings without adding any additional assembly height.

Tables 48 and 49 report the mass and dimensional measurements of the polyethylene reflector caps. A description of these measurements is included in Section 1.2.5.

Table 48: Mass and dimensions of the 0-BOTCAP and 0-CAP parts (see Figure 22).

Part ID	**Mass (g)**	**Outer Diameter, *a* [in. (cm)]**	**Inner Diameter, *b* [in. (cm)]**	**Thickness, *d* [in. (cm)]**
0-BOTCAP-1	48.2	16.0530 (40.7746)	15.0660 (38.2676)	0.1310 (0.3327)
0-BOTCAP-2	48.0	16.0530 (40.7746)	15.0650 (38.2651)	0.1250 (0.3175)
0-CAP-1	50.7	17.0465 (43.2981)	16.0785 (40.8394)	0.1260 (0.3200)
0-CAP-2	50.8	17.0460 (43.2968)	16.0770 (40.8356)	0.1255 (0.3188)
0-CAP-3	50.9	17.0470 (43.2994)	16.0710 (40.8203)	0.1250 (0.3175)

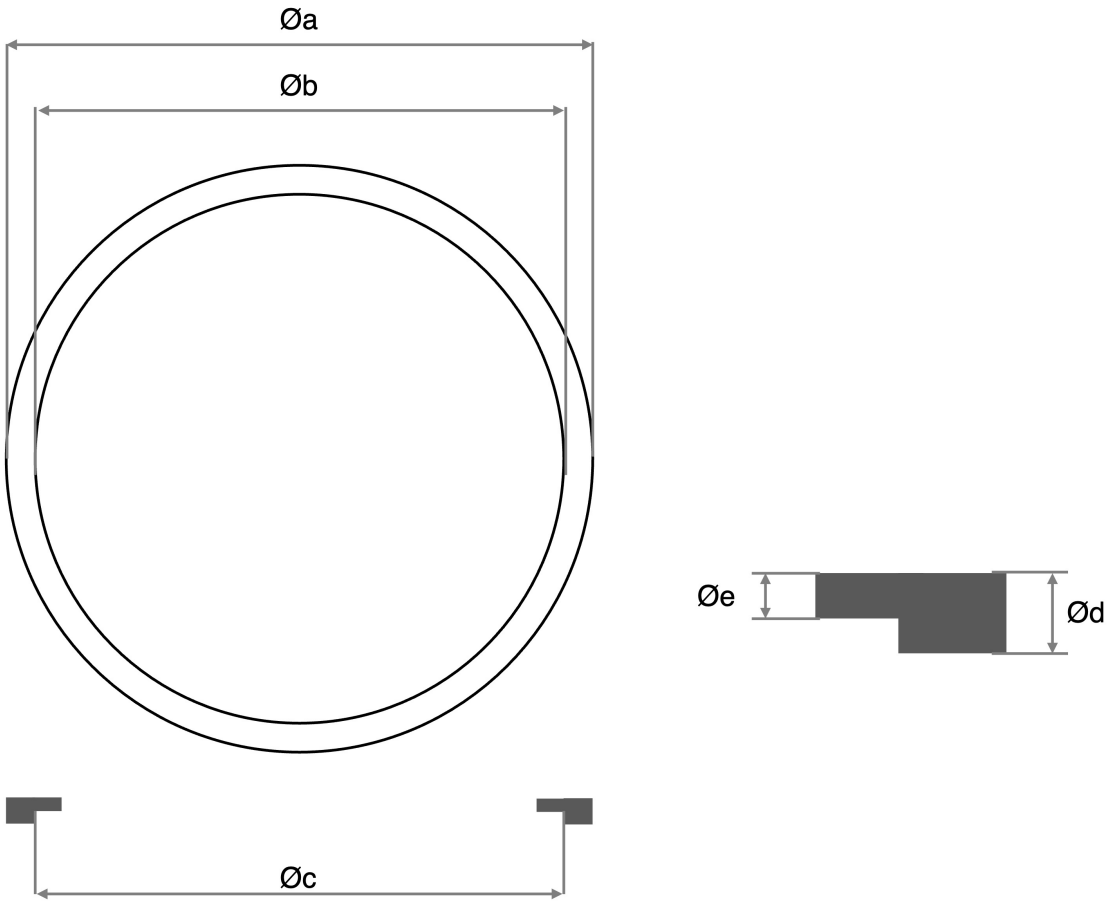

Figure 21: Diagram of the reflector cap (dimensions in inches)

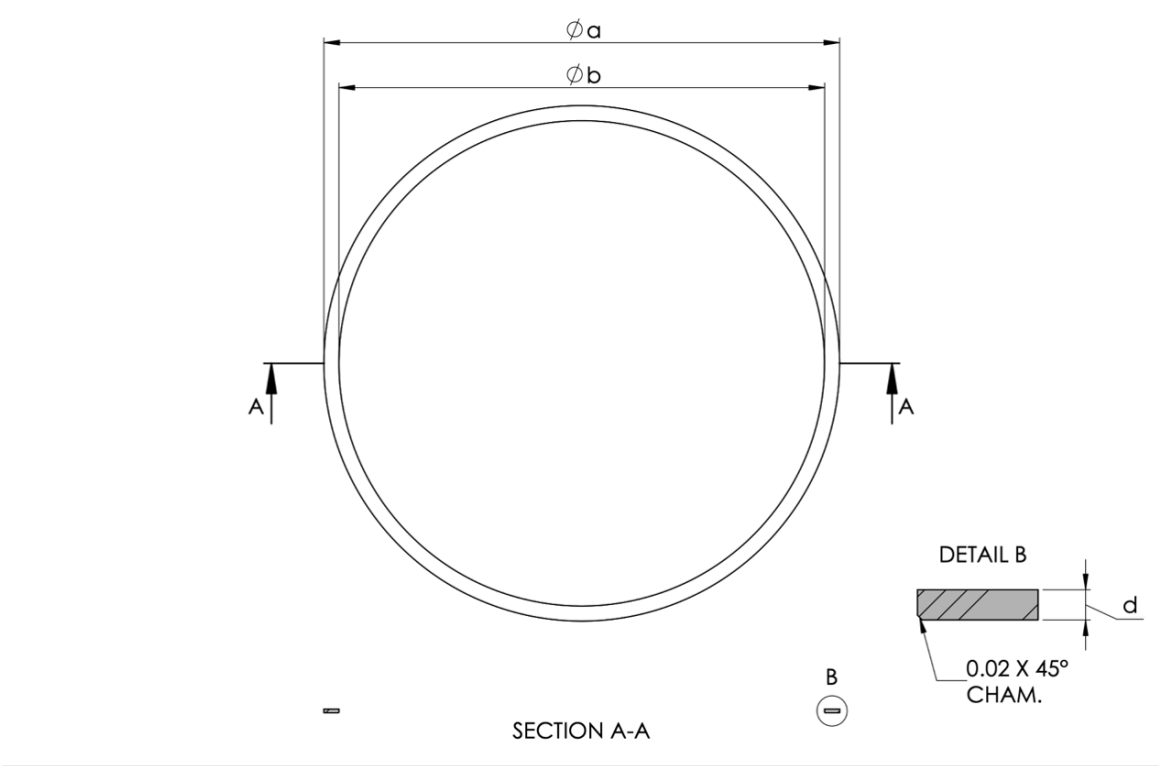

Figure 22: Diagram of the 0-BOTCAP and 0-CAP parts (dimensions in inches).

Table 49: Mass and dimensions of the reflector cap parts (see Figure 21).

Part ID	Mass (g)	Outer Diameter, *a* [in. (cm)]			Inner Diameter, *b* [in. (cm)]		
		Min	Max	Average	Min	Max	Average
1/32-CAP-1	76.8	17.0612	17.0763	17.0689 (43.3550)	15.0604	15.0828	15.0738 (38.2875)
1/32-CAP-2	76.8	17.0620	17.0804	17.0711 (43.3606)	15.0645	15.0875	15.0769 (38.2953)
1/32-CAP-3	76.9	17.0651	17.0758	17.0710 (43.3603)	15.0731	15.0847	15.0773 (38.2963)
1/16-CAP-1	101.5	17.0457	17.1074	17.0794 (43.3817)	15.0554	15.1168	15.0842 (38.3139)
1/16-CAP-2	101.2	17.0690	17.0906	17.0803 (43.3840)	15.0741	15.0933	15.0850 (38.3159)
1/16-CAP-3	101.0	17.0496	17.1070	17.0765 (43.3743)	15.0456	15.1037	15.0773 (38.2963)
3/32-CAP-1	127.9	17.0414	17.1020	17.0725 (43.3642)	15.0511	15.1100	15.0807 (38.3050)
3/32-CAP-2	126.7	17.0687	17.0734	17.0713 (43.3611)	15.0821	15.0893	15.0850 (38.3159)
3/32-CAP-3	127.5	17.0620	17.0836	17.0728 (43.3649)	15.0676	15.0920	15.0796 (38.3022)
1/8-CAP-1	149.0	17.0753	17.0845	17.0788 (43.3802)	15.0748	15.0873	15.0824 (38.3093)
1/8-CAP-2	148.9	17.0692	17.0909	17.0791 (43.3809)	15.0748	15.0921	15.0817 (38.3075)
1/8-CAP-3	149.0	17.0582	17.0977	17.0781 (43.3784)	15.0652	15.1004	15.0815 (38.3070)
5/32-CAP-1	173.7	17.0691	17.0927	17.0788 (43.3802)	15.0714	15.0913	15.0836 (38.3123)
5/32-CAP-2	173.7	17.0668	17.0892	17.0775 (43.3769)	15.0752	15.0944	15.0847 (38.3151)
5/32-CAP-3	172.9	17.0664	17.0908	17.0787 (43.3799)	15.0733	15.0934	15.0848 (38.3154)
3/16-CAP-1	198.2	17.0697	17.0946	17.0797 (43.3824)	15.0708	15.0966	15.0851 (38.3162)
3/16-CAP-2	194.1	17.0714	17.0906	17.0806 (43.3847)	15.0781	15.0972	15.0867 (38.3202)
3/16-CAP-3	193.9	17.0754	17.0867	17.0808 (43.3852)	15.0828	15.0950	15.0876 (38.3225)
7/32-CAP-1	225.4	17.0781	17.0919	17.0860 (43.3984)	15.0790	15.0933	15.0861 (38.3187)
7/32-CAP-2	225.2	17.0662	17.0774	17.0706 (43.3593)	15.0692	15.0857	15.0780 (38.2981)
7/32-CAP-3	225.6	17.0548	17.0841	17.0686 (43.3542)	15.0602	15.0909	15.0774 (38.2966)

Table 49 (continued): Mass and dimensions of the reflector cap parts (see Figure 21).

Part ID	Top Step (Male) Diameter, *c* [in. (cm)]			Outer Edge Height, *d* [in. (cm)]	Inner Edge Height, *e* [in. (cm)]
	Min	Max	Average		
1/32-CAP-1	16.0833	16.1000	16.0930 (40.8762)	0.1647 (0.4183)	0.0344 (0.0874)
1/32-CAP-2	16.0874	16.1030	16.0950 (40.8813)	0.1649 (0.4188)	0.0351 (0.0892)
1/32-CAP-3	16.0906	16.0989	16.0943 (40.8795)	0.1664 (0.4227)	0.0350 (0.0889)
1/16-CAP-1	16.0727	16.1328	16.1012 (40.8970)	0.1953 (0.4961)	0.0681 (0.1730)
1/16-CAP-2	16.0898	16.1123	16.1025 (40.9004)	0.1912 (0.4856)	0.0673 (0.1709)
1/16-CAP-3	16.0673	16.1258	16.0999 (40.8937)	0.1904 (0.4836)	0.0729 (0.1852)
3/32-CAP-1	16.0645	16.1234	16.0946 (40.8803)	0.2431 (0.6175)	0.1006 (0.2555)
3/32-CAP-2	16.0948	16.1025	16.0978 (40.8884)	0.2443 (0.6205)	0.1000 (0.2540)
3/32-CAP-3	16.0813	16.1057	16.0930 (40.8762)	0.2451 (0.6226)	0.1005 (0.2553)
1/8-CAP-1	16.0928	16.1036	16.0993 (40.8922)	0.2531 (0.6429)	0.1292 (0.3282)
1/8-CAP-2	16.0913	16.1076	16.0981 (40.8892)	0.2540 (0.6452)	0.1290 (0.3277)
1/8-CAP-3	16.0838	16.1214	16.1011 (40.8968)	0.2535 (0.6439)	0.1281 (0.3254)
5/32-CAP-1	16.0874	16.1091	16.0999 (40.8937)	0.2832 (0.7193)	0.1618 (0.4110)
5/32-CAP-2	16.0905	16.1128	16.1009 (40.8963)	0.2836 (0.7203)	0.1620 (0.4115)
5/32-CAP-3	16.0889	16.1098	16.1009 (40.8963)	0.2824 (0.7173)	0.1606 (0.4079)
3/16-CAP-1	16.0891	16.1102	16.1020 (40.8991)	0.3147 (0.7993)	0.1935 (0.4915)
3/16-CAP-2	16.0982	16.1164	16.1070 (40.9118)	0.3116 (0.7915)	0.1866 (0.4740)
3/16-CAP-3	16.1019	16.1163	16.1086 (40.9158)	0.3116 (0.7915)	0.1856 (0.4714)
7/32-CAP-1	16.0990	16.1155	16.1073 (40.9125)	0.3444 (0.8748)	0.2290 (0.5817)
7/32-CAP-2	16.0823	16.0973	16.0904 (40.8696)	0.3517 (0.8933)	0.2242 (0.5695)
7/32-CAP-3	16.0723	16.1012	16.0887 (40.8653)	0.3531 (0.8969)	0.2251 (0.5718)

1.2.5.4 Bottom Reflector

A set of new bottom reflector pieces (BOTREFSRC) were designed and procured for this experimental campaign, and moving forward with TEX-HEU-based designs. The new design, shown in Figure 23, includes a source cavity and a matching source insert, shown in Figure 24, which allows easy installation and removal of the source. The source holder, which is a solid piece of polyethylene during the benchmark measurements, known as the BLNKINSRT, fits within the cavity of the bottom reflector marked with the dimensions *e* and *f* of Figure 23. The thickness of the insert, labeled *j* in Figure 24, fits within the dimension *e* of Figure 23.

This design change compliments the design change of the adapter plate described in Section 1.2.2.2. The bottom reflectors have a nominal thickness of 1.00 in. (2.54 cm) (1.0-BOTREFSRC) and 1.50 in. (3.81 cm) (1.5-BOTREFSRC) and outer diameters of 17.1 in. (43.434 cm). Each bottom reflector has a feature that protrudes from the top surface with a thickness of 0.125 in. (0.3175 cm) and outer diameter of 16.08 in. (40.8432 cm). On the bottom of each part is a channel which may be filled with either the source holder or a solid plug. The channel has a nominal width of 0.563 in. (1.430 cm) and a depth of 0.50 in. (1.27 cm). Measurements of the mass and select features were perfomed with a CMM at LANL and are tabulated in Table 50.

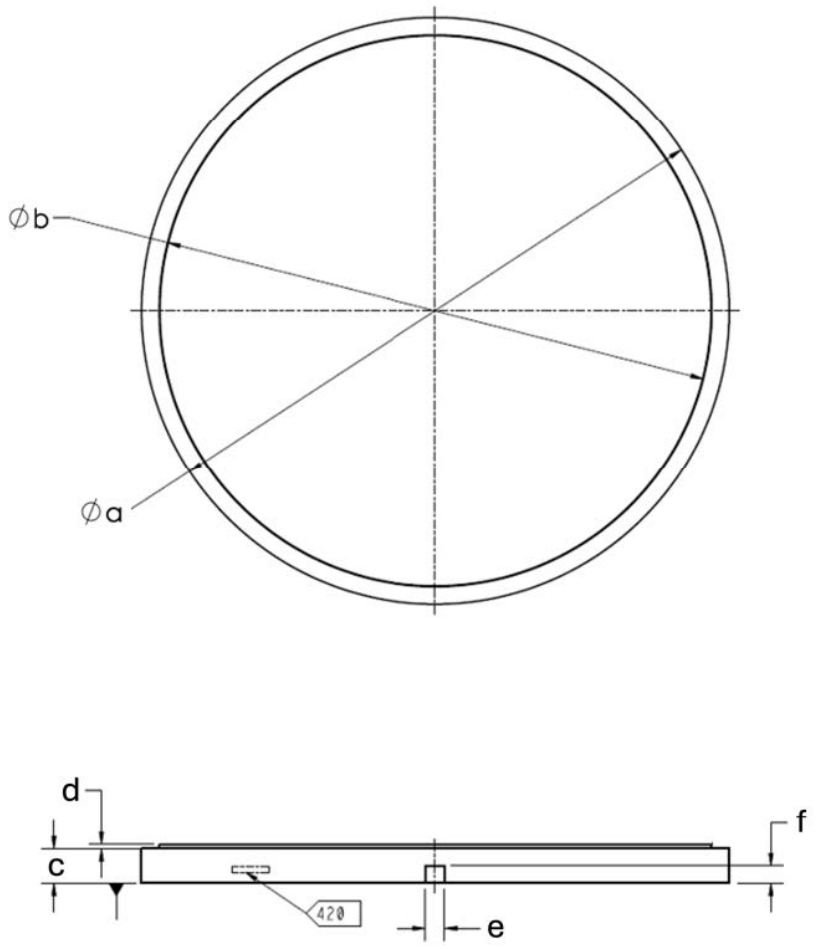

Figure 23: Diagram of the bottom reflector plate. The box labeled 420 represents the location of the part ID number.

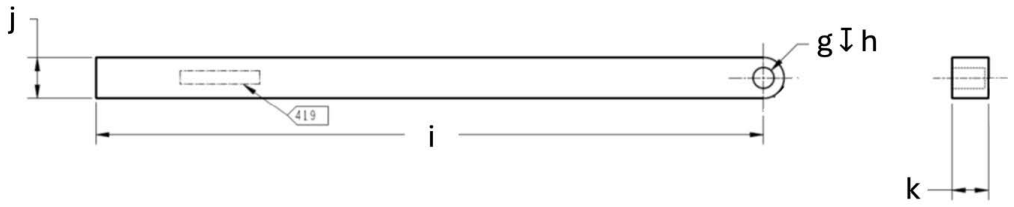

Figure 24: Diagram of the source and blank insert. The box labeled 419 represents the location of the part ID number.

Table 50: Mass and CMM measurements of the BOTREFSRC parts (see Figure 23).

Part ID	Mass (g)	Outer Diameter, *a* [in. (cm)]	Thickness, *c* [in. (cm)]		
			Measurement 1	Measurement 2	Average
1.0-BOTREFSRC-1	3976.0	17.0780 (43.37812)	1.0015 (2.54381)	1.0015 (2.54381)	1.0015 (2.54381)
1.0-BOTREFSRC-2	3976.7	17.0840 (43.39336)	1.0000 (2.54000)	1.0030 (2.54762)	1.0015 (2.54381)
1.5-BOTREFSRC-1	5783.6	17.0785 (43.37939)	1.4995 (3.80873)	1.4990 (3.80746)	1.4993 (3.80810)
1.5-BOTREFSRC-2	5784.7	17.0890 (43.40606)	1.5005 (3.81127)	1.4965 (3.80111)	1.4985 (3.80619)

Table 51: Hand measurements of the BOTREFSRC parts (see Figure 23).

Part ID	Outer Diameter, *a* [in. (cm)]	Thickness, *c* [in. (cm)]	Lip Diameter, *b* [in. (cm)]
1.0-BOTREFSRC-1	17.0950 (43.42130)	1.0020 (2.54508)	16.0750 (40.83050)
1.0-BOTREFSRC-2	17.0960 (43.42384)	1.0015 (2.54381)	16.0775 (40.83685)
1.5-BOTREFSRC-1	17.1000 (43.43400)	1.4970 (3.80238)	16.0840 (40.85336)
1.5-BOTREFSRC-2	17.0990 (43.43146)	1.4970 (3.80238)	16.0850 (40.85590)

Part ID	Lip Thickness, *d* [in. (cm)]	Slot Width, *e* [in. (cm)]	Slot Thickness, *f* [in. (cm)]
1.0-BOTREFSRC-1	0.126 (0.3200)	0.558 (1.4173)	0.500 (1.2700)
1.0-BOTREFSRC-2	0.128 (0.3239)	0.559 (1.4199)	0.497 (1.2624)
1.5-BOTREFSRC-1	0.127 (0.3226)	0.564 (1.4326)	0.504 (1.2802)
1.5-BOTREFSRC-2	0.127 (0.3226)	0.564 (1.4326)	0.501 (1.2725)

Table 52: Mass and CMM measurements of the SRCINSRT parts (see Figure 24).

Part ID	Mass (g)	Hole Diameter, *g* [in. (cm)]	Hole Depth, *i* [in. (cm)]
SRCINSRT-1	39.5	0.285 (0.7239)	0.439 (1.1138)
SRCINSRT-2	39.4	0.284 (0.7214)	0.438 (1.1113)
SRCINSRT-3	39.3	0.285 (0.7239)	0.436 (1.1074)
SRCINSRT-4	39.3	0.283 (0.7188)	0.440 (1.1163)
BLNKINSRT-1	38.6	-	-
BLNKINSRT-2	39.5	-	-
BLNKINSRT-3	39.8	-	-
BLNKINSRT-4	39.9	-	-

Part ID	Hole Distance or Length, *i* [in. (cm)]	Width, *j* [in. (cm)]	Thickness, *k* [in. (cm)]
SRCINSRT-1	9.012 (22.8905)	0.554 (1.4072)	0.492 (1.2497)
SRCINSRT-2	8.999 (22.8575)	0.554 (1.4072)	0.492 (1.2484)
SRCINSRT-3	9.005 (22.8727)	0.555 (1.4084)	0.492 (1.2497)
SRCINSRT-4	9.009 (22.8829)	0.554 (1.4072)	0.492 (1.2497)
BLNKINSRT-1	9.000 (22.8600)	0.554 (1.4072)	0.492 (1.2497)
BLNKINSRT-2	8.998 (22.8549)	0.556 (1.4122)	0.492 (1.2497)
BLNKINSRT-3	9.006 (22.8740)	0.554 (1.4072)	0.492 (1.2497)
BLNKINSRT-4	9.003 (22.8671)	0.555 (1.4084)	0.492 (1.2497)

1.2.6 Aluminum Inserts

Al-6061 inserts were placed in the annuli of the HEU plates to prevent sagging in the polyethylene moderator and reflectors, which may have formed due to the weight of the stack. The aluminum inserts have a nominal thickness of 0.125 in. (0.3175 cm) and varying diameters, reported in Table 53 and shown in Figure 53. The inserts are nominally 0.1 in. (0.254 cm) smaller in diameter than the corresponding HEU plate annuli: 2.5-DISK for 15/2.5-HEU, 6-DISK for 15/6-HEU, and 10-DISK for 15/10-HEU.

Table 54 reports the mass and dimensional measurements of the aluminum inserts. Table 55 reports the derived volumes and masses of the aluminum inserts. The dimensional measurements of the diameters and thicknesses were performed by LLNL's Dimensional Inspection Laboratory using a caliper having a precision of 0.0005 in..

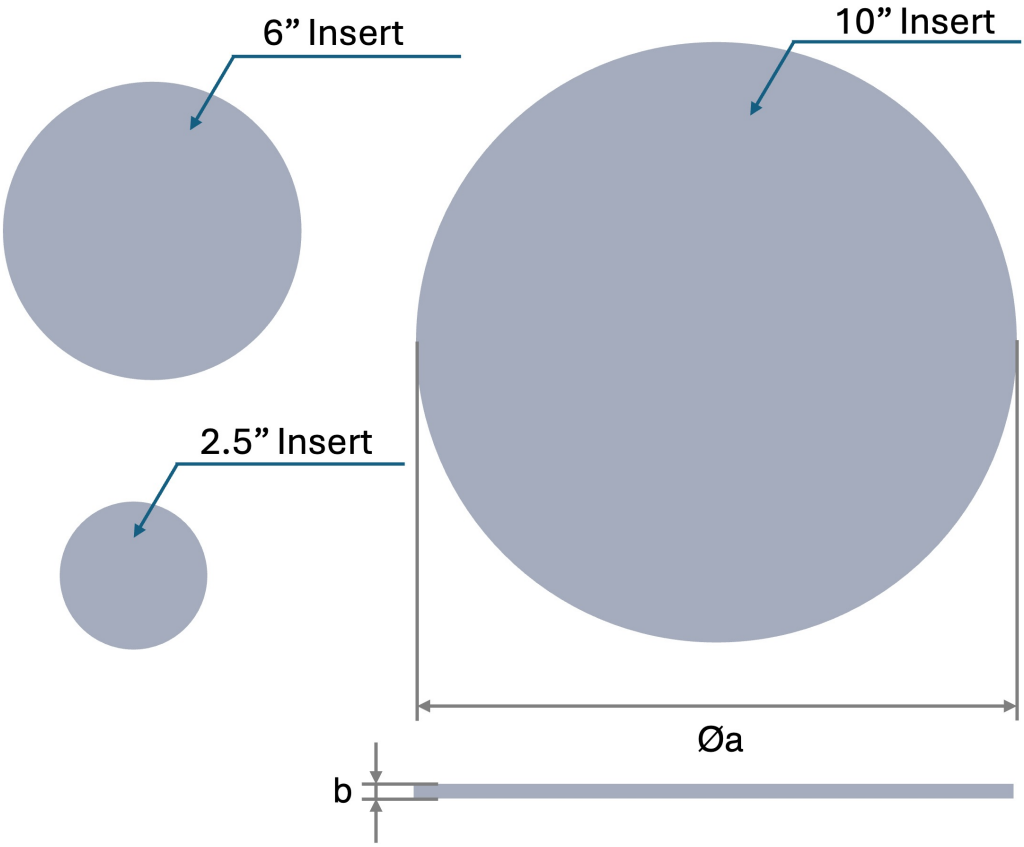

Figure 25: Schematic of the aluminum inserts.

Table 53: Aluminum insert nominal dimensions (see Fig. 25).

Part Type	**Diameter, *a* [in. (cm)]**	**Thickness, *b* [in. (cm)]**
2.5-DISK	2.4 (6.096)	0.125 (0.3175)
6-DISK	5.9 (14.986)	
10-DISK	9.9 (25.146)	

Table 54: Mass and dimensions of the aluminum insert parts (see Fig. 25).

Part Type	Mass (g)	Thickness, *b* [in. (cm)]	Diameter, *a* [in. (cm)]		
			Min	Max	Average
2.5-DISK-1	24.6	0.1240 (0.3150)	2.3945	2.3945	2.3945 (6.0820)
2.5-DISK-2	24.8	0.1245 (0.3162)	2.3955	2.3960	2.3958 (6.0858)
2.5-DISK-3	24.7	0.1245 (0.3162)	2.3960	2.3960	2.3960 (6.0858)
2.5-DISK-4	24.9	0.1255 (0.3188)	2.3960	2.3960	2.3960 (6.0858)
2.5-DISK-5	24.9	0.1250 (0.3175)	2.3950	2.3950	2.3950 (6.0833)
2.5-DISK-6	25.0	0.1255 (0.3188)	2.3940	2.3950	2.3945 (6.0833)
2.5-DISK-7	24.9	0.1250 (0.3175)	2.3950	2.3955	2.3953 (6.0846)
2.5-DISK-8	24.8	0.1250 (0.3175)	2.3945	2.3950	2.3948 (6.0833)
2.5-DISK-9	24.6	0.1240 (0.3150)	2.3945	2.3950	2.3948 (6.0833)
2.5-DISK-10	24.9	0.1250 (0.3175)	2.3955	2.3955	2.3955 (6.0846)
6-DISK-1	149.9	0.1240 (0.3150)	5.8935	5.8945	5.8940 (14.9720)
6-DISK-2	149.7	0.1235 (0.3137)	5.8915	5.8915	5.8915 (14.9644)
6-DISK-3	151.1	0.1250 (0.3175)	5.8915	5.8915	5.8920 (14.9644)
6-DISK-4	151.3	0.1250 (0.3175)	5.8930	5.8935	5.8933 (14.9695)
6-DISK-5	150.1	0.1240 (0.3150)	5.8905	5.8915	5.8910 (14.9644)
6-DISK-6	150.4	0.1245 (0.3162)	5.8920	5.8925	5.8923 (14.9670)
10-DISK-1	423.9	0.1240 (0.3150)	9.8915	9.8920	9.8918 (25.1257)
10-DISK-2	424.0	0.1245 (0.3162)	9.8920	9.8935	9.8928 (25.1295)
10-DISK-3	426.5	0.1250 (0.3175)	9.8925	9.8925	9.8925 (25.1270)
10-DISK-4	426.3	0.1250 (0.3175)	9.8925	9.8930	9.8928 (25.1282)
10-DISK-5	426.9	0.1255 (0.3188)	9.8880	9.8900	9.8890 (25.1206)
10-DISK-6	427.1	0.1250 (0.3175)	9.8935	9.8940	9.8938 (25.1308)
10-DISK-7	426.5	0.1250 (0.3175)	9.8910	9.8920	9.8915 (25.1257)
10-DISK-8	426.2	0.1250 (0.3175)	9.8915	9.8920	9.8918 (25.1257)
10-DISK-9	425.3	0.1245 (0.3162)	9.8915	9.8925	9.8920 (25.1270)
10-DISK-10	423.1	0.1245 (0.3162)	9.8900	9.8925	9.8913 (25.1270)

Table 55: Derived volumes and densities of the aluminum insert parts.

Part ID	**Mass (g)**	**Volume (cm^3)**	**Density (g/cm^3)**
2.5-DISK-1	**24.6**	**9.1504**	**2.6884**
2.5-DISK-2	24.8	9.1973	2.6964
2.5-DISK-3	24.7	9.1989	2.6851
2.5-DISK-4	24.9	9.2727	2.6853
2.5-DISK-5	24.9	9.2281	2.6983
2.5-DISK-6	25	9.2611	2.6995
2.5-DISK-7	24.9	9.2304	2.6976
2.5-DISK-8	24.8	9.2266	2.6879
2.5-DISK-9	24.6	9.1527	2.6877
2.5-DISK-10	24.9	9.2319	2.6972
6-DISK-1	149.9	55.4412	2.7038
6-DISK-2	149.7	55.1709	2.7134
6-DISK-3	151.1	55.8504	2.7054
6-DISK-4	151.3	55.8751	2.7078
6-DISK-5	150.1	55.3848	2.7101
6-DISK-6	150.4	55.6327	2.7034
10-DISK-1	423.9	156.1577	2.7146
10-DISK-2	424	156.8191	2.7038
10-DISK-3	426.5	157.4393	2.7090
10-DISK-4	426.3	157.4489	2.7075
10-DISK-5	426.9	157.9572	2.7026
10-DISK-6	427.1	157.4807	2.7121
10-DISK-7	426.5	157.4075	2.7095
10-DISK-8	426.2	157.4170	2.7075
10-DISK-9	425.3	156.7937	2.7125
10-DISK-10	423.1	156.7715	2.6988

1.2.7 Height Measurements

Stack height uncertainties were the leading uncertainty of the past TEX-HEU evaluations ([3, 4]). In the previous evaluations a 24-inch Westward Electronic Height Gauge (Model No. 2YND5; Calibration No. 018643) was used to perform the stack height measurements. In the current evaluation only one confirmatory measurement was performed with the height gauge. The rest of the stack height measurements were performed with an Articulated Arm Coordinate Measuring Machine (CMM) (Calibration No. 240116-14017-UC) with a Hexagon Absolute Arm 8525-7. The measurements were performed in place, on Comet, and after restacking on a granite plate.

The new adapter plate, discussed in Section 1.2.2.2, was designed to allow the height gauge to zero at the bottom of the bottom reflector. The new lip feature of the adapter plate provides the necessary room to be able to zero on the bottom reflector. In the past, the lip of the adapter plate created an offset in the measurement. The face of the adapter plate served as the zero point for both the height gauge and the CMM. Figure 26 shows the measurement locations on Comet using the height gauge.

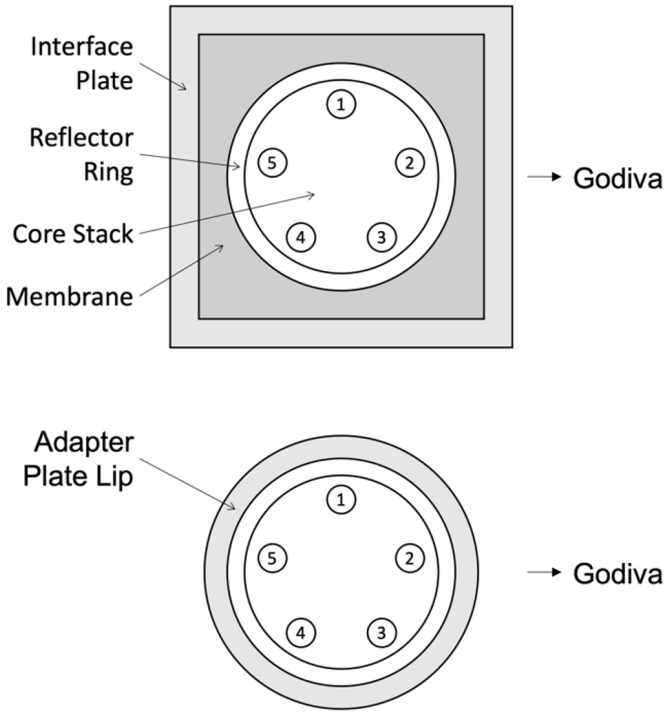

Figure 26: Upper (top) and lower (bottom) stack height measurement locations with the height gauge for Case 1.

CMM measurements were performed on Comet by placing the CMM on a tripod which stood either next to Comet or on the Comet platform. Figure 27 shows the measurement locations on Comet and the granite plate after restacking for Case 1. The "X" in Figure 27 denotes the location of the CMM. The three measurement locations, H_1 through H_3, were not single measurements, but rather a set of measurements that were averaged to obtain a single value for each region. Height gauge measurements were performed on the upper stack of Case 1 and were compared with the CMM measurements to verify agreement. The reflector rings were measured

using an average value to represent the total height.

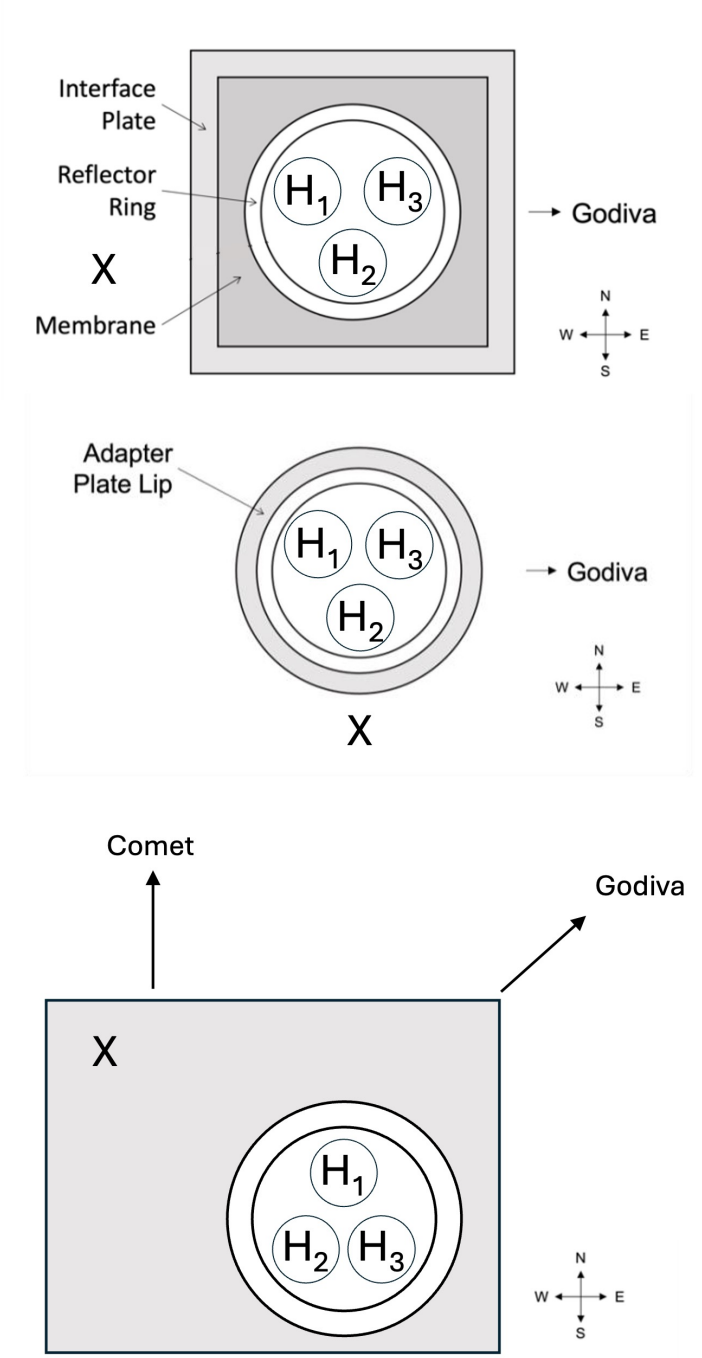

Figure 27: Upper (top), lower (middle), and granite surface plate (bottom) stack height measurement locations with the CMM for Cases 2 and 3.

CMM measurements for Case 2 and 3 adopted a cardinal measurement scheme where the center of the plate and the points in the cardinal N/S/E/W directions were measured, shown in Figure 28.

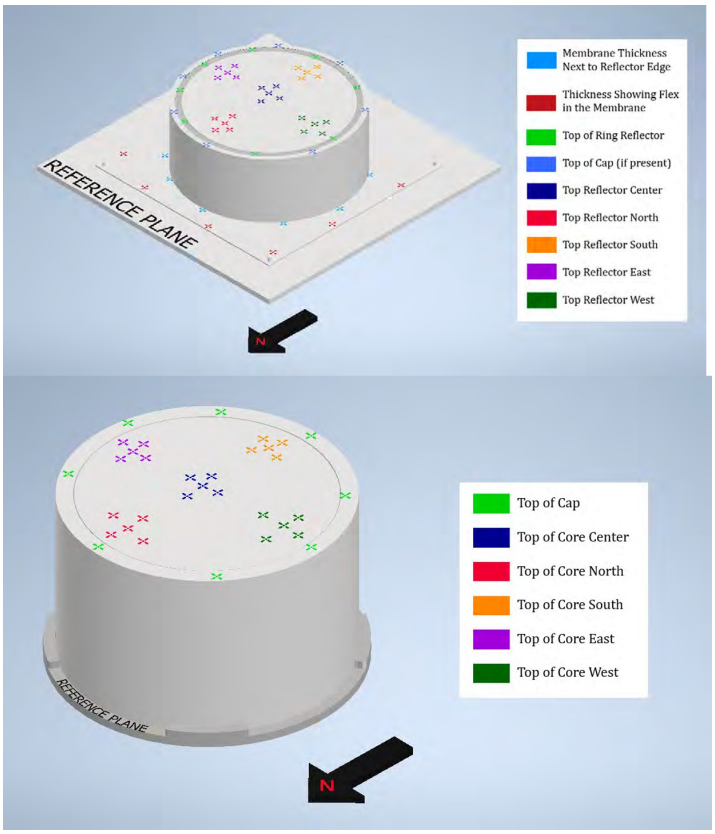

Figure 28: Upper (top) and lower (bottom) stack height measurement locations with the CMM using cardinal directions used for Cases 2 and 3.

Table 56 summarizes the core stack and reflector height measurements for Case 1 using the height gauge. This was the only case that utilized the height gauge as it was used to verify the CMM measurements. Table 57 summarizes the core stack and reflector height measurements for Case 1 using the CMM while on Comet and Table 58 summarizes the same information after restacking on the granite plate. Note that the averages for the CMM measurements are not the averages of the measurements listed in the tables, but rather the average value reported by the CMM.

Table 56: Summary of upper and lower core stack and reflector ring height measurements for Case 1 using the height gauge (see Figure 26).

Location	Upper (mm)		Lower (mm)	
	Measurement	Re-Zero	Measurement	Re-Zero
1	167.52	0.02	*Not Measured*	
2	167.34	0.00	*Not Measured*	
3	166.59	0.15	*Not Measured*	
4	167.88	0.05	*Not Measured*	
5	167.32	0.56	*Not Measured*	
Average	167.33	-	*Not Measured*	
Reflector Ring	168.65	0.23	*Not Measured*	

[(a)] Re-zero refers to returning the height gauge to the zero position after completing the measurement to quantify the amount of drift in the gauge during the measurement.

Table 57: Summary of upper and lower core stack and reflector ring height measurements for Case 1 using the CMM while on Comet (see Figure 27).

Location	Upper (mm)	Lower (mm)
1	167.31	240.51
2	167.61	240.54
3	167.15	240.69
Average	167.38	240.54
Reflector Ring	167.70	240.41
Reflector Cap	168.15	-

Table 58: Summary of upper and lower core stack and reflector ring height measurements for Case 1 using the CMM after restacking on the granite plate (see Figure 27).

Location	Upper (mm)	Lower (mm)
1	168.29	240.97
2	168.01	240.46
3	168.06	240.68
Average	168.19	240.67
Reflector Ring	168.22	240.79
Reflector Cap	168.66	-

Table 59 and Table 60 summarize the core stack and reflector height measurements for Case 2 using the CMM while on Comet and after restacking on the granite plate, respectively.

Table 59: Summary of upper and lower core stack and reflector ring height measurements for Case 2 using the CMM while on Comet (see Figure 28).

Location	Upper (mm)	Lower (mm)
Center	195.55	263.96
North	195.25	264.12
South	195.36	263.92
East	195.39	263.70
West	195.79	263.99
Average	195.67	263.94
1/2-RING-2	196.29	-
0-CAP-1	196.82	-
1/32-CAP-1	-	264.55

Table 60: Summary of upper and lower core stack and reflector ring height measurements for Case 2 using the CMM after restacking on the granite plate (see Figure 28).

Location	Upper (mm)	Lower (mm)
Center	194.04	264.12
North	194.18	264.03
South	193.36	264.11
East	193.15	264.06
West	193.62	264.41
Average	193.67	264.15
1/2-RING-2	193.68	-
0-CAP-1	194.15	-
1/32-CAP-1	-	264.82

Table 61 and Table 62 summarize the core stack and reflector height measurements for Case 3 using the CMM while on Comet and after restacking on the granite plate, respectively.

Table 61: Summary of upper and lower core stack and reflector ring height measurements for Case 3 using the CMM while on Comet (see Figure 28).

Location	Upper (mm)	Lower (mm)
Center	127.34	203.71
North	127.27	203.30
South	128.21	203.55
East	127.94	203.84
West	127.79	203.44
Average	127.71	203.57
1/32-CAP-12	127.55	-
1/8-CAP-2	-	203.35

Table 62: Summary of upper and lower core stack and reflector ring height measurements for Case 3 using the CMM after restacking on the granite plate (see Figure 28).

Location	**Upper (mm)**	**Lower (mm)**
Center	125.81	204.14
North	125.97	203.58
South	125.48	204.65
East	126.31	203.87
West	126.10	203.74
Average	125.92	204.00
1/32-CAP-12	125.10	-
1/8-CAP-2	-	203.65

1.2.8 Reactor Period

Reactor period measurements of the experimental configurations were performed using four ^{3}He proportional counters, referred to as the start-up (SU) detectors, and three compensated ion chambers, referred to as the linear channels (LC). Figure 29 shows an example of the period measurement and fit for the Case 1 experimental configuration using the linear channels (LC) detectors. The fit is performed in the LC detectors as the SU detectors begin to saturate due to the high neutron count rates.

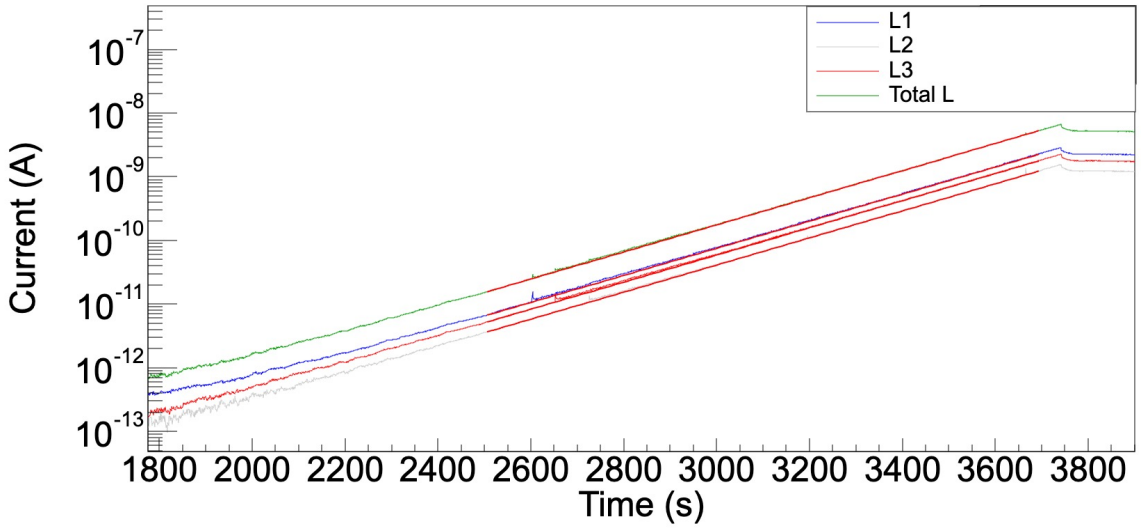

Figure 29: Example period measurement of the Case 1 experimental configuration, showing the LCs. The plot is in logarithmic scale on the y axis. The drop off represents the separation of the two halves of the assembly.

Table 63 reports the measured reactor periods and the *in-situ* calculated excess reacitivities from the Comet logbook. The SU measurements are reported as the sum of all four ^{3}He proportional counters (SU_{sum}), to improve the counting statistics. The *in-situ* calculated excess reactivity is based on a preliminary fit of the measured neutron count rate data using the Keepin delayed neutron parameters [0].

In addition to the benchmark period measurements, reproducibility measurements of configurations 2 and 3 were performed to measure the potential impact of inconsistencies when assembling the experimental configurations. The reproducibility measurements were performed by completely disassembling and reassembling the assembly, ensuring that the parts were placed in the same order and orientation. The two reproduced cases cover the thermal (configuration 2) and the intermediate/fast (configuration 3) neutron energy regimes. The reproducibility measurements are also reported in Table 63.

Table 63: Benchmark period measurements, in seconds (s), and *in-situ* calculated excess reactivity, in cents (¢).

Configuration	Measured Reactor Period & *In-Situ* Calculated Excess Reactivity [s (¢)][a]			
	LC_1	LC_2	LC_3	SU_{sum}
1	206.03 (5.44)	205.69 (5.45)	205.59 (5.45)	216.76 (5.21)
2	118.86 (8.62)	119.72 (8.57)	118.91 (8.62)	127.54 (8.15)
2R[b]	160.39 (6.74)	158.9 (6.79)	162.66 (6.66)	173.34 (6.31)
3	47.71 (16.33)	47.77 (16.31)	48.08 (16.24)	49.92 (15.83)
3R[b]	57.01 (14.45)	57.20 (14.42)	56.72 (14.50)	60.18 (13.91)

[a] Based on preliminary fits of the measured neutron count rate data as reported in the Comet logbook.
[b] R represents a reproducibility measurement.

1.2.9 Experimental Configurations

The following sections describe the three experimental configurations. Each section includes a listing and diagram of the parts used in the experimental configuration. Table 64 summarizes the characteristics of the experimental configurations.

Table 64: Overview of the experimental configurations.

Configuration	Number of HEU Plates	Total HEU Mass (kg)	Total NaCl Mass (kg)	Nominal Moderator Thickness [in. (cm)]	Nominal Top Reflector Thickness [in. (cm)]
1	8	48.6	4.6	0.750 (1.905) [a]	0.2500 (0.6350)
2	8	48.6	4.6	1.750 (4.445)	0.5000 (1.2700)
3	18	110.2	8.7	0.125 (0.3175)	1.0625 (2.69875)

[a] Sodium chloride absorbers are sandwiched between two nominal 0.750 in. thick polyethylene moderator plates (Section 1.2.1).

1.2.9.1 Case 1

The Case 1 experimental configuration included 8 HEU plates, 7 0.250-inch sodium chloride absorbers, 14 0.750-inch moderator plates, and a nominal 0.250-inch upper reflector. The 8 HEU plates consisted of five 15/0-HEU, one 15/6-HEU, one 15/10-HEU plates, and the Q2-16 insert, for a total mass of 48.6 kg. This configuration used the sandwich stacking method described in Section 1.2.1.

Figure 30 and Tables 65 and 66 list the parts used in the experimental configuration. The measured reactor period is reported in Section 1.2.8. The stack height measurements are reported in Section 1.2.7.

Table 65: Parts used in the upper (left) and lower (right) core stacks of Case 1, using the sandwich stacking method.

Layer	Upper Core Stack
14	1/4-MOD-1
13	10458 & 10-DISK-2
12	3/4-MOD-14
11	Salt Plate 1/4-9
10	3/4-MOD-13
9	10487 & 2.5-DISK-1
8	3/4-MOD-12
7	Salt Plate 1/4-8
6	3/4-MOD-11
5	11018 & Q2-16
4	3/4-MOD-10
3	Salt Plate 1/4-7
2	3/4-MOD-9
1	11147

Part	Lower Core Stack
17	3/4-MOD-8
16	Salt Plate 1/4-5
15	3/4-MOD-7
14	11149
13	3/4-MOD-6
12	Salt Plate 1/4-4
11	3/4-MOD-5
10	11019
9	3/4-MOD-4
8	Salt Plate 1/4-3
7	3/4-MOD-3
6	11017
5	3/4-MOD-2
4	Salt Plate 1/4-2
3	3/4-MOD-1
2	11150
1	1.0-BOTREFSRC-2

Table 66: Parts used in the upper (left) and lower (right) reflector rings of Case 1.

Layer	Upper Reflector Ring
5	0-CAP-1
4	1/2-RING-1
3	3-RING-4
2	3-RING-1
1	0-BOTCAP-1

Layer	Lower Reflector Ring
6	1/16-CAP-3
5	1/4-RING-1
4	1-RING-3
3	3-RING-2
2	1-RING-1
1	3-RING-3

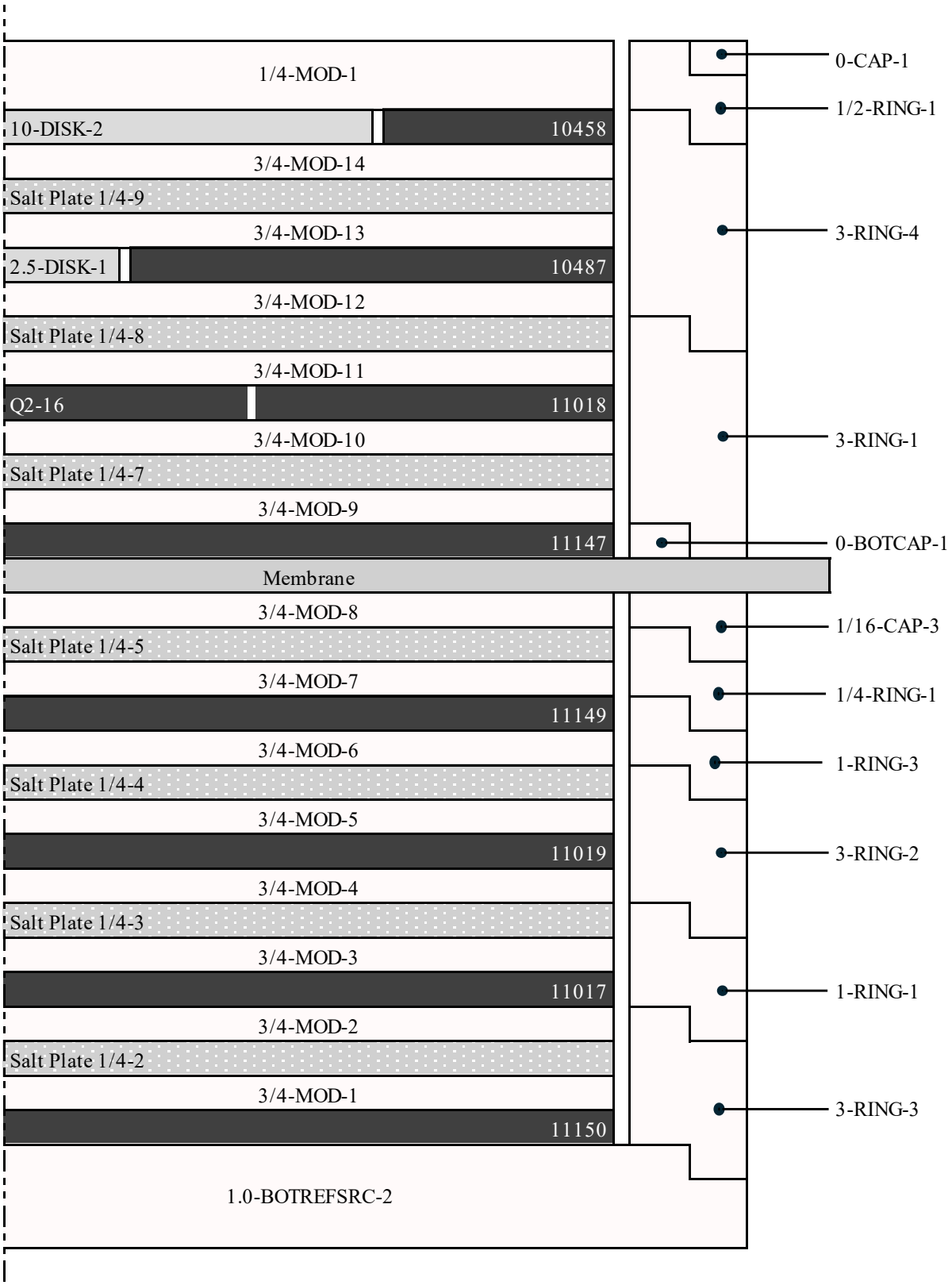

Figure 30: Axisymmetric diagram of the Case 1 experimental configuration (not to scale).

1.2.9.2 Case 2

The Case 2 experimental configuration included 8 HEU plates, 7 0.250-inch sodium chloride absorbers, 7 1.500-inch moderator plates, 7 0.250-inch moderator plates, and a nominal 0.500-inch upper reflector. The 8 HEU plates consisted of five 15/0-HEU, one 15/6-HEU, one 15/10-HEU plates, and the Q2-16 insert, for a total mass of 48.6 kg. This configuration used the standard stacking method described in Section 1.2.1.

Figure 31 and Tables 67 and 68 list the parts used in the experimental configuration. The measured reactor period is reported in Section 1.2.8. The stack height measurements are reported in Section 1.2.7.

Table 67: Parts used in the upper (left) and lower (right) core stacks of Case 2, using the sandwich stacking method.

Layer	Upper Core Stack
14	1/2-MOD-1
13	10458 & 10-DISK-2
12	Salt Plate 1/4-09
11	1.5-MOD-8
10	1/4-MOD-7
9	10487 & 2.5-DISK-1
8	Salt Plate 1/4-08
7	1.5-MOD-7
6	1/4-MOD-6
5	11018 & Q2-16
4	Salt Plate 1/4-07
3	1.5-MOD-6
2	1/4-MOD-5
1	11147

Part	Lower Core Stack
17	Salt Plate 1/4-05
16	1.5-MOD-5
15	1/4-MOD-4
14	11149
13	Salt Plate 1/4-04
12	1.5-MOD-4
11	1/4-MOD-3
10	11019
9	Salt Plate 1/4-03
8	1.5-MOD-3
7	1/4-MOD-2
6	11017
5	Salt Plate 1/4-02
4	1.5-MOD-1
3	1/4-MOD-1
2	11150
1	1-BOTREFSRC-2

Table 68: Parts used in the upper (left) and lower (right) reflector rings of Case 2.

Layer	Upper Reflector Ring
6	0-CAP-1
5	1/2-RING-2
4	3-RING-5
3	3-RING-4
2	1-RING-5
1	0-BOTCAP-1

Layer	Lower Reflector Ring
5	1/32-CAP-1
4	1/4-RING-2
3	3-RING-2
2	3-RING-3
1	3-RING-1

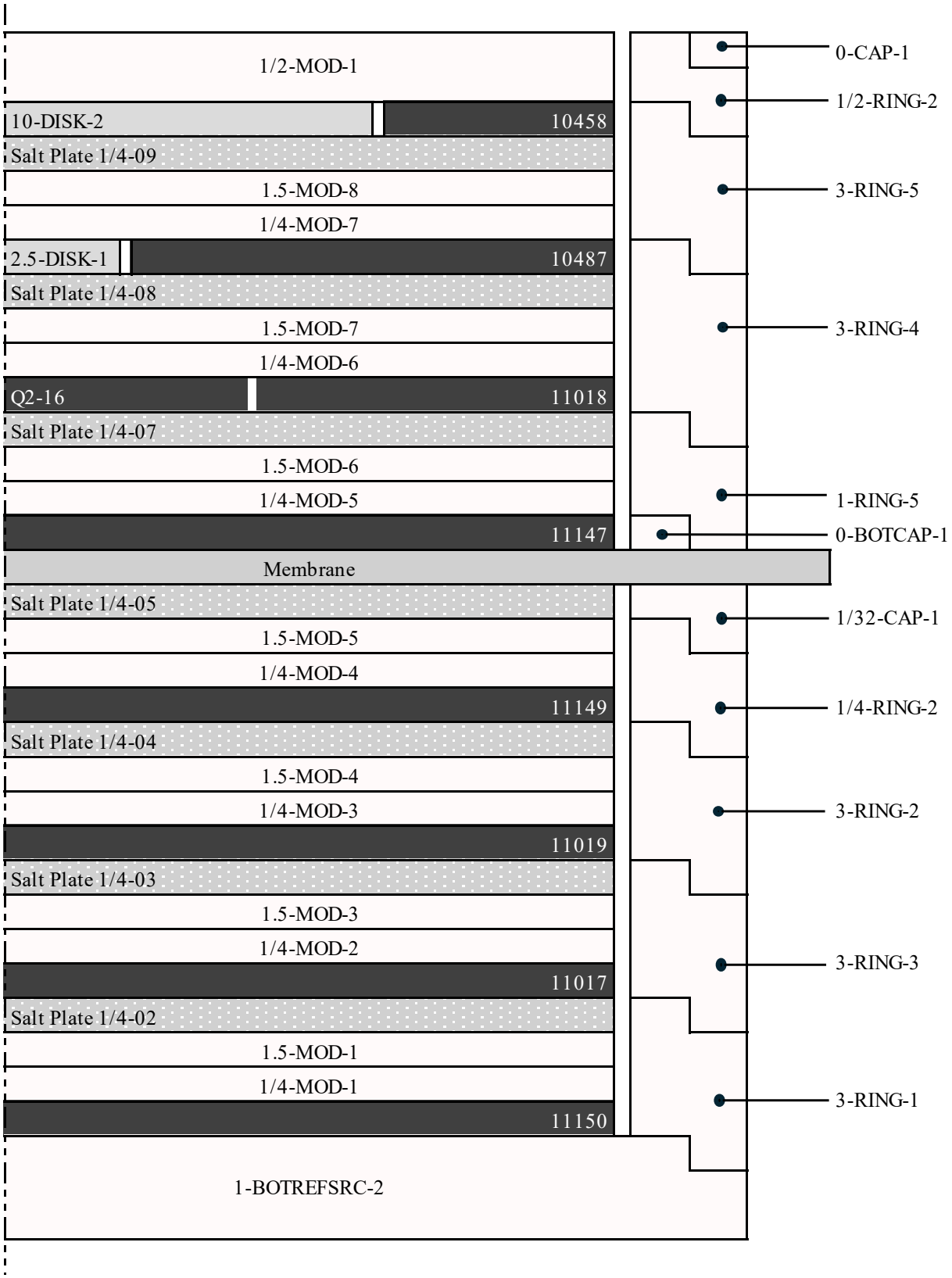

Figure 31: Axisymmetric diagram of the Case 2 experimental configuration (not to scale).

1.2.9.3 Case 3

The Case 3 experimental configuration included 18 HEU plates, 17 0.1875-inch sodium chloride absorbers, 17 0.125-inch moderator plates, and a nominal 1.0625-inch upper reflector. The 18 HEU plates consisted of five 15/0-HEU, seven 15/2.5-HEU, six 15/6-HEU, and the Q2-16 insert, for a total mass of 110.2 kg. This configuration used the standard stacking method described in Section 1.2.1.

Figure 32 and Tables 69 and 70 list the parts used in the experimental configuration. The measured reactor period is reported in Section 1.2.8. The stack height measurements are reported in Section 1.2.7.

Table 69: Parts used in the upper (left) and lower (right) core stacks of Case 3, using the sandwich stacking method.

Layer	Upper Core Stack
21	1-REF-1
20	1/16-REF-1
19	10935 & 6-DISK-5
18	Salt Plate 3/16-19
17	1/8-MOD-17
16	10933 & 6-DISK-4
15	Salt Plate 3/16-18
14	1/8-MOD-16
13	10570 & 2.5-DISK-7
12	Salt Plate 3/16-17
11	1/8-MOD-15
10	10475 & 2.5-DISK-6
9	Salt Plate 3/16-16
8	1/8-MOD-14
7	10489 & 2.5-DISK-5
6	Salt Plate 3/16-15
5	1/8-MOD-13
4	11018 & Q2-16
3	Salt Plate 3/16-14
2	1/8-MOD-12
1	11017

Part	Lower Core Stack
34	Salt Plate 3/16-13
33	1/8-MOD-11
32	11150
31	Salt Plate 3/16-12
30	1/8-MOD-10
29	11019
28	Salt Plate 3/16-11
27	1/8-MOD-9
26	11147
25	Salt Plate 3/16-10
24	1/8-MOD-8
23	11149
22	Salt Plate 3/16-09
21	1/8-MOD-7
20	10467 & 2.5-DISK-4
19	Salt Plate 3/16-08
18	1/8-MOD-6
17	10464 & 2.5-DISK-3
16	Salt Plate 3/16-06
15	1/8-MOD-5
14	10487 & 2.5-DISK-2
13	Salt Plate 3/16-05
12	1/8-MOD-4
11	10491 & 2.5-DISK-1
10	Salt Plate 3/16-04
9	1/8-MOD-3
8	10932 & 6-DISK-3
7	Salt Plate 3/16-03
6	1/8-MOD-2
5	10457 & 6-DISK-2
4	Salt Plate 3/16-02
3	1/8-MOD-1
2	10477 & 6-DISK-1
1	1.0-BOTREFSRC-2

Table 70: Parts used in the upper (left) and lower (right) reflector rings of Case 3.

Layer	Upper Reflector Ring
6	1/32-CAP-2
5	1-RING-5
4	1/2-RING-2
3	1/4-RING-1
2	3-RING-3
1	0-BOTCAP-1

Layer	Lower Reflector Ring
5	1/8-CAP-2
4	1/2-RING-3
3	1/4-RING-2
2	3-RING-2
1	3-RING-1

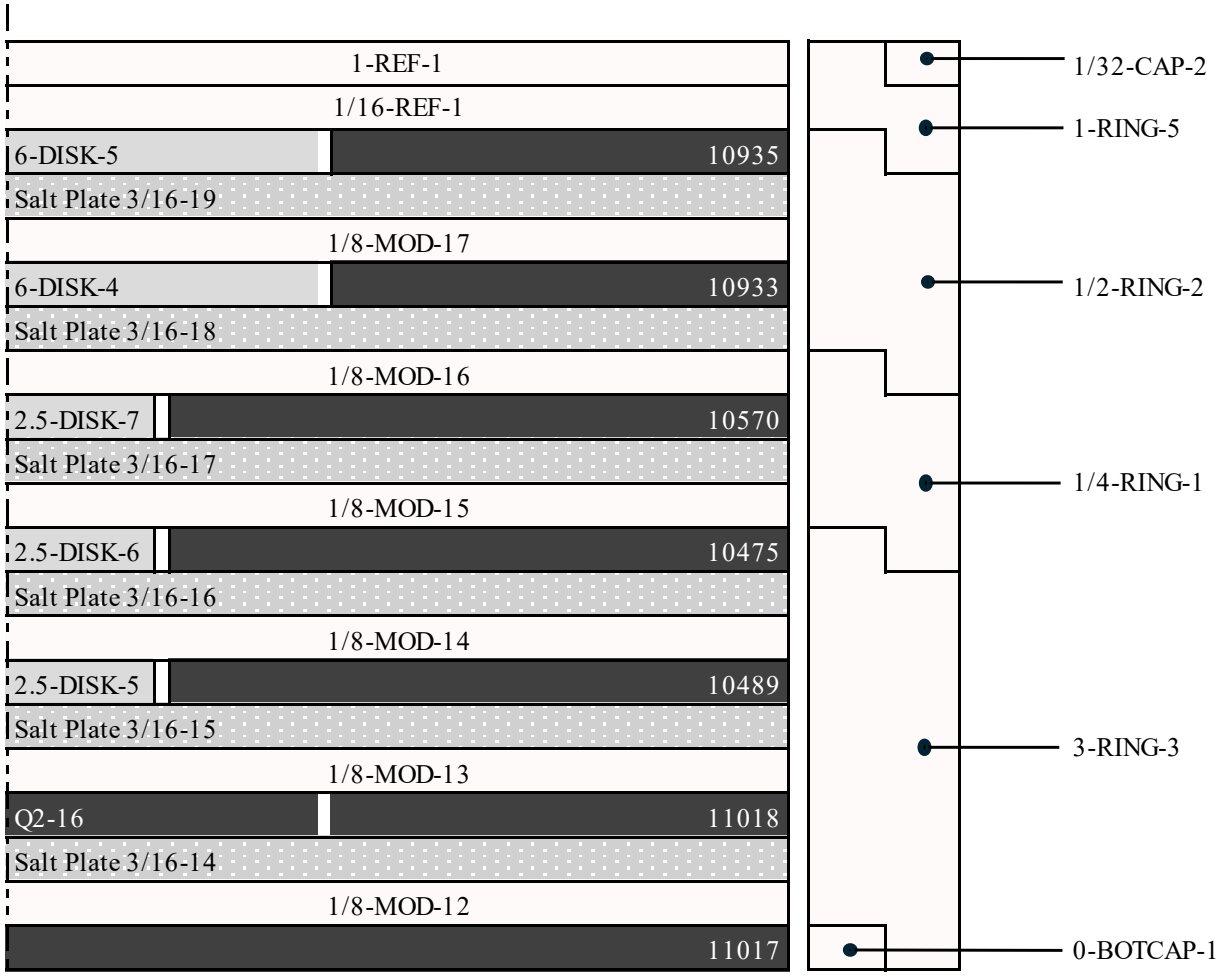

Figure 32: Axisymmetric diagram of the Case 3 experimental configuration (not to scale).

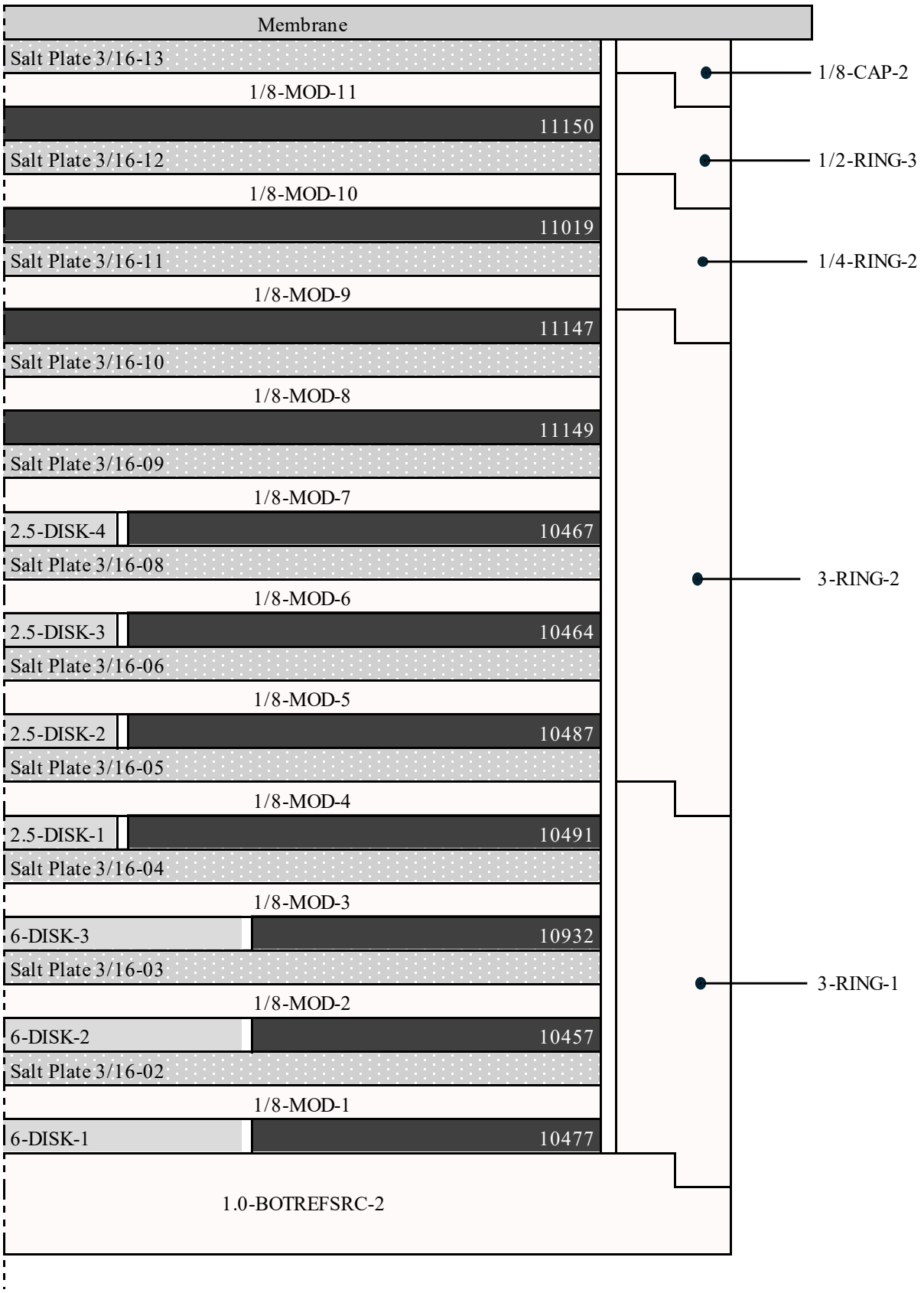

Figure 32 continued.

1.3 Description of Material Data

The following material descriptions are reproduced from HEU-MET-INTER-013 and HEU-MET-MIXED-021, which is nearly identical apart from the inclusion of sodium chloride absorbers instead of Hf absorbers.

1.3.1 Highly Enriched Uranium

Sections 1.3.1.1 and 1.3.1.2 summarize and reproduce relevant material descriptions from HEU-MET-INTER-013 and HEU-MET-FAST-072, which use the same HEU plates. The 15/2.5-HEU, 15/6-HEU, and 15/10-HEU plate types, identified as Id No. 403, 401, and 402, are used in HEU-MET-INTER-013. The 15/0-HEU and 15/2.5-HEU plate types, identified as HEU1 and HEU2, are used in HEU-MET-FAST-072.

1.3.1.1 ^{235}U Enrichment

Table 71 reproduces the mass spectrometry measurements from HEU-MET-INTER-013 and HEU-MET-FAST-072, reporting the uranium isotopic content of the HEU plates. The measurements are reported as atomic ratios relative to ^{235}U and the uncertainties are at the 95% confidence level (2σ), as noted in IEU-MET-FAST-007.

Table 71: HEU plate uranium isotopic content measurements.

Part Type	Part ID	Uranium Isotope (Atom Ratio Relative to ^{235}U)			
		^{234}U	^{235}U	^{236}U	^{238}U
15/10-HEU	10458	0.0111 ± 0.0002	1.00	<2E-5	0.0577 ± 0.0012
15/6-HEU	10493	0.0115 ± 0.0001	1.00	(8.40 ± 0.42)E-4	0.0592 ± 0.0002
	10932	0.0108 ± 0.0001	1.00	(3.50 ± 0.04)E-3	0.0586 ± 0.0002
	11018	0.0110 ± 0.0001	1.00	(5.56 ± 0.06)E-3	0.0555 ± 0.0002

Table 72 reproduces the relevant HEU plate enrichments from HEU-MET-INTER-013 and HEU-MET-FAST-072. The enrichments were obtained from Material Controls and Accountability for the plates used in the Big Ten assembly and a letter from Dixon Callihan (ORNL) to Hugh Paxton (LANL) dated May 20, 1960. The HEU plates in HEU-MET-INTER-013 are not individually identified, instead it lists individual enrichment values grouped by part type. Some of the HEU plate Part IDs in HEU-MET-FAST-072 are prefaced with "B10" which has been removed in favor of the ending 5-digit identifier.

Table 72: HEU plate ^{235}U enrichment.

Part Type	Part ID	Enrichment
15/0-HEU	11150	93.17
	11149	93.24
	11147	93.17
	11019	93.18
	11017	93.31
15/2.5-HEU	10491	93.37
	10489	93.39
	10487	93.26
	10475	93.40
	10470	93.41
	10467	93.41
	10464	93.38
6/0-HEU	Q2-16	-

Part Type	Part ID	Enrichment
15/6-HEU	11018	93.19
	10935	93.18
	10933	93.16
	10932	93.15
	10477	93.35
	10457	93.44
15/10-HEU	10485	93.24
	10481	93.23
	10479	-
	10473	-
	10472	-
	10463	-
	10458	93.4

1.3.1.2 Uranium Impurities

Table 73 reproduces the HEU plate impurity measurements from HEU-MET-INTER-013 and HEU-MET-FAST-072. The analysis reports did not distinguish whether the impurities were atom fractions or mass fractions. Therefore, the reported impurities are assumed to be by weight, as is done in HEU-MET-INTER-013.

Table 73: Measured HEU plate impurities.

Impurity (ppm U)	15/0-HEU			15/6-HEU	
	11147	11149	11150	10932	10933
Li	<0.1	<0.1	<0.1	<0.1	<0.1
Be	<0.1	<0.1	<0.1	<0.1	<0.1
B	0.6	0.6	0.3	0.2	<0.1
C	1100	270	320	170	170
Na	<1	<1	<1	<1	<1
Mg	<1	<1	<1	<1	1
Al	50	40	20	150	100
Si	300	400	210	80	130
Ca	<2	<2	<2	<2	<2
V	<20	<20	<20	<20	<20
Cr	5	15	5	2	3
Mn	4	7	6	7	6
Fe	100	190	90	70	30
Co	<5	<5	<5	<5	<5
Ni	20	30	20	15	15
Cu	6	5	4	4	3
Mo	50	<25	<25	-	-
Sn	<1	<1	<1	-	-
Pb	5	<1	<1	-	-

1.3.2 Sodium Chloride

NaCl salt impurity analysis was performed on a random subset of the sodium chloride absorbers. At the time of filling, salt samples were taken from twelve randomly selected sodium chloride absorbers. These twelve samples were then combined into four samples to meet the minimum mass requirements for the impurity tests. The four blended samples were sent to Eurofins (Liverpool, New York, USA) who performed Glow Discharge Mass Spectrometry (GDMS) to determine the chemical impurities of the salt samples and Intersitial Gas Analysis (IGA) to determine the water concentration of the salt, i.e. the moisture of the salt. The precision of the GDMS technique is 20% relative to the reported value and has a detection limit down to the part-per-billion (ppb) level. The IGA technique has a detection limit and precision of 0.01 wt%.

A sample was collected for each of the 36 sodium chloride absorbers that were fabricated. As stated above, a random sample of twelve of the NaCl samples were blended into four final samples, which were taken as a representative sample of all sodium chloride absorbers as the salt came from a single batch.. Table 74 summarizes the identifiers of the sodium chloride absorbers that were fabricated and which were included in the final samples for analysis.

NaCl salt impurities were checked against 77 elements, but was insensitive to C, N, and O. Additionally, Na and Cl were not reported as they are the main constituents of the salt. Arsenic (As) was marked as interference due to spectral interference and was not reported. The electrode used was made of Ta, which was also not reported. The impurities are reported in Table 75 and are given in ppm NaCl. A minimum detection threshold for various elements were set and are reported as the upper limit.

NaCl salt is hygroscopic, meaning that it will accumulate moisture over time if exposed to a source of water, such as air. While NaCl is lowly hygroscopic compared to many other salts, an accurate quantification of the moisture content is important. Mass measurements of the filled sodium chloride absorbers, reported in Section 1.2.4.4 and 1.2.4.3, were performed to measure any water retention that occurred before the experiment took place. Samples of NaCl salt were taken during the filling process and sent to Eurofins to perform IGA Multiphase Analysis. Table 76 reports the moisture content of the sodium chloride absorbers and are given in ppm NaCl.

Table 74: NaCl salt sample identifiers (IDs).

Part ID	Original NaCl Sample ID	Final NaCl Sample ID
SaltPlate3/16-1	001	-
SaltPlate3/16-2	002	-
SaltPlate3/16-3	003	-
SaltPlate3/16-4	004	-
SaltPlate3/16-5	005	-
SaltPlate3/16-6	006	-
SaltPlate3/16-7	007	-
SaltPlate3/16-8	008	-
SaltPlate3/16-9	009	-
SaltPlate3/16-10	010	01-13
SaltPlate3/16-11	011	-
SaltPlate3/16-12	012	-
SaltPlate3/16-13	013	-
SaltPlate3/16-14	014	-
SaltPlate3/16-15	015	-
SaltPlate3/16-16	016	-
SaltPlate3/16-17	017	-
SaltPlate3/16-18	018	-
SaltPlate3/16-19	019	-
SaltPlate3/16-20	020	01-11
SaltPlate3/16-21	021	01-10
SaltPlate3/16-22	022	01-11
SaltPlate3/16-23	023	01-08
SaltPlate1/4-1	01-01	01-08
SaltPlate1/4-2	01-02	01-13
SaltPlate1/4-3	01-03	-
SaltPlate1/4-4	01-04	01-10
SaltPlate1/4-5	01-05	-
SaltPlate1/4-6	01-06	-
SaltPlate1/4-7	01-07	-
SaltPlate1/4-8	01-08	01-08
SaltPlate1/4-9	01-09	-
SaltPlate1/4-10	01-10	01-10
SaltPlate1/4-11	01-11	01-11
SaltPlate1/4-12	01-12	-
SaltPlate1/4-13	01-13	01-13

Table 75: NaCl salt impurity analysis results from GDMS analysis.

Element	Composition [ppm NaCl]			
	01-08	**01-10**	**01-11**	**01-13**
Li	0.01	<0.01	<0.01	<0.01
Be	<0.01	<0.01	<0.01	<0.01
B	<0.05	<0.05	<0.05	<0.05
C	-	-	-	-
N	-	-	-	-
O	-	-	-	-
F	<1	<1	<1	<1
Na	Matrix	Matrix	Matrix	Matrix
Mg	0.86	0.47	0.39	0.47
Al	0.05	0.18	0.05	0.07
Si	0.07	0.33	0.05	0.12
P	<0.1	<0.1	<0.1	<0.1
S	1.20	5.10	3.40	3.10
Cl	Matrix	Matrix	Matrix	Matrix
K	4.30	7.80	14.00	17.00
Ca	0.90	2.10	2.00	1.60
Sc	<0.01	<0.01	<0.01	<0.01
Ti	<0.05	<0.05	<0.05	<0.05
V	<0.05	<0.05	<0.05	<0.05
Cr	<0.05	<0.05	<0.05	<0.05
Mn	<0.05	<0.05	<0.05	<0.05
Fe	<0.1	<0.1	<0.1	<0.1
Co	<0.05	<0.05	<0.05	<0.05
Ni	<0.1	<0.1	<0.1	<0.1
Cu	<1	<1	<1	<1
Zn	<0.1	<0.1	<0.1	<0.1
Ga	<0.05	<0.05	<0.05	<0.05
Ge	<0.5	<0.5	<0.5	<0.5
As	Interference	Interference	Interference	Interference
Se	<0.5	<0.5	<0.5	<0.5
Br	2.70	12.00	16.00	13.00
Rb	<0.01	<0.01	<0.01	<0.01
Sr	0.12	0.19	0.11	0.23
Y	<0.01	<0.01	<0.01	<0.01
Zr	<0.05	<0.05	<0.05	<0.05
Nb	<50	<50	<50	<50
Mo	<20	<20	<20	<20
Ru	<0.05	<0.05	<0.05	<0.05

Table 75 Continued.

Element	Composition [ppm NaCl]			
	01-08	**01-10**	**01-11**	**01-13**
Rh	<5	<5	<5	<5
Pd	<0.05	<0.05	<0.05	<0.05
Ag	<0.1	<0.1	<0.1	<0.1
Cd	<0.1	<0.1	<0.1	<0.1
In	<1	<1	<1	<1
Sn	<0.10	<0.10	<0.10	<0.10
Sb	<0.05	<0.05	<0.05	<0.05
Te	<0.05	<0.05	<0.05	<0.05
I	<0.05	<0.05	<0.05	<0.05
Cs	<0.5	<0.5	<0.5	<0.5
Ba	<0.05	<0.05	<0.05	<0.05
La	<0.05	<0.05	<0.05	<0.05
Ce	<0.05	<0.05	<0.05	<0.05
Pr	<0.05	<0.05	<0.05	<0.05
Nd	<0.05	<0.05	<0.05	<0.05
Sm	<0.05	<0.05	<0.05	<0.05
Eu	<0.05	<0.05	<0.05	<0.05
Gd	<0.05	<0.05	<0.05	<0.05
Tb	<0.05	<0.05	<0.05	<0.05
Dy	<0.05	<0.05	<0.05	<0.05
Ho	<0.05	<0.05	<0.05	<0.05
Er	<0.05	<0.05	<0.05	<0.05
Tm	<0.05	<0.05	<0.05	<0.05
Yb	<0.05	<0.05	<0.05	<0.05
Lu	<0.1	<0.1	<0.1	<0.1
Hf	<0.50	<0.50	<0.50	<0.50
Ta	Electrode	Electrode	Electrode	Electrode
W	<5	<5	<5	<5
Re	<0.1	<0.1	<0.1	<0.1
Os	<0.01	<0.01	<0.01	<0.01
Ir	<0.01	<0.01	<0.01	<0.01
Pt	<0.05	<0.05	<0.05	<0.05
Au	<5	<5	<5	<5
Hg	<0.1	<0.1	<0.1	<0.1
Tl	<0.0	<0.0	<0.0	<0.0
Pb	<0.1	<0.1	<0.1	<0.1
Bi	<0.0	<0.0	<0.0	<0.0
Th	<0.01	<0.01	<0.01	<0.01
U	<0.01	<0.01	<0.01	<0.01

Table 76: NaCl salt moisture analysis results from IGA.

Water Concentration [ppm NaCl]			
01-08	**01-10**	**01-11**	**01-13**
120	160	120	130

1.3.3 Polyethylene

1.3.3.1 Polyethylene Density Measurements

The density of the polyethylene parts used in TEX-Hf was analyzed at LLNL by performing high-precision volume and mass measurements of small samples taken from seven different polyethylene parts. The volume measurements were performed using a Micromeritics AccuPyc II gas displacement pycnometry system. The system used a 100 cm^3 sample chamber and was calibrated using a 51.08755 cm^3 calibration ball prior to each series of sample measurements. Each volume measurement was performed 10 times per sample. The mass measurements were performed on a balance with a precision of 10 µg. Each sample was weighed three times.

Table 77 reports the results of density measurements performed on the seven polyethylene samples. The uncertainty in the mass and volume measurements is reported as the standard deviation of the three mass measurements and 10 volume measurements. These uncertainties are then propagated in quadrature to determine the standard deviation of the calculated density.

Table 77: Polyethylene part density measurements.

Part ID	Mass (g)	Volume (cm^3)	Density (g/cm^3)
0-CAP-3	39.92816 ± 0.00003	41.1483 ± 0.0047	0.9703 ± 0.0001
3/32-CAP-3	48.90154 ± 0.00004	50.4268 ± 0.0033	0.9698 ± 0.0001
1-RING-6	44.30622 ± 0.00001	45.6667 ± 0.0063	0.9702 ± 0.0001
1/8-MOD-38	46.37212 ± 0.00007	48.1521 ± 0.0047	0.9630 ± 0.0001
1/4-MOD-36	58.59803 ± 0.00001	61.2725 ± 0.0043	0.9564 ± 0.0001
1/2-MOD-32	57.58423 ± 0.00007	60.1526 ± 0.0022	0.9573 ± 0.0000
1.5-MOD-12	42.35975 ± 0.00002	44.2152 ± 0.0059	0.9580 ± 0.0001

1.3.3.2 Polyethylene Impurity Analysis

Elemental analysis by Inductively Coupled Plasma Mass Spectrometry (ICP-MS) was performed on a 246.97 µg sample of the polyethylene. This process involved adding the sample to a digestion pressure vessel with 10 mL of 6M nitric acid (HNO_3) and then digesting it in a MARS6 Microwave Digestion System (Model 910900) following the CEM "Polyethylene" procedure in the semi-quantitative, MS/MS mode. The measured elemental impurities are reported in Table 78. The selection criteria required >5000 counts per second, elements included in the analysis were as follows: Mg, V, Mn, Ni, Cu, Zn, Ga, Zr, Mo, Sn, La, and Pb.

Table 78: Polyethylene impurity analysis results. Elements not meeting the selection criteria are not reported.

Elemental Impurity	Unit	Average	Standard Deviation
Na	$\mu g\,g^{-1}$	14.38	1.82
Al	$\mu g\,g^{-1}$	23.92	1.74
Si	$mg\,g^{-1}$	1.17	0.06
Cr	$ng\,g^{-1}$	921.35	7.08

1.3.4 Aluminum

All aluminum parts in the experimental configuration are aluminum alloy 6061 (Al-6061), except for the NaCl encapsulation screws. Table 79 presents standard data for Al-6061[4].

Table 79: Elemental composition limits for aluminum alloy 6061.

Element	Wt.%
Al[(a)]	95.8 - 98.6
Mg	0.8 - 1.2
Si	0.4 - 0.8
Cu	0.15 - 0.4
Cr	0.04 - 0.35

[(a)] Aluminum content reported is calculated as the remainder.

Element	Wt.%
Fe	Max 0.7
Zn	Max 0.25
Mn	Max 0.15
Ti	Max 0.15
Other, each	Max 0.05
Other, total	Max 0.15

The screws used in the encapsulation are aluminum alloy 2024 (Al-2024). Table 80 presents standard data for Al-2024[5].

Table 80: Elemental composition limits for aluminum alloy 2024.

Element	Wt.%
Al[(a)]	90.7 - 94.7
Mg	1.2 - 1.8
Si	Max 0.5
Cu	3.8 - 4.9
Cr	Max 0.1

[(a)] Aluminum content reported is calculated as the remainder.

Element	Wt.%
Fe	Max 0.5
Zn	Max 0.25
Mn	0.3 - 0.9
Ti	Max 0.15
Other, each	Max 0.05
Other, total	Max 0.15

[4] *ASTM B209M-14, Standard Specification for Aluminum and Aluminum-Alloy Sheet and Plate (Metric).* West Conshohocken, PA: ASTM International. DOI: 10.1520/b0209m-14.

[5] *ASTM B209M-14, Standard Specification for Aluminum and Aluminum-Alloy Sheet and Plate (Metric).* West Conshohocken, PA: ASTM International. DOI: 10.1520/b0209m-14.

1.3.5 Comet General Purpose Critical Assembly Machine

The additional parts on Comet, described in Section 1.2.2, also used in the TEX-HEU and TEX-Hf experiments were weighed and reported in HEU-MET-MIXED-021. These parts include the membrane, the experiment platform, and the lower adapter. The weights are reported in Table 81 and were measured during the TEX-HEU experiment using a Mettler Toledo SB16001 High Capacity Precision Balance under the NCERC Calibration Program (Cal No. 012708). The calibration for this balance was certified on May 2, 2019, and was valid through May 2, 2020. These measurements were taken on February 24, 2020. The manufacturer of the SB16001 reports a maximum capacity of 16,100 grams, precision of 0.1 grams, and linearity of 0.3 grams. All parts are Al-6061.

Table 81: Mass measurements of the additional parts on Comet.

Part Type		**Mass (g)**
Membrane		2396.1
Experiment Platform	Interface Plate	11242.5
	Standoffs	633.8
		634.4
		634.0
		635.0
Lower Adpater	Adapter Plate	5014.7
	Adapter Extension	8365.3

1.4 Temperature Data

The temperature of the each experimental configuration was measured by placing a resistance temperature detector (RTD) on Comet to measure the ambient temperature in the room. For two measurements, an RTD was placed on the upper reflector during the approach to critical. This RTD was removed prior to the reactivity measurement for the benchmark configuration. Table 82 reports the ambient and top reflector temperature measurements taken during the benchmark period measurements. The uncertainties in the temperature measurements is ± 2°C. Since the uncertainty in the measurement is greater than the difference for either of the two top reflector measurements, and the top reflector measurement wasn't performed for case 2, the temperature is assumed to be the ambient temperature.

Table 82: Temperature measurements of the experimental configurations. "R" represents a reproducibility measurement.

Case	Temperature (°C)	
	Ambient	Top Reflector
1	14.9	15.4
2	14.9	-
2R	14.8	-
3	14.6	13.9
3R	15.1	-

1.5 Supplemental Experimental Measurements

No additional experimental measurements were performed.

2.0 EVALUATION OF EXPERIMENTAL DATA

Each configuration was evaluated using MCNP® 6.3 with ENDF/B-VIII.0 neutron cross section libraries[6,7], using the re-release of the NJOY2016 processed thermal scattering law library[8]. The calculations are typically run with 1,000 generations of 500,000 particles per generation, skipping the first 50 generations, resulting in a total of 475 million active histories and a typical statistical uncertainty of ± 0.00004 in k_{eff}. Therefore, the threshold for negligible is defined to be less than or equal to 0.00004 (4 pcm) in k_{eff}.

For a given parameter i with a mean value $x_{0,i}$ and a perturbation δx_i, the resulting effect in k_{eff} is calculated using

$$\Delta k_{\text{eff},i} = \frac{k_{\text{eff}}(x_{0,i} + \delta x_i) - k_{\text{eff}}(x_{0,i} - \delta x_i)}{2} \tag{1}$$

The effect of the perturbation in k_{eff} for parameter i is symmetric unless otherwise stated. The standard uncertainty in k_{eff}, $u_{k,i}$, is then calculated with the evaluated uncertainty in parameter i, u_i, and the sensitivity in k_{eff} to the perturbation δx_i from Eq. 1:

$$u_{k,i}^2 = u_i^2 \left(\frac{\Delta k_{\text{eff},i}}{\delta x_i} \right)^2 \tag{2}$$

When the sensitivity in k_{eff} to parameter i, as defined in Eq. 1, can be assumed to be independent for multiple perturbations δx_i, Eq. 2 may be represented as

$$(u_{k,i}) = (u_i \sqrt{N}) \left(\frac{\Delta k_{\text{eff},i}}{\Delta x_i} \right) \tag{3}$$

where $u_i\sqrt{N}$ is the resulting sum in quadrature of N independent uncertainties in parameter i, u_i, and Δx_i is the sum of the individual perturbations δx_i. This form is useful when evaluating the uncertainty in a parameter i involving multiple parts of a similar type, allowing N perturbations to be performed with a single calculation. This approach is used for components of the mass uncertainty in Section 2.2, dimensional uncertainty in Section 2.3, and material uncertainty in Section 2.4.

[6] Christopher John Werner et al. *MCNP User's Manual Code Version 6.2*. LA-UR-17-29981. Los Alamos National Laboratory, 2017.

[7] J. L. Conlin et al. *Release of ENDF/B-VIII.0-Based ACE Data Files*. LA-UR-18-24034. Los Alamos National Laboratory, 2018. DOI: 10.2172/1438139.

[8] D. K. Parsons and C. A. Toccoli. *Re-Release of the ENDF/B VIII.0 S(α,β) Data Processed by NJOY2016*. LA-UR-20-24456. Los Alamos National Laboratory, 2020. DOI: 10.2172/1634930.

2.1 Reactor Period

Reactor period measurements of the experimental configurations are described in Section 1.2.8. The four ^{3}He proportional counters (SU) typically saturated prior to the end of the experimental measurements. Therefore, only the data from the compensated ion chambers (LC) is considered for the benchmark reactor period.

The measurements reported in Table 63 of Section 1.2.8 are based on preliminary fits of the neutron count rate data performed during the experiment and documented in the Comet logbook. Table 83 reports the final fits of the neutron count rate data following the conclusion of the experiment. The uncertainty in the fits are negligible for all measurements. The LC_{avg} is the average and standard deviation of the three LC detectors and represents the evaluated benchmark reactor periods.

Table 83: Measured reactor period based on exponential fitting of the neutron count rate data.

Case	Reactor Period (s)			
	LC_1	LC_2	LC_3	LC_{avg}
1	204.1	204.0	203.6	203.9 ± 0.3
2	116.7	117.5	116.2	116.8 ± 0.7
3	45.6	45.8	45.6	45.7 ± 0.1
2[(a)]	151.9	151.8	152.2	152.0 ± 0.2
3[(a)]	52.1	52.2	52.0	52.1 ± 0.1

[(a)] Reproducibility measurement.

The measured reactor period is used to estimate the excess reactivity of the experimental configuration using the following form of the Inhour equation

$$\rho(T) = \frac{\Lambda}{T\beta_{\text{eff}}} + \sum_{i=1}^{6} \frac{a_i}{(1+\lambda_i T)} \tag{4}$$

where $\rho(T)$ is the excess reactivity, as a function of the measured reactor period T, Λ is the mean generation time, and a_i and λ_i are the abundance ($\beta_i/\beta_{\text{eff}}$) and decay constant of the i^{th} delayed neutron precursor group, respectively.

The ENDF/B-VIII.0 six-group delayed neutron abundances and decay constants[9] for ^{235}U were used and are reproduced in Table 84. The ENDF-6 Delayed Neutron Data format does not store values for the uncertainties in the parameters. Therefore, the uncertainties in the abundances and decay constants are based on the six-group parameters for ^{235}U as recommended by Tuttle[10]. These delayed neutron abundances, decay constants, and uncertainties are similar to, but not the same as, the six-group parameters as reported by Keepin for fast ^{235}U fission[11].

[9] ENDF-6 Formats Manual, File 1, Delayed Neutron Data (MT=455). DOI: 10.2172/1425114

[10] R. J. Tuttle. "Delayed-Neutron Data for Reactor-Physics Analysis". *Nuclear Science and Engineering* 56.1 (1975), pp. 37–71. DOI: 10.13182/NSE75-A26620.

[11] G. R. Keepin. *Physics of Nuclear Kinetics*. Reading, Massachusetts: Wesley Publishing Company, 1956.

Table 84: ENDF/B-VIII.0 six-group delayed neutron abundances and decay constants for ^{235}U.

Group	Abundance, a_i	Decay Constant, λ_i (s^{-1})
1	0.036 ± 0.004	0.0133 ± 0.0003
2	0.236 ± 0.007	0.0309 ± 0.0012
3	0.179 ± 0.024	0.1134 ± 0.0040
4	0.327 ± 0.010	0.2925 ± 0.0120
5	0.170 ± 0.012	0.8575 ± 0.1200
6	0.051 ± 0.004	2.7297 ± 0.5500

The delayed neutron fraction, β_{eff}, and the mean generation time, Λ, are system-dependent. Furthermore, no measurements were performed to infer these quantities experimentally. Therefore, β_{eff} and Λ must be based on calculation. To do so, the iterated fission probability method, as implemented in the KOPTS card of MCNP® 6.3, was used. The results of these calculations using the benchmark models are reported in Table 85. The uncertainties in these calculated parameters are based on the Monte Carlo statistical uncertainty of the calculation.

Table 85: Delayed neutron fraction and mean generation time (based on calculations using MCNP® 6.3 with ENDF/B-VIII.0).

Case	Delayed Neutron Fraction, β_{eff}	Mean Generation Time, Λ (s)
1	0.00735 ± 0.00005	1.612E−5 ± 2.168E-8
2	0.00729 ± 0.00004	3.072E−5 ± 2.815E-8
3	0.00757 ± 0.00005	2.357E−6 ± 6.100E-9

Table 86 reports the results of the experimental configurations. The excess reactivity is calculated using Eq. 4 with the LC_{avg} period. The uncertainty in the excess reactivity is propagated from the delayed neutron parameters (Table 84), calculated β_{eff} and Λ (Table 85), and standard deviation of LC_{avg} (Table 86). Finally, the following relationship is used to determine the k_{eff} of the experimental configurations

$$\rho(\$) = \frac{k_{\text{eff}} - 1}{k_{\text{eff}}\,\beta_{\text{eff}}} \tag{5}$$

where $\rho(\$)$ is the excess reactivity in dollars and β_{eff} is the delayed neutron fraction (Table 85).

Table 86: Measured reactor period, excess reactivity, and k_{eff} for the experimental configurations.

Case	Reactor Period (s)[(a)]	Excess Reactivity ($)	Experimental k_{eff}
1	203.9 ± 0.3	0.056 ± 0.002	1.00041 ± 0.00002
2	116.8 ± 0.7	0.089 ± 0.004	1.00065 ± 0.00003
3	45.7 ± 0.1	0.177 ± 0.007	1.00134 ± 0.00005

[(a)] Based on LC_{avg} reported in Table 86.

In addition to the reactor period measurements of the three experimental configurations documented in this evaluation, two additional period measurements were performed to characterize the reproducibility of the experimental configurations. These reproducibility measurements were performed for the Case 2 and 3 experimental configurations by completely disassembling, then reassembling and remeasuring the reactor period. No reproducibility measurements were performed for Case 1.

Table 87 reports the measured results of the reproducibility measurements. In both instances, the change in the neutron multiplication factor is greater than one sigma. The majority of the parts, save the HEU fuel plates, have physical identifiers that may were used during the stacking process to ensure no rotation of the parts when restacking. For instance, each of the sodium chloride absorber plates have a unique part ID engraved along the outer surface of the encapsulations, which allowed the practitioners to restack in a repeatable way. While this doesn't necessarily preclude the possibility of small effects from rotation or gaps, this is a best estimate for exact reproducility. Therefore an encompassing uncertainty of 13 pcm is assigned to the experimental keff values. The final experimental k_{eff} values, with their assigned uncertainties, are provided in Table 88.

Table 87: Measured reactor period, excess reactivity, and k_{eff} for the reproducibility measurements for Case 2 and 3. The experimental Δk_{eff} is with respect to the non-reproducibility measurements to highlight the difference between the two measurements of each case.

Case	**Reactor Period (s)[(a)]**	**Excess Reactivity ($)**	**Experimental Δk_{eff}**
2	152.0 ± 0.2	0.072 ± 0.003	-0.00013 ± 0.00003
3	52.1 ± 0.1	0.162 ± 0.006	-0.00011 ± 0.00007

[(a)] Based on LC_{avg} reported in Table 86.

Table 88: Final experimental k_{eff} values for the experimental configurations.

Case	**Experimental k_{eff}**
1	1.00041 ± 0.00013
2	1.00065 ± 0.00013
3	1.00134 ± 0.00013

2.2 Mass Uncertainty

Uncertainty analysis of part masses was done with constant volume, which requires that the part density be adjusted to conserve mass. The evaluated uncertainties are typically based on the distribution of the individual part measurements within a given part type, unless otherwise noted. This distribution represents the standard deviation,

$$\sigma = \sqrt{\sum_{i=1}^{N} (x_i - \bar{x})^2} \tag{6}$$

where $\bar{x}$ is the average mass of the part type and σ is the resulting uncertainty for the part type, assuming N parts of that part type, each having a measured mass x_i. The mass measurements are assumed to be independent. While measurements were performed with the same instrument, the random uncertainty component, which would be the correlated uncertainty component, is assumed to be significantly dwarfed by the uncertainty in the distribution of the part masses, and can be neglected in this analysis.

As described in Section 2.0, the perturbations related to mass uncertainties are performed by collectively perturbing all parts of a given part type at once, unless noted otherwise. This allows Eq. 3 to be used in determining the standard uncertainty in k_{eff}.

2.2.1 Highly Enriched Uranium Mass

Mass measurements of the HEU plates are reported in Table 5 of Section 1.2.3, including measurements from 2023, 2022, 2020 HEU-MET-MIXED-021, and 2005. The measurements from 2022 and 2020 were performed using a balance with a reported linearity of ± 0.3 g, representing the uncertainty in the measurement.

Table 89 compares the differences in the measured HEU plate masses from the 2022 and 2020 measurements, using the 2005 measurements for plates that were not measured in 2020. The largest difference in mass is a loss of 5.6 grams. The measurements have an average difference of -1.2 ± 1.7 g, generally with the plate mass decreasing over time due to oxidation. The evaluated uncertainty for the HEU plate mass is ± 1.7 g. This uncertainty is significantly larger than the measurement uncertainty (± 0.3 g). Since the measurements were two years apart, and another two years had elapsed before this experiment was executed, the mass difference is assumed to be double that evaluated in TEX-Hf. Therefore the largest mass difference is assumed to be 12 grams.

The masses measured in 2023 were only a subset of the plates, so the measurements from 2022 were used. The difference in the mass measurements between 2022 and 2023 are enveloped in the associated uncertainty of 12 grams, so the effect of choosing one over the other is negligible.

Table 89: Difference in the HEU plate mass measurements.

Part Type	Part ID	Difference (g)
6/0-HEU	Q2-16[a]	-2.2
15/0-HEU	11150	-5.6
	11149	-1.4
	11147	-4.9
	11019	-0.8
	11017	-3.8
15/2.5-HEU	10491	-0.8
	10489	-0.1
	10487	0.5
	10475	-1.5
	10470	-0.4
	10467	-0.2
	10464	-0.1
15/6-HEU	11018	-0.3
	10935[a]	-1.0
	10933[a]	-2.5
	10932[a]	-3.6
	10477	-0.3
	10457	-0.2
15/10-HEU	10485[a]	-1.2
	10481[a]	0.7
	10479	-0.1
	10473[a]	-0.4
	10472	0.7
	10463	0.0
	10458[a]	-0.4
Average Difference (g)		**−1.2 ± 1.7**

[a] Compared to the mass measurement performed in 2005.

Table 90 summarizes the HEU plate mass uncertainty calculation parameters and sensitivity in k_{eff} for the three configurations. The total HEU mass is the sum of all HEU plates in the experimental configurations. The calculations vary the HEU mass by collectively perturbing the mass of all HEU plates in the experimental configurations by ± 12.0 g. Therefore, the standard uncertainty in k_{eff} is calculated using Eq. 3 where N is the number of HEU plates in the experimental configuration and u_i is the evaluated uncertainty in the HEU plate mass of ± 1.7 g. Table 90 is reproduced alongside the other evaluated uncertainties in Section 2.6.

Table 90: Summary of sensitivity in k_{eff} to uncertainties in the HEU plate mass.

Case	Number of Plates	Total HEU Mass (g)	Parameter Variation in Calculation	Calculated Effect in k_{eff}	Standard Uncertainty	Standard Uncertainty in k_{eff}
1	8	48604.8	$\pm 12.0 \times 8$	0.00059	$\pm 1.7\sqrt{8}$	Negligible
2	8	48604.8	$\pm 12.0 \times 8$	0.00057	$\pm 1.7\sqrt{8}$	Negligible
3	18	110201.3	$\pm 12.0 \times 18$	0.00143	$\pm 1.7\sqrt{18}$	Negligible

2.2.2 Sodium Chloride Absorber Mass

2.2.2.1 Encapsulations

Mass measurements for both the 3/16-inch and 1/4-inch plates were performed for each component and combined assembly. The measurements, shown in Sections 1.2.4.3 and 1.2.4.4, were performed with a balance with a total reported uncertainty of ± 0.3 g. The measurements were performed for the individual components, i.e. the base, the lid, and the entire assembly. Mass measurements of the entire assembly, without the salt in the plate, were performed three times and agreed with the individual component mass measurements. Table 91 summarizes the sodium chloride absorber encapsulation mass measurements, reporting the average and standard deviation of the measurements.

Table 91: Average sodium chloride absorber encapsulation mass.

Part Type	N	Mass (g)
SaltPlate3/16 - Base	23	1208.6 ± 5.6
SaltPlate3/16 - Lid	23	720.5 ± 1.1
SaltPlate3/16 - Total (with screws)	23	1931.8 ± 5.9
SaltPlate1/4 - Base	13	1386.2 ± 7.5
SaltPlate1/4 - Lid	13	721.7 ± 1.0
SaltPlate1/4 - Total (with screws)	13	2110.7 ± 8.2

Table 92 summarizes the sodium chloride absorber encapsulation mass uncertainty calculation parameters and sensitivity in k_{eff}. The total encapsulation mass is the sum of all encapsulation plates in the experimental configurations. The calculations vary the encapsulation mass by collectively perturbing the mass of all sodium chloride absorber encapsulations in the experimental configurations by ± 9 g (1/4-inch plates) and ± 7 g (3/16-inch plates), which encompasses the variance of the mass measurements for lids and bases for all components. Therefore, the standard uncertainty in k_{eff} is calculated using Eq. 3 where N is the number of absorber plates in the experimental configuration and u_i is the evaluated uncertainty in the encapsulation mass of ± 9 g (1/4-inch plates) and ± 7 g (3/16-inch plates) . Table 92 is reproduced alongside the other evaluated uncertainties in Section 2.6.

Table 92: Summary of sensitivity in k_{eff} to uncertainties for the NaCl salt plate encapsulation mass.

Case	Number of Plates	Total Encapsulation Mass (g)	Parameter Variation in Calculation	Calculated Effect in k_{eff}	Standard Uncertainty	Standard Uncertainty in k_{eff}
1	7	14771.2	$\pm 9.0 \times 7$	-0.00001	$\pm 8.2\sqrt{7}$	Negligible
2	7	14771.2	$\pm 9.0 \times 7$	-0.00013	$\pm 8.2\sqrt{7}$	Negligible
3	17	32802.9	$\pm 7.0 \times 17$	0.00044	$\pm 7.0\sqrt{17}$	± 0.00005

2.2.2.2 NaCl Salt

Mass measurements for both the filled 3/16-inch and 1/4-inch absorbers were performed three times, at the time of fill, prior to shipping the absorbers, and immediately after the experiments were performed. Table 91 summarizes the mass measurements, reporting the average and standard deviation of the measurements. The filled plate masses, along with the empty plate masses from Section 2.2.2.1, were used to infer the NaCl salt

mass of each plate. Table 94 summarizes the inferred salt masses, reporting the average and standard deviation of the measurements.

Table 93: Average sodium chloride absorber encapsulation mass.

Part Type	N	Initial Filled Mass (g)	Pre-Shipment Filled Mass (g)	Post-Experiment Filled Mass (g)[a]
SaltPlate3/16	23	2443.3 ± 11.8	2443.7 ± 12.0	2443.3 ± 10.4
SaltPlate1/4	13	2772.2 ± 12.5	2772.2 ± 12.6	2768.0 ± 8.5

Table 94: Average NaCl salt mass.

Part Type	N	NaCl Mass (g)
SaltPlate3/16	23	655.0 ± 6.5
SaltPlate1/4	13	510.9 ± 5.3

Table 95 summarizes the NaCl salt mass uncertainty calculation parameters and sensitivity in k_{eff}. The total salt mass is the sum of all salt in the experimental configurations. The calculations vary the salt mass by collectively perturbing the mass of all salt in the experimental configurations by ± 10 g. Therefore, the standard uncertainty in k_{eff} is calculated using Eq. 3 where N is the number of salt plates in the experimental configuration and u_i is the evaluated uncertainty in the NaCl mass of ± 6.5 g (3/16-inch plates) and ± 5.3 g (1/4-inch plates). Table 95 is reproduced alongside the other evaluated uncertainties in Section 2.6.

Table 95: Summary of sensitivity in k_{eff} to uncertainties for the NaCl salt mass.

Case	Number of Plates	Total NaCl Mass (g)	Parameter Variation in Calculation	Calculated Effect in k_{eff}	Standard Uncertainty	Standard Uncertainty in k_{eff}
1	7	4585.0	$\pm 10.0 \times 7$	-0.00172	$\pm 5.3\sqrt{7}$	± 0.00017
2	7	4585.0	$\pm 10.0 \times 7$	-0.00243	$\pm 5.3\sqrt{7}$	± 0.00025
3	17	8685.7	$\pm 10.0 \times 17$	0.00012	$\pm 6.5\sqrt{17}$	Negligible

2.2.3 Polyethylene Moderator Mass

Mass measurements of the polyethylene moderator plates are reported in Tables 36, 38, 40, 42, and 44. These measurements were performed using a balance with a precision of 0.1 g. Table 96 summarizes the polyethylene moderator plate mass measurements, reporting the average and standard deviation of the masses by part type. The uncertainties are represented as the standard deviation of the mass measurements from parts of the same type. As found in HEU-MET-INTER-013, there was a grouping in the 1/8-MOD parts and this is addressed by assigning different uncertainties for each group. However, only the first 17 1/8-MOD plates were utilized, all of which share the same uncertainty.

A set of 3/4-inch moderator parts were procured for this experimental campaign, and as such the masses were measured at a separate time. The mass measurements are reported in Table 42 The measurements were performed using a balance with a precision of 0.3 g.

Table 96: Average polyethylene moderator plate mass by part type.

Part Type	N	Mass (g)
1/8-MOD-{1-18}	18	344.1 ± 0.9
1/4-MOD	36	688.4 ± 0.7
1/2-MOD	32	1380.6 ± 3.3
3/4-MOD	22	2115.5 ± 3.0
1.5-MOD	12	4152.5 ± 17.9

The evaluated uncertainties in the polyethylene moderator plate types are: ± 0.9 g for 1/8-MOD-{1-18}; ± 0.7 g for 1/4-MOD; ± 3.3 g for 1/2-MOD; ± 3.0 g for 3/4-MOD; and ± 17.9 g for 1.5-MOD. Table 97 summarizes the polyethylene moderator plate mass uncertainty calculation parameters and sensitivity in k_{eff}. The total moderator mass is the sum of all polyethylene moderator plates in the experimental configurations. The calculations vary the moderator mass by collectively perturbing the mass of all polyethylene moderator plates in the experimental configurations by their respective evaluated uncertainties. The standard uncertainty in k_{eff} is calculated using Eq. 3 where N is the number of polyethylene moderator plates in the experimental configuration and u_i is the evaluated uncertainty for the polyethylene moderator plate type used in the experimental configuration. Table 97 is reproduced alongside the other evaluated uncertainties in Section 2.6.

Table 97: Summary of sensitivity in k_{eff} to uncertainties for the polyethylene moderator plate mass.

Case	Number of Plates	Total Moderator Mass (g)	Parameter Variation in Calculation	Calculated Effect in k_{eff}	Standard Uncertainty	Standard Uncertainty in k_{eff}
1	14	29612.3	$\pm 3.0 \times 14$	0.00008	$\pm 3.0\sqrt{14}$	Negligible
2	7	33898.2	$\pm 18.6 \times 7$	-0.00085	$\pm 18.6\sqrt{7}$	± 0.00016
3	17	5848.4	$\pm 0.9 \times 17$	0.00152	$\pm 0.9\sqrt{17}$	± 0.00018

2.2.4 Polyethylene Reflector Mass

The reflector parts consist of a bottom reflector, a top reflector, and annular reflector rings, as shown in Figure 33. The bottom reflector is a single unit (BOTREFSRC) and the top reflector may consist of multiple parts, including the use of moderator (MOD) or reflector (REF) parts. The upper and lower reflector rings consist of the interlocking RING and CAP parts. The base of the upper reflector ring is the BOTCAP part. The base of the lower reflector ring is the BOTREFSRC-1 for all configurations.

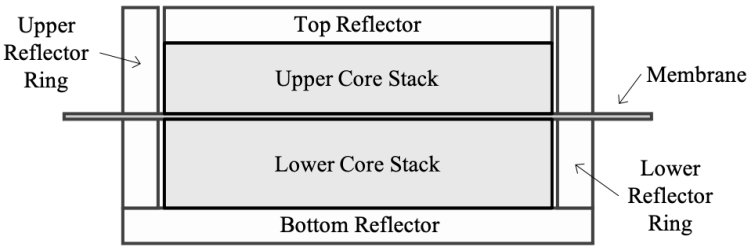

Figure 33: Diagram of the reflector components surrounding the upper and lower core stacks.

Mass measurements of the polyethylene reflector parts are report in Table 46 (REF), Table 47 (RING), Table 48 (CAP and BOTCAP), Table 49 (CAP), and Table 50 (BOTREFSRC). These measurements were performed using a balance with a precision of 0.1 g. Table 98 summarizes the polyethylene reflector part mass measurements, reporting the average and standard deviation of the masses by part type. The uncertainties are represented as the standard deviation of the mass measurements from parts of the same type. The BOTREFSRC and BLNKINSRT parts were procured for this experiment and were therefore measured independently of the other parts. The BOTREFSRC and BLNKINSRT parts were measured using a balance with a precision of 0.3 g.

Table 98: Average polyethylene reflector part mass by part type (s).

Part Type	N	Mass (g)
1/16-REF	2	182.7 ± 0.4
1-REF	2	2767.1 ± 0.2
1/4-RING	4	199.0 ± 0.3
1/2-RING	4	393.7 ± 0.7
1-RING	6	805.5 ± 0.5
3-RING	6	2386.3 ± 2.0
0-BOTCAP	2	48.1 ± 0.1
0-CAP	3	50.8 ± 0.1
1/32-CAP	3	76.8 ± 0.1
1/16-CAP	3	101.2 ± 0.3
1/8-CAP	3	149.0 ± 0.1
BOTREFSRC[(a)]	2	3976.4 ± 0.5
BLNKINSRT[(a)]	4	39.5 ± 0.3
1/4-MOD	36	688.4 ± 0.7
1/2-MOD	32	1380.6 ± 3.3

[(a)] Measured independently of other parts in 2024.

The uncertainties in the reflector part mass measurements are typically less than ± 0.7 g, except for the higher mass parts (3-RING, 1/2-MOD). As such, the evaluated uncertainties in the reflecotr part mass components are: ± 2.0 g for the 3-RING, ± 3.3 g for the 1/2-MOD and ± 0.7 g for all other parts.

Table 99: Total masses of the reflector components.

Case	Reflector Component (g)				Total Mass (g)
	Top Plate	Upper Ring	Lower Ring	Bottom Plate[(a)]	
1	690.2 ± 0.7	5265.8 ± 2.9	6687.5 ± 2.9	4016.15 ± 0.60	16659.7 ± 4.2
2	1377.9 ± 3.3	6070.4 ± 3.0	7436.2 ± 3.5	4016.15 ± 0.60	18900.7 ± 5.7
3	2949.3 ± 0.4	3912.1 ± 2.2	5512.4 ± 2.9	4016.15 ± 0.60	16390.0 ± 3.7

[(a)] All cases use the BOTREF-1 part as the bottom reflector plate.

Table 100 summarizes the polyethylene reflector mass uncertainty calculation parameters and sensitivity in k_{eff}. The total reflector mass is the sum of all reflector parts, as reported in Table 99. The calculations vary the reflector mass by collectively perturbing the mass of all reflector part in the experimental configurations by ± 0.5 %. This large perturbation was chosen to improve the statistics in Δk_{eff} used in Eq. 2. Therefore, the standard uncertainty in k_{eff} is calculated using Eq. 3 where N is the number of reflector parts in the experimental configuration and u_i is the evaluated uncertainty in the total polyethylene reflector mass reported in Table 99. Table 100 is reproduced alongside the other evaluated uncertainties in Section 2.6.

Table 100: Summary of sensitivity in k_{eff} to uncertainties for the polyethylene reflector mass.

Case	Number of Parts	Total Reflector Mass (g)	Parameter Variation in Calculation	Calculated Effect in k_{eff}	Standard Uncertainty	Standard Uncertainty in k_{eff}
1	13	16659.7	± 0.5 %	0.00054	$\pm 4.2\sqrt{13}$	± 0.00005
2	13	18900.7		0.00061	$\pm 5.7\sqrt{13}$	± 0.00007
3	14	16390.0		0.00153	$\pm 3.7\sqrt{14}$	± 0.00012

2.2.5 Aluminum Insert Mass

Mass measurements of the aluminum inserts are reported in Table 54. These measurements were performed using a balance with a precision of 0.1 g. Table 101 summarizes the aluminum insert mass measurements by part type, reporting the average and standard deviation of the measurements.

Table 101: Average aluminum insert mass by part type.

Part Type	N	Mass (g)
2.5-DISK	10	24.8 ± 0.1
6-DISK	6	150.4 ± 0.7
10-DISK	10	425.6 ± 1.4

Table 102 summarizes the aluminum insert mass uncertainty calculation parameters and sensitivity in k_{eff}. The total insert mass is the sum of all aluminum inserts in the experimental configurations. The calculations vary the insert mass by collectively perturbing the mass of all aluminum inserts in the experimental configurations by ± 3.0 g. Therefore, the standard uncertainty in k_{eff} is calculated using Eq. 3 where N is the number of aluminum inserts in the experimental configuration and u_i is the evaluated uncertainty in the aluminum insert mass of ± 0.5 g. Table 102 is reproduced alongside the other evaluated uncertainties in Section 2.6.

Table 102: Summary of sensitivity in k_{eff} to uncertainties for the aluminum insert mass.

Case	Number of Inserts	Total Insert Mass (g)	Parameter Variation in Calculation	Calculated Effect in k_{eff}	Standard Uncertainty	Standard Uncertainty in k_{eff}
1	2	448.6	$\pm 3.0 \times 2$	0.00006	$\pm 0.5\sqrt{2}$	Negligible
2	2	624.5	$\pm 3.0 \times 2$	-0.00005	$\pm 0.5\sqrt{2}$	Negligible
3	7	925.9	$\pm 3.0 \times 7$	0.00015	$\pm 0.5\sqrt{7}$	Negligible

2.2.6 Membrane Mass

The mass measurement of the membrane is reported in Table 81. This measurement was performed using a balance with a reported linearity of ± 0.3 g, representing the uncertainty in the measurement. Therefore, the evaluated uncertainty in the membrane mass is ± 0.3 g.

Table 103 summarizes the membrane mass uncertainty calculation parameters and sensitivity in k_{eff}. The calculations vary the membrane mass by perturbing its mass by ± 20.0 g. This large perturbation was chosen to improve the statistics in Δk_{eff} used in Eq. 2. The standard uncertainty in k_{eff} is calculated using Eq. 2 where u_i is the evaluated uncertainty in the membrane mass of ± 0.3 g. Table 103 is reproduced alongside the other evaluated uncertainties in Section 2.6.

Table 103: Summary of sensitivity in k_{eff} to uncertainties in the membrane mass.

Case	Membrane Mass (g)	Parameter Variation in Calculation	Calculated Effect in k_{eff}	Standard Uncertainty	Standard Uncertainty in k_{eff}
1	2396.1	±20.0	0.00010	±0.3	Negligible
2			−0.00003		Negligible
3			−0.00010		Negligible

2.2.7 Structure Mass

The effect on k_{eff} due to perturbations of the structure mass were investigated in both HEU-MET-INTER-013 (TEX-Hf) and HEU-MET-MIXED-021 (TEX-HEU Baseline Assemblies). In both cases, the structure mass was found to be negligible. Therefore, the same is assumed for this evaluation.

2.3 Dimensional Uncertainty

All dimensional uncertainties are evaluated by perturbing the dimensions at a constant mass, requiring the part density to be adjusted in order to conserve mass. The dimensional uncertainties are based on both measured quantities and tolerances from engineering drawings.

As described in Section 2.0, the perturbations related to dimensional uncertainties are performed by collectively perturbing all parts of a given part type at once, unless noted otherwise. This allows Eq. 3 to be used in determining the standard uncertainty in k_{eff}.

2.3.1 Highly Enriched Uranium Plate Dimensions

The nominal dimensions and tolerances of the HEU plates are reported in Table 4 of Section 1.2.3. The nominal dimensions for the inner and outer diameters of the HEU plates were recently verified through CMM measurements [12]. Thickness measurements of the HEU plates are reported in Table 5 of Section 1.2.3. Table 104 summarizes the measured HEU plate diameters and average measured thickness. The tolerance of the diameters has been converted from one-sided to symmetric by selecting the midpoint of the tolerance interval. The uncertainty in the thickness is reported as the standard deviation of all available thickness measurements, regardless of part type. Therefore, the evaluated uncertainty in the HEU plate diameters and thickness are ± 0.00635 cm and ± 0.0060 cm, respectively. The uncertainty in the diameters is assumed be uniform within the tolerance interval.

The HEU plate thicknesses are addressed as part of the core stack height uncertainty in 2.3.5. Only the uncertainty in the inner and outer diameters are addressed here.

Table 104: HEU plate average thickness and diameters by part type.

Part Type	N	Diameter (cm)		Thickness (cm)
		Inner	Outer	
15/0-HEU	5	-	38.0937 ± 0.0064	0.3108 ± 0.0060
15/2.5-HEU	7	6.3818 ± 0.0064		
15/6-HEU	6	15.2591 ± 0.0064		
15/10-HEU	7	25.4191 ± 0.0064		
6/0-HEU	1	-	15.2337 ± 0.0064	

Table 105 summarizes the HEU plate diameter uncertainty calculation parameters and sensitivity in k_{eff}. The calculations vary the parameter by collectively perturbing all HEU plate diameters by ± 0.02 cm. This perturbation is performed for both the inner and outer diameters at the same time but in opposite directions such that the outer diameter is increased by 0.02 cm and the inner diameter is decreased by 0.02 cm, and vice versa. Since the evaluated uncertainty in the diameters represents a uniform tolerance interval, the standard uncertainty is $\pm 0.00635/\sqrt{12}$ cm or approximately ± 0.002 cm. Therefore, the standard uncertainty in k_{eff} is calculated using Eq. 3 where N is the number of HEU plates in the experimental configuration and u_i is the evaluated uncertainty in the HEU plate diameter of ± 0.002 cm. Table 105 is reproduced alongside the other evaluated uncertainties in Section 2.6.

[12] K. Amundson, T. Cutler, C. Kiehne, *et al.*, *HEU Pancake (Jemima) Plate Preliminary Characterization Report*, Los Alamos National Laboratory, LA-UR-24-20414 (2024)

Table 105: Summary of sensitivity in k_{eff} to uncertainties for the HEU plate diameters.

Case	Number of Plates	Parameter Value (cm)	Parameter Variation in Calculation	Calculated Effect in k_{eff}	Standard Uncertainty	Standard Uncertainty in k_{eff}
1	8	Varies (Table 104)	$\pm 0.02(8)$	0.00000	$\pm 0.002\sqrt{8}$	Negligible
2	8		$\pm 0.02(8)$	-0.00013	$\pm 0.002\sqrt{8}$	Negligible
3	18		$\pm 0.02(18)$	-0.00053	$\pm 0.002\sqrt{18}$	Negligible

2.3.2 Sodium Chloride Absorber Dimensions

Due to the dependence of the core stack height on the thickness of the sodium chloride absorbers, the uncertainty in the plate thickness is evaluated as part of the core stack height uncertainty in Section 2.3.5. The following analysis is limited to the uncertainty in the diameter of the sodium chloride absorbers, encapsulations, and the pocket depth within the encapsulation.

The nominal and measured dimensions of the sodium chloride absorber encapsulations are reported in Section 1.2.4. Table 106 summarizes the NaCl salt and encapsulation dimensional measurements, reporting the average thickness and diameter. The uncertainties are reported as the standard deviation of the measurements. The average diameter is based on measurements performed using a CMM with a resolution of 0.00635 cm. The average thickness is based on the measurements reported in Table 9,10,24, and 25. These measurements were performed with the CMM and the result is an average of multiple points taken across the surfaces via a best fit cylinder. The evaluated uncertainty for these measurements is taken to be the population variance (variance of the measurements for all of the plates measured). The evaluated uncertainties are given in Section 1.2.4.

The dimensions described are of the encapsulation. The dimensions of the NaCl salt is determined by the inner diameter and pocket depth of the encapsulation.

Table 106: Average sodium chloride absorber encapsulation dimensions.

Part Type	N	Inner Diameter (cm)	Outer Diameter (cm)	Pocket Depth (cm)	Bottom Thickness (cm)
SaltPlate3/16	23	30.479 ± 0.002	38.091 ± 0.003	0.490 ± 0.005	0.244 ± 0.007
SaltPlate1/4	23	30.478 ± 0.003	38.095 ± 0.005	0.643 ± 0.009	0.236 ± 0.006

2.3.2.1 Sodium Chloride Diameter

Table 107 summarizes the sodium chloride absorber diameter uncertainty calculation parameters and sensitivity in k_{eff}. The calculations vary the sodium chloride diameter by perturbing all sodium chloride absorber diameters (inner encapsulation diameters) by ± 0.02 cm. The standard uncertainty in k_{eff} is calculated using Eq. 3 where N is the number of absorber plates in the experimental configuration and u_i is the evaluated uncertainty in the sodium chloride absorber diameter of ± 0.002 cm or ± 0.003 cm. Table 107 is reproduced alongside the other evaluated uncertainties in Section 2.6.

Table 107: Summary of sensitivity in k_{eff} to uncertainties in the sodium chloride absorber diameters.

Case	Number of Plates	Parameter Value (cm)	Parameter Variation in Calculation	Calculated Effect in k_{eff}	Standard Uncertainty	Standard Uncertainty in k_{eff}
1	7	30.479	$\pm 0.02(7)$	0.00002	$\pm 0.002\sqrt{7}$	Negligible
2	7		$\pm 0.02(7)$	0.00012	$\pm 0.002\sqrt{7}$	Negligible
3	17	30.478	$\pm 0.02(17)$	-0.00008	$\pm 0.003\sqrt{17}$	Negligible

2.3.2.2 Sodium Chloride Absorber Pocket Depth

Table 108 summarizes the sodium chloride absorber pocket depth uncertainty calculation parameters and sensitivity in k_{eff}. The calculations vary the sodium chloride absorber thickness by perturbing all sodium chloride absorber pocket depths by ± 0.02 cm and perturbing all bottom encapsulation thicknesses equally in the opposite direction to maintain the overall absorber thickness. The mass was held constant, so the density was perturbed. The standard uncertainty in k_{eff} is calculated using Eq. 3 where N is the number of absorber plates in the experimental configuration and u_i is the evaluated uncertainty in the sodium chloride absorber thickness of ± 0.003 cm. Table 108 is reproduced alongside the other evaluated uncertainties in Section 2.6.

Table 108: Summary of sensitivity in k_{eff} to uncertainties in the sodium chloride absorber thicknesses.

Case	Number of Plates	Parameter Value (cm)	Parameter Variation in Calculation	Calculated Effect in k_{eff}	Standard Uncertainty	Standard Uncertainty in k_{eff}
1	7	0.490	$\pm 0.02(7)$	0.00374	$\pm 0.003\sqrt{7}$	± 0.00011
2	7		$\pm 0.02(7)$	0.00525	$\pm 0.003\sqrt{7}$	± 0.00015
3	17	0.643	$\pm 0.02(17)$	0.00137	$\pm 0.003\sqrt{17}$	± 0.00004

2.3.2.3 Encapsulation Diameter

Table 109 summarizes the encapsulation diameter uncertainty calculation parameters and sensitivity in k_{eff}. The calculations vary the encapsulation diameter by perturbing all encapsulation absorber diameters by ± 0.02 cm. The standard uncertainty in k_{eff} is calculated using Eq. 3 where N is the number of absorber plates in the experimental configuration and u_i is the evaluated uncertainty in the encapsulation diameter of ± 0.003 cm or ± 0.005 cm. Table 109 is reproduced alongside the other evaluated uncertainties in Section 2.6.

Table 109: Summary of sensitivity in k_{eff} to uncertainties in the encapsulation diameters.

Case	Number of Plates	Parameter Value (cm)	Parameter Variation in Calculation	Calculated Effect in k_{eff}	Standard Uncertainty	Standard Uncertainty in k_{eff}
1	7	38.091	$\pm 0.02(7)$	0.00005	$\pm 0.003\sqrt{7}$	Negligible
2	7		$\pm 0.02(7)$	-0.00002	$\pm 0.003\sqrt{7}$	Negligible
3	17	38.095	$\pm 0.02(17)$	0.00019	$\pm 0.005\sqrt{17}$	Negligible

2.3.3 Polyethylene Plate Dimensions

Due to the dependence of the core stack height on the thickness of the polyethylene plates, the uncertainty in the plate thickness is evaluated as part of the core stack height uncertainty in Section 2.3.5. The following analysis is limited to the uncertainty in the diameter of the polyethylene plates.

The polyethylene plates include the moderator (MOD), top reflector (REF), and bottom reflector source (BOTREFSRC) part types. The nominal and measured dimensions of the MOD and REF plates are reported in Tables 35, 46, 44, 36, 38, 40, and 42 of Section 1.2.5.1. The nominal and measured dimensions of the BOTREFSRC plates are reported in Table 50 of Section 1.2.5.4. Table 110 summarizes the polyethylene plate dimension measurements, reporting the average thickness and diameter by part type. The diameter of the BOTREFSRC plates in Table 110 corresponds to the outer diameter in Table 50. The uncertainties are reported as the standard deviation of the measured dimensions for each part type. These measurements were performed using a coordinate measuring machine, as described in Section 1.2.5.

Table 110: Average polyethylene moderator and reflector plate by part type.

Part Type	N	Thickness (cm)	Diameter (cm)		
			Min	Max	Average
1/8-MOD	39	0.3221 ± 0.0047	38.0655	38.0840	38.0888 ± 0.0022
1/4-MOD	36	0.6464 ± 0.0093	38.0413	38.0619	38.0642 ± 0.0030
1/2-MOD	32	1.2850 ± 0.0084	38.0556	38.0746	38.0739 ± 0.0037
3/4-MOD	22	1.9369 ± 0.0141	38.0746	38.0949	38.0889 ± 0.0055
1.5-MOD	12	3.8373 ± 0.0237	38.0451	38.0919	38.0826 ± 0.0168
1/16-REF	2	0.1777 ± 0.0102	38.0566	38.0571	38.0637 ± 0.0004
1-REF	2	2.5413 ± 0.0036	38.0604	38.0644	38.0727 ± 0.0034
BOTREFSRC	2	2.5438 ± 0.0021	43.3781	43.3934	43.3857 ± 0.0108

The evaluated uncertainty in the polyethylene plate diameter and thickness are reported in Table 111. These uncertainties are based on the standard deviations of the average part types reported in Table 110, except for the thickness of the BOTREFSRC which inherited the measurement uncertainty of the CMM.

Table 111: Evaluated uncertainty in the polyethylene plate thickness and diameter by part type.

Part Type	Evaluated Uncertainty (cm)	
	Thickness	Diameter
1/8-MOD	± 0.005	± 0.005
1/4-MOD	± 0.010	
1/2-MOD	± 0.010	
3/4-MOD	± 0.014	± 0.020
1.5-MOD	± 0.025	± 0.020
1/16-REF	± 0.010	± 0.010
1-REF		
BOTREFSRC	± 0.0021	± 0.011

Table 112 summarizes the polyethylene moderator and reflector plate diameter uncertainty calculation param-

eters and sensitivity in k_{eff}. The calculations vary the parameter by collectively perturbing all polyethylene plate diameters by ± 0.02 cm. Therefore, the standard uncertainty in k_{eff} is calculated using Eq. 3 where N is the number of polyethylene plates in the experimental configuration and u_i is the evaluated uncertainty in the polyethylene plate diameter as reported in Table 111. Table 112 is reproduced alongside the other evaluated uncertainties in Section 2.6.

Table 112: Summary of sensitivity in k_{eff} to uncertainties in the polyethylene moderator and reflector plate diameters.

Case	**Number of Plates**	**Parameter Value (cm)**	**Parameter Variation in Calculation**	**Calculated Effect in k_{eff}**	**Standard Uncertainty**	**Standard Uncertainty in k_{eff}**
1	16	Varies (Table 110)	$\pm 0.02(16)$	0.00027	$\pm 0.02\sqrt{16}$	Negligible
2	16		$\pm 0.02(16)$	0.00076	$\pm 0.02\sqrt{9}$	± 0.00013
3	20		$\pm 0.02(20)$	-0.00038	$\pm 0.02\sqrt{20}$	± 0.00004

2.3.4 Aluminum Insert Dimensions

Due to the dependence of the core stack height on the thickness of the aluminum inserts, the uncertainty in the insert thickness is evaluated as part of the core stack height uncertainty in Section 2.3.5. The following analysis is limited to the uncertainty in the diameter of the aluminum inserts.

The nominal and measured dimensions of the aluminum inserts are reported in Tables 53 and 54 of Section 1.2.6. Table 113 summarizes the dimensional measurements, reporting the average thickness and diameter by part type. The uncertainties are reported as the standard deviation of the measurements. Therefore, the evaluated uncertainty in the aluminum insert diameter and thickness are ± 0.005 cm and ± 0.0015 cm, respectively, for all part types.

Table 113: Average aluminum insert dimensions by part type.

Part Type	N	Thickness (cm)	Diameter (cm)		
			Min	Max	Average
2.5-DISK	10	0.3170 ± 0.0014	6.0808	6.0858	6.0838 ± 0.0015
6-DISK	6	0.3158 ± 0.0015	14.9619	14.9695	14.9665 ± 0.0028
10-DISK	10	0.3170 ± 0.0011	25.1155	25.1295	25.1254 ± 0.0032

Table 114 summarizes the aluminum insert diameter uncertainty calculation parameters and sensitivity in k_{eff}. The calculations vary the parameter by collectively perturbing all aluminum insert diameters by ± 0.005 cm. Therefore, the standard uncertainty in k_{eff} is calculated using Eq. 3 where N is the number of aluminum inserts in the experimental configuration and u_i is the evaluated uncertainty in the aluminum insert diameter of ± 0.005 cm. Table 114 is reproduced alongside the other evaluated uncertainties in Section 2.6.

Table 114: Summary of sensitivity in k_{eff} to uncertainties in the aluminum insert diameters.

Case	Number of Inserts	Parameter Value (cm)	Parameter Variation in Calculation	Calculated Effect in k_{eff}	Standard Uncertainty	Standard Uncertainty in k_{eff}
1	2	Varies (Table 113)	$\pm 0.005(2)$	0.00002	$\pm 0.005\sqrt{2}$	Negligible
2	2		$\pm 0.005(2)$	0.00003	$\pm 0.005\sqrt{2}$	Negligible
3	12		$\pm 0.005(12)$	0.00005	$\pm 0.005\sqrt{12}$	Negligible

2.3.5 Core Stack Height

The core stack height measurements are described in Section 1.2.7. These measurements are reported for each experimental configuration in the subsections of Section 1.2.9 and summarized in multiple tables in Section 1.2.7. The measurements were performed with a CMM, with one measurement corroborated with height gauge measurements, using varying techniques for each of the configurations. Since this is the first time that the CMM is used for these types of measurements, a single height gauge measurement was performed to verify the accuracy of the CMM measurements. Aside from this single height gauge measurements, all other measurements were performed using the CMM and therefore only the CMM measurements are analyzed in this section. The CMM has a measurement uncertainty of ± 0.0635 mm. The measurement techniques are described in detail in Section 1.2.7. For each set of measurements, data were taken at multiple locations on the superior surface being measured. The uncertainty in the core stack height is based on the standard deviation of the measurements at the multiple locations. Stack height measurements were performed while the stack was on Comet as well as after being restacked on a granite surface plate.

The lower stack height measurement was taken relative to the surface of the adapter plate where the bottom reflector sat. The upper stack height measurement was taken relative to the interface plate. Table 115 reports the measured core stack heights, utilizing the raw CMM data which is notably different from Section 1.2.7. Instead of the best fit cylinder that is found using the included software for the CMM, the raw data points were analyzed to determine stack heights and the associated uncertainties based on data point averages and standard deviations.

Table 115: Summary of upper and lower core stack height measurements.

Case	Core Stack Height (cm)			
	On Comet		On Granite Surface Plate	
	Upper	Lower	Upper	Lower
1	16.835 ± 0.356[a]	24.158 ± 0.203	16.792 ± 0.056	24.067 ± 0.055
2	19.532 ± 0.356	26.378 ± 0.031	19.349 ± 0.058	26.400 ± 0.025
3	12.768 ± 0.073[b]	20.357 ± 0.021	12.561 ± 0.064[b]	20.400 ± 0.042

[a] Accounts for a flipped CMM tip which leads to an adjustment of 3 mm.
[b] On Comet and surface plate measurements disagree significantly.

The core stacks consist of HEU plates, sodium chloride absorber plates, polyethylene moderator plates, and polyethylene reflector plates. Some of the HEU plates have aluminum inserts filling the inner annuli. The aluminum inserts are typically thicker than the HEU plates, and therefore contribute to the stack height in those instances. Each part has a measured thickness as reported in the subsections of Section 1.2. Each of the individual part thicknesses can be summed together to calculate an expected core stack height, given the configurations, and compared to the measured core stack height to infer gaps within the configuration. It should be expected that the sum of the individual parts is less than or equal to the measured core stack height, within uncertainty. If this sum of individual parts is less than the measured core stack height, accounting for the propagated statistical uncertainty in the difference, this would indicate the presence of gaps between the layers. These gaps may manifest due to any given part not being perfectly flat. Table 116 compares the calculated stack heights with the CMM measurements performed on Comet. Table 117 compares the calculated stack heights with the CMM measurements performed on the granite surface plate.

Table 116: Comparison of the calculated and measured upper and lower core stack heights on Comet. The calculated core stack heights are based on the individual part measurements.

Case	Upper Core Stack (cm)		Lower Core Stack (cm)	
	Calculated[(a)]	Difference[(b)]	Calculated[(a)]	Difference[(b)]
1	16.801 ± 0.040	-0.035 ± 0.359	24.133 ± 0.044	-0.025 ± 0.208
2	19.375 ± 0.051	-0.158 ± 0.360	26.244 ± 0.057	0.046 ± 0.065
3	12.661 ± 0.026	-0.107 ± 0.048	20.485 ± 0.032	0.095 ± 0.038

[(a)] Sum of the individual part thicknesses, with propagated uncertainty based on uncertainty in part thicknesses.
[(b)] (Calculated) - (Measured), refer to Table 115 for measured core stack heights while on Comet.

Table 117: Comparison of the calculated and measured upper and lower core stack heights on the granite surface plate. The calculated core stack heights are based on the individual part measurements.

Case	Upper Core Stack (cm)		Lower Core Stack (cm)	
	Calculated[(a)]	Difference[(b)]	Calculated[(a)]	Difference[(b)]
1	16.801 ± 0.040	0.008 ± 0.069	24.133 ± 0.044	0.066 ± 0.070
2	19.375 ± 0.051	0.026 ± 0.077	26.244 ± 0.057	0.024 ± 0.063
3	12.661 ± 0.026	0.100 ± 0.069	20.485 ± 0.036	0.052 ± 0.053

[(a)] Sum of the individual part thicknesses, with propagated uncertainty based on uncertainty in part thicknesses.
[(b)] (Calculated) - (Measured), refer to Table 115 for measured core stack heights while on the granite surface plate.

The difference in the upper core stack height and the CMM measurements of the same are negative if gaps exist in the system. The upper core stack of the Case 3 is the only instance where there is a statistical ($> 1\sigma$) difference between the calculated and measured stack heights in the appropriate direction to imply gaps in the stack, but only for the measurements on Comet. There is a statistical difference between the calculated and measured stack heights for most measurements in the opposite direction, which would imply an unphysical relationship between the two, since it would be impossible to have negative gaps in the system. This phenomenon was also observed in HEU-MET-INTER-013 (TEX-Hf) and was addressed by analyzing the total core stack heights, i.e. combining the upper and lower core stacks for each configuration to determine the total core stack height and compare that to the measured core stack heights.

The deviation between the on Comet and the granite surface plate indicates an issue with the measurement as the two measurements are not statistically similar ($> 1\sigma$). The measurements on Comet suggest the precense of gaps by a total of 1 mm while the granite surface plate measurements suggest the presence of 'negative' gaps of 1 mm. The on Comet measurement of the lower stack of Case 3 shows a statistically significant core stack that is shorter than the individual pieces. However, the granite surface plate measurement shows agreement with the calculated stack height, which implied concurrence between the calculated stack height and the CMM measurements. The granite table measurements are deemed to be more reliable measurements due to the positioning of the CMM, considering anchoring of the machine itself, sagging due to the weight of the top stack, and space for the operator to work, and therefore it is determined that it is more likely to produce an accurate measurement. Given the large uncertainties of the on Comet CMM measurements, as well as the apparent self disagreement with some of the measurements, the granite surface plate measurements are used to determine that no gaps were present in the stack.

To encompass the measurement uncertainty, as well as the uncertainty in gaps in the system, the evaluated uncertainty of the difference measurements for the granite surface plate measurements presented in Table 117 were taken to be the evaluated stack height uncertainties, the same methodology used in HEU-MET-INTER-013.

Table 118 summarizes the upper and lower core stack height uncertainty calculation parameters and sensitivity in k_{eff}. The calculations vary the parameter by perturbing the thickness[13] of each part within the stack based on the evaluated uncertainty in the thicknesses reported in Section 2.3. Each component was simultaneously perturbed by the components uncertainty in thickness. The standard uncertainty in k_{eff} is calculated using Eq. 2 where u_i is the evaluated uncertainty in the core stack height measurements reported in Table 118. Table 118 is reproduced alongside the other evaluated uncertainties in Section 2.6.

Table 118: Summary of sensitivity in k_{eff} to uncertainties in the upper and lower core stack height.

Parameter (unit of measured)	Case	Parameter Value	Perturbation	Calculated Effect in k_{eff}	Standard Uncertainty	Standard Uncertainty in k_{eff}
Upper Core Stack Height (cm)	1	16.738	0.139	−0.00109	±0.069	±0.00027
	2	19.567	0.166	0.00122	±0.077	±0.00028
	3	12.771	0.110	0.00081	±0.069	±0.00025
Lower Core Stack Height (cm)	1	24.054	0.169	−0.00249	±0.070	±0.00052
	2	26.394	0.197	−0.00455	±0.063	±0.00066
	3	20.357	0.211	−0.00467	±0.053	±0.00059

While no gaps are expected in the stacks, they may exist. To account for gaps in the stack a similar simulation was performed to the positive perturbation stack height simulations. Instead of positively perturbing each part in the stack a gap was added above each part with the same magnitude as the perturbation. For example, if for in the stack height perturbation each HEU fuel plate was positively perturbed by 0.006 cm, the gap analysis used a gap of 0.006 cm above each HEU fuel plates. This was performed to study the difference in effect from positive stack height perturbation and gap analysis. It was found that both simulations resulted in the same neutron multiplication factor, within Monte Carlo uncertainties, which suggests that the major contribution to the stack height analysis may be leakage and suggests that, without evidence of significant gaps in the stack, the stack height measurements encompass adding gaps to the system.

2.3.6 Polyethylene Reflector Ring Diameters

The polyethylene reflector rings includes the ring (RING) and cap (CAP, BOTCAP) parts. Since the RING parts make up the majority of the upper and lower reflector rings, while the CAP parts provide only minor height adjustment, the uncertainty is the reflector ring diameter is based only on the RING parts.

The measured diameters of the polyethylene rings are reported in Table 47 of Section 1.2.5.2. Table 119 summarizes the dimensional measurements, reporting the average dimension by part type. As discussed in Section 1.2.5, these measurements were performed using a coordinate measuring machine (CMM) by LLNL's Dimensional Inspection Laboratory. The uncertainties are reported as the standard deviation of the measurements. The uncertainties in the inner and outer diameters are less than 0.003 cm for the 1/4-RING, 1/2-RING, and 3-RING part types. The standard deviation of the diameter measurements for the 1-RING part type is

[13] As noted in Section 2.3, all dimensional perturbations are performed at a constant mass by adjusting density.

0.006 cm, excluding the parts that were not used in this experiment. Three of the 1-RING parts, the 1-RING-2, 1-RING-4, and 1-RING-6, contribute significantly towards the standard deviation of the measurements. None of these parts were used in this experiment, therefore they were removed from the sample, and the values in Table 119 do not reflect those parts. The evaluated uncertainty in the reflector ring inner and outer diameters is ± 0.006 cm.

Table 119: Average polyethylene ring inner and outer diameters by part type.

Part ID	N	Inner Diameter (cm)			Outer Diameter (cm)		
		Min	Max	Average	Min	Max	Average
1/4-RING	4	38.2732	38.3315	38.3035 ± 0.0032	43.3894	43.4452	43.4172 ± 0.0013
1/2-RING	4	38.2640	38.2829	38.2720 ± 0.0013	43.3814	43.3987	43.3894 ± 0.0014
1-RING	3	38.2513	38.2688	38.2613 ± 0.0120	43.3757	43.3902	43.3917 ± 0.0021
3-RING	6	38.3239	38.3345	38.3299 ± 0.0017	43.4014	43.4151	43.4086 ± 0.0028

Table 120 summarizes the polyethylene reflector ring diameter uncertainty calculation parameters and sensitivity in k_{eff}. The calculations vary the parameter by collectively perturbing all polyethylene ring diameters by ± 0.02 cm. Therefore, the standard uncertainty in k_{eff} is calculated using Eq. 3 where N is the number of polyethylene ring parts in the experimental configuration and u_i is the evaluated uncertainty in the polyethylene ring diameter of ± 0.006 cm. Table 120 is reproduced alongside the other evaluated uncertainties in Section 2.6.

Table 120: Summary of sensitivity in k_{eff} to uncertainties in the reflector ring diameters.

Case	Number of Parts	Parameter Variation in Calculation	Calculated Effect in k_{eff}	Standard Uncertainty	Standard Uncertainty in k_{eff}
1	8	± 0.02	-0.00008	± 0.006	Negligible
2	8	± 0.02	-0.00002	± 0.006	Negligible
3	8	± 0.02	-0.00017	± 0.006	Negligible

2.3.7 Polyethylene Reflector Ring Height

The polyethylene reflector rings include the ring (RING) and cap (CAP, BOTCAP) part types. These parts are used to assemble the upper and lower reflector rings in each experimental configuration. This dimensional uncertainty evaluates the uncertainty in the height of the upper and lower reflector rings, based on measurements, similar to the stack height analysis performed in Section 2.3.5.

The reflector ring height measurements are reported for each experimental configuration in the subsections of Section 1.2.9. These measurements were performed in a similar fashion as the core stack height measurements described in Section 1.2.7. A detailed description of the measurement method is presented in Section 1.2.7. The measurements were performed with a CMM using varying techniques for each of the configurations. The CMM has a measurement uncertainty of ± 0.00635 cm.

Table 121 reports the upper and lower reflector ring height measurements. The reflector rings were averaged in-situ to provide a single height measurement. Since no other data exists, the measurement uncertainty was assumed to be the uncertainty of the CMM which is ± 0.00635 cm. However, the lower reflector ring height is

limited to be the same height or less than the core stack height, otherwise a gap would form in the highest worth region of the assembly. This was confirmed visually for all three configurations.

The upper reflector rings do not have the same requirement, they may be taller than the core stack height. Any excess in the upper reflector rings above the core stack is deemed to have a negligible effect in the reactivity of the system as it is in a low worth location. Therefore, the CMM uncertainty is retained for these measurements.

In some instances the lower ring reflector height is greater than the lower core stack height, which as described before would create a high worth gap in the assembly. As we have two measurements of the reflector ring heights, one on Comet and one on the granite surface plate, the standard deviation of the two measurements is assigned as the measurement uncertainty of the on Comet measurements, since these are the measurements used to determine the uncertainty in k_{eff}. This solves the issue of the lower ring reflector heights being greater than the lower core stack. These evaluated uncertainties are presented in Table 121.

Table 121: Summary of upper and lower reflector ring height measurements.

Case	**Reflector Ring Height (cm)**			
	On Comet		**On Granite Surface Plate**	
	Upper	Lower	Upper	Lower
1	16.770 ± 0.026	24.041 ± 0.027	16.822 ± 0.006	24.079 ± 0.006
2	19.432 ± 0.011	26.455 ± 0.019	19.415 ± 0.006	26.482 ± 0.006
3	12.755 ± 0.174	20.335 ± 0.021	12.510 ± 0.006	20.365 ± 0.006

Table 122 summarizes the upper and lower reflector ring height uncertainty calculation parameters and sensitivity in k_{eff}. The calculations vary the parameter by perturbing the reflector height by various quantities representing the sum of 1σ of each part thickness. The standard uncertainty in k_{eff} is calculated using Eq. 2 where u_i is the evaluated uncertainty in the reflector ring height of ± 0.00635 cm. Table 122 is reproduced alongside the other evaluated uncertainties in Section 2.6.

Table 122: Summary of sensitivity in k_{eff} to uncertainties in the upper and lower reflector ring height.

Parameter (unit of measured)	**Case**	**Parameter Value**	**Parameter Variation in Calculation**	**Calculated Effect in k_{eff}**	**Standard Uncertainty**	**Standard Uncertainty in k_{eff}**
Upper Reflector Ring Height (cm)	1	16.770	Various	0.00001	0.00635	Negligible
	2	19.432		0.00008		Negligible
	3	12.755		-0.00012		Negligible
Lower Reflector Ring Height (cm)	1	24.041	Various	0.00011	0.00635	Negligible
	2	26.455		-0.00055		± 0.00009
	3	20.335		-0.00091		± 0.00012

2.3.8 Membrane Thickness

The nominal dimensions of the membrane are reported in Table 2. No other dimensional measurements were documented. The drawing reports a thickness tolerance of ± 0.010 in. (± 0.0254 cm). Therefore, the evaluated uncertainty in the membrane thickness is based on this tolerance. The same membrane was used in all

experimental configurations.

These calculations were performed by perturbing the membrane thickness by ± 0.0254 cm, representing the reported tolerance, while keeping the density constant. A comparison between performing these calculations with a constant mass and constant density was performed in HEU-MET-INTER-013, and the constant mass approach was more conservative but it would produce unphysical densities since the membrane is Al-6061, which has a well known density of $2.70\,\mathrm{g\,cm^{-3}}$. Therefore, the constant density approach was used for this evaluation as well.

Table 123 summarizes the membrane thickness uncertainty calculation parameters and sensitivity in k_{eff}. The calculations vary the parameter by perturbing the membrane thickness by ± 0.0254 cm. Since the evaluated uncertainty in the thickness represents a uniform tolerance interval, the standard uncertainty is $\pm 0.0254/\sqrt{12}$ cm or approximately ± 0.0073 cm. The standard uncertainty in k_{eff} is calculated using Eq. 2 where u_i is the evaluated uncertainty in the membrane thickness of ± 0.0073 cm. Table 123 is reproduced alongside the other evaluated uncertainties in Section 2.6.

Table 123: Summary of sensitivity in k_{eff} to uncertainties in membrane thickness.

Case	Parameter Value (cm)	Parameter Variation in Calculation	Calculated Effect in k_{eff}	Standard Uncertainty	Standard Uncertainty in k_{eff}
1	0.3175	± 0.0254	-0.00062	± 0.0073	± 0.00005
2			-0.00063		± 0.00005
3			-0.00065		± 0.00005

2.3.9 Membrane Lift

The effect in k_{eff} due to the lift of the membrane was found to be negligible for all configurations in HEU-MET-INTER-013. The same is assumed for this evaluation.

2.3.10 Positional Uncertainty

The effect in k_{eff} due to the horizontal position of the core stack within the annular reflector was found to be negligible for all configurations in HEU-MET-INTER-013. The same is assumed for this evaluation.

2.4 Material Uncertainty

The material uncertainties were analyzed using the adjoint-based sensitivity method used to evaluate the sensitivities to material constituents and impurities[14]. This method was used to analyze the impurities by calculating the sensitivity of k_{eff} for each isotopic and then adding the individual contributions in quadrature to determine an overall relative uncertainty in k_{eff} for all impurities in the material. The uncertainty from the adjoint-based sensitivity method is represented as a fractional standard deviation (FSD), defined as the calculated uncertainty divided by its associated sensitivity. The control parameter adjusted (CPA) renormalization method was used. For this renormalization, the majority constituent is each material was chosen as the balance. These are uranium (U) in the HEU plates, sodium chloride (NaCl) in the sodium chloride absorbers, CH_2 in the polyethylene, and aluminum (Al) in the aluminum membrane, structure, and inserts. The calculations were performed using the KSEN card in MCNP® 6.3 with ENDF/B-VIII.0 cross sections and were performed by Jesse Norris of LLNL.

2.4.1 U-235 Enrichment

The uranium isotopic distribution in the HEU is based on the mass spectrometry measurements reported in Table 71 of Section 1.3.1.1. This mass spectrometry data is available for four plates, all of which were used in this experiment. Table 124 summarizes the uranium composition, reporting the average and standard deviation of the measurements. The reported isotopic range is relative to ^{235}U to match Table 71. Based on these measurements, the HEU is 93.232 ± 0.392 % enriched, by weight.

Table 124: Measured HEU isotopic content.

Element	Range (ng/g)	Elemental Composition (Wt.%)	
		Average	Uncertainty
U-234	10.8 - 11.5	1.03046	±2.76710E−04
U-235	-	9.32324E+01	±3.91961E−03
U-236	0.02 - 5.56	2.32202E-01	±2.37288E−03
U-238	57.7 - 59.2	5.50498	±7.31459E−04

In addition to the mass spectrometry measurements, individual plate enrichment values are available for the HEU plates used in the Big Ten experiment, based on Material Control & Accountability records. These values are reported in previous benchmarks and are reproduced in Table 71 of Section 1.3.1.1. Based on these values, the HEU is 93.287 ± 0.103 % enriched, by weight.

The calculated ^{235}U enrichments, based on the mass spectrometry measurements and data available from Material Controls and Accountability (MC&A), are consistent and in good agreement. However, the uncertainty of the mass spectrometry measurements is four times larger than the uncertainty of the MC&A enrichments. Therefore, the ^{235}U enrichment is based on the isotopic distribution reported in Table 124, from the mass spectrometry measurements, with an evaluated uncertainty of ± 0.103 %, based on the distribution of MC&A enrichments.

Table 125 summarizes the ^{235}U enrichment uncertainty calculation parameters and sensitivity in k_{eff}. These calculations were performed via sensitivity analysis. All HEU plates were perturbed at once so the standard uncertainty was scaled by the number of plates. Table 125 is reproduced alongside the other evaluated uncer-

[14] J. A. Favorite et al. "Adjoint Based Sensitivity and Uncertainty Analysis for Density and Composition: A User's Guide". *Nuclear Science and Engineering* 185.3 (2017), pp. 384–405. DOI: 10.1080/00295639.2016.1272990.

tainties in Section 2.6.

Table 125: Summary of sensitivity in k_{eff} to uncertainties in the ^{235}U enrichment.

Case	Number of Plates	^{235}U Enrichment (Wt.%)	$S_{k,x_i} \pm 1\sigma_{MC}[\%\ \%]$	Standard Uncertainty	Standard Uncertainty in k_{eff}
1	8	93.232	1.4109E-01 ± 1.5520E-04	$\pm 0.103/\sqrt{8}$	±0.00005
2	8		1.3512E-01 ± 1.4863E-04	$\pm 0.103/\sqrt{8}$	±0.00005
3	18		3.3772E-01 ± 2.0263E-04	$\pm 0.103/\sqrt{18}$	±0.00008

In addition to the uncertainty from the ^{235}U enrichment, the other uranium isotopics were evaluated. ^{234}U and ^{238}U have assigned compositional uncertainties of 1 wt-% while the ^{236}U has an assigned compositional uncertainty of 100 wt-%. Table 126 summarized the ^{234}U abundance uncertainties in k_{eff} for the three cases. Table 127 summarized the ^{236}U abundance uncertainties in k_{eff} for the three cases. Table 128 summarized the ^{238}U abundance uncertainties in k_{eff} for the three cases. Each of these tables are reproduced alongside the other evaluated uncertainties in Section 2.6.

Table 126: Summary of sensitivity in k_{eff} to uncertainties in the ^{234}U abundance.

Case	Number of Plates	^{234}U Abundance (Wt.%)	$S_{k,x_i} \pm 1\sigma_{MC}[\%\ \%]$	Standard Uncertainty	Standard Uncertainty in k_{eff}
1	8	1.0305	-1.7567E-03 ± -1.0716E-05	$\pm 1/\sqrt{8}$	Negligible
2	8		-1.5535E-03 ± -9.7871E-06	$\pm 1/\sqrt{8}$	Negligible
3	18		2.6120E-04 ± 2.0243E-05	$\pm 1/\sqrt{18}$	Negligible

Table 127: Summary of sensitivity in k_{eff} to uncertainties in the ^{236}U abundance.

Case	Number of Plates	^{236}U Abundance (Wt.%)	$S_{k,x_i} \pm 1\sigma_{MC}[\%\ \%]$	Standard Uncertainty	Standard Uncertainty in k_{eff}
1	8	0.2322	-4.3299E-04 ± -6.1485E-06	$\pm 100/\sqrt{8}$	Negligible
2	8		-3.2880E-04 ± -4.4059E-06	$\pm 100/\sqrt{8}$	Negligible
3	18		-2.4721E-04 ± -9.6412E-06	$\pm 100/\sqrt{18}$	Negligible

Table 128: Summary of sensitivity in k_{eff} to uncertainties in the ^{238}U abundance.

Case	Number of Plates	^{238}U Abundance (Wt.%)	$S_{k,x_i} \pm 1\sigma_{MC}[\%\ \%]$	Standard Uncertainty	Standard Uncertainty in k_{eff}
1	8	5.5050	-8.8393E-04 ± -2.5457E-05	$\pm 1/\sqrt{8}$	Negligible
2	8		-4.8782E-04 ± -2.2976E-05	$\pm 1/\sqrt{8}$	Negligible
3	18		2.2206E-03 ± 4.7743E-05	$\pm 1/\sqrt{18}$	Negligible

2.4.2 Highly Enriched Uranium Composition

The HEU composition is based on the impurity analysis reported in Table 73 of Section 1.3.1.2. The impurity analysis was performed on five HEU plates. Based on these measurements, there is less than 2000 $\mu g\,g^{-1}$ U (parts-per-million U) of impurities. Table 129 presents the elemental composition for the HEU, treating U as the remainder. For elements measured to be less than a given threshold (Li, Be, Na, Mg, Ca, V, Co, and Sn), the lower bound is assumed to be 0. For these eight elements, the impurity content is assumed to be a uniform distribution centered at the midpoint within the range. For the two elements (Mo and Pb), not included with HEU plates 10932 and 10933, the average impurity content and uncertainty in the average is based only on the measurements of HEU plates 11147, 11149, and 11150. For the remaining elements, the uncertainty in the average impurity content is the standard deviation of the five measurements.

Table 129: HEU impurity content, elemental composition, and uncertainties.

Element	Range (ug/g)	Elemental Composition (Wt.%)	
		Average	Uncertainty
U[(a)]	-	9.99898E-01	-
Li	0.1	2.91573E-09	±1.45787E−09
Be	0.1	3.78579E-09	±1.89290E−09
B	0.1 - 0.6	1.63491E-08	±1.04551E−08
C	170 - 1100	2.04848E-05	±1.98469E−05
Na	1	9.65742E-08	±4.82871E−08
Mg	1	1.02099E-07	±5.10495E−08
Al	20 - 150	8.16065E-06	±5.96530E−06
Si	80 - 400	2.64275E-05	±1.52144E−05
Ca	2	3.36715E-07	±1.68357E−07
V	20	4.27984E-06	±2.13992E−06
Cr	2 - 15	1.31053E-06	±1.13495E−06
Mn	4 - 7	1.38468E-06	±2.82647E−07
Fe	30 - 190	2.25215E-05	±1.38393E−05
Co	5	1.23782E-06	±6.18908E−07
Ni	15 - 30	4.93083E-06	±1.50975E−06
Cu	3 - 6	1.17454E-06	±3.04359E−07
Mo	0 - 50	8.06038E-06	±5.81708E−06
Sn	0 - 1	2.99202E-07	±8.97159E−12
Pb	0 - 5	1.21855E-06	±2.01009E−06

[(a)] Treated as the remainder.

Table 130 summarizes the HEU composition uncertainty calculation parameters and sensitivity in k_{eff}. The calculated effect in k_{eff} is based on the sum of the effect in k_{eff} to the constrained sensitivities as described in Section 2.4 and the standard uncertainty in k_{eff} is the contribution from each plate. The standard uncertainty is based on the impurity content reported in Table 129. Table 130 is reproduced alongside the other evaluated uncertainties in Section 2.6.

Table 130: Summary of sensitivity in k_{eff} to uncertainties in the HEU composition.

Case	Number of Plates	Parameter Value (Wt.%)	Calculated Effect in k_{eff}	Standard Uncertainty	Standard Uncertainty in k_{eff}
1	8	Varies (Table 129)	0.00000	Varies (Table 129)	Negligible
2	8		0.00000		Negligible
3	18		0.00001		Negligible

The following tables report the unconstrained and constrained elemental density sensitivities for the HEU composition, calculated as described in Section 2.4. These tables include: Table 131 for Case 1, Table 132 for Case 2, and Table 133 for Case 3.

Table 131: Elemental density sensitivities in k_{eff} for the HEU composition in Case 1.

Element	**Unconstrained Sensitivity, $S_{k,i}$**	**FSD, $\sigma(S_{k,i})/S_{k,i}$**	**Constrained Sensitivity, $S_{k,i}^{CPA}$**	**u_k/k**
U	1.3802E-01	1.1430E-03	-	-
Li	-1.9132E-09	4.2870E+00	-2.3157E-09	1.1578E-09
Be	1.1308E-08	1.5493E+00	1.0785E-08	5.3927E-09
B	-3.4446E-07	1.4025E-01	-3.4672E-07	2.2172E-07
C	1.0553E-06	1.1113E+00	-1.7723E-06	1.7171E-06
Na	-9.7176E-08	2.5750E-01	-1.1051E-07	5.5253E-08
Mg	-1.0089E-08	4.7629E+00	-2.4182E-08	1.2091E-08
Al	3.4869E-07	1.4548E+00	-7.7773E-07	5.6851E-07
Si	1.0313E-06	8.2869E-01	-2.6165E-06	1.5063E-06
Ca	9.5920E-09	5.2675E+00	-3.6885E-08	1.8442E-08
V	-1.7142E-07	1.9079E+00	-7.6216E-07	3.8108E-07
Cr	7.1099E-08	2.2360E+00	-1.0979E-07	9.5084E-08
Mn	-1.7477E-07	1.7131E+00	-3.6590E-07	7.4689E-08
Fe	1.0592E-06	7.6265E-01	-2.0494E-06	1.2594E-06
Co	-1.4675E-07	1.4954E+00	-3.1761E-07	1.5880E-07
Ni	4.6760E-07	9.3929E-01	-2.1300E-07	6.5218E-08
Cu	-7.1958E-07	2.7264E-01	-8.8170E-07	2.2848E-07
Mo	-1.4526E-06	3.5449E-01	-2.5652E-06	1.8513E-06
Sn	-8.4203E-08	8.0831E-01	-1.2550E-07	3.7632E-12
Pb	2.7410E-08	4.8920E+00	-1.4079E-07	2.3224E-07
Total	**1.3802E-01**	**1.1431E-03**	**-**	**3.3018E-06**

Table 132: Elemental density sensitivities in k_{eff} for the HEU composition in Case 2.

Element	**Unconstrained Sensitivity, $S_{k,i}$**	**FSD, $\sigma(S_{k,i})/S_{k,i}$**	**Constrained Sensitivity, $S_{k,i}^{CPA}$**	**u_k/k**
U	1.3275E-01	1.1358E-03	-	-
Li	-2.8425E-09	1.7605E+00	-3.2296E-09	1.6148E-09
Be	4.2768E-08	8.7190E-01	4.2265E-08	2.1133E-08
B	-4.3136E-07	2.8820E-02	-4.3353E-07	2.7724E-07
C	1.2031E-06	8.6461E-01	-1.5166E-06	1.4693E-06
Na	6.8418E-08	9.2260E-01	5.5596E-08	2.7798E-08
Mg	-2.7400E-11	1.5673E+03	-1.3582E-08	6.7912E-09
Al	-6.3777E-07	7.2340E-01	-1.7212E-06	1.2582E-06
Si	1.7751E-06	4.5582E-01	-1.7335E-06	9.9797E-07
Ca	1.8261E-08	2.8527E+00	-2.6443E-08	1.3221E-08
V	-1.5048E-08	1.6602E+01	-5.8325E-07	2.9163E-07
Cr	-2.9229E-07	4.6118E-01	-4.6628E-07	4.0381E-07
Mn	-4.8865E-07	5.5270E-01	-6.7249E-07	1.3727E-07
Fe	-5.1470E-07	1.2193E+00	-3.5047E-06	2.1536E-06
Co	-6.9834E-08	2.7454E+00	-2.3417E-07	1.1709E-07
Ni	-1.5766E-07	2.4256E+00	-8.1229E-07	2.4871E-07
Cu	-1.1048E-06	1.3271E-01	-1.2608E-06	3.2670E-07
Mo	-7.4399E-08	6.5353E+00	-1.1445E-06	8.2599E-07
Sn	-6.8636E-08	8.1312E-01	-1.0836E-07	3.2491E-12
Pb	4.2137E-08	3.0023E+00	-1.1964E-07	1.9736E-07
Total	**1.3275E-01**	**1.1359E-03**	**-**	**3.2596E-06**

Table 133: Elemental density sensitivities in k_{eff} for the HEU composition in Case 3.

Element	Unconstrained Sensitivity, $S_{k,i}$	FSD, $\sigma(S_{k,i})/S_{k,i}$	Constrained Sensitivity, $S_{k,i}^{CPA}$	u_k/k
U	3.3995E-01	6.1592E-04	-	-
Li	4.7234E-09	3.6534E+00	3.7321E-09	1.8660E-09
Be	1.6518E-09	1.1560E+01	3.6467E-10	1.8234E-10
B	-2.5639E-07	1.8122E-01	-2.6195E-07	1.6751E-07
C	1.2168E-05	1.9255E-01	5.2035E-06	5.0415E-06
Na	-5.8773E-08	1.7292E+00	-9.1607E-08	4.5804E-08
Mg	1.9918E-08	6.0660E+00	-1.4795E-08	7.3973E-09
Al	1.5855E-06	6.4450E-01	-1.1890E-06	8.6916E-07
Si	4.7195E-06	3.6066E-01	-4.2656E-06	2.4557E-06
Ca	6.6206E-08	1.5593E+00	-4.8273E-08	2.4137E-08
V	1.4886E-06	4.0421E-01	3.3481E-08	1.6740E-08
Cr	1.0845E-07	3.1978E+00	-3.3711E-07	2.9195E-07
Mn	9.9423E-07	7.9650E-01	5.2345E-07	1.0685E-07
Fe	2.1653E-06	5.6702E-01	-5.4918E-06	3.3747E-06
Co	3.0385E-07	1.4395E+00	-1.1699E-07	5.8497E-08
Ni	6.7529E-07	1.2155E+00	-1.0011E-06	3.0653E-07
Cu	-5.8111E-07	6.0141E-01	-9.8044E-07	2.5406E-07
Mo	-3.0101E-07	3.4726E+00	-3.0415E-06	2.1950E-06
Sn	1.0572E-08	1.7856E+01	-9.1154E-08	2.7332E-12
Pb	8.6923E-08	3.1597E+00	-3.2737E-07	5.4002E-07
Total	**3.3998E-01**	**6.1598E-04**	**-**	**6.9993E-06**

2.4.3 NaCl Salt Composition

The NaCl composition is based on the measured elemental composition reported in Table 75 of Section 1.3.2. The element composition measurements were performed with four samples of the salt that was sourced at the time of plate fabrication. There is a measured range in the impurities of $170\,\mu g\,g^{-1}$ to $196\,\mu g\,g^{-1}$, with an average of $187.5\,\mu g\,g^{-1}$. Table 134 presents the elemental composition for the NaCl based on these measurements, treating Na and Cl as the remainder. The uncertainty is based on the standard deviation of the measurements.

Table 134: NaCl impurity content, elemental composition, and uncertainties.

Element	Range (ug/g)	Elemental Composition (Wt.%)	
		Average	Uncertainty
Na[(a)]	-	3.9367E+01	-
Cl[(a)]	-	6.0614E+01	-
H	13.3 - 17.8	8.8889E-04	2.1000E-06
O	106.7 - 142.2	1.4222E-02	1.6800E-05
Li	0 - 0.01	1.0000E-06	5.0000E-07
Mg	0.39 - 0.86	8.6000E-05	2.1172E-05
Al	0 - 0.18	1.8000E-05	7.0000E-06
Si	0 - 0.33	3.3000E-05	1.1265E-05
S	1.2 - 5.1	3.3000E-05	1.5979E-04
K	4.3 - 17	1.7000E-03	5.7714E-04
Ca	0.9 - 2.1	2.1000E-04	5.4467E-05
Br	2.7 - 16	1.6000E-03	5.7407E-04
Sr	0.11 - 0.23	2.3000E-05	5.7373E-06

[(a)] Treated as the remainder.

Table 135 summarizes the NaCl composition uncertainty calculation parameters and sensitivity in k_{eff}. The calculated effect in k_{eff} is based on the sum of the effect in k_{eff} to the constrained sensitivities as described in Section 2.4 and the standard uncertainty in k_{eff} is the contribution from each absorber. All sodium chloride absorbers in each configuration are included. The standard uncertainty is based on the impurity content reported in Table 134. Table 135 is reproduced alongside the other evaluated uncertainties in Section 2.6.

Table 135: Summary of sensitivity in k_{eff} to uncertainties in the sodium chloride composition.

Case	Number of Plates	Parameter Value (Wt.%)	Calculated Effect in k_{eff}	Standard Uncertainty	Standard Uncertainty in k_{eff}
1	7	Varies (Table 134)	0.00000	Varies (Table 134)	Negligible
2	7		0.00000		Negligible
3	17		0.00000		Negligible

Similarly, the uncertainty due to the ^{35}Cl abundance was studied. An associated uncertainty in the ^{35}Cl was estimated from the impurities. The chemical analysis suggests a salt purity of greater than 99.98% (which surpasses the reported $\geq$99.5%). The total uncertainty from impurities was found to be 0.00143 weight percent. Since no measurement was performed that would provide a direct uncertainty on the NaCl abundance, this uncertainty was assumed as the total uncertainty for NaCl. Using the known abundance of each isotope in natural NaCl, the ^{35}Cl abundance uncertainty was determined to be 0.00065. To encompass this uncertainty the associated composition uncertainty for the salt was assumed to be 0.001. The same constrained sensitivities used above were used to calculate the standard uncertainty in k_{eff}. Table 136 reports the standard uncertainty due to the uncertainty in the ^{35}Cl abundance. Table 136 is reproduced alongside the other evaluated uncertainties in Section 2.6.

Table 136: Summary of sensitivity in k_{eff} to uncertainties in the ^{35}Cl abundance

Case	Number of Plates	Parameter Value (Wt.%)	Calculated Effect in k_{eff}	Standard Uncertainty	Standard Uncertainty in k_{eff}
1	7	45.396%	0.00000	$0.001/\sqrt{7}$	Negligible
2	7		0.00000	$0.001/\sqrt{7}$	Negligible
3	17		0.00000	$0.001/\sqrt{17}$	Negligible

The following tables report the unconstrained and constrained elemental density sensitivities for the sodium chloride composition, calculated as described in Section 2.4. These tables include: Table 137 for Case 1, Table 138 for Case 2, and Table 139 for Case 3.

Table 137: Elemental density sensitivities in k_{eff} for the NaCl composition in Case 1.

Element	Unconstrained Sensitivity, $S_{k,i}$	FSD, $S_{k,i}/\sigma(S_{k,i})$	Constrained Sensitivity, $S_{k,i}^{CPA}$	u_k/k
Na	7.2452E-04	6.0800E-02	-	-
Cl	-5.7770E-02	1.0243E-03	-	-
H	-8.9339E-07	1.5548E+00	-9.0975E-07	2.1493E-09
O	6.1169E-07	1.4105E+00	3.4993E-07	4.1336E-10
Li	-1.4483E-08	4.2062E-04	-1.4502E-08	7.2508E-09
Mg	8.8269E-08	7.8847E-01	8.6686E-08	2.1341E-08
Al	-1.3723E-08	6.3690E-01	-1.4054E-08	5.4656E-09
Si	-2.1277E-08	7.0188E-01	-2.1884E-08	7.4702E-09
S	2.1554E-08	1.8614E+00	2.0947E-08	1.0143E-07
K	2.3081E-06	2.5842E-01	2.2768E-06	7.7295E-07
Ca	1.8063E-06	1.4034E-01	1.8024E-06	4.6749E-07
Br	-5.9217E-07	1.7134E+00	-6.2161E-07	2.2303E-07
Sr	-4.2479E-07	1.2626E+00	-4.2521E-07	1.0607E-07
Total	**-5.7043E-02**	**-1.2938E-03**	**-**	**9.4227E-07**

Table 138: Elemental density sensitivities in k_{eff} for the NaCl composition in Case 2.

Element	Unconstrained Sensitivity, $S_{k,i}$	FSD, $S_{k,i}/\sigma(S_{k,i})$	Constrained Sensitivity, $S_{k,i}^{CPA}$	u_k/k
Na	-6.2358E-04	7.0400E-02	-	-
Cl	-7.9262E-02	5.3218E-04	-	-
H	2.1645E-06	6.5275E-01	2.1786E-06	5.1469E-09
O	5.4667E-09	1.4291E+02	2.3075E-07	2.7257E-10
Li	-1.7380E-08	2.5367E-04	-1.7364E-08	8.6822E-09
Mg	3.7762E-08	1.6853E+00	3.9124E-08	9.6319E-09
Al	2.9462E-08	9.9330E-01	2.9747E-08	1.1568E-08
Si	9.3770E-10	3.2705E+01	1.4604E-09	4.9852E-10
S	1.6009E-08	1.2676E+00	1.6532E-08	8.0052E-08
K	-3.3346E-07	3.6491E-01	-3.0653E-07	1.0407E-07
Ca	-1.1591E-07	1.8729E-01	-1.1258E-07	2.9200E-08
Br	-8.5603E-07	1.8426E-01	-8.3069E-07	2.9805E-07
Sr	-4.9886E-09	3.0506E+00	-4.6243E-09	1.1535E-09
Total	**-7.9885E-02**	**-7.6238E-04**	**-**	**3.2749E-07**

Table 139: Elemental density sensitivities in k_{eff} for the NaCl composition in Case 3.

Element	Unconstrained Sensitivity, $S_{k,i}$	FSD, $S_{k,i}/\sigma(S_{k,i})$	Constrained Sensitivity, $S_{k,i}^{CPA}$	u_k/k
Na	9.3097E-03	1.0300E-02	-	-
Cl	-6.9022E-03	1.0266E-02	-	-
H	1.8751E-05	1.5991E-01	1.8540E-05	4.3802E-08
O	6.0968E-06	2.8753E-01	2.7334E-06	3.2289E-09
Li	-1.1772E-08	1.9289E-02	-1.2009E-08	6.0044E-09
Mg	2.5131E-07	5.9750E-01	2.3098E-07	5.6863E-08
Al	4.5863E-08	2.0487E+00	4.1606E-08	1.6180E-08
Si	5.5300E-08	1.3456E+00	4.7495E-08	1.6212E-08
S	-6.3925E-08	4.0672E-01	-7.1729E-08	3.4732E-07
K	-2.7045E-09	1.1542E+02	-4.0473E-07	1.3740E-07
Ca	5.1475E-08	2.0909E+00	1.8130E-09	4.7023E-10
Br	-1.0413E-06	3.5649E-01	-1.4197E-06	5.0937E-07
Sr	2.8405E-08	1.4332E+00	2.2966E-08	5.7287E-09
Total	**2.4317E-03**	**4.9053E-02**	**-**	**6.3619E-07**

2.4.4 Polyethylene Composition

The polyethylene composition is based on the measured elemental composition reported in Section 1.3.3.2. The elemental composition measurements were performed on a 246.97 µg sample of the polyethylene. Based on these measurements, there was less than 0.3 µg of impurities in the sample. Table 140 presents the elemental composition for the polyethylene based on these measurements. The reported elemental uncertainties are based on the standard deviation of the measurements. The remainder of the sample is assumed to be polyethylene (CH_2).

Table 140: Polyethylene elemental composition and uncertainties.

Element	Elemental Composition (Wt.%)	
	Average	Uncertainty
H[(a)]	1.43573E+01	-
C[(a)]	8.55467E+01	-
Na	1.43800E-03	±1.82000E–06
Al	2.39200E-03	±1.74000E–06
Si	1.17000E-04	±6.00000E–08
Cr	9.21350E-02	±7.08000E–06

[(a)] Treated as the remainder (CH_2).

Table 141 summarizes the polyethylene composition uncertainty calculation parameters and sensitivity in k_{eff}. The calculated effect in k_{eff} is based on the sum of the effect in k_{eff} to the constrained sensitivities as described in Section 2.4 and the standard uncertainty in k_{eff} is the contribution from each plate. All polyethylene components in each configuration are included. All polyethylene materials were perturbed collectively, including the moderator and reflector parts. The standard uncertainty is based on the impurity content reported in Table 140. Table 141 is reproduced alongside the other evaluated uncertainties in Section 2.6.

Table 141: Summary of sensitivity in k_{eff} to uncertainties in the polyethylene composition.

Case	Parameter Value (Wt.%)	Calculated Effect in k_{eff}	Standard Uncertainty	Standard Uncertainty in k_{eff}
1	Varies (Table 140)	0.00000	Varies (Table 140)	Negligible
2		0.00000		Negligible
3		0.00000		Negligible

The following tables report the unconstrained and constrained elemental density sensitivities for the polyethylene composition, calculated as described in Section 2.4. These tables include: Table 142 for Case 1, Table 143 for Case 2, and Table 144 for Case 3.

Table 142: Elemental density sensitivities in k_{eff} for the polyethylene composition in Case 1.

Element	Unconstrained Sensitivity, $S_{k,i}$	FSD, $S_{k,i}/\sigma(S_{k,i})$	Constrained Sensitivity, $S_{k,i}^{CPA}$	u_k/k
H	1.4588E-01	2.6998E-03	-	-
C	5.3842E-02	4.1794E-03	-	-
Na	-9.8691E-07	7.6440E-01	-3.8617E-06	4.8876E-09
Al	7.6849E-07	7.3860E-01	-4.0135E-06	2.9195E-09
Si	1.9480E-05	2.2905E-01	1.9246E-05	9.8699E-09
Cr	2.2312E-08	5.3231E+00	-1.8417E-04	1.4152E-08
Total	**1.9974E-01**	**2.2710E-03**	**-**	**1.8169E-08**

Table 143: Elemental density sensitivities in k_{eff} for the polyethylene composition in Case 2.

Element	Unconstrained Sensitivity, $S_{k,i}$	FSD, $S_{k,i}/\sigma(S_{k,i})$	Constrained Sensitivity, $S_{k,i}^{CPA}$	u_k/k
H	5.2746E-02	7.2983E-03	-	-
C	5.0685E-02	4.1829E-03	-	-
Na	3.3768E-07	2.4139E+00	-1.1511E-06	1.4569E-09
Al	-9.1139E-07	6.0980E-01	-3.3878E-06	2.4644E-09
Si	9.3923E-06	4.7332E-01	9.2712E-06	4.7544E-09
Cr	-1.3660E-07	8.6510E-01	-9.5525E-05	7.3405E-09
Total	**1.0344E-01**	**4.2489E-03**	**-**	**9.2023E-09**

Table 144: Elemental density sensitivities in k_{eff} for the polyethylene composition in Case 3.

Element	Unconstrained Sensitivity, $S_{k,i}$	FSD, $S_{k,i}/\sigma(S_{k,i})$	Constrained Sensitivity, $S_{k,i}^{CPA}$	u_k/k
H	2.7746E-01	1.1000E-03	-	-
C	7.8228E-02	1.7922E-03	-	-
Na	7.9477E-07	7.3400E-01	-4.3249E-06	5.4738E-09
Al	1.7252E-06	2.7150E-01	-6.7910E-06	4.9399E-09
Si	3.5740E-05	8.9289E-02	3.5324E-05	1.8115E-08
Cr	1.0276E-07	9.8578E-01	-3.2792E-04	2.5199E-08
Total	**3.5572E-01**	**9.4418E-04**	**-**	**3.1898E-08**

2.4.5 Aluminum Composition

The aluminum composition is based on the handbook data reported for Al-6061 in Table 79 of Section 1.3.4. The Al-2024 screws have a negligible impact on the material uncertainty so they were excluded. There is an average 2.695 Wt.% impurities in the reported Al-6061 composition. The elemental compositions presented in Table 79 represent an upper and lower bound (Mg, Si, Cu, and Cr), a maximum upper bound with no lower bound (Fe, Zn, Mn, and Ti), or the main constituent as the remainder (Al). Table 145 presents the evaluated elemental composition for Al-6061. The uncertainty of the elemental composition is based on the range of the

specification, assuming a lower bound of 0 if not given. The standard uncertainty assumes a uniform distribution within this range. Aluminum is treated as the remainder, including the other and unknown impurities.

Table 145: Aluminum elemental composition and uncertainties.

Element	Elemental Composition (Wt.%)	
	Average	Uncertainty
Al[(a)]	9.73050E+01	-
Mg	1.00000E+00	1.15470E-01
Si	6.00000E-01	1.15470E-01
Cu	2.75000E-01	7.21688E-02
Cr	1.95000E-01	8.94893E-02
Fe	3.50000E-01	1.01036E-01
Zn	1.25000E-01	3.60844E-02
Mn	7.50000E-02	2.16506E-02
Ti	7.50000E-02	2.16506E-02

[(a)] Treated as the remainder.

Table 146 summarizes the aluminum composition uncertainty calculation parameters and sensitivity in k_{eff}. The calculated effect in k_{eff} is based on the sum of the effect in k_{eff} to the constrained sensitivities as described in Section 2.4 and the standard uncertainty in k_{eff} is the contribution from each plate. All aluminum components in each configuration are included. The standard uncertainty is based on the impurity content reported in Table 145. Table 146 is reproduced alongside the other evaluated uncertainties in Section 2.6.

Table 146: Summary of sensitivity in k_{eff} to uncertainties in the aluminum composition.

Case	**Parameter Value (Wt.%)**	**Calculated Effect in k_{eff}**	**Standard Uncertainty**	**Standard Uncertainty in k_{eff}**
1	Varies (Table 145)	0.00000	Varies (Table 145)	Negligible
2		0.00000		Negligible
3		0.00001		Negligible

The following tables report the unconstrained and constrained elemental density sensitivities for the aluminum composition, calculated as described in Section 2.4. These tables include: Table 147 for Case 1, Table 148 for Case 2, and Table 149 for Case 3.

Table 147: Elemental density sensitivities in k_{eff} for the aluminum composition in Case 1.

Element	**Unconstrained Sensitivity, $S_{k,i}$**	**FSD, $S_{k,i}/\sigma(S_{k,i})$**	**Constrained Sensitivity, $S_{k,i}^{CPA}$**	**u_k/k**
Al	1.3252E-03	5.6700E-02	-	-
Mg	1.7855E-05	5.3270E-01	4.2356E-06	4.8908E-07
Si	1.7884E-05	3.4941E-01	9.7121E-06	1.8691E-06
Ti	7.1520E-06	3.1869E-01	3.4068E-06	8.9406E-07
Cr	7.6063E-06	4.1014E-01	4.9505E-06	2.2719E-06
Mn	9.4528E-06	3.8200E-01	4.6861E-06	1.3528E-06
Fe	5.6596E-06	8.7603E-01	3.9572E-06	1.1423E-06
Cu	9.1588E-06	3.3832E-01	8.1374E-06	2.3491E-06
Zn	4.8867E-06	5.3598E-01	3.8653E-06	1.1158E-06
Total	**1.4049E-03**	**5.4417E-02**	**-**	**4.3992E-06**

Table 148: Elemental density sensitivities in k_{eff} for the aluminum composition in Case 2.

Element	**Unconstrained Sensitivity, $S_{k,i}$**	**FSD, $S_{k,i}/\sigma(S_{k,i})$**	**Constrained Sensitivity, $S_{k,i}^{CPA}$**	**u_k/k**
Al	1.8250E-03	2.8100E-02	-	-
Mg	2.6912E-05	2.8055E-01	8.1563E-06	9.4181E-07
Si	1.6840E-06	6.3461E-01	-9.5693E-06	1.8416E-06
Ti	7.2894E-06	2.3133E-01	2.1317E-06	5.5942E-07
Cr	5.6716E-06	3.7632E-01	2.0142E-06	9.2438E-07
Mn	4.7453E-06	5.4480E-01	-1.8191E-06	5.2513E-07
Fe	9.9450E-06	3.5832E-01	7.6006E-06	2.1941E-06
Cu	7.4482E-06	3.8664E-01	6.0415E-06	1.7440E-06
Zn	1.7555E-06	1.1131E+00	3.4887E-07	1.0071E-07
Total	**1.8905E-03**	**2.7623E-02**	**-**	**3.5638E-06**

Table 149: Elemental density sensitivities in k_{eff} for the aluminum composition in Case 3.

Element	**Unconstrained Sensitivity, $S_{k,i}$**	**FSD, $S_{k,i}/\sigma(S_{k,i})$**	**Constrained Sensitivity, $S_{k,i}^{CPA}$**	**u_k/k**
Al	2.8707E-03	1.1900E-02	-	-
Mg	4.5490E-05	1.0368E-01	1.5988E-05	1.8461E-06
Si	1.6735E-05	1.7166E-01	-9.6656E-07	1.8601E-07
Ti	3.1463E-06	4.1894E-01	-4.9668E-06	1.3034E-06
Cr	4.2923E-06	3.4523E-01	-1.4606E-06	6.7032E-07
Mn	-2.8463E-07	6.1731E+00	-1.0610E-05	3.0629E-06
Fe	7.3652E-06	2.6407E-01	3.6774E-06	1.0616E-06
Cu	-4.1061E-05	4.3742E-02	-4.3274E-05	1.2492E-05
Zn	1.7289E-06	6.7798E-01	-4.8373E-07	1.3964E-07
Total	**2.9081E-03**	**1.1976E-02**	**-**	**1.2991E-05**

2.5 Temperature Uncertainty

The ambient temperature of the experimental configurations were measured for all cases when they were critical. While the ambient temperature was the only temperature measured, the relationship between the ambient temperture and the Comet temperature from HEU-MET-INTER-013 was used to estimate the experimental temperature. It should be noted that the evaluated uncertainty is $\pm 2.0\,^{\circ}\mathrm{C}$, which represents the tolerance that the RTDs are annually measured to be compliant with, encompasses the vast majority of the difference, so minimal deviations due to this estimation are negligible in comparison. All experiments were conducted at slightly below $20.5\,^{\circ}\mathrm{C}$ (293.6 K), which is what MCNP calculations are typically performed at. The ambient room temperature was taken as the evaluated temperature and ranged from $14.8\,^{\circ}\mathrm{C}$ (287.95 K) to $14.9\,^{\circ}\mathrm{C}$ (288.05 K). Table 150 reports the evaluated temperatures of the experimental configurations.

Table 150: Temperatures of the experimental configurations.

Case	Temperature (°C)
1	14.9
2	14.9
3	14.6

2.5.1 Thermal Contraction

The thermal contraction uncertainty evaluates the effect of thermal contraction due to change in temperature. The thermal contraction is modeled using linear contraction in each dimension to capture the overall contraction of the volume. Linear contraction is defined as

$$\frac{\Delta L}{L} = \alpha_L \Delta T \tag{7}$$

where L is the dimension, ΔT is the change in temperature, and α_L is the linear coefficient of thermal expansion (CTE). Table 151 shows the linear coefficients of thermal expansion for uranium, NaCl, polyethylene, and aluminum.

Table 151: Linear coefficients of thermal expansion.

Material	CTE, α_L ($\frac{\mu m}{m\,^\circ C}$)
Uranium, U; Cast	19.0[a]
Sodium Chloride, NaCl	44[c]
Aluminum, Al	24.0[a]
High Density Polyethylene, Extruded	110.0[b]

[a] Based on a reference value provided by the manufacturer.
[b] Based on a values from HEU-MET-INTER-013.
[c] Based on a values from [5].

Table 152 summarizes the calculation parameters and sensitivity in k_{eff} of thermal contraction due to uncertainty in temperature. The calculations use Eq. 7 with the CTE values from Table 151 to perturb each part within the experimental configurations by $\pm 10.0\,^\circ$C. The standard uncertainty is calculated using Eq. 2 with the evaluated uncertainty of $\pm 2.0\,^\circ$C. Table 152 is reproduced alongside the other evaluated uncertainties in Section 2.6.

Table 152: Summary of sensitivity in k_{eff} to thermal contraction due to uncertainties in temperature.

Case	Parameter Value (°C)	Parameter Variation in Calculation	Calculated Effect in k_{eff}	Standard Uncertainty	Standard Uncertainty in k_{eff}
1	14.9	±10.0	−0.00062	±2.0	±0.00006
2	14.9		−0.00036		±0.00004
3	14.6		−0.00014		Negligible

2.5.2 Doppler Broadening

Doppler broadening was evaluated in-depth in HEU-MET-INTER-013, which utilizes very similar designs as those presented in this benchmark, and was deemed negligible for every one of the 7 experimental configurations. None of the cross sections utilized here, including the sodium or chlorine cross sections, are expected to behave any differently to the same analysis, therefore the effect of doppler broadening is also deemed negligible for each of the three experimental configurations evaluated here.

2.5.3 Thermal Scattering Law

The thermal scattering law uncertainty evaluates the effect in k_{eff} due to changes in temperature of the thermal scattering laws. The thermal scattering laws in ENDF/B-VIII.0 relevant to these experimental configurations are polyethylene (^{1}H in CH_2) and aluminum (^{27}Al). This uncertainty evaluation is specific to the polyethylene thermal scattering law as the aluminum thermal scattering law does not have a significant effect in k_{eff}.

The ACE-formatted thermal scattering laws based on ENDF/B-VIII.0 for polyethylene distributed for use with MCNP® include the following temperatures (with ACE library identifier)[15]: 300 K (44t), 303 K (45t), 313 K (46t), 323 K (47t), 333 K (48t), and 343 K (49t). By default, MCNP® 6.3 uses thermal scattering laws at 293.6 K (20.5 °C), referred to here as room temperature. In MCNP® 6.3, thermal scattering laws replace the free-gas incident neutron interaction cross sections when the MT card is used and the thermal scattering law exists at the given energy of incident interaction. The polyethylene thermal scattering law is specific to the ^{1}H neutron cross section.

Table 153 reports the temperatures of the ten polyethylene thermal scattering laws evaluated as part of this uncertainty. The temperatures used are the ones that are distributed with ENDF/B-V.III.

Table 153: Thermal scattering law temperatures evaluated for polyethylene (^{1}H in CH_2).

Temperature (K)	Temperature (°C)
293.6[(a)]	20.5
300.0	26.9
303.0	29.9
313.0	39.9
323.0	49.9
333.0	59.9
343.0	69.9

[(a)] Room temperature.

Figure 34 shows a plot of δk_{eff}, defined as the change in k_{eff} compared to room temperature, for the polyethylene thermal scattering laws for Case 1. The results are fit using linear least squares where the slope represents the sensitivity in k_{eff} to the temperature of the polyethylene thermal scattering law. Table 154 reports the parameters of a linear least squares fit to the all nine standard temperatures available in MCNP. All fits have a coefficient of determination exceeding 0.988.

[15] The original ACE-formatted thermal scattering law library based on ENDF/B-VIII.0 distributed for MCNP® in 2018 included a processing error. This processing error was corrected and the ACE-formatted thermal scattering law library re-released in 2020. These calculations use the corrected thermal scattering law library. For more information, refer to: D. K. Parsons and C. A. Toccoli. *Re-Release of the ENDF/B VIII.0 S(α,β) Data Processed by NJOY2016*. LA-UR-20-24456. Los Alamos National Laboratory, 2020. DOI: 10.2172/1634930.

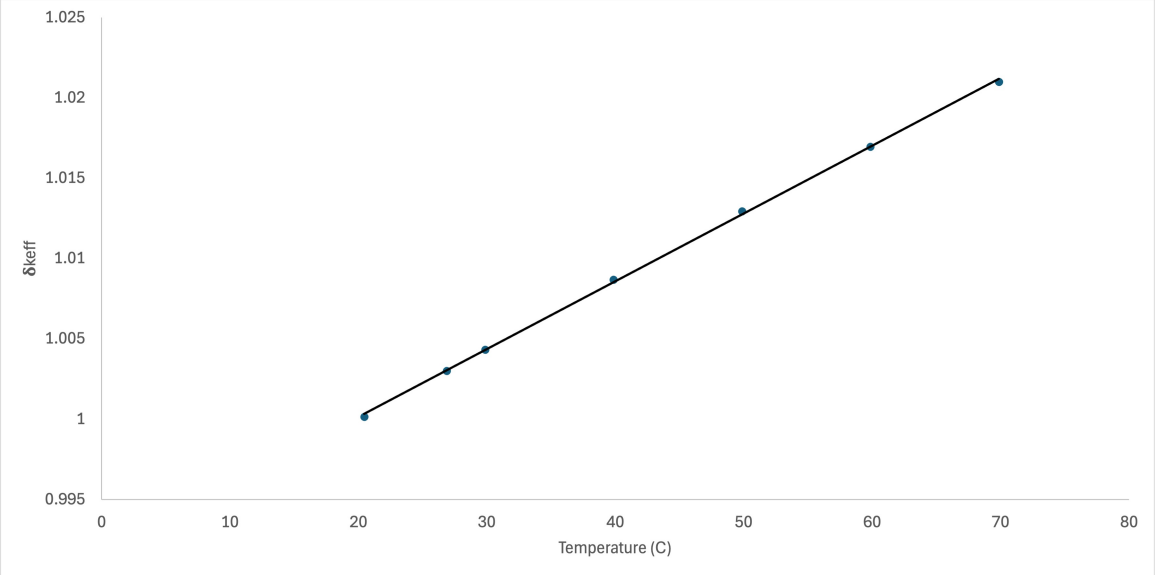

Figure 34: Effect of the polyethylene thermal scattering law at various temperatures for Case 1. The plot includes error bars for the Monte Carlo statistical uncertainty (±0.00004) and the linear least-squares fit.

Table 154: Parameters of the least squares fit for the change in k_{eff} due to the temperature of the polyethylene (^{1}H in CH_2) thermal scattering law.

Case	Slope (K^{-1})	y-Intercept	Coefficient of Determination, R^2
1	2.83903E-04	9.89912E-01	0.99640
2	5.77012E-04	9.85903E-01	0.98919
3	2.78450E-05	9.93849E-01	0.98470

Table 155 summarizes the calculation parameters and sensitivity in k_{eff} of the polyethylene (^{1}H in CH_2) thermal scattering law due to uncertainty in temperature. The effect in k_{eff} is based on the slope of the linear least squares fit reported in Table 154. The standard uncertainty is calculated using Eq. 2 with the evaluated uncertainty of ±2.0 °C. Table 155 is reproduced alongside the other evaluated uncertainties in Section 2.6.

Table 155: Summary of sensitivity in k_{eff} to the polyethylene thermal scattering law due to uncertainties in temperature.

Case	Parameter Value (°C)	Calculated Effect in k_{eff}	Standard Uncertainty	Standard Uncertainty in k_{eff}
1	14.9	−0.00023/°C	±2.0	±0.00046
2	14.9	−0.00042/°C		±0.00084
3	14.6	−0.00002/°C		±0.00004

2.6 Combined Uncertainty

Table 156 presents the total combined uncertainty for the experimental configurations. These combined uncertainties are broken down into individual parameters for mass, dimension, material, and temperature in Table 157 (Case 1), Table 158 (Case 2), and Table 159 (Case 3). These tables summarize the uncertainty calculations previously described in Sections 2.1, 2.2, 2.3, 2.4, and 2.5.

Table 156: Summary of calculated uncertainties for the experimental configurations.

Case	Standard Uncertainty in k_{eff}
1	±0.00078
2	±0.00117
3	±0.00070

All configurations are found to be acceptable for use as benchmark data.

2.6.1 Case 1

Table 157: Summary of sensitivity in k_{eff} to uncertainties in Case 1.

Parameter (unit of measured)	N	Parameter Value	Parameter Variation in Calculation	Calculated Effect in k_{eff}	Standard Uncertainty	Standard Uncertainty in k_{eff}
Mass Uncertainty						
HEU Mass (g)	8	48604.8	$\pm 12.0 \times 8$	0.00059	$\pm 1.7\sqrt{8}$	Negligible
Absorber Encapsulation Mass (g)	7	14771.2	$\pm 9.0 \times 7$	-0.00001	$\pm 9.0\sqrt{7}$	Negligible
NaCl Mass (g)	7	4585.0	$\pm 10.0 \times 7$	-0.00172	$\pm 5.3\sqrt{7}$	± 0.00017
Polyethylene Moderator Mass (g)	14	29612.3	$\pm 3.0 \times 14$	0.00008	$\pm 3.0\sqrt{7}$	Negligible
Polyethylene Reflector Mass (g)	13	16659.7	$\pm 0.5\,\%$	0.00054	$\pm 4.2\sqrt{13}$	± 0.00005
Aluminum Insert Mass (g)	2	448.6	$\pm 7.0 \times 2$	0.00006	$\pm 0.5\sqrt{2}$	Negligible
Membrane Mass (g)	-	2396.1	± 20.0	0.00010	± 0.3	Negligible
Structure Mass (g)	-	-	-	-	-	Negligible
					Sum in Quadrature (Mass Uncertainty)	± 0.00018
Dimensional Uncertainty						
HEU Plate Dimensions (cm)	8	Varies (Table 104)	$\pm 0.02 \times 8$	0.00000	$\pm 0.002/\sqrt{8}$	Negligible
NaCl Absorber Diameter (cm)	7	30.479	$\pm 0.02 \times 7$	0.00002	$\pm 0.002/\sqrt{7}$	Negligible
NaCl Absorber Pocket Depth (cm)	7	0.490	$\pm 0.02 \times 7$	0.00374	$\pm 0.003/\sqrt{7}$	± 0.00011
Absorber Encapsulation Diameter (cm)	7	38.091	$\pm 0.02 \times 7$	0.00005	$\pm 0.003/\sqrt{7}$	Negligible
Polyethylene Plate Dimensions (cm)	16	Varies (Table 110)	$\pm 0.02 \times 16$	0.00027	$\pm 0.02/\sqrt{16}$	Negligible
Polyethylene Ref. Dimensions (cm)	8	Varies (Table 119)	± 0.02	-0.00008	± 0.006	Negligible
Aluminum Insert Dimensions (cm)	2	Varies (Table 113)	$\pm 0.005 \times 2$	0.00002	$\pm 0.005/\sqrt{2}$	Negligible

Table 157 (continued): Summary of sensitivity in k_{eff} to uncertainties in Case 1.

Parameter (unit of measured)	N	Parameter Value	Parameter Variation in Calculation	Calculated Effect in k_{eff}	Standard Uncertainty	Standard Uncertainty in k_{eff}
Upper Core Stack Height (cm)	-	16.738	0.139	-0.00109	± 0.069	± 0.0027
Lower Core Stack Height (cm)	-	24.054	0.169	-0.00249	± 0.070	± 0.0052
Upper Reflector Ring Height (cm)	-	16.770	Various	0.00001	± 0.00635	Negligible
Lower Reflector Ring Height (cm)	-	24.041	Various	0.00011	± 0.00635	Negligible
Membrane Thickness (cm)	-	0.3175	± 0.0254	-0.00062	± 0.0073	± 0.0005
Membrane Lift (cm)	-	-	-	-	-	Negligible
Sum in Quadrature (Dimensional Uncertainty)						± 0.00060
Composition Uncertainty						
^{234}U Abundance (Wt.%)	8	1.031	± 1	-	$\pm 1/\sqrt{8}$	Negligible
^{235}U Enrichment (Wt.%)	8	93.232	± 0.103	-	$\pm 0.103/\sqrt{8}$	± 0.00005
^{236}U Abundance (Wt.%)	8	0.232	± 100	-	$\pm 100/\sqrt{8}$	Negligible
^{238}U Abundance (Wt.%)	8	5.505	± 1	-	$\pm 1/\sqrt{8}$	Negligible
HEU Impurities (Wt.%)	8	Varies (Table 129)	-	0.00000	Varies (Table 129)	Negligible
NaCl Impurities (Wt.%)	7	Varies (Table 134)	-	0.00000	Varies (Table 134)	Negligible
^{35}Cl Abundance (Wt.%)	7	45.396	$\pm .001$	-	$\pm .001/\sqrt{7}$	Negligible
Polyethylene Impurities (Wt.%)	-	Varies (Table 140)	-	0.00000	Varies (Table 140)	Negligible
Aluminum Impurities (Wt.%)	-	Varies (Table 145)	-	0.00000	Varies (Table 145)	Negligible
Sum in Quadrature (Composition Uncertainty)						± 0.00005
Temperature Uncertainty						
Thermal Contraction (°C)	-	20.5	± 10.0	-0.00062	± 2.0	± 0.00006
Neutron Cross Sections (°C)	-	-	-		-	Negligible
Thermal Scattering Laws (°C)	-	20.5	Refer to Section 2.5.3	-0.00023/°C	± 2.0	± 0.00046
Sum in Quadrature (Temperature Uncertainty)						± 0.00047
Sum in Quadrature (Total Uncertainty)						± 0.00078

2.6.2 Case 2

Table 158: Summary of sensitivity in k_{eff} to uncertainties in Case 2.

Parameter (unit of measured)	N	Parameter Value	Parameter Variation in Calculation	Calculated Effect in k_{eff}	Standard Uncertainty	Standard Uncertainty in k_{eff}
Mass Uncertainty						
HEU Mass (g)	8	48604.8	$\pm 12.0 \times 8$	0.00057	$\pm 1.7\sqrt{8}$	Negligible
Absorber Encapsulation Mass (g)	7	14771.2	$\pm 9.0 \times 7$	-0.00013	$\pm 9.0\sqrt{7}$	Negligible
NaCl Mass (g)	7	4585.0	$\pm 10.0 \times 7$	-0.00243	$\pm 5.3\sqrt{7}$	± 0.00025
Polyethylene Moderator Mass (g)	7	33898.2	$\pm 18.6 \times 7$	-0.00085	$\pm 18.6\sqrt{7}$	± 0.00016
Polyethylene Reflector Mass (g)	13	18900.7	$\pm 0.5\,\%$	0.00061	$\pm 5.7\sqrt{13}$	± 0.00007
Aluminum Insert Mass (g)	2	624.5	$\pm 3.0 \times 2$	-0.00005	$\pm 0.5\sqrt{2}$	Negligible
Membrane Mass (g)	-	2396.1	± 20.0	-0.00003	± 0.3	Negligible
Structure Mass (g)	-	-	-	-	-	Negligible
					Sum in Quadrature (Mass Uncertainty)	± 0.00030
Dimensional Uncertainty						
HEU Plate Dimensions (cm)	8	Varies (Table 104)	$\pm 0.02 \times 8$	-0.00013	$\pm 0.002/\sqrt{8}$	Negligible
NaCl Absorber Diameter (cm)	7	30.479	$\pm 0.02 \times 7$	0.00012	$\pm 0.002/\sqrt{7}$	Negligible
NaCl Absorber Pocket Depth (cm)	7	0.490	$\pm 0.02 \times 7$	0.00525	$\pm 0.003/\sqrt{7}$	± 0.00015
Absorber Encapsulation Diameter (cm)	7	38.091	$\pm 0.02 \times 7$	-0.00002	$\pm 0.003/\sqrt{7}$	Negligible
Polyethylene Plate Dimensions (cm)	16	Varies (Table 110)	$\pm 0.02 \times 16$	0.00076	$\pm 0.02/\sqrt{16}$	± 0.00013
Polyethylene Ref. Dimensions (cm)	8	Varies (Table 119)	± 0.02	-0.00002	± 0.006	Negligible
Aluminum Insert Dimensions (cm)	2	Varies (Table 113)	$\pm 0.005 \times 2$	0.00003	$\pm 0.005/\sqrt{2}$	Negligible

Table 158 (continued): Summary of sensitivity in k_{eff} to uncertainties in Case 2.

Parameter (unit of measured)	N	Parameter Value	Parameter Variation in Calculation	Calculated Effect in k_{eff}	Standard Uncertainty	Standard Uncertainty in k_{eff}
Upper Core Stack Height (cm)	-	19.567	0.166	0.00122	$\pm$0.077	$\pm$0.00028
Lower Core Stack Height (cm)	-	26.394	0.217	$-$0.00455	$\pm$0.063	$\pm$0.00066
Upper Reflector Ring Height (cm)	-	19.432	Various	0.00008	$\pm$0.00635	Negligible
Lower Reflector Ring Height (cm)	-	26.455	Various	$-$0.00055	$\pm$0.00635	$\pm$0.00009
Membrane Thickness (cm)	-	0.3175	$\pm$0.0254	$-$0.00063	$\pm$0.0073	$\pm$0.00005
Membrane Lift (cm)	-	-	-	-	-	Negligible
Sum in Quadrature (Dimensional Uncertainty)						$\pm$0.00075
Composition Uncertainty						
^{234}U Abundance (Wt.%)	8	1.031	$\pm$1	-	$\pm 1/\sqrt{8}$	Negligible
^{235}U Enrichment (Wt.%)	8	93.232	$\pm$0.103	-	$\pm 0.103/\sqrt{8}$	$\pm$0.00005
^{236}U Abundance (Wt.%)	8	0.232	$\pm$100	-	$\pm 100/\sqrt{8}$	Negligible
^{238}U Abundance (Wt.%)	8	5.505	$\pm$1	-	$\pm 1/\sqrt{8}$	Negligible
HEU Impurities (Wt.%)	8	Varies (Table 129)	-	0.00000	Varies (Table 129)	Negligible
NaCl Impurities (Wt.%)	7	Varies (Table 134)	-	0.00000	Varies (Table 134)	Negligible
^{35}Cl Abundance (Wt.%)	7	45.396	$\pm$.001	-	$\pm .001/\sqrt{7}$	Negligible
Polyethylene Impurities (Wt.%)	-	Varies (Table 140)	-	0.00000	Varies (Table 140)	Negligible
Aluminum Impurities (Wt.%)	-	Varies (Table 145)	-	0.00000	Varies (Table 145)	Negligible
Sum in Quadrature (Composition Uncertainty)						$\pm$0.00006
Temperature Uncertainty						
Thermal Contraction (°C)	-	20.5	$\pm$10.0	$-$0.00036	$\pm$2.0	$\pm$0.00004
Neutron Cross Sections (°C)	-	-	-	-	-	Negligible
Thermal Scattering Laws (°C)	-	20.5	Refer to Section 2.5.3	-0.00042/°C	$\pm$2.0	$\pm$0.00084
Sum in Quadrature (Temperature Uncertainty)						$\pm$0.00085
Sum in Quadrature (Total Uncertainty)						$\pm$0.00117

2.6.3 Case 3

Table 159: Summary of sensitivity in k_{eff} to uncertainties in Case 3.

Parameter (unit of measured)	N	Parameter Value	Parameter Variation in Calculation	Calculated Effect in k_{eff}	Standard Uncertainty	Standard Uncertainty in k_{eff}
Mass Uncertainty						
HEU Mass (g)	18	110201.3	$\pm 12.0 \times 18$	0.00143	$\pm 1.7\sqrt{18}$	Negligible
Absorber Encapsulation Mass (g)	17	32802.9	$\pm 7.0 \times 17$	0.00044	$\pm 7.0\sqrt{17}$	± 0.00005
NaCl Mass (g)	17	8685.7	$\pm 10.0 \times 17$	0.00012	$\pm 6.5\sqrt{17}$	Negligible
Polyethylene Moderator Mass (g)	17	12432.6	$\pm 0.9 \times 17$	0.00152	$\pm 0.9\sqrt{17}$	± 0.00018
Polyethylene Reflector Mass (g)	14	16390.0	$\pm 0.5\,\%$	0.00153	$\pm 3.7\sqrt{11}$	± 0.00012
Aluminum Insert Mass (g)	7	925.9	$\pm 3.0 \times 7$	0.00015	$\pm 0.5\sqrt{7}$	Negligible
Membrane Mass (g)	-	2396.1	± 20.0	-0.00010	± 0.3	Negligible
Structure Mass (g)	-	-	-	-	-	Negligible
					Sum in Quadrature (Mass Uncertainty)	± 0.00023
Dimensional Uncertainty						
HEU Plate Dimensions (cm)	18	Varies (Table 104)	$\pm 0.02 \times 18$	-0.00053	$\pm 0.002/\sqrt{18}$	Negligible
NaCl Absorber Diameter (cm)	17	30.478	$\pm 0.02 \times 17$	-0.00008	$\pm 0.003/\sqrt{17}$	Negligible
NaCl Absorber Pocket Depth (cm)	17	0.643	$\pm 0.02 \times 17$	0.00137	$\pm 0.003/\sqrt{17}$	± 0.00004
Absorber Encapsulation Diameter (cm)	17	38.095	$\pm 0.02 \times 17$	0.00019	$\pm 0.005/\sqrt{17}$	Negligible
Polyethylene Plate Dimensions (cm)	20	Varies (Table 110)	$\pm 0.02 \times 20$	-0.00038	$\pm 0.02/\sqrt{20}$	± 0.00004
Polyethylene Ref. Dimensions (cm)	8	Varies (Table 119)	± 0.02	-0.00017	± 0.006	Negligible
Aluminum Insert Dimensions (cm)	12	Varies (Table 113)	$\pm 0.005 \times 12$	0.00005	$\pm 0.005/\sqrt{12}$	Negligible

Table 159 (continued): Summary of sensitivity in k_{eff} to uncertainties in Case 3.

Parameter (unit of measured)	N	Parameter Value	Parameter Variation in Calculation	Calculated Effect in k_{eff}	Standard Uncertainty	Standard Uncertainty in k_{eff}
Upper Core Stack Height (cm)	-	12.771	0.110	0.00081	$\pm$0.069	$\pm$0.00025
Lower Core Stack Height (cm)	-	20.357	0.211	$-$0.00467	$\pm$0.053	$\pm$0.00059
Upper Reflector Ring Height (cm)	-	12.755	Various	$-$0.00012	$\pm$0.00635	Negligible
Lower Reflector Ring Height (cm)	-	20.355	Various	$-$0.00091	$\pm$0.00635	$\pm$0.00012
Membrane Thickness (cm)	-	0.3175	$\pm$0.0254	$-$0.00065	$\pm$0.0073	$\pm$0.00005
Membrane Lift (cm)	-	-	-	-	-	Negligible
Sum in Quadrature (Dimensional Uncertainty)						$\pm$0.00066
Composition Uncertainty						
^{234}U Abundance (Wt.%)	18	1.031	$\pm$1	-	$\pm1/\sqrt{18}$	Negligible
^{235}U Enrichment (Wt.%)	18	93.232	$\pm$0.103	-	$\pm0.103/\sqrt{18}$	$\pm$0.00008
^{236}U Abundance (Wt.%)	18	0.232	$\pm$100	-	$\pm100/\sqrt{18}$	Negligible
^{238}U Abundance (Wt.%)	18	5.505	$\pm$1	-	$\pm1/\sqrt{18}$	Negligible
HEU Impurities (Wt.%)	18	Varies (Table 129)	-	0.00001	Varies (Table 129)	Negligible
NaCl Impurities (Wt.%)	17	Varies (Table 134)	-	0.00000	Varies (Table 134)	Negligible
^{35}Cl Abundance (Wt.%)	17	45.396	$\pm$.001	-	$\pm.001/\sqrt{17}$	Negligible
Polyethylene Impurities (Wt.%)	-	Varies (Table 140)	-	0.00000	Varies (Table 140)	Negligible
Aluminum Impurities (Wt.%)	-	Varies (Table 145)	-	0.00001	Varies (Table 145)	Negligible
Sum in Quadrature (Composition Uncertainty)						$\pm$0.00008
Temperature Uncertainty						
Thermal Contraction (°C)	-	20.5	$\pm$10.0	$-$0.00014	$\pm$2.0	Negligible
Neutron Cross Sections (°C)	-	-	-	-	-	Negligible
Thermal Scattering Laws (°C)	-	20.5	Refer to Section 2.5.3	-0.00002/°C	$\pm$2.0	$\pm$0.00004
Sum in Quadrature (Temperature Uncertainty)						$\pm$0.00004
Sum in Quadrature (Total Uncertainty)						$\pm$0.00070

3.0 BENCHMARK SPECIFICATIONS

3.1 Description of Model

The models presented in this section are simplified models of the benchmark configurations. The models utilize simplified material descriptions, simplified parts, and averaged geometries and densities to increase the ease of model reproduction. Each of the models are in vacuum and with the room removed, both of which are taken as simplifications. The simplifications to the models are described in more detail in the following section, Section 3.1.1, with a calculated simplification bias to determine the respective effect on the neutron multiplication factor.

Each of the models utilize HEU plates, sodium chloride absorbers, aluminum inserts, and polyethylene moderator and reflector plates and rings. The annular reflector rings, which are nested rings, are modeled as solid polyethylene reflectors. The Comet structure includes the stationary platform, movable platen, interface plate, adapter plate, adapter extension, and membrane. The adapter extension connects the adapter plate to the movable platen. The four standoffs connecting the interface plate to the stationary platform are not included in the models. The lower half of the experimental configuration sits in the adapter plate and the upper half of the experimental configuration sits on the membrane. These two halves are separated by the membrane, which sits on top of the interface plate.

The models are solely represented by simplified models and the detailed models are not described in this report beyond the simplification biases. Input decks are included in Appendix A.

3.1.1 Model Simplification and Bias

Given an unbiased model with calculated multiplication factor k_{eff} and a biased model, due to a simplification in component *i*, resulting in a calculated multiplication factor $k'_{eff,i}$, the simplification bias is defined as

$$\text{Bias}_i = k'_{\text{eff},i} - k_{\text{eff}} \tag{8}$$

Therefore, the simplification bias for component *i* is negative when the simplification results in a reduction in k_{eff}, and vice verse.

These model simplification and bias calculations use the same calculational parameters as Section 2.0. Therefore, the threshold for negligible is defined to be less than or equal to 0.00006 (6 pcm) in k_{eff}, which represents the propagated uncertainty in Δk_{eff} given a statistical uncertainty of ± 0.00004.

3.1.1.1 Comet and Room Removal

The experimental configurations were assembled using Comet located at National Criticality Experiments Research Center. In this subsection, Comet, the room, and the air simplifications were considered. Other components, or machines (Godiva), the four start-up detectors, and other contents in the room were not included as they were judged to have a negligible effect in k_{eff}.

Figure 35 shows a diagram of the room model, including Comet and an example experimental configuration. This room model is based on a previous study with additional measurement performed during this experiment[16]. The room is approximately 4.7 m tall with the stationary platform of Comet standing approximately 2.1 m from

[16] S. S. Kim. *12-Rad Zone Analysis for CAAS Placement at the Device Assembly Facility*. CSM 1531. Lawrence Livermore National Laboratory, 2008.

the floor. The closest wall and ceiling were measured relative to the interface plate. The interface plate was rigidly attached to the stationary platform of Comet by four 30.48 cm standoffs, described in Section 1.2.2.1. The ceiling was approximately 2.3 m from the top face of the interface plate and the nearest wall was approximately 3.1 m away from the side of the interface plate. The walls are modeled with a thickness of 0.3 m. The components of Comet are modeled using the engineering drawings provided in Appendix **??**.

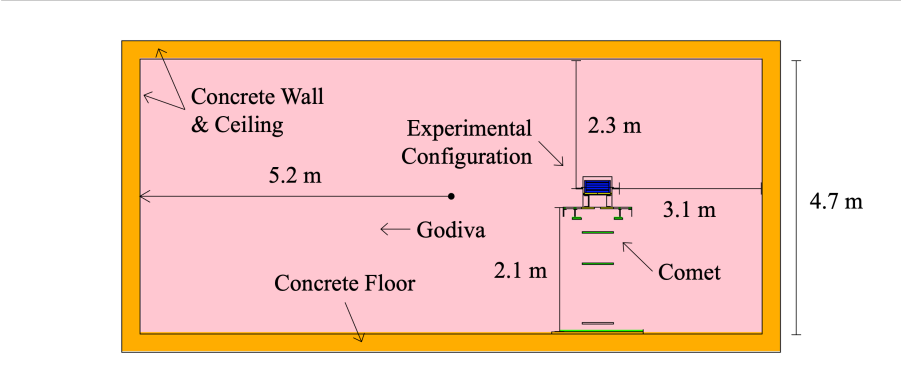

Figure 35: Diagram of the room containing Comet and the location of the experimental configurations.

The room is filled with air (75.5 % nitrogen (N), 23.2 % oxygen (O), and 1.3 % argon (Ar), by weight)[17] modeled with a density of 0.001225 $\mathrm{g\,cm^{-3}}$. The concrete walls are modeled as Portland Cement[17,18] with a density of 2.3 $\mathrm{g\,cm^{-3}}$. The Comet components, separate of those already included in the benchmark model, are modeled as iron[19] with a density of 7.8 $\mathrm{g\,cm^{-3}}$.

Table 160 summarizes the simplification bias due to removal of Comet, the room, and air. This table is reproduced alongside the other simplification biases in Section 3.1.2.

[17] R. J. McConn Jr. et al. *Compendium of Material Composition Data for Radiation Transport Modeling*. PNNL-15870 Rev. 1. Pacific Northwest National Laboratory, 2011. DOI: 10.2172/1023125.

[18] Referred to as "Portland Concrete" in the reference.

[19] These components are A36 Steel which is greater than 98% iron.

Table 160: Summary of simplification bias for removal of the room, Comet, and air.

Bias Component	Case 1	Case 2	Case 3
Baseline[a]	0.99824 ±0.00004	1.00138 ±0.00004	0.99202 ±0.00004
Comet Removed	0.99811 ±0.00004	1.00136 ±0.00004	0.99192 ±0.00004
Difference[b]	-0.00013 ±0.00006	-0.00002 ±0.00006	-0.00010 ±0.00006
Room Removed	0.99779 ±0.00004	1.00086 ±0.00004	0.99060 ±0.00004
Difference[c]	-0.00032 ±0.00006	-0.00050 ±0.00006	-0.00132 ±0.00006
Air Removed	0.99765 ±0.00004	1.00081 ±0.00004	0.99037 ±0.00004
Difference[d]	-0.00014 ±0.00006	-0.00005 ±0.00006	-0.00023 ±0.00006
Total[e]	**-0.00059 ±0.00010**	**-0.00050 ±0.00010**	**-0.00165 ±0.00010**

[a] The baseline model includes the detailed experimental configuration, the room, air, and Comet.
[b] (Comet Removed) - (Baseline), the worth of the room.
[c] (Room Removed) - (Comet Removed), the worth of the air.
[d] (Air Removed) - (Room Removed), the worth of Comet.
[e] The sum of the biases.

3.1.1.2 Simplified Absorbers

The absorber encapsulations were designed to maximize the density and security of the NaCl salt, as described in Section 1.2.4. In doing so, the encapsulations were designed with 16 screws and a lip on the outer diameter to retain the lid. The screws were made from Al-2024 which was simplified to be removed in favor of Al-6061. Both the screws and the lip feature of the encapsulation were removed in this step, shown in Figure 36, to form a simplified encapsulation which includes a base and a lid which share a common outer diameter. The simplification bias from removing the screws and simplifying the encapsulation geometry is summarized in Table 161. The effect is significantly greater for Case 3 as it utilized more than double the amound of absorber plates, with thicker aluminum encapsulation and thinner absorbers, increasing the importance of the material in the model.

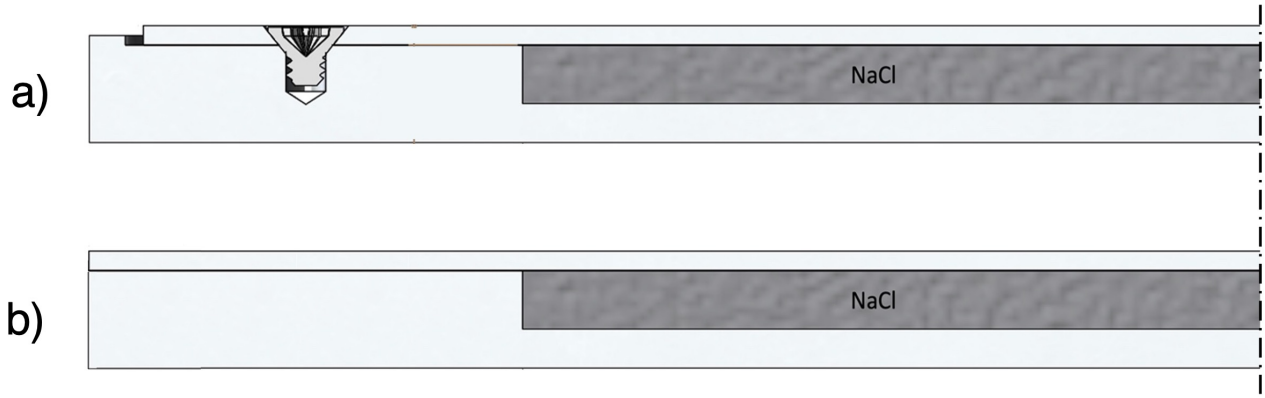

Figure 36: (A) An axis-symmetric drawing of the detailed NaCl absorber encapsulations. (B) An axis-symmetric drawing of the simplified NaCl absorber encapsulations.

Table 161: Summary of simplification bias for the simplification of the absorber encapsulations.

Case	Effect in k_{eff}
1	0.00018 ± 0.00006
2	0.00022 ± 0.00006
3	0.00106 ± 0.00006

3.1.1.3 HEU Impurity

The impurities in the HEU are reported in Section 2.4.2. The average impurities were measured to be $885.5\,\mu g\,g^{-1}$. The largest impurities are carbon (C), silicon (Si), aluminum (Al), and iron (Fe), making up just over 90% of the impurity content. Table 162 summarizes the effect in k_{eff} due to the removal of the HEU impurities. The HEU impurities were modeled as void which reduced the HEU plate densities by 0.08855 %.

Table 162: Summary of simplification bias for the removal of the HEU impurities.

Case	Effect in k_{eff}
1	-0.00025 ± 0.00006
2	-0.00012 ± 0.00006
3	-0.00025 ± 0.00006

3.1.1.4 Sodium Chloride Impurity

The impurities in the sodium chloride salt are described in detail in Section 2.4.3. The average impurities were measured to be $41.8\,\mu g\,g^{-1}$, excluding water which will be addressed in the following section. The largest contributors to the impurities were potassium (K), sulfur (S), and bromine (Br), which made up approximately 90% of the total impurity content. Table 163 summarizes the effect in k_{eff} due to the removal of the sodium chloride impurities. The sodium chloride impurities were modeled as void which reduced the sodium chloride density by 0.00418 %.

Table 163: Summary of simplification bias for the removal of the sodium chloride impurities.

Case	Effect in k_{eff}
1	0.00014 ± 0.00006
2	-0.00005 ± 0.00006
3	0.00004 ± 0.00006

3.1.1.5 Sodium Chloride Moisture

The moisture (water) in the sodium chloride salt is also described in Section 2.4.3. The average moisture was measured to be $160\,\mu g\,g^{-1}$. Table 164 summarized the effect in k_{eff} due to the removal of the moisture in the sodium chloride salt. The moisture was modeled as void whcih further reduced the sodium chloride density by 0.0160 %.

Table 164: Summary of simplification bias for the removal of the sodium chloride moisture.

Case	Effect in k_{eff}
1	-0.00004 ± 0.00006
2	0.00015 ± 0.00006
3	-0.00003 ± 0.00006

3.1.1.6 Polyethylene Impurity

The impurities in the polyethylene are reported in Section 2.4.4. These impurities were measured to be $960.8\,\mu g\,g^{-1}$. The elemental impurities include Na, Al, Si, and Cr. Of which, none are significant neutron absorbers. Table 165 summarizes the effect in k_{eff} due to the removal of the polyethylene impurities. In the benchmark models, the polyethylene impurities are modeled as void by reducing the polyethylene part densities by 0.09608 %. These parts include all the polyethylene parts described in Section 1.2.5.

Table 165: Summary of simplification bias for the removal of the polyethylene impurities.

Case	Effect in k_{eff}
1	-0.00020 ± 0.00006
2	-0.00008 ± 0.00006
3	0.00003 ± 0.00006

3.1.1.7 Aluminum Impurity

The impurities in the aluminum are reported in Section 2.4.5. This impurity content ranges from 1.4 Wt % to 4.2 Wt %, with an average of 2.695 Wt %. The largest elemental impurities include magnesium (Mg), silicon (Si), iron (Fe), copper (Cu), and chromium (Cr), making up just under 90% of the total impurity content. Unlike the other impurities, the aluminum composition was not probed empircally, but rather was mased on handbook data. Due to the large abundance of aluminum in the core, magnesium (Mg), copper (Cu), and iron (Fe) were left in the final aluminum composition which the aluminum serving as the balance for the removed impurities. Since the accepted density of aluminum is $2.7\,g\,cm^{-3}$, the Comet components were assigned that

density. For the stack components, empirical mass and dimensional measurements provided part densities which were reduced by 1.07 % to model the removed impurities as void. Table 166 summarizes the effect in k_{eff} due to the removal of the aluminum impurities.

Table 166: Summary of simplification bias for the removal of the aluminum impurities.

Case	Effect in k_{eff}
1	0.00002 ± 0.00006
2	-0.00007 ± 0.00006
3	-0.00053 ± 0.00006

3.1.1.8 Temperature Correction

As described in Section 1.4, the temperatures of the experimental configurations during operation were typically around 14.9 °C. To simplify the model, these temperatures are corrected to 293.6 K (20.45 °C).

The bias in this simplification is determined based on the sensitivities calculated during the temperature uncertainty analysis described in Section 2.5. This analysis shows that the sensitivity in k_{eff} due to temperature results from thermal contraction and the polyethylene thermal scattering law. The sensitivity due to the neutron cross section data is negligible.

Table 167 summarizes simplification bias due to correcting the model temperature. The experiment temperature is evaluated in Section 2.5. This table is reproduced alongside the other simplification biases in Section 3.1.2.

Table 167: Summary of simplification bias for the temperature correction to 293.6 K (20.5 °C).

Case	Sensitivity in k_{eff} [a]	Temperature (°C)			Effect in k_{eff} [c]
		Model	Experiment	Difference[b]	
1	-0.00023/°C	20.5	14.9	-5.6	0.00130 ± 0.00010
2	-0.00042/°C		14.9	-5.6	0.00236 ± 0.00010
3	-0.00002/°C		14.6	-5.9	0.00012 ± 0.00010

[a] Sum of sensitivities in k_{eff} to thermal contraction (Section 2.5.1) and thermal scattering law (Section 2.5.3).
[b] (Experiment Temperature) - (Model Temperature)
[c] Uncertainty is due to uncertainty in the least squares fit.

3.1.1.9 Reflector Rings, Caps, and Bottom Reflector

The polyethylene reflector parts are designed to be stacked. Namely, the annular reflector rings were designed with step joints to allow them to be nested together to form a completed annular reflector, minimizing the neutron streaming pathways. The tops and bottoms of the annular reflector rings were completed with caps so that a bare step joint was not exposed, i.e. forming a complete reflector ring. Additionally, the bottom reflector was designed with a step on the outer diameter to seat the annular reflector rings. The bottom reflector also included a polyethylene plug on the bottom surface, which could be removed in favor of a source holder during the approach to critical.

Simplifications to the reflectors are shown in Figure 37 and Figure 38. The top reflectors were simplified into a single unit for each configuration and were given the reflector density regardless if moderator plates were used as reflectors. These simplifications removed the complex features of the reflectors in favor of solid, easy to model geometries. The total mass of the reflectors were conserved by using a bulk density, which was based on the combined measured masses and the modeled volumes.

The effect of these simplifications to the polyethylene reflector parts is analyzed as part of the average geometry simplification in Section 3.1.1.10.

3.1.1.10 Average Geometry

The core stacks were simplified by using averaged geometries for the HEU, sodium chloride absorbers, and polyethylene parts. A bulk density was used for each of the part types, and was calculed to conserve the total measured mass of the parts used in each of the experimental configurations. An exception is the structural aluminum, which used a nominal $2.70\,\mathrm{g\,cm^{-3}}$ density.

All parts use nominal diameters, including the HEU plates, sodium chloride absorbers, polyethylene moderator and reflector plates, and aluminum inserts. The inner and outer diameters for the annular reflectors were based on teh average inner any outer diameters for the parts in each configuration. The thickness of each part is the average thickness of each part type used in the configuration.

As assessed in Section 2.2.1, there is a bias of -1.2 grams. This mass bias is insignificant and therefore was not included in the simplification bias for the HEU plates.

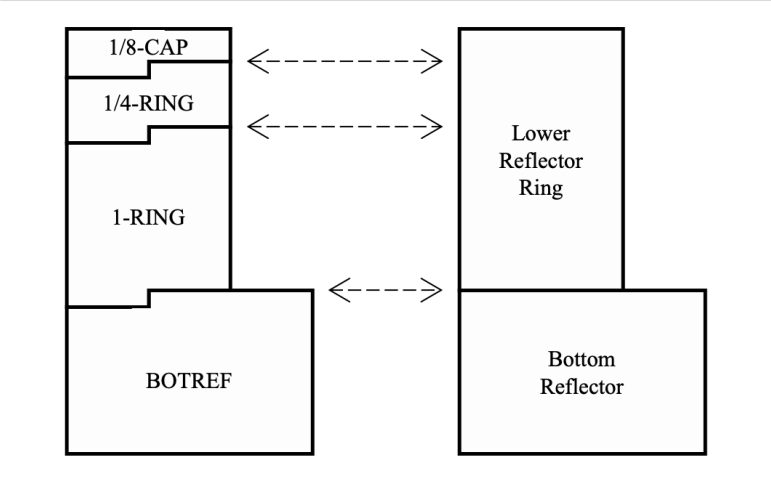

Figure 37: Example of the reflector simplification, showing the lower reflector rings and bottom reflector. The left shows the actual ring reflectors including the step joints while the right shows the model simplification which removes the step joints.

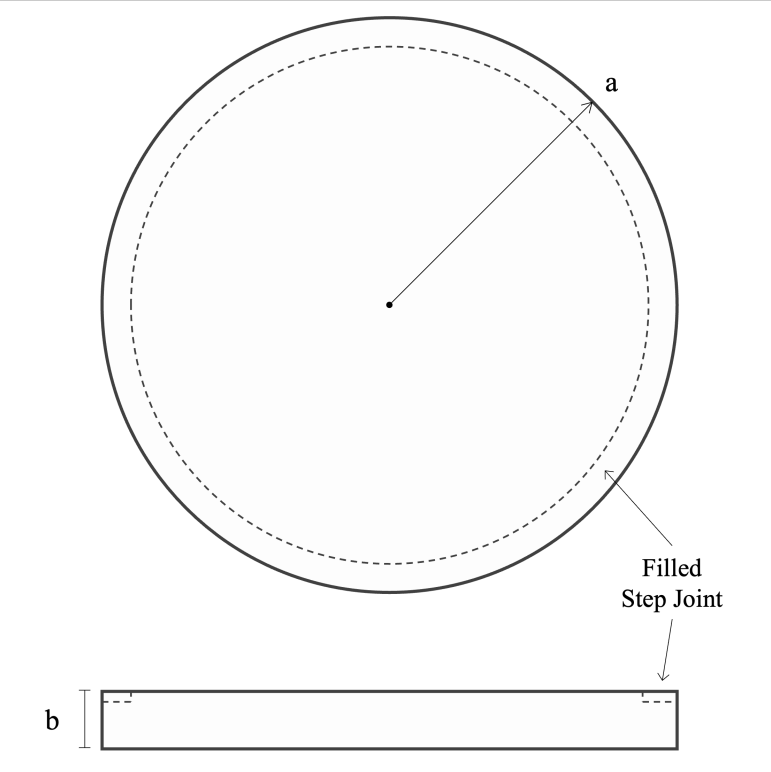

Figure 38: Simplifications to the bottom reflector plate, removing the step joint and neutron source hole. The dimensions are reported in Table 175 of Section 3.2.6.

Table 168 summarizes the simplification bias due to the average geometry and reflector simplifications. This table is reproduced alongside the other simplification biases in Section 3.1.2.

Table 168: Summary of simplification bias for the average geometry and reflector simplifications.

Case	Effect in k_{eff}
1	-0.00081 ± 0.00006
2	-0.00047 ± 0.00006
3	-0.00168 ± 0.00006

3.1.2 Summary of Bias Calculations

Table 169 presents the bias calculations for the benchmark model. The experimental k_{eff} will be adjusted by adding the total bias reported in this table.

Table 169: Summary of bias calculation results due to model simplification.

Bias Component	Case 1	Case 2	Case 3
Room, Air, and Comet Removal	−0.00059 ±0.00010	−0.00050 ±0.00006	−0.00165 ±0.00010
Absorber Simplification	+0.00018 ±0.00006	+0.00022 ±0.00006	+0.00106 ±0.00006
Impurity Removal	−0.00031 ±0.00010	−0.00012 ±0.00011	−0.00074 ±0.00008
Average Geometry	−0.00081 ±0.00006	−0.00047 ±0.00006	−0.00168 ±0.00006
Temperature Correction	+0.00130 ±0.00010	+0.00236 ±0.00010	+0.00012 ±0.00010
Total	**−0.00023 ±0.00019**	**+0.00149 ±0.00018**	**−0.00289 ±0.00018**

3.2 Dimensions

3.2.1 Comet General Purpose Critical Assembly Machine

The model of Comet consists of six components, shown in Figure 39. The interface plate and stationary platform form the upper stationary platform, shown in Figure 5 of Section 1.2.2.1. The adapter plate, adapter extension, and movable platen form the lower movable platen, shown in Figure 8 of Section 1.2.2.2. The upper stationary platform is fixed in place, where the interface plate and stationary platform are separated by four 30.48 cm standoffs. The position of the lower movable platen varies along the vertical axis depending on the height of the lower half of the experiment. The membrane sits on top of the interface plate for all configurations, separating the upper and lower halves of the configurations.

Tables 170 and 171 report the part dimensions for the upper stationary platform and lower movable platen, respectively. Since the upper stationary platform is fixed in place across all models, Table 170 also reports the upper and lower z-planes that bound the extent, or thicknesses, of the parts. The same is done for the lower movable platen, but the positions along the vertical axis depend on the height of the lower half of the experimental configuration, so the values are reported in the relevant model sections. In addition to these tables, each component is described in detail in the following sections.

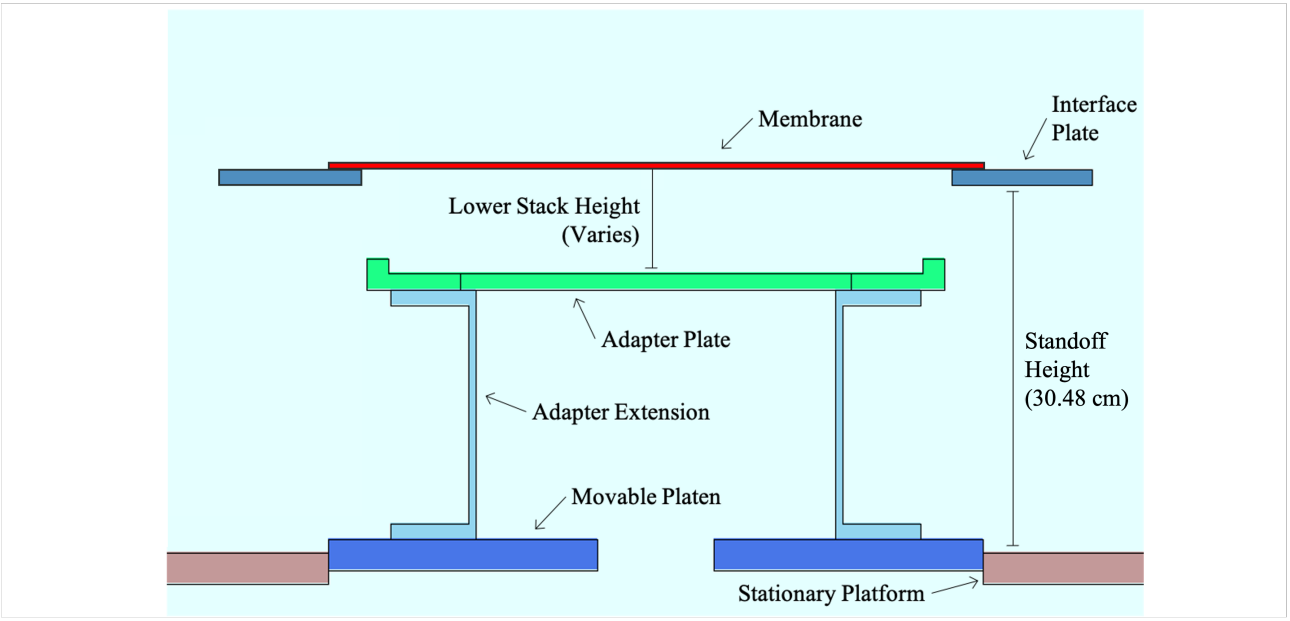

Figure 39: Comet structure components: membrane (red), interface plate (dark blue), adapter plate (teal), adapter extension (light blue), movable platen (blue), and stationary platform (brown).

Table 170: Model dimensions for the upper stationary platform of Comet.

Part	Density (g/cm^3)	Side Length (cm)	Inner Radius (cm)	Thickness (cm)	Lower z Plane (cm)	Upper z Plane (cm)
Membrane	2.6525	53.34	-	0.3175	See model-specific tables in each section.	
Interface Plate	2.7	71.12	24.13	1.27		
Stationary Platform		114.3	26.797	2.54		

Table 171: Model dimensions for the lower movable platen of Comet.

Part		Density (g/cm^3)	Outer Radius (cm)	Inner Radius (cm)	Thickness (cm)	Lower z Plane (cm)	Upper z Plane (cm)
Adapter Plate	Lip	2.7	23.495	21.7805	1.1938	See model-specific tables in each section.	
	Plate			15.875	1.3462		
Adapter Extension			21.59	14.605	1.27		
			15.24		17.78		
			21.59		1.27		
Movable Plate			26.67	4.7625	2.54		

3.2.1.1 Membrane

The membrane was modeled as shown in Figure 40. The membrane is a square aluminum sheet with a side length of 53.34 cm and thickness of 0.3175 cm. There are four small holes in the corners of the membrane. These holes are removed in the model as they have a negligible impact on the calculation. The membrane is the same for all experimental configurations.

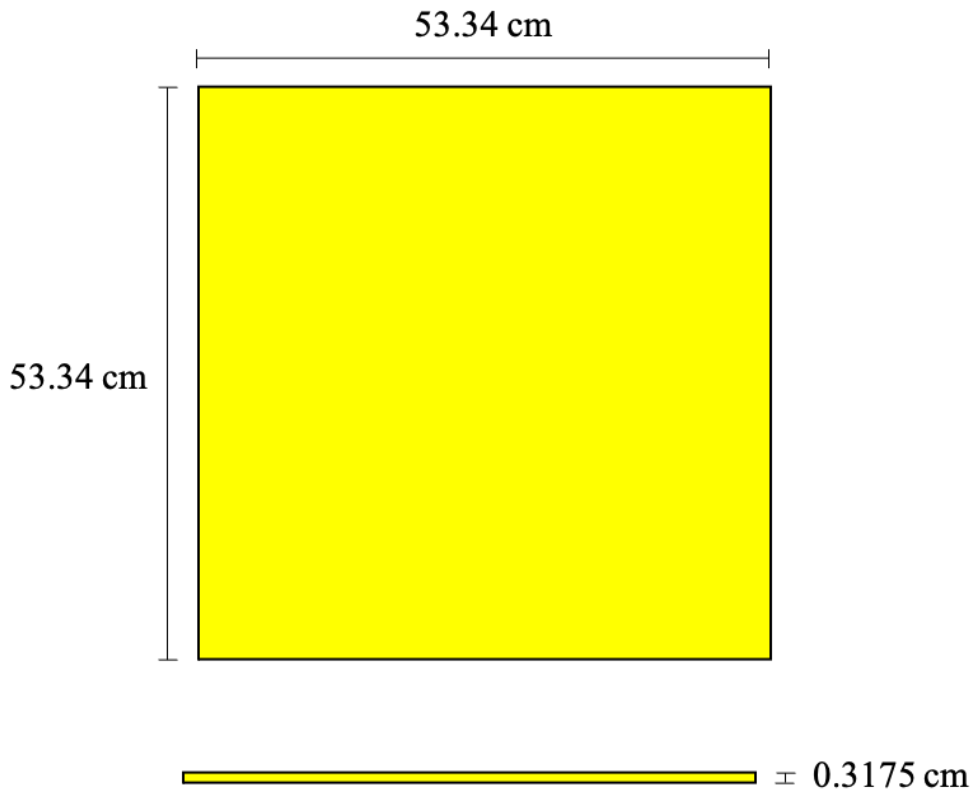

Figure 40: Membrane model dimensions (not to scale).

3.2.1.2 Interface Plate

The interface plate is modeled as shown in Figure 41. The interface plate is a square aluminum plate with a side length of 71.12 cm and thickness of 1.27 cm. There is a 48.26 cm diameter hole through the center of the interface plate. There are various holes for affixing the standoffs to the interface plate and four protruding pegs to align the membrane. These components are removed in the model as they have a negligible impact on the calculation. The interface plate is the same for all experimental configurations.

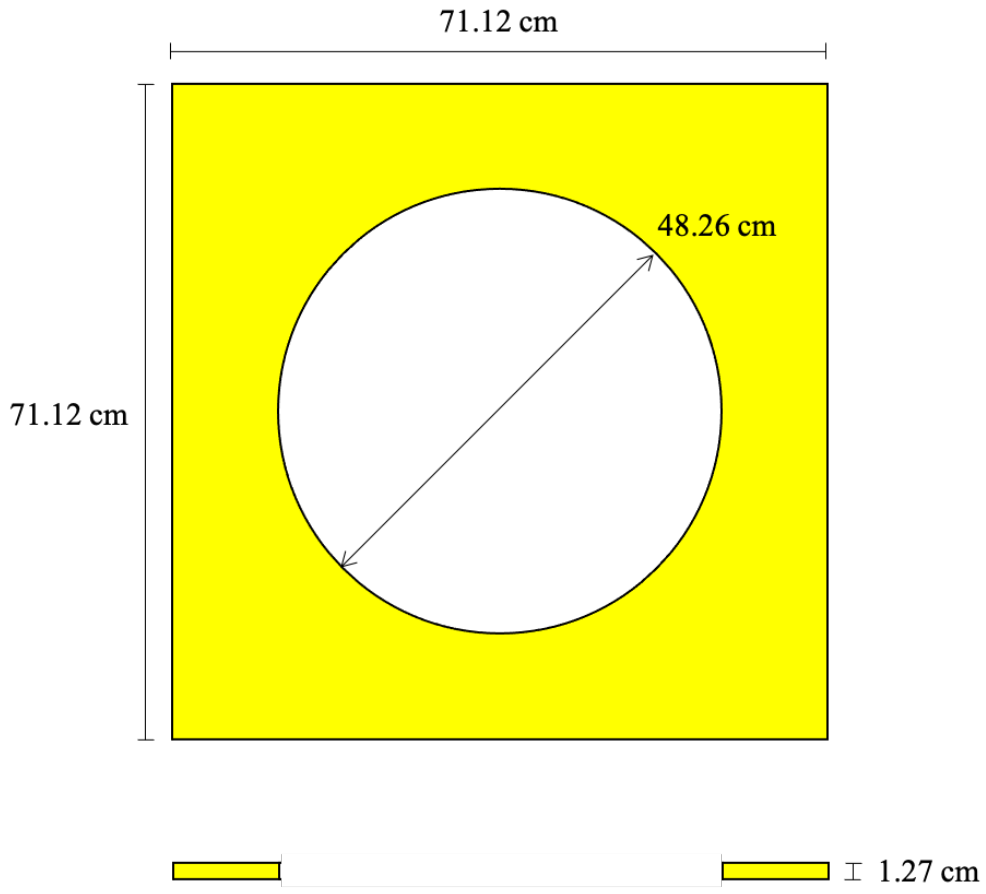

Figure 41: Interface plate model dimensions (figure not to scale).

3.2.1.3 Adapter Plate

The adapter plate is modeled as shown in Figure 42. The adapter plate is an annular cylinder with an outer lip and inner crossbars to hold the bottom reflector (BOTREF) in place. The adapter plate features multiple lip regions to retain the bottom reflector, but they were simplified to a single lip ring around the circumference. There are various holes for affixing the adapter plate to the adapter extension. These holes are removed within the model as they have a negligible impact on the calculation. The adapter plate is the same for all experimental configurations.

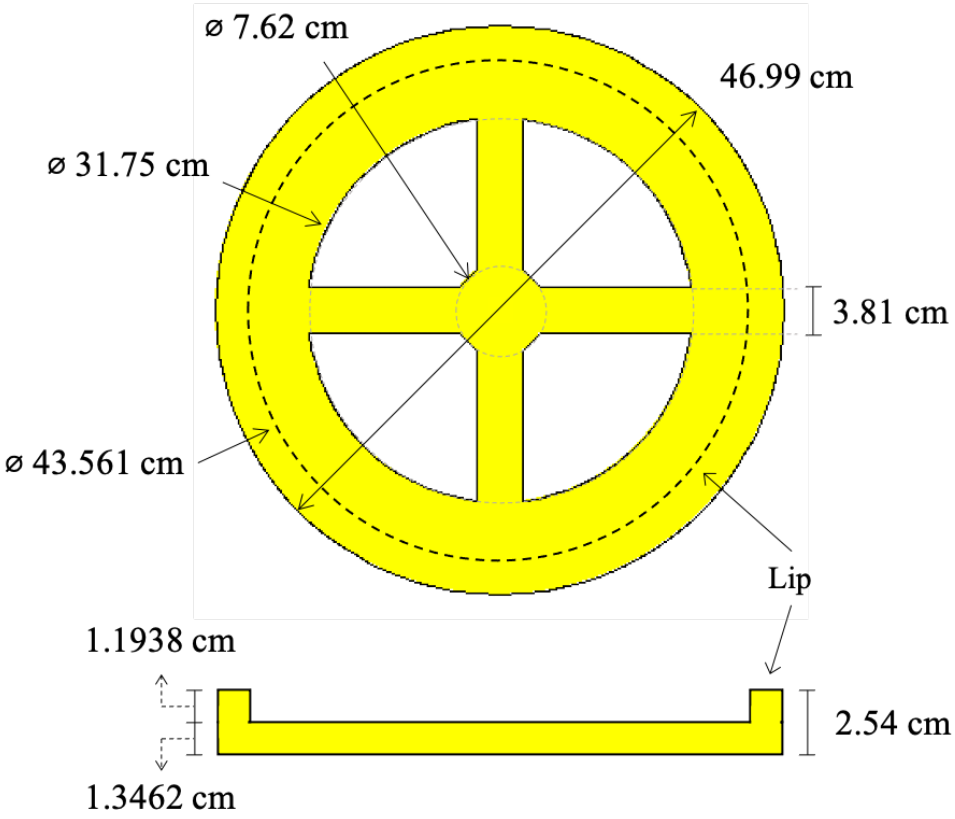

Figure 42: Adapter plate model dimensions (figure not to scale).

3.2.1.4 Adapter Extension

The adapter extension is modeled as shown in Figure 43. The adapter extension consists of a thin-walled aluminum cylinder with a top and bottom flange extending off the cylinder to affix the adapter extension to the adapter plate on top and the Comet movable platen on bottom. The annular cylinder has an inner diameter of 29.21 cm and a height of 20.32 cm with a wall thickness of 0.635 cm. The top and bottom lips have an outer diameter of 43.18 cm and thickness of 1.27 cm. There are various holes for affixing the adapter extension to both the adapter plate and movable platen. These holes are removed within the model as they have a negligible impact on the calculation. The adapter extension is the same for all experimental configurations.

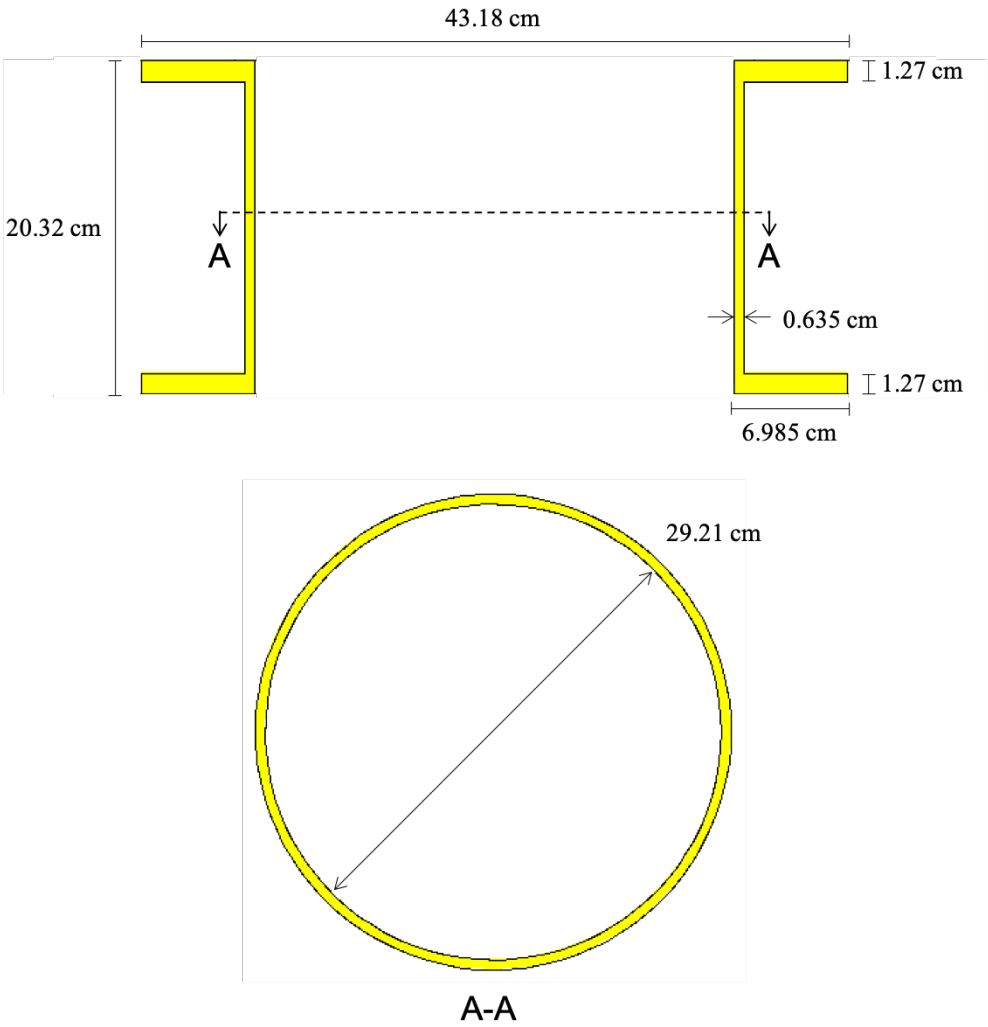

Figure 43: Adapter extension model dimensions (figure not to scale).

3.2.1.5 Comet Movable Platen

The Comet movable platen is modeled as shown in Figure 44. The platen is a circular aluminum plate with a diameter of 53.34 cm and thickness of 2.54 cm. There is a 9.525 cm diameter hole through the center of the platen. There are various holes through the movable platen for fixturing. These holes are removed within the model as they have a negligible impact on the calculation. The movable platen is the same for all experimental configurations.

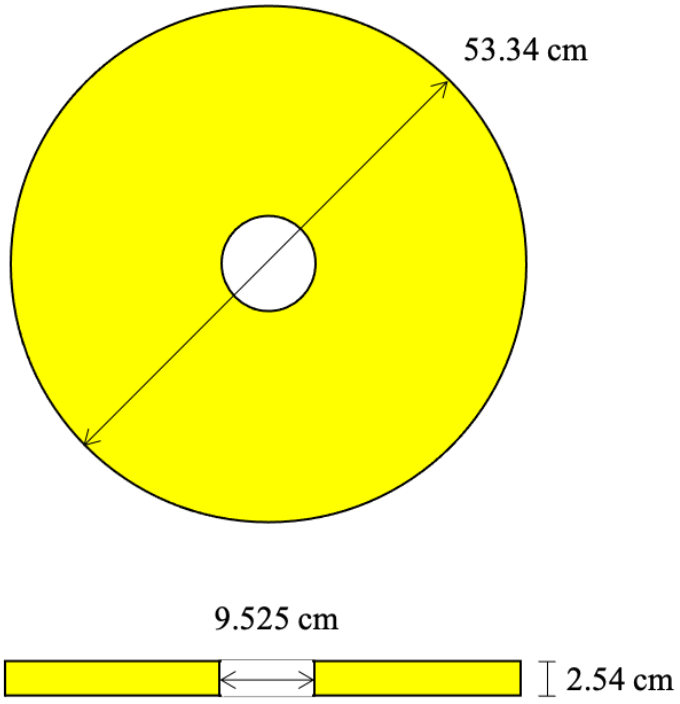

Figure 44: Comet movable platen model dimensions (figure not to scale).

3.2.1.6 Comet Stationary Platform

The Comet stationary platform is modeled as shown in Figure 45. The platform is a square aluminum plate with a side length of 114.3 cm and thickness of 2.54 cm. There is a 53.594 cm diameter hole through the center of the platform. There are various holes through the stationary platform for fixturing and the four corners chamfered. These holes are removed, and the corners are filled within the model as they have a negligible impact on the calculation. The stationary platform is the same for all experimental configurations.

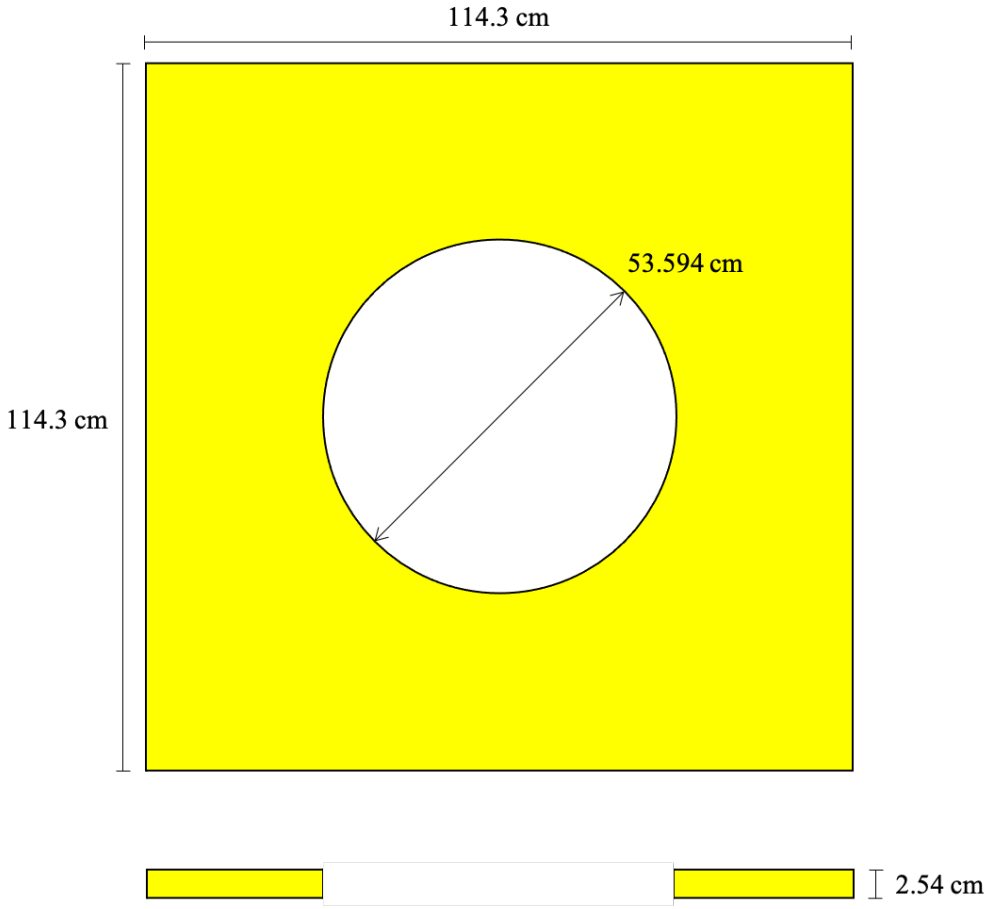

Figure 45: Comet stationary platform model dimensions (figure not to scale).

3.2.2 Highly Enriched Uranium Plates

The HEU plates are modeled as shown in Figure 46. There are five types of HEU plates: 15/0-HEU, 15/2.5-HEU, 15/6-HEU, 15/10-HEU, and 6/0-HEU. Each part type uses the nominal inner and outer radii. All part types use the same thickness, based on an average of all the measured plate thicknesses, as described in Section 2.3.1. Table 172 reports the dimensions of the HEU plates used in the benchmark models. The HEU plates are concentric with the vertical axis.

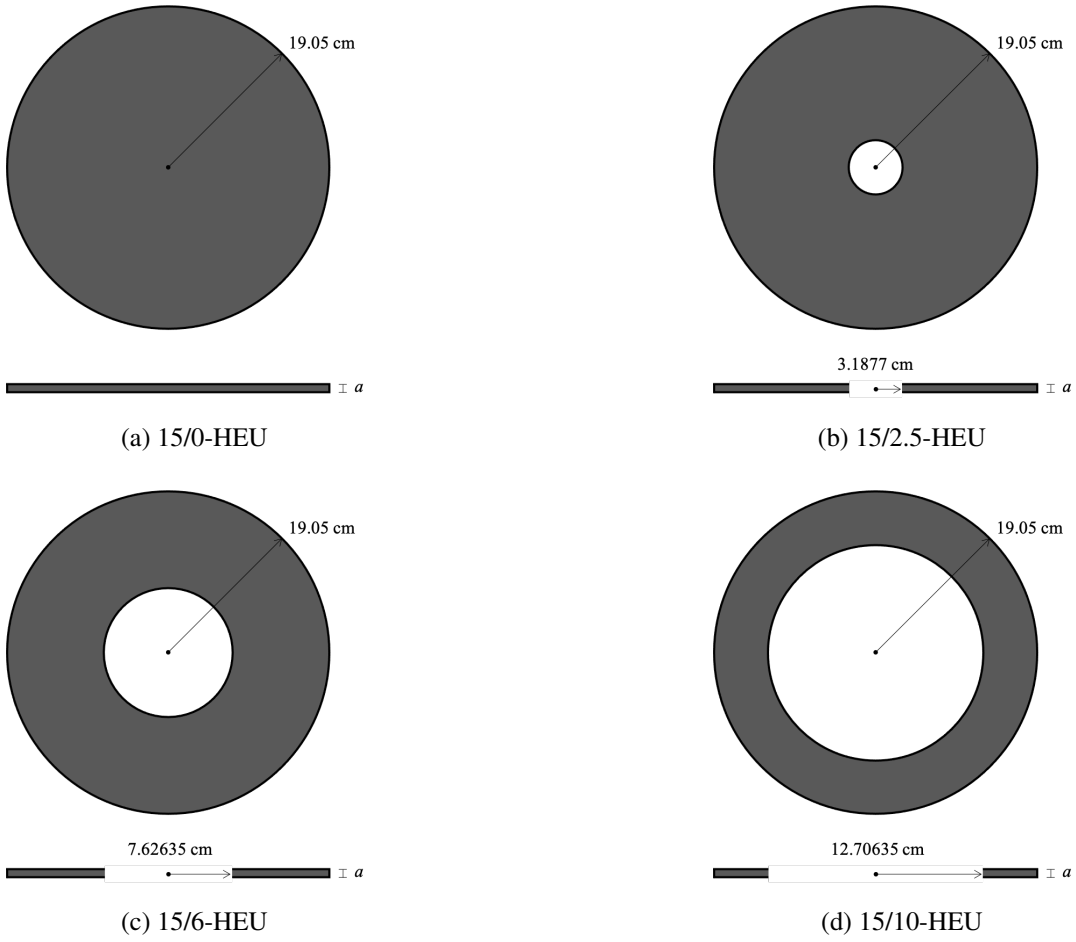

(a) 15/0-HEU

(b) 15/2.5-HEU

(c) 15/6-HEU

(d) 15/10-HEU

Figure 46: HEU plate model (not to scale).

Table 172: HEU plate model dimensions (see Figure 46).

Part Type	Inner Radius (cm)	Outer Radius (cm)	Thickness, *a* (cm)
15/0-HEU	-	19.05	0.31083
15/2.5-HEU	3.19		
15/6-HEU	7.629		
15/10-HEU	12.699		
6/0-HEU	-	7.607	

3.2.3 Sodium Chloride Absorbers

The sodium chloride absorbers are modeled as shown in Figure 47. The geometry has been simplified as a cylindrical sodium chloride absorber region surrounded by encapsulation. The encapsulation is made of aluminum. The sodium chloride absorber region has a nominal radius of 15.24 cm and either a nominal thickness of 0.635 cm or 0.490 cm. The encapsulation has a nominal outer radius of 19.05 cm. Table 173 reports the dimensions of the sodium chloride absorber plates used in the benchmark models. The sodium chloride absorber plates are concentric with the vertical axis.

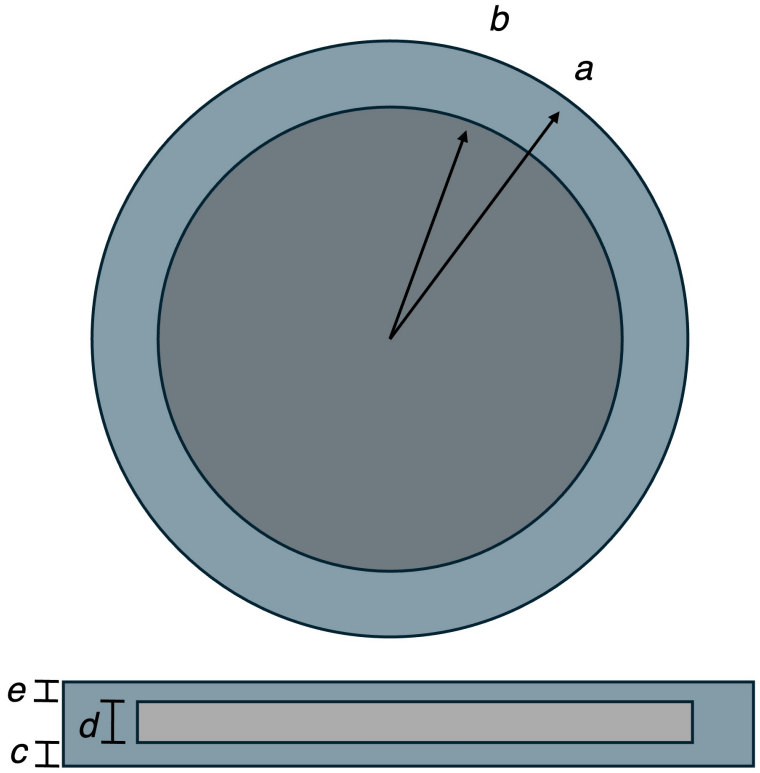

Figure 47: Sodium chloride absorber plate model (not to scale).

Table 173: Sodium chloride absorber plate model dimensions (see Figure 47).

Part Type	Outer Radius, *a* (cm)	Inner Radius, *b* (cm)	Absorber Thickness, *d* (cm)	Lower Encap. Thickness, *c* (cm)	Upper Encap. Thickness, *e* (cm)
1/4" Sodium Chloride Absorber	19.05	15.24	0.645	0.233	0.251
3/16" Sodium Chloride Absorber	19.05	15.24	0.4893	0.245	0.254

3.2.4 Polyethylene Moderator and Reflector Plates

The polyethylene moderator (MOD) and reflector (REF) plates are modeled as shown in Figure 48. There are seven types of polyethylene moderator and reflector plates: 1/8-MOD, 1/4-MOD, 1/2-MOD, 1.5-MOD, 1/16-REF, and 1-REF. The top reflector for each experimental configuration consists of a combination of these moderator and reflector plates. However, as part of the simplification bias the top reflector components were simplified to a single reflector plate with the density for reflectors. The benchmark models represent the top reflector as the sum of the individual part types. All part types use a nominal radius of 19.05 cm and an average thickness based on the part type, as described in Section 2.3.3. Table 174 reports the dimensions of the polyethylene moderator and reflector plates used in the benchmark models.

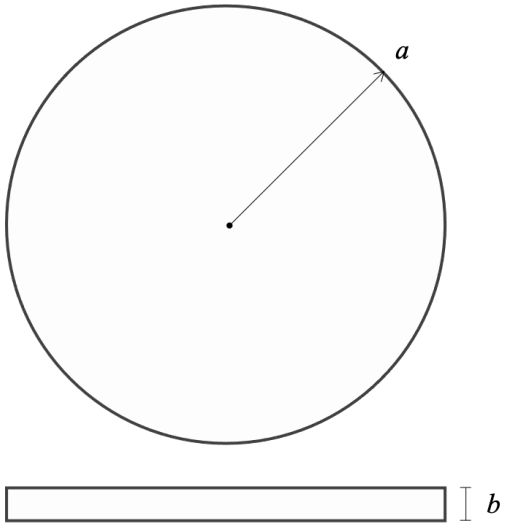

Figure 48: Polyethylene moderator and reflector plate model (not to scale).

Table 174: Polyethylene moderator and reflector plate model dimensions (see Figure 48).

Part Type	Thickness, *b* (cm)	Radius, *a* (cm)
1/8-MOD	0.3183	19.05
1/4-MOD	0.6431	
1/2-MOD	1.2901	
3/4-MOD	1.9367	
1.5-MOD	3.8321	
1/16-REF	0.1849	
1-REF	2.5387	

3.2.5 Polyethylene Reflector Rings and Caps

The polyethylene reflector rings surround the core stack to provide an additional 2.54 cm of radial reflection. These rings include male (top) and female (bottom) steps joints which mate with one another as the rings are stacked to provide structural support and reduce neutron streaming paths. The stack of reflector rings is finished using a reflector cap which only has the female (bottom) step joint to provide a flat top surface to the reflector stack.

The upper and lower reflectors are modeled as shown in Figure 49. These dimensions are reported for each benchmark model in Section 3.2.8.

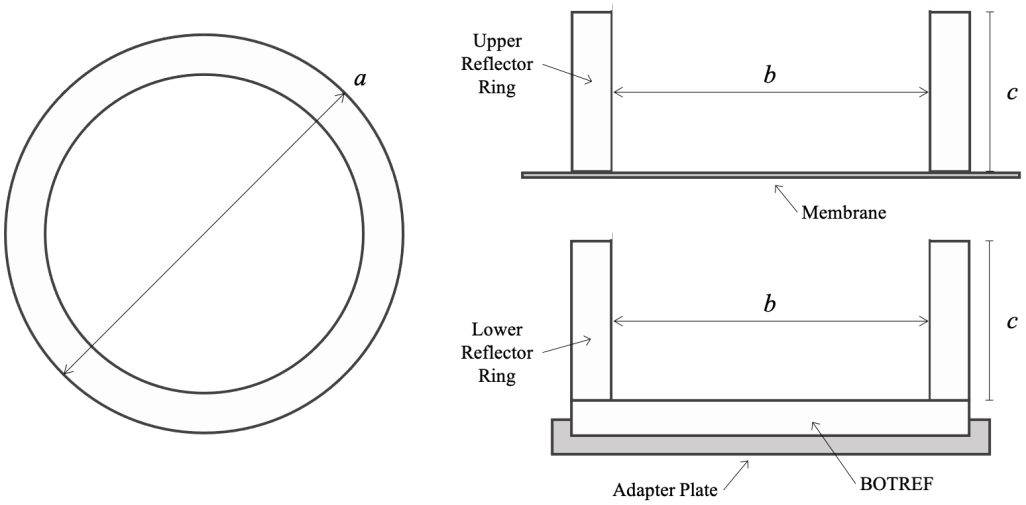

Figure 49: Polyethylene reflector ring model and dimensions. The left figure shows a cross section of the reflector which is an annular cylinder. The right figures show the upper ring reflector, which sits on top of the membrane, and the lower ring reflector, which sits on top of the bottom reflector within the adapter plate.

3.2.6 Polyethylene Bottom Reflector

The polyethylene bottom reflector (BOTREFSRC) is modeled as shown in Figure 50. This model includes the simplifications described in Section 3.1.1. These simplifications include removal of the step joint and neutron source hole. Table 175 reports the dimensions of the bottom reflector used in the benchmark models.

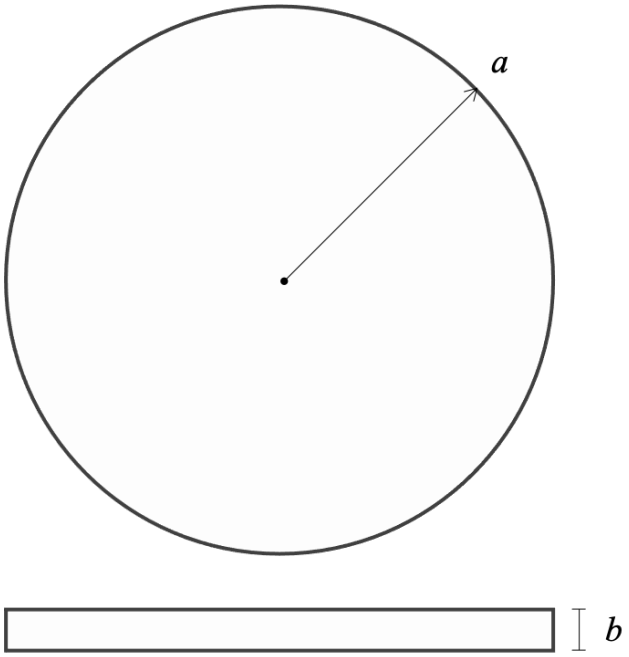

Figure 50: Polyethylene bottom reflector model (not to scale).

Table 175: Polyethylene bottom reflector model dimensions (see Figure 50).

Part Type	Radius, *a* (cm)	Thickness, *b* (cm)
BOTREF	21.7119	2.8677

3.2.7 Aluminum Inserts

The aluminum inserts are modeled as shown in Figure 51. There are three types of aluminum inserts, differentiated by their diameter, corresponding to the annuli of the 15/2.5-HEU, 15/6-HEU, and 15/10-HEU plates. The aluminum insert models are concentric with the vertical axis and fit within the center of the HEU plate annuli. Table 176 reports the dimensions of the aluminum inserts used in the benchmark models.

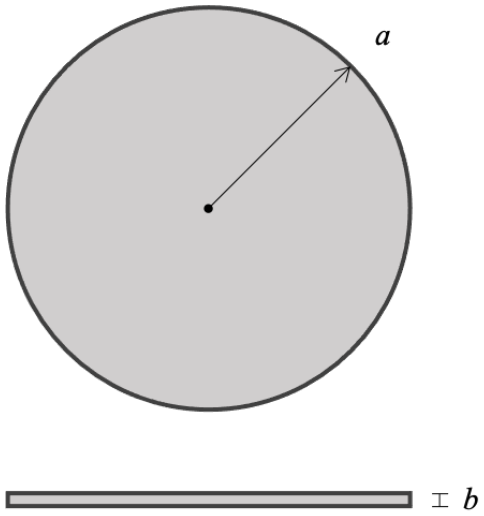

Figure 51: Aluminum insert model (not to scale).

Table 176: Aluminum insert model dimensions (see Figure 51).

Part Type	Thickness, *a* (cm)	Radius, *b* (cm)
2.5-DISK	0.31672	3.19
6-DISK		7.629
10-DISK		12.699

3.2.8 Case Models

Each experimental configuration presents a benchmark model, with accompanying tables and figures to fully describe the experimental configuration including the dimensions, masses, and axial positions that describe each part. The origin of the benchmark models is at center of the top face of the interface plate. All axial positions reported in the following sections are relative to this origin. All parts are centered about the vertical axis (z-axis).

3.2.8.1 Case 1

The Case 1 model includes 8 HEU plates, 7 sodium chloride absorbers between each HEU plate, 7 sets of 0.25" and 1.5" HDPE moderators, and a 0.5079 in. (1.2901 cm) top HDPE reflector. These 8 HEU plates consist of five 15/0-HEU plates, one 15/2.5-HEU plate, one 15/6-HEU plate, and one 15/10-HEU plate. Figure 52 shows a cross sectional view of the model. The aluminum parts (structural components, membrane, and inserts) are shown in yellow, the HEU plates in green, the sodium chloride absorbers in blue, and the polyethylene reflector in pink.

Tables 178 and 179 report the upper and lower core stack dimensions, including: part densities (in g/cm^3), dimensions, and axial position (z-axis). Table 180 reports similar dimensions for the upper and lower reflector rings. Table 177 reports the axial positions of the Comet lower movable platen components specific to the Case 1 model, as reference in Table 171 of Section 3.2.1.

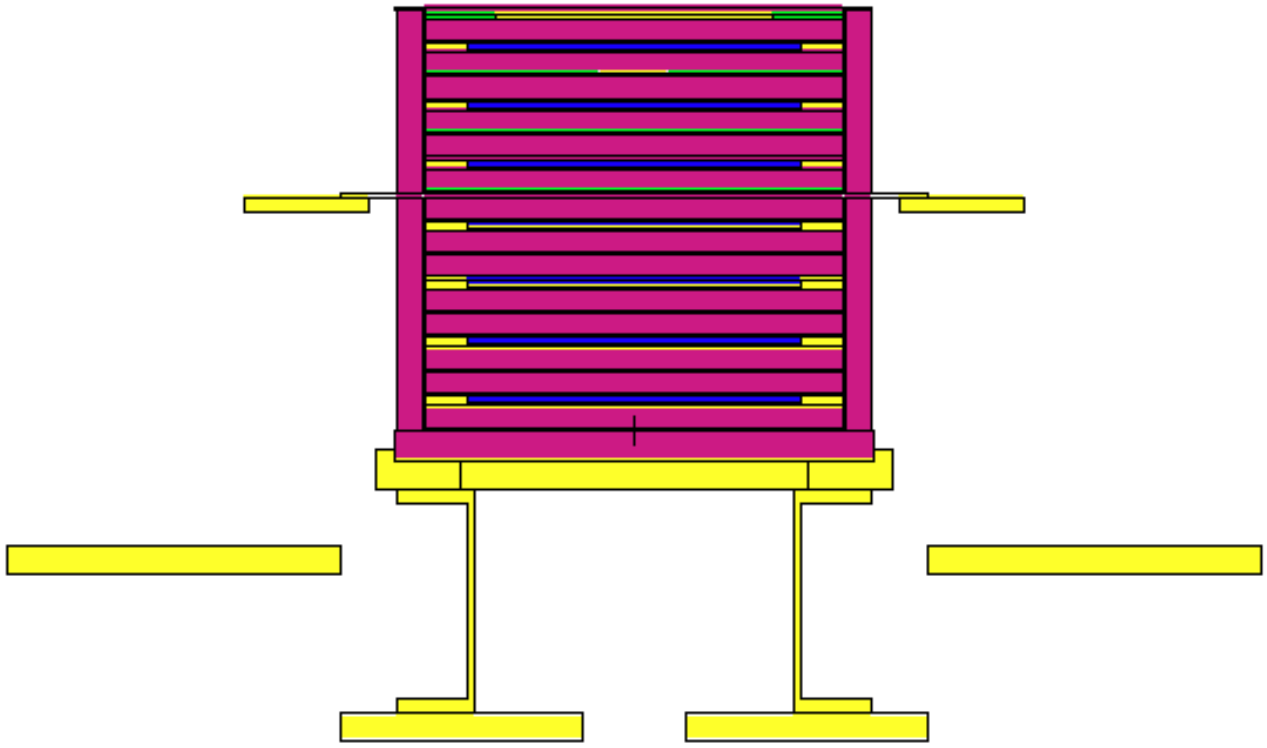

Figure 52: Case 1 model (HEU in green , sodium chloride absorber in blue, polyethylene in pink, and aluminum in yellow).

Table 177: Case 1 model lower movable platen axial positions (see Section 3.2.1).

Part		Density (g/cm^3)	z-Plane (cm)	
			Lower	**Upper**
Membrane		2.65250	21.25292	21.57042
Interface Plate		2.7	19.98292	21.25292
Stationary Platform			-13.03708	-10.49708
Adapter Plate	Lip		-2.86770	-1.67390
	Plate		-4.20831	-2.86770
Adapter Extension			-5.47831	-4.20831
			-23.25830	-5.47831
			-24.52831	-23.25830
Movable Platen			-27.06831	-24.52831

Table 178: Case 1 model upper core stack dimensions.

Layer	Part ID	Density (g/cm^3)	Radius (cm)		Thickness (cm)	z-Plane (cm)	
			Inner	Outer		Lower	Upper
14	Top Reflector	0.95715	-	19.05	0.64300	37.83268	38.47478
13	10458	18.20662	12.699	19.05	0.31083	37.51598	37.82681
	10-DISK-2	2.66926	-	12.699	0.31672	37.51598	37.83268
12	3/4-MOD-14	0.95703	-	19.05	1.9367	35.57928	37.51598
11	Upper Encap	2.46174	-	19.05	0.251	35.32828	35.57928
	SaltPlate1/4-09	1.39146	-	15.24	0.645	34.68328	35.32828
	Side Encap	2.58759	15.24	19.05	0.645		
	Lower Encap	2.58759	-	19.05	0.2223	34.45028	34.68328
10	3/4-MOD-13	0.95703	-	19.05	1.9367	32.51358	34.45028
9	10487	18.20662	3.19	19.05	0.31083	32.19688	32.50771
	2.5-DISK-1	2.66926	-	3.19	0.31672	32.19688	32.51358
8	3/4-MOD-12	0.95703	-	19.05	1.9367	30.26018	32.19688
7	Upper Encap	2.46174	-	19.05	0.251	30.00918	30.26018
	SaltPlate1/4-08	1.39146	-	15.24	0.645	29.36418	30.00918
	Side Encap	2.58759	15.24	19.05	0.645		
	Lower Encap	2.58759	-	19.05	0.2223	29.13118	29.36418
6	3/4-MOD-11	0.95703	-	19.05	1.9367	27.19448	29.13118
5	11018	18.20662	7.629	19.05	0.31083	26.88365	27.19448
	Q2-16	18.20662	-	7.629	0.31083		
4	3/4-MOD-10	0.95703	-	19.05	1.9367	24.94695	26.88365
3	Upper Encap	2.46174	-	19.05	0.251	24.69595	24.94695
	SaltPlate1/4-07	1.39146	-	15.24	0.645	24.05095	24.69595
	Side Encap	2.58759	15.24	19.05	0.645		
	Lower Encap	2.58759	-	19.05	0.2223	23.81795	24.05095
2	3/4-MOD-9	0.95703	-	19.05	1.9367	21.88125	23.81795
1	11147	18.20662	-	19.05	0.31083	21.57042	21.88125

Table 179: Case 1 model lower core stack dimensions.

Layer	Part ID	Density (g/cm^3)	Radius (cm)		Thickness (cm)	z-Plane (cm)	
			Inner	Outer		Lower	Upper
17	3/4-MOD-8	0.95703	-	19.05	1.9367	19.31622	21.25292
16	Upper Encap	2.46174	-	19.05	0.251	19.06522	19.31622
	SaltPlate1/4-02	1.39146	-	15.24	0.645	18.42022	19.06522
	Side Encap	2.58759	15.24	19.05	0.645		
	Lower Encap	2.58759	-	19.05	0.2223	18.18722	18.42022
15	3/4-MOD-7	0.95703	-	19.05	1.9367	16.25052	18.18722
14	11149	18.20662	-	19.05	0.31083	15.93969	16.25052
13	3/4-MOD-6	0.95703	-	19.05	1.9367	14.00299	15.93969
12	Upper Encap	2.46174	-	19.05	0.251	13.75199	14.00299
	SaltPlate1/4-02	1.39146	-	15.24	0.645	13.10699	13.75199
	Side Encap	2.58759	15.24	19.05	0.645		
	Lower Encap	2.58759	-	19.05	0.2223	12.87399	13.10699
11	3/4-MOD-5	0.95703	-	19.05	1.9367	10.93729	12.87399
10	11019	18.20662	-	19.05	0.31083	10.62646	10.93729
9	3/4-MOD-4	0.95703	-	19.05	1.9367	8.68976	10.62646
8	Upper Encap	2.46174	-	19.05	0.251	8.43876	8.68976
	SaltPlate1/4-02	1.39146	-	15.24	0.645	7.79376	8.43876
	Side Encap	2.58759	15.24	19.05	0.645		
	Lower Encap	2.58759	-	19.05	0.2223	7.56076	7.79376
7	3/4-MOD-3	0.95703	-	19.05	1.9367	5.62406	7.56076
6	11017	18.20662	-	19.05	0.31083	5.31323	5.62406
5	3/4-MOD-2	0.95703	-	19.05	1.9367	3.37653	5.31323
4	Upper Encap	2.46174	-	19.05	0.251	3.12553	3.37653
	SaltPlate1/4-02	1.39146	-	15.24	0.645	2.48053	3.12553
	Side Encap	2.58759	15.24	19.05	0.645		
	Lower Encap	2.58759	-	19.05	0.2223	2.24753	2.48053
3	3/4-MOD-1	0.95703	-	19.05	1.9367	0.31083	2.24753
2	11150	18.20662	-	19.05	0.31083	0.00000	0.31083
1	BOTREF-1	0.95715	-	21.71192	2.86770	-2.86770	0.00000

Table 180: Case 1 model upper and lower reflector ring dimensions (see Section 3.2.5).

Layer	Density (g/cm^3)	Radius (cm)		Thickness (cm)	z-Plane (cm)	
		Inner	Outer		Lower	Upper
Upper	0.95715	19.149	21.694	16.827	21.5704	38.3974
Lower				21.1714	0.0000	21.1714

3.2.8.2 Case 2

The Case 2 model includes 8 HEU plates, 7 sodium chloride absorbers, 7 sets of 0.25" and 1.5" HDPE moderators, and a 0.5079 in. (1.2901 cm) top HDPE reflector. These 8 HEU plates consist of five 15/0-HEU plates, one 15/2.5-HEU plate, one 15/6-HEU plate, and one 15/10-HEU plate. Figure 53 shows a cross sectional view of the model. The aluminum parts (structural components, membrane, and inserts) are shown in yellow, the HEU plates in green, the sodium chloride absorbers in blue, and the polyethylene reflector in pink.

Tables 182 and 183 report the upper and lower core stack dimensions, including: part densities (in g/cm^3), dimensions, and axial position (z-axis). Table 184 reports similar dimensions for the upper and lower reflector rings. Table 181 reports the axial positions of the Comet lower movable platen components specific to the Case 2 model, as reference in Table 171 of Section 3.2.1.

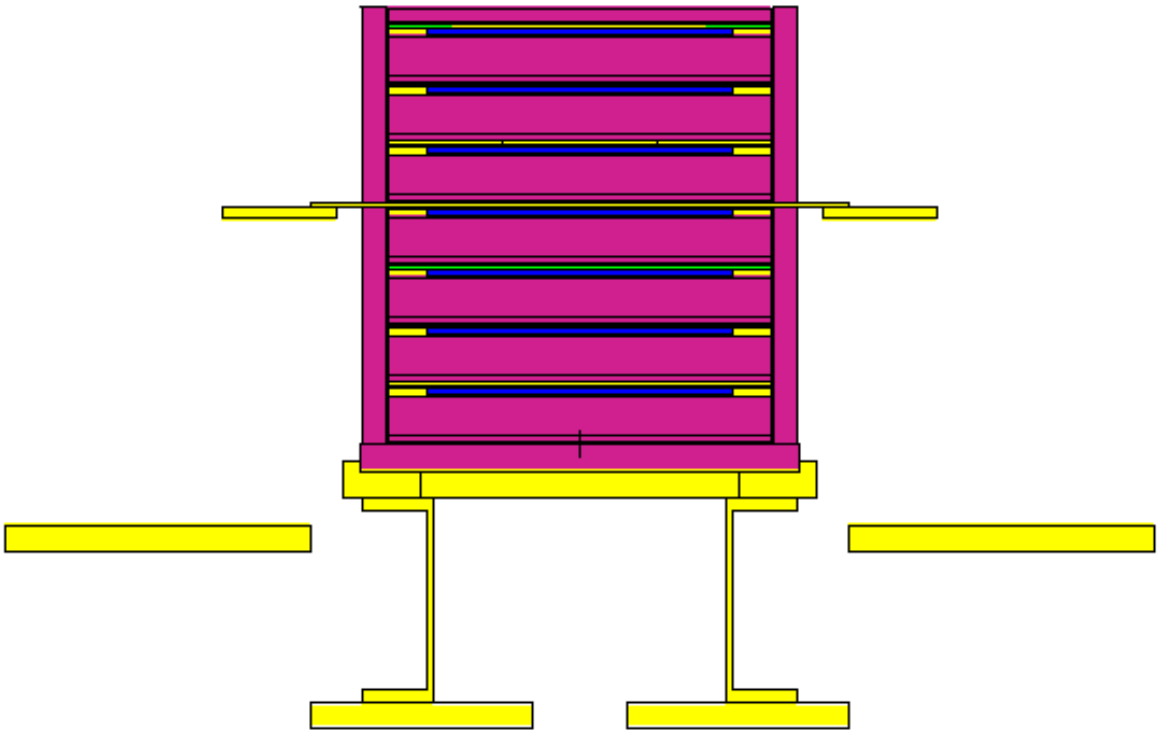

Figure 53: Case 2 model (HEU in green , NaCl absorber in blue, polyethylene in pink, and aluminum in yellow).

Table 181: Case 2 model lower movable platen axial positions (see Section 3.2.1).

Part		Density (g/cm^3)	z-Plane (cm)	
			Lower	**Upper**
Membrane		2.65250	23.66012	23.97762
Interface Plate		2.7	22.39012	23.66012
Stationary Platform			-10.62988	-8.08988
Adapter Plate	Lip		-2.86770	-1.67390
	Plate		-4.20831	-2.86770
Adapter Extension			-5.47831	-4.20831
			-23.25831	-5.47831
			-24.52831	-23.25831
Movable Platen			-27.06831	-24.52831

Table 182: Case 2 model upper core stack dimensions.

Layer	Part ID	Density (g/cm^3)	Radius (cm)		Thickness (cm)	z-Plane (cm)	
			Inner	Outer		Lower	Upper
14	Top Reflector	0.95721	-	19.05	1.2901	42.04532	43.33542
13	10458	18.20662	12.699	19.05	0.31083	41.7286	42.03943
	10-DISK-2	2.66926	-	12.699	0.31672		42.04532
12	Upper Encap	2.49604	-	19.05	0.251	41.4776	41.7286
	SaltPlate1/4-07	1.39231	-	15.24	0.645	40.8326	41.4776
	Side Encap	2.58759	15.24	19.05	0.645		
	Lower Encap	2.58759	-	19.05	0.233	40.5996	40.8326
11	1.5-MOD-8	0.94822	-	19.05	3.8321	36.7675	40.5996
10	1/4-MOD-7	0.94822	-	19.05	0.6431	36.1244	36.7675
9	10487	18.20662	3.19	19.05	0.31083	35.80768	36.11851
	2.5-DISK-1	2.66926	-	3.19	0.31672	35.80768	36.1244
8	Upper Encap	2.49604	-	19.05	0.251	35.55668	35.80768
	SaltPlate1/4-07	1.39231	-	15.24	0.645	34.91168	35.55668
	Side Encap	2.58759	15.24	19.05	0.645		
	Lower Encap	2.58759	-	19.05	0.233	34.67868	34.91168
7	1.5-MOD-7	0.94822	-	19.05	3.8321	30.84658	34.67868
6	1/4-MOD-6	0.94822	-	19.05	0.6431	30.20348	30.84658
5	11018	18.20662	7.629	19.05	0.31083	29.89265	30.20348
	Q2-16	18.20662	-	7.629	0.31083		
4	Upper Encap	2.49604	-	19.05	0.251	29.64165	29.89265
	SaltPlate1/4-07	1.39231	-	15.24	0.645	28.99665	29.64165
	Side Encap	2.58759	15.24	19.05	0.645		
	Lower Encap	2.58759	-	19.05	0.233	28.76365	28.99665
3	1.5-MOD-6	0.94822	-	19.05	3.8321	24.93155	28.76365
2	1/4-MOD-5	0.94822	-	19.05	0.6431	24.28845	24.93155
1	11147	18.20662	-	19.05	0.31083	23.97762	24.28845

Table 183: Case 2 model lower core stack dimensions.

Layer	Part ID	Density (g/cm^3)	Radius (cm)		Thickness (cm)	z-Plane (cm)	
			Inner	Outer		Lower	Upper
17	Upper Encap	2.49604	-	19.05	0.251	23.40912	23.66012
	SaltPlate1/4-05	1.39231	-	15.24	0.645	22.76412	23.40912
	Side Encap	2.58759	15.24	19.05	0.645		
	Lower Encap	2.58759	-	19.05	0.233	22.53112	22.76412
16	1.5-MOD-5	0.94822	-	19.05	3.8321	18.69902	22.53112
15	1/4-MOD-4	0.94822	-	19.05	0.6431	18.05592	18.69902
14	11149	18.20662	-	19.05	0.31083	17.74509	18.05592
13	Upper Encap	2.49604	-	19.05	0.251	17.49409	17.74509
	SaltPlate1/4-04	1.39231	-	15.24	0.645	16.84909	17.49409
	Side Encap	2.58759	15.24	19.05	0.645		
	Lower Encap	2.58759	-	19.05	0.233	16.61909	16.84909
12	1.5-MOD-4	0.94822	-	19.05	3.8321	12.78399	16.61909
11	1/4-MOD-3	0.94822	-	19.05	0.6431	12.14089	12.78399
10	11019	18.20662	-	19.05	0.31083	11.83006	12.14089
9	Upper Encap	2.49604	-	19.05	0.251	11.57906	11.83006
	SaltPlate1/4-03	1.39231	-	15.24	0.645	10.93406	11.57906
	Side Encap	2.58759	15.24	19.05	0.645		
	Lower Encap	2.58759	-	19.05	0.233	10.70106	10.93406
8	1.5-MOD-3	0.94822	-	19.05	3.8321	6.86896	10.70106
7	1/4-MOD-2	0.94822	-	19.05	0.6431	6.22586	6.86896
6	11017	18.20662	-	19.05	0.31083	5.91503	6.22586
5	Upper Encap	2.49604	-	19.05	0.251	5.66403	5.91503
	SaltPlate1/4-02	1.39231	-	15.24	0.645	5.01903	5.66403
	Side Encap	2.58759	15.24	19.05	0.645		
	Lower Encap	2.58759	-	19.05	0.233	4.78603	5.01903
4	1.5-MOD-1	0.94822	-	19.05	3.8321	0.95393	4.78603
3	1/4-MOD-1	0.94822	-	19.05	0.6431	0.31083	0.95393
2	11150	18.20662	-	19.05	0.31083	0.00000	0.31083
1	BOTREF-1	0.95721	-	21.71192	2.86770	-2.86770	0.00000

Table 184: Case 2 model upper and lower reflector ring dimensions (see Section 3.2.5).

Layer	Density (g/cm^3)	Radius (cm)		Thickness (cm)	z-Plane (cm)	
		Inner	Outer		Lower	Upper
Upper	0.95721	19.155	21.695	19.3848	23.9896	43.3624
Lower				23.5908	0.0000	23.5908

3.2.8.3 Case 3

The Case 3 model includes 18 HEU plates, 17 sodium chloride absorbers, 17 0.125" HDPE moderator, and a nominally 1.0625 in. (2.69875 cm) top HDPE reflector. These 18 HEU plates consist of five 15/0-HEU plates, seven 15/2.5-HEU plate, ans six 15/6-HEU plate. Figure 54 shows a cross sectional view of the model. The aluminum parts (structural components, membrane, and inserts) are shown in yellow, the HEU plates in green, the sodium chloride absorbers in blue, and the polyethylene reflector in pink.

Tables 186 and 187 report the upper and lower core stack dimensions, including: part densities (in g/cm^3), dimensions, and axial position (z-axis). Table 188 reports similar dimensions for the upper and lower reflector rings. Table 185 reports the axial positions of the Comet lower movable platen components specific to the Case 3 model, as reference in Table 171 of Section 3.2.1.

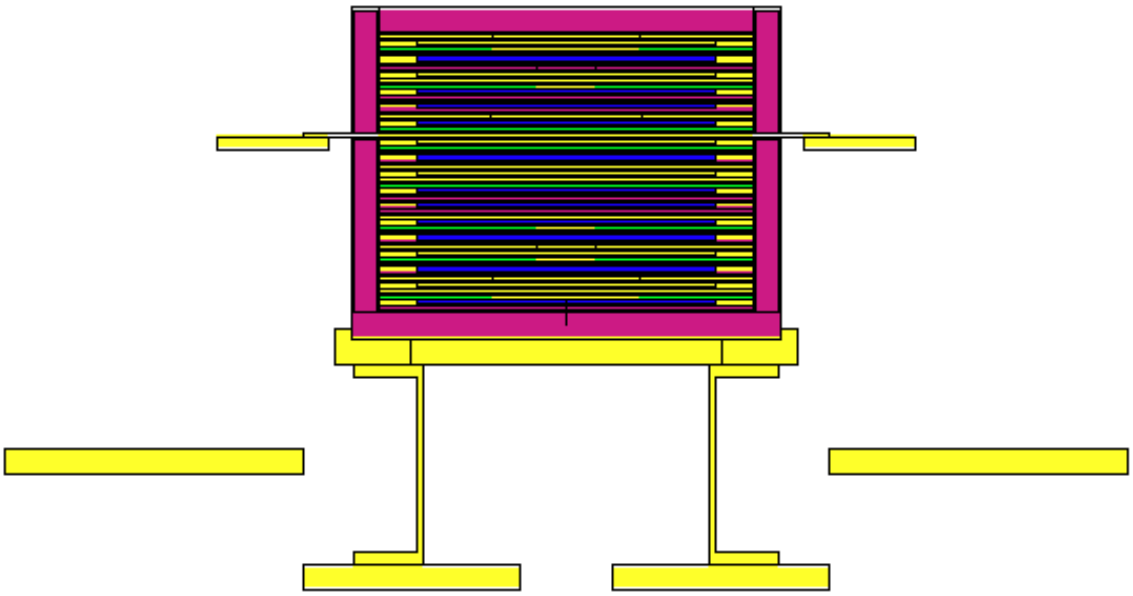

Figure 54: Case 3 model (HEU in green , NaCl absorber in blue, polyethylene in pink, and aluminum in yellow).

Table 185: Case 3 model lower movable platen axial positions (see Section 3.2.1).

Part		Density (g/cm^3)	z-Plane (cm)	
			Lower	**Upper**
Membrane		2.65250	17.83296	18.15046
Interface Plate		2.7	16.56296	17.83296
Stationary Platform			-16.45704	-13.91704
Adapter Plate	Lip		-2.86770	-1.67390
	Plate		-5.40211	-2.86770
Adapter Extension			-6.67211	-5.40211
			-24.45211	-6.67211
			-28.26211	-24.45211
Movable Platen			-25.72211	-28.26211

Table 186: Case 3 model upper core stack dimensions.

Layer	Part ID	Density (g/cm^3)	Radius (cm)		Thickness (cm)	z-Plane (cm)	
			Inner	Outer		Lower	Upper
20	Top Reflector	0.95721	-	19.05	2.7236	28.19532	30.91892
19	10935	18.27542	7.629	19.05	0.31083	27.8786	28.18943
	6-DISK-5	2.67045	-	7.629	0.31672	27.8786	28.19532
18	Upper Encap	2.46174	-	19.05	0.254	27.6246	27.8786
	SaltPlate3/16-19	1.43078	-	15.24	0.4893	27.1353	27.6246
	Side Encap	2.49347	15.24	19.05	0.4893		
	Lower Encap	2.49347	-	19.05	0.245	26.8903	27.1353
17	1/8-MOD-17	0.94710	-	19.05	0.3183	26.572	26.8903
16	10933	18.27542	7.629	19.05	0.31083	26.25528	26.56611
	6-DISK-4	2.67045	-	7.629	0.31672	26.25528	26.572
15	Upper Encap	2.46174	-	19.05	0.254	26.00128	26.25528
	SaltPlate3/16-18	1.43078	-	15.24	0.4893	25.51198	26.00128
	Side Encap	2.49347	15.24	19.05	0.4893		
	Lower Encap	2.49347	-	19.05	0.245	25.26698	25.51198
14	1/8-MOD-16	0.94710	-	19.05	0.3183	24.94868	25.26698
13	10570	18.27542	3.19	19.05	0.31083	24.63196	24.94279
	2.5-DISK-7	2.67045	-	3.19	0.31672	24.63196	24.94868
12	Upper Encap	2.46174	-	19.05	0.254	24.37796	24.63196
	SaltPlate3/16-17	1.43078	-	15.24	0.4893	23.88866	24.37796
	Side Encap	2.49347	15.24	19.05	0.4893		
	Lower Encap	2.49347	-	19.05	0.245	23.64366	23.88866
11	1/8-MOD-15	0.94710	-	19.05	0.3183	23.32536	23.64366
10	10475	18.27542	3.19	19.05	0.31083	23.00864	23.31947
	2.5-DISK-6	2.67045	-	3.19	0.31672	23.00864	23.32536
9	Upper Encap	2.46174	-	19.05	0.254	22.75464	23.00864
	SaltPlate3/16-16	1.43078	-	15.24	0.4893	22.26534	22.75464
	Side Encap	2.49347	15.24	19.05	0.4893		
	Lower Encap	2.49347	-	19.05	0.245	22.02034	22.26534
8	1/8-MOD-14	0.94710	-	19.05	0.3183	21.70204	22.02034
7	10489	18.27542	3.19	19.05	0.31083	21.38532	21.69615
	2.5-DISK-5	2.67045	-	3.19	0.31672	21.38532	21.70204

Layer	Part ID	Density (g/cm^3)	Radius (cm)		Thickness (cm)	z-Plane (cm)	
			Inner	Outer		Lower	Upper
6	Upper Encap	2.46174	-	19.05	0.254	21.13132	21.38532
	SaltPlate3/16-15	1.43078	-	15.24	0.4893	20.64202	21.13132
	Side Encap	2.49347	15.24	19.05	0.4893		
	Lower Encap	2.49347	-	19.05	0.245	20.39702	20.64202
5	1/8-MOD-13	0.94710	-	19.05	0.3183	20.07872	20.39702
4	11018	18.27542	7.629	19.05	0.31083	19.76789	20.07872
	Q2-16	18.27542	-	7.607	0.31083		
3	Upper Encap	2.46174	-	19.05	0.254	19.51389	19.76789
	SaltPlate3/16-14	1.43078	-	15.24	0.4893	19.02459	19.51389
	Side Encap	2.49347	15.24	19.05	0.4893		
	Lower Encap	2.49347	-	19.05	0.245	18.77959	19.02459
2	1/8-MOD-12	0.94710	-	19.05	0.3183	18.46129	18.77959
1	11017	18.27542	-	19.05	0.31083	18.15046	18.46129

Table 187: Case 3 model lower core stack dimensions.

Layer	Part ID	Density (g/cm^3)	Radius (cm)		Thickness (cm)	z-Plane (cm)	
			Inner	Outer		Lower	Upper
34	Upper Encap	2.46174	-	19.05	0.254	17.57896	17.83296
	SaltPlate3/16-13	1.43078	-	15.24	0.4893	17.08966	17.57896
	Side Encap	2.49347	15.24	19.05	0.4893		
	Lower Encap	2.49347	-	19.05	0.245	16.84466	17.08966
33	1/8-MOD-11	0.94710	-	19.05	0.3183	16.52636	16.84466
32	11150	18.27542	-	19.05	0.31083	16.21553	16.52636
31	Upper Encap	2.46174	-	19.05	0.254	15.96153	16.21553
	SaltPlate3/16-12	1.43078	-	15.24	0.4893	15.47223	15.96153
	Side Encap	2.49347	15.24	19.05	0.4893		
	Lower Encap	2.49347	-	19.05	0.245	15.22723	15.47223
30	1/8-MOD-10	0.94710	-	19.05	0.3183	14.90893	15.22723
29	11019	18.27542	-	19.05	0.31083	14.5981	14.90893
28	Upper Encap	2.46174	-	19.05	0.254	14.3441	14.5981
	SaltPlate3/16-11	1.43078	-	15.24	0.4893	13.8548	14.3441
	Side Encap	2.49347	15.24	19.05	0.4893		
	Lower Encap	2.49347	-	19.05	0.245	13.6098	13.8548
27	1/8-MOD-9	0.94710	-	19.05	0.3183	13.2915	13.6098
26	11147	18.27542	-	19.05	0.31083	12.98067	13.2915
25	Upper Encap	2.46174	-	19.05	0.254	12.72667	12.98067
	SaltPlate3/16-10	1.43078	-	15.24	0.4893	12.23737	12.72667
	Side Encap	2.49347	15.24	19.05	0.4893		
	Lower Encap	2.49347	-	19.05	0.245	11.99237	12.23737
24	1/8-MOD-8	0.94710	-	19.05	0.3183	11.67407	11.99237
23	11149	18.27542	-	19.05	0.31083	11.36324	11.67407
22	Upper Encap	2.46174	-	19.05	0.254	11.10924	11.36324
	SaltPlate3/16-09	1.43078	-	15.24	0.4893	10.61994	11.10924
	Side Encap	2.49347	15.24	19.05	0.4893		
	Lower Encap	2.49347	-	19.05	0.245	10.37494	10.61994
21	1/8-MOD-7	0.94710	-	19.05	0.3183	10.05664	10.37494
20	10467	18.27542	3.19	19.05	0.31083	9.73992	10.05075
	2.5-DISK-4	2.67045	-	3.19	0.31672	9.73992	10.05664
19	Upper Encap	2.46174	-	19.05	0.254	9.48592	9.73992
	SaltPlate3/16-08	1.43078	-	15.24	0.4893	8.99662	9.48592
	Side Encap	2.49347	15.24	19.05	0.4893		
	Lower Encap	2.49347	-	19.05	0.245	8.75162	8.99662

Layer	Part ID	Density (g/cm^3)	Radius (cm)		Thickness (cm)	z-Plane (cm)	
			Inner	Outer		Lower	Upper
18	1/8-MOD-6	0.94710	-	19.05	0.3183	8.43332	8.75162
17	10464	18.27542	3.19	19.05	0.31083	8.1166	8.42743
	2.5-DISK-3	2.67045	-	3.19	0.31672	8.1166	8.43332
16	Upper Encap	2.46174	-	19.05	0.254	7.8626	8.1166
	SaltPlate3/16-06	1.43078	-	15.24	0.4893	7.3733	7.8626
	Side Encap	2.49347	15.24	19.05	0.4893		
	Lower Encap	2.49347	-	19.05	0.245	7.1283	7.3733
15	1/8-MOD-5	0.94710	-	19.05	0.3183	6.8100	7.1283
14	10487	18.27542	3.19	19.05	0.31083	6.49328	6.80411
	2.5-DISK-2	2.67045	-	3.19	0.31672	6.49328	6.8100
13	Upper Encap	2.46174	-	19.05	0.254	6.23928	6.49328
	SaltPlate3/16-05	1.43078	-	15.24	0.4893	5.74998	6.23928
	Side Encap	2.49347	15.24	19.05	0.4893		
	Lower Encap	2.49347	-	19.05	0.245	5.50498	5.74998
12	1/8-MOD-4	0.94710	-	19.05	0.3183	5.18668	5.50498
11	10491	18.27542	3.19	19.05	0.31083	4.86996	5.18079
	2.5-DISK-1	2.67045	-	3.19	0.31672	4.86996	5.18668
10	Upper Encap	2.46174	-	19.05	0.254	4.61596	4.86996
	SaltPlate3/16-04	1.43078	-	15.24	0.4893	4.12666	4.61596
	Side Encap	2.49347	15.24	19.05	0.4893		
	Lower Encap	2.49347	-	19.05	0.245	3.88166	4.12666
9	1/8-MOD-3	0.94710	-	19.05	0.3183	3.56336	3.88166
8	10932	18.27542	7.629	19.05	0.31083	3.24664	3.55747
	6-DISK-3	2.67045	-	7.629	0.31672	3.24664	3.56336
7	Upper Encap	2.46174	-	19.05	0.254	2.99264	3.24664
	SaltPlate3/16-03	1.43078	-	15.24	0.4893	2.50334	2.99264
	Side Encap	2.49347	15.24	19.05	0.4893		
	Lower Encap	2.49347	-	19.05	0.245	2.25834	2.50334
6	1/8-MOD-2	0.94710	-	19.05	0.3183	1.94004	2.25834
5	10457	18.27542	7.629	19.05	0.31083	1.62332	1.93415
	6-DISK-2	2.67045	-	7.629	0.31672	1.62332	1.94004
4	Upper Encap	2.46174	-	19.05	0.254	1.36932	1.62332
	SaltPlate3/16-02	1.43078	-	15.24	0.4893	0.88002	1.36932
	Side Encap	2.49347	15.24	19.05	0.4893		
	Lower Encap	2.49347	-	19.05	0.245	0.63502	0.88002
3	1/8-MOD-1	0.94710	-	19.05	0.3183	0.31672	0.63502
2	10477	18.27542	7.629	19.05	0.31083	0.00000	0.31083
	6-DISK-1	2.67045	-	7.629	0.31672	0.00000	0.31672
1	BOTREF-1	0.95607	-	21.71192	2.86770	-2.86770	0.00000

Table 188: Case 3 model upper and lower reflector ring dimensions (see Section 3.2.5).

Layer	**Density (g/cm^3)**	**Radius (cm)**		**Thickness (cm)**	**z-Plane (cm)**	
		Inner	**Outer**		**Lower**	**Upper**
Upper	0.95607	19.15	21.699	12.4036	18.15046	30.55406
Lower				17.4770	0.0000	17.4770

3.3 Material Data

3.3.1 Highly Enriched Uranium

The HEU composition is modeled with a ^{235}U enrichment of 93.232%, by weight. The impurities were removed from the HEU based on the simplification bias analyzed in Section 3.1.1.3. Table 189 reports the elemental and isotopic composition of the HEU material used in all benchmark models, renormalized following the removal of the impurities. Table 190 reports the densities of the HEU plates used in the benchmark models. These densities represent a bulk density per benchmark model, conserving the total HEU mass in each experimental configuration. Table 191 reports the atom densities for the HEU used in the benchmark models.

Table 189: HEU elemental and isotopic composition used in all benchmark models.

Element	Wt.%	Isotope	Wt.%	At.%
U	1.00000E+02	^{234}U	1.03046E+00	1.03556E+00
		^{235}U	9.32324E+01	9.32940E+01
		^{236}U	2.32202E-01	2.31369E-01
		^{238}U	5.50498E+00	5.43904E+00

Table 190: HEU plate density by case.

Case	Density (g/cm^3)
1	18.20662
2	18.20662
3	18.27542

Table 191: HEU plate atom densities by case.

Isotope	Atom Density (atoms-b/cm)		
	Case 1	Case 2	Case 3
^{234}U	4.8274E-04	4.8274E-04	4.8456E-04
^{235}U	4.3490E-02	4.3490E-02	4.3654E-02
^{236}U	1.0785E-04	1.0785E-04	1.0826E-04
^{238}U	2.5355E-03	2.5355E-03	2.5450E-03
Total	**4.6616E-02**	**4.6616E-02**	**4.6792E-02**

3.3.2 Sodium Chloride

The NaCl composition is modeled based on sample measurements, described in Section 1.3.2. The impuritied were removed from the NaCl based on the simplification bias analyzed in Section 3.1.1.4. Similarly, the moisture in the NaCl was removed based on the simplification bias analyzed in Section 3.1.1.5. Table 192 reports the elemental and isotopic composition of the NaCl salt used in all benchmark models, renormalized following the removal of all impurities, including moisture.

Table 193 reports the densities of the sodium chloride absorbers used in the benchmark models. These den-

sities represent a bulk density per benchmark model, conserving the total NaCl mass in each experimental configuration. Table 194 reports the atom densities for the sodium chloride absorbers used in the benchmark models.

Table 192: NaCl elemental and isotopic composition used in all benchmark models.

Element	Wt.%	Isotope	Wt.%	At.%
Na	3.9374E+01	^{23}Na	3.9374E+01	5.0039E+01
Cl	6.0626E+01	^{35}Cl	4.5303E+01	3.7850E+01
		^{37}Cl	1.5323E+01	1.2111E+01

Table 193: Sodium chloride absorber plate density by case.

Case	Density (g/cm^3)
1	1.39146
2	1.39146
3	1.43078

Table 194: Sodium chloride absorber plate atom densities by case.

Isotope	Atom Density (atoms-b/cm)		
	Case 1	Case 2	Case 3
^{23}Na	1.4351E-02	1.4351E-02	1.4757E-02
^{35}Cl	1.0856E-02	1.0856E-02	1.1163E-02
^{37}Cl	3.4735E-03	3.4735E-03	3.5716E-03
Total	**2.8681E-02**	**2.8681E-02**	**2.9491E-02**

3.3.3 Polyethylene

The polyethylene composition is modeled as CH_2. The impurities were removed from the polyethylene based on the simplification bias analyzed in Section 3.1.1.6. Table 195 reports the elemental and isotopic composition of the polyethylene material used in all benchmark models, renormalized following the removal of the impurities. Table 196 reports the densities of the polyethylene moderator and reflector used in the benchmark models. The polyethylene reflector consists of the top reflector plate, bottom reflector plate, and upper and lower reflector rings. These densities represent a bulk density per benchmark model, conserving the total polyethylene mass in each experimental configuration. Table 197 reports the atom densities for the polyethylene moderator used in the benchmark models. Table 198 reports the atom densities for the polyethylene reflector used in the benchmark models.

Table 195: Polyethylene elemental and isotopic composition used in all models.

Element	Wt.%	Isotope	Wt.%	At.%
H	1.43711E+01	^{1}H	1.43689E+01	6.6661E+01
		^{2}H	2.15566E-03	5.0040E-03
C	8.56289E+01	^{12}C	8.46870E+01	3.2996E+01
		^{13}C	9.41918E-01	3.3867E-01

Table 196: Polyethylene moderator and reflector densities by case.

Case	Density (g/cm^3)	
	Moderator	Reflector
1	0.95703	0.95715
2	0.94822	0.95721
3	0.94710	0.95607

Table 197: Polyethylene moderator atom densities by case.

Isotope	Atom Density (atoms-b/cm)		
	Case 1	Case 2	Case 3
^{1}H	3.72873E-01	3.78450E-01	3.7790E-01
^{2}H	1.40057E-05	1.42152E-05	1.4194E-05
^{12}C	1.55003E-02	1.57321E-02	1.5709E-02
^{13}C	1.46820E-04	1.49016E-04	1.4880E-04
Total	**3.88387E-01**	**3.94196E-01**	**3.9362E-01**

Table 198: Polyethylene reflector atom densities by case.

Isotope	Atom Density (atoms-b/cm)		
	Case 1	**Case 2**	**Case 3**
^{1}H	3.81484E-01	3.81115E-01	3.8047E-01
^{2}H	1.43291E-05	1.43152E-05	1.4291E-05
^{12}C	1.58582E-02	1.58429E-02	1.5816E-02
^{13}C	1.50210E-04	1.50065E-04	1.4981E-04
Total	**3.97356E-01**	**3.96972E-01**	**3.9630E-01**

3.3.4 Aluminum

The aluminum composition is based on the generic composition of Al-6061 with most of the impurities and alloy components removed. As aluminum accounts for a significant part of the assembly, some of the impurities and alloy components have a notable impact on the reactivity, and were therefore left in the model. Table 199 reports the elemental and isotopic composition of the aluminum used in the benchmark models. Table 202 reports the atom densities for the aluminum used in the benchmark models.

The density of the aluminum for the Comet components is modeled at the theoretical 2.7 g cm^{-3} (6.02623E-02 atom-b/cm). Bulk part densities were assigned for the spacer plates, the absorber encapsulation bases, and absorber encapsulation lids conserving total part masses for each configuration using the modeled volumes. Table 200 reports the densities used for the aluminum for each case.

Table 199: Aluminum elemental and isotopic composition used in all models.

Element	Wt.%	Isotope	Wt.%	At.%
Al	9.83750E+01	^{27}Al	9.83750E+01	9.86000E+01
Mg	1.00000E+00	^{24}Mg	7.89900E-01	8.9062E-01
		^{25}Mg	1.00000E-01	1.0823E-01
		^{26}Mg	1.10100E-01	1.1459E-01
Cu	2.75000E-01	^{63}Cu	1.90218E-01	8.1744E-02
		^{65}Cu	8.47825E-02	3.5313E-02
Fe	3.50000E-01	^{54}Fe	2.06500E-02	1.0353E-02
		^{56}Fe	3.21020E-01	1.5521E-01
		^{57}Fe	7.35000E-03	3.4911E-03
		^{58}Fe	9.80000E-04	4.5746E-04

Table 200: Aluminum density by case.

Case	Density (g/cm^3)		
	Al Spacer	Encap. Base	Encap. Lid
1	2.66926	2.58759	2.49604
2	2.66926	2.58759	2.49604
3	2.67045	2.49347	2.46174

Table 201: Aluminum atom density for structural components.

Isotope	Atom Density (atoms-b/cm)
^{27}Al	**5.9419E-02**
^{24}Mg	6.0376E-04
^{25}Mg	7.0434E-05
^{26}Mg	7.1712E-05
^{63}Cu	2.1121E-05
^{65}Cu	8.8433E-06
^{54}Fe	3.1209E-06
^{56}Fe	4.5117E-05
^{57}Fe	9.9699E-07
^{58}Fe	1.2839E-07
Total	**6.0244E-02**

Table 202: Aluminum atom density for aluminum inserts.

Isotope	Atom Density (atoms-b/cm)		
	Case 1	**Case 2**	**Case 3**
^{27}Al	5.87421E-02	5.87421E-02	5.87683E-02
^{24}Mg	5.96884E-04	5.96884E-04	5.97150E-04
^{25}Mg	6.96323E-05	6.96323E-05	6.96633E-05
^{26}Mg	7.08956E-05	7.08956E-05	7.09272E-05
^{63}Cu	2.08803E-05	2.08803E-05	2.08896E-05
^{65}Cu	8.74263E-06	8.74263E-06	8.74652E-06
^{54}Fe	3.08533E-06	3.08533E-06	3.08671E-06
^{56}Fe	4.46029E-05	4.46029E-05	4.46228E-05
^{57}Fe	9.85643E-07	9.85643E-07	9.86082E-07
^{58}Fe	1.26931E-07	1.26931E-07	1.26987E-07
Total	**5.95580E-02**	**5.95580E-02**	**5.95845E-02**

Table 203: Aluminum atom density for encapsulation bases.

Isotope	Atom Density (atoms-b/cm)		
	Case 1	**Case 2**	**Case 3**
^{27}Al	5.6945E-02	5.6945E-02	5.4874E-02
^{24}Mg	5.7862E-04	5.7862E-04	5.5758E-04
^{25}Mg	6.7502E-05	6.7502E-05	6.5047E-05
^{26}Mg	6.8726E-05	6.8726E-05	6.6227E-05
^{63}Cu	2.0242E-05	2.0242E-05	1.9505E-05
^{65}Cu	8.4751E-06	8.4751E-06	8.1669E-06
^{54}Fe	2.9909E-06	2.9909E-06	2.8821E-06
^{56}Fe	4.3238E-05	4.3238E-05	4.1666E-05
^{57}Fe	9.5549E-07	9.5549E-07	9.2073E-07
^{58}Fe	1.2305E-07	1.2305E-07	1.1857E-07
Total	**5.7736E-02**	**5.7736E-02**	**5.5636E-02**

Table 204: Aluminum atom density for encapsulation lids.

Isotope	Atom Density (atoms-b/cm)		
	Case 1	**Case 2**	**Case 3**
^{27}Al	5.4930E-02	5.4930E-02	5.4175E-02
^{24}Mg	5.5815E-04	5.5815E-04	5.5048E-04
^{25}Mg	6.5114E-05	6.5114E-05	6.4219E-05
^{26}Mg	6.6295E-05	6.6295E-05	6.5384E-05
^{63}Cu	1.9525E-05	1.9525E-05	1.9257E-05
^{65}Cu	8.1753E-06	8.1753E-06	8.0629E-06
^{54}Fe	2.8851E-06	2.8851E-06	2.8455E-06
^{56}Fe	4.1709E-05	4.1709E-05	4.1135E-05
^{57}Fe	9.2168E-07	9.2168E-07	9.0902E-07
^{58}Fe	1.1869E-07	1.1869E-07	1.1706E-07
Total	**5.5693E-02**	**5.5693E-02**	**5.4928E-02**

3.4 Temperature Data

All benchmark cases use a temperature of 293.6 K (20.45°C).

3.5 Experimental and Benchmark-Model k_{eff}

As discussed in Section 2.1, the k_{eff} of the experimental configurations was calculated based on the measured reactor period. The experimental k_{eff} uncertainty was calculated by summing the combined modeling uncertainty (Section 2.6) and the experiment measurement uncertainty (Section 2.1) in quadrature. A calculation bias was determined based on the model simplification described in Section 3.1.1. The expected benchmark k_{eff} is determined by adding the bias to the experimental k_{eff}, summarized for the benchmark models in Table 169 of Section 3.1.1. The benchmark model uncertainty was calculated by summing the experimental k_{eff} uncertainty and the bias uncertainty in quadrature.

Table 205: Expected benchmark model k_{eff}.

Case	Experimental $k_{eff} \pm 1\sigma$	Bias in $k_{eff} \pm 1\sigma$	Benchmark Model k_{eff}
1	1.00041 ± 0.00078	-0.00023 ± 0.00019	1.00017 ± 0.00080
2	1.00065 ± 0.00114	0.00149 ± 0.00018	1.00214 ± 0.00115
3	1.00134 ± 0.00070	-0.00289 ± 0.00018	0.99845 ± 0.00072

4.0 RESULTS OF SAMPLE CALCULATIONS

Calculated fission fractions using MCNP® 6.3 with ENDF/B-VIII.0 cross sections are presented in Table 206. These calculated fission fractions are also shown in Table 1 of Section 1.0.

Table 206: Fission fractions calculated using MCNP® 6.3 with ENDF/B-VIII.0 (United States).

Case	Calculated Fission Fractions		
	Thermal (<0.625 eV)	**Intermediate (0.625 eV - 100 keV)**	**Fast (>100 keV)**
1	58.07%	30.15%	11.78%
2	62.99%	25.51%	11.50%
3	13.64%	51.10%	35.26%

Results are presented for MCNP® 6.3 using ENDF/B-VIII.0 cross section libraries[20,21] in Table 207 and MCNP® 6.3 using ENDF/B-VII.1 cross section libraries[22] in Table 208. Both tables include the associated calculated-over-experiment results, comparing to the benchmark model k_{eff} results reported in Table 205 of Section 3.5. Sample MCNP® 6.3 input files using ENDF/B-VIII.0 cross section libraries are included as attachments to Section A.1 of Appendix A.

Table 207: Sample k_{eff} and C/E results with combined experimental and calculational uncertainties using MCNP® 6.3 with ENDF/B-VIII.0 (United States).

Case	MCNP® 6.3 (Continuous Energy ENDF/B-VIII.0)	
	Calculated k_{eff}	**C/E**
1	0.99670 ± 0.00004	0.99653 ± 0.00078
2	1.00036 ± 0.00004	0.99822 ± 0.00117
3	0.98900 ± 0.00004	0.99054 ± 0.00069

Table 208: Sample k_{eff} and C/E results with combined experimental and calculational uncertainties using MCNP® 6.3 with ENDF/B-VII.1 (United States).

Case	MCNP® 6.3 (Continuous Energy ENDF/B-VII.1)	
	Calculated k_{eff}	**C/E**
1	1.00051 ± 0.00004	1.00034 ± 0.00078
2	1.00536 ± 0.00004	1.00321 ± 0.00118
3	0.98701 ± 0.00004	0.98855 ± 0.00069

[20] J. L. Conlin et al. *Release of ENDF/B-VIII.0-Based ACE Data Files*. LA-UR-18-24034. Los Alamos National Laboratory, 2018. DOI: 10.2172/1438139.

[21] D. K. Parsons and C. A. Toccoli. *Re-Release of the ENDF/B VIII.0 S(α,β) Data Processed by NJOY2016*. LA-UR-20-24456. Los Alamos National Laboratory, 2020. DOI: 10.2172/1634930.

[22] J. L. Conlin et al. *Release of ENDF/B-VII.1-based Continuous Energy Neutron Cross Section Data Tables for MCNP*. LA-UR-13-20240. Los Alamos National Laboratory, 2013.

Results are presented for COG 11.3 using ENDF/B-VIII.0 cross section libraries in Table 209. The table include the associated C/E results, comparing to the benchmark model k_{eff} results reported in Table 205 of Section 3.5. These results were provided by Paul Maggi of Lawrence Livermore National Laboratory.

Table 209: Sample k_{eff} and C/E results with combined experimental and calculational uncertainties using COG 11.3 with ENDF/B-VIII.0 (United States).

Case	**COG 11.3 (Continuous Energy ENDF/B-VIII.0)**	
	Calculated k_{eff}	**C/E**
1	0.99756 ± 0.00009	0.99739 ± 0.00078
2	1.00232 ± 0.00009	1.00018 ± 0.00118
3	0.98620 ± 0.00010	0.98773 ± 0.00070

Results are presented for MONK11A (RU0) using ENDF/B-VIII.0 cross section libraries in Table 210 and JEFF3.3 cross section libraries in Table 211. The table include the associated C/E results, comparing to the benchmark model k_{eff} results reported in Table 205 of Section 3.5. These results were provided by Alfie O'Neill of the UK National Nuclear Laboratory.

Table 210: Sample k_{eff} and C/E results with combined experimental and calculational uncertainties using MONK11A (RU0) with ENDF/B-VIII.0 (United States).

Case	**MONK 11A (Continuous Energy ENDF/B-VIII.0)**	
	Calculated k_{eff}	**C/E**
1	0.99488 ± 0.00049	0.99471 ± 0.00092
2	0.99868 ± 0.00049	0.99654 ± 0.00127
3	0.98779 ± 0.00050	0.98933 ± 0.00085

Table 211: Sample k_{eff} and C/E results with combined experimental and calculational uncertainties using MONK11A (RU0) with JEFF3.3 (NEA/OECD).

Case	**MONK 11A (Continuous Energy JEFF3.3)**	
	Calculated k_{eff}	**C/E**
1	0.99883 ± 0.00050	0.99866 ± 0.00093
2	1.00235 ± 0.00049	1.00021 ± 0.00127
3	0.99021 ± 0.00050	0.99175 ± 0.00085

5.0 REFERENCES

[1] J. M. Goda. *HEU Data Jemima Plates 2019*. LA-UR-19-24229. Los Alamos National Laboratory, 2019.

[2] H.Y. Sohn and C. Moreland. *The Effect of Particle Size Distribution on Packing Density*. Department of Chemical Engineering, University of New Brunswick, Fredericton, N.B., 1968.

[3] J. D. Norris. *TEX-HEU Baseline Assemblies: Highly Enriched Uranium Plates with Polyethylene Moderator and Polyethylene Reflector*. HEU-MET-MIXED-021, Rev. 0. International Handbook of Evaluated Criticality Safety Benchmark Experiments, NEA/NSC/DOC(95)03/II, Nuclear Energy Agency of the Organisation for Economic Co-operation and Development, 2020.

[4] J. D. Norris. *TEX-HF Assemblies: Highly Enriched Uranium Plates with Hafnium Using Polyethylene Moderator and Polyethylene Reflector*. HEU-MET-INTER-013, Rev. 0. International Handbook of Evaluated Criticality Safety Benchmark Experiments, NEA/NSC/DOC(95)03/II, Nuclear Energy Agency of the Organisation for Economic Co-operation and Development, 2024.

[5] Lewis S Combes, Stanley S Ballard, and Kathryn A McCarthy. “Mechanical and thermal properties of certain optical crystalline materials”. *Journal of the Optical Society of America* 41.4 (1951), pp. 215–222.

APPENDIX A: TYPICAL INPUT LISTINGS

A.1 MCNP® 6.3.0 Input Listings

All cases listed use ENDF/B-VIII.0 nuclear data.

A.1.1 Case 1

Input: MCNP® 6.3.0 Case 1

A.1.2 Case 2

Input: MCNP® 6.3.0 Case 2

A.1.3 Case 3

Input: MCNP® 6.3.0 Case 3